ISSN

Period.

VOL. 545 NO. 2 JUNE 7, 1991

THIS ISSUE COMPLETES VOL. 545

7th Int. Symp. on CE and ITP
Tatranská Lomnica, Oct. 2–4, 1990

JOURNAL OF CHROMATOGRAPHY

INCLUDING ELECTROPHORESIS AND OTHER SEPARATION METHODS

ELSEVIER

Scope. The *Journal of Chromatography* publishes papers on all aspects of chromatography, electrophoresis and related methods. Contributions consist mainly of research papers dealing with chromatographic theory, instrumental development and their applications. The section *Biomedical Applications*, which is under separate editorship, deals with the following aspects: developments in and applications of chromatographic and electrophoretic techniques related to clinical diagnosis or alterations during medical treatment; screening and profiling of body fluids or tissues with special reference to metabolic disorders; results from basic medical research with direct consequences in clinical practice; drug level monitoring and pharmacokinetic studies; clinical toxicology; analytical studies in occupational medicine.

Submission of Papers. Manuscripts (in English; *four* copies are required) should be submitted to: Editorial Office of *Journal of Chromatography*, P.O. Box 681, 1000 AR Amsterdam, The Netherlands, Telefax (+31-20) 5862 304, or to: The Editor of *Journal of Chromatography, Biomedical Applications*, P.O. Box 681, 1000 AR Amsterdam, The Netherlands. Review articles are invited or proposed by letter to the Editors. An outline of the proposed review should first be forwarded to the Editors for preliminary discussion prior to preparation. Submission of an article is understood to imply that the article is original and unpublished and is not being considered for publication elsewhere. For copyright regulations, see below.

Publication. The *Journal of Chromatography* (incl. *Biomedical Applications*) has 38 volumes in 1991. The subscription prices for 1991 are:

J. Chromatogr. (incl. *Cum. Indexes, Vols. 501–550*) + *Biomed. Appl.* (Vols. 535–572):
Dfl. 7220.00 plus Dfl. 1140.00 (p.p.h.) (total *ca.* US$ 4519.00)

J. Chromatogr. (incl. *Cum. Indexes, Vols. 501–550*) only (Vols. 535–561):
Dfl. 5859.00 plus Dfl. 810.00 (p.p.h.) (total *ca.* US$ 3604.75)

Biomed. Appl. only (Vols. 562–572):
Dfl. 2387.00 plus Dfl. 330.00 (p.p.h.) (total *ca.* US$ 1468.75).

Subscription Orders. The Dutch guilder price is definitive. The US$ price is subject to exchange-rate fluctuations and is given as a guide. Subscriptions are accepted on a prepaid basis only, unless different terms have been previously agreed upon. Subscriptions orders can be entered only by calender year (Jan.–Dec.) and should be sent to Elsevier Science Publishers, Journal Department, P.O. Box 211, 1000 AE Amsterdam, The Netherlands, Tel. (+31-20) 5803 642, Telefax (+31-20) 5803 598, or to your usual subscription agent. Postage and handling charges include surface delivery except to the following countries where air delivery via SAL (Surface Air Lift) mail is ensured: Argentina, Australia, Brazil, Canada, Hong Kong, India, Israel, Japan*, Malaysia, Mexico, New Zealand, Pakistan, PR CHina, Singapore, South Africa, South Korea, Taiwan, Thailand, USA. * For Japan air delivery (SAL) requires 50% additional charge of the normal postage and handling charge. For all other countries airmail rates are available upon request. Claims for missing issues must be made within three months of our publication (mailing) date, otherwise such claims cannot be honoured free of charge. Back volumes of the *Journal of Chromatography* (Vols. 1–534) are available at Dfl. 208.00 (plus postage). Customers in the USA and Canada wishing information on this and other Elsevier journals, please contact Journal Information Center, Elsevier Science Publishing Co. Inc., 655 Avenue of the Americas, New York, NY 10010, USA, Tel. (+1-212) 633 3750, Telefax (+1-212) 633 3990.

Abstracts/Contents Lists published in Analytical Abstracts, Biochemical Abstracts, Biological Abstracts, Chemical Abstracts, Chemical Titles, Chromatography Abstracts, Clinical Chemistry Lookout, Current Contents/Life Sciences, Current Contents/Physical, Chemical & Earth Sciences, Deep-Sea Research/Part B: Oceanographic Literature Review, Excerpta Medica, Index Medicus, Mass Spectrometry Bulletin, PASCAL-CNRS, Pharmaceutical Abstracts, Referativnyi Zhurnal, Research Alert, Science Citation Index and Trends in Biotechnology.

See inside back cover for Publication Schedule, Information for Authors and information on Advertisements.

0021-9673/91/$03.50

Printed in The Netherlands

For Contents, see p. III

For Superior Chiral Separation From Analytical To Preparative.

The finest from DAICEL……

Why look beyond DAICEL? We have developed the finest CHIRALCEL, CHIRALPAK and CROWNPAK with up to 17 types of HPLC columns, all providing superior resolution of racemic compounds.

NEW CHIRALPAK AS

● CHIRALPAK AS

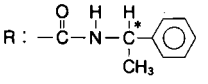

for β-Lactam antibiotics

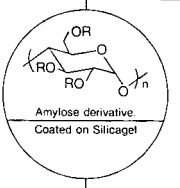

NEW CHIRALPAK AD

● CHIRALPAK AD

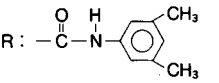

4-Acetoxy-2-azetidine

Eluent : Hexane/Ethanol = 8/2
Flow rate : 1.0ml/min
Temperature : r.t.
Detection : UV254nm

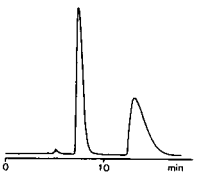

Oxyphencyclimine

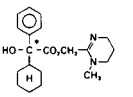

Eluent : Hexane/2-Propanol = 9/1
Flow rate : 1.0ml/min
Temperature : r.t.
Detection : UV254nm

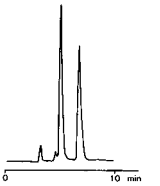

Ofloxacine methyl ester

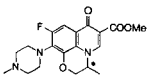

Eluent : Hexane/EtOH = 8/2
Flow rate : 1.2ml/min
Temperature : 40°C
Detection : UV254nm

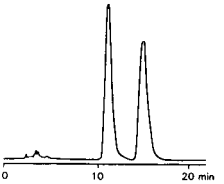

Verapamil

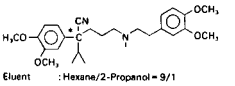

Eluent : Hexane/2-Propanol = 9/1
Flow rate : 1.0ml/min
Temperature : r.t.
Detection : UV254nm

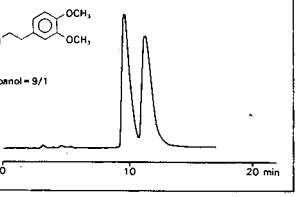

Analytical column 0.46cm × 25cm(10μm)

CHIRALCEL OA
OB
OC
OD
OJ
OF
OG
OK

CHIRALPAK AS
AD

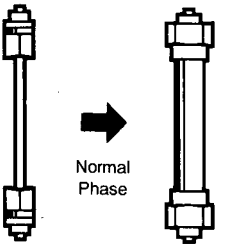

Semi-preparative column 2cm × 25cm(10μm)

You can have Pure enantiomer quickly!!

■Separation Service

- A pure enantiomer separation in the amount of 100g~10kg is now available.
- Please contact us for additional information regarding the manner of use and application of our chiral columns and how to procure our separation service.

DAICEL CHEMICAL INDUSTRIES, LTD.

chiral chemicals division.
8-1, Kasumigaseki 3-chome, Chiyoda-ku, Tokyo 100, Japan Phone: 03 (507) 3151 FAX: 03 (507) 3193

DAICEL(U.S.A.),INC.
Fort Lee Executive Park
Two Executive Drive, Fort Lee,
New Jersey 07024
Phone: (201) 461-4466
FAX: (201) 461-2776

DAICEL(U.S.A.),INC.
23456 Hawthorne Blvd.
Bldg. 5, Suit 130
Torrance, CA 90505
Phone: (213) 791-2030
FAX: (213) 791-2031

DAICEL(EUROPA)GmbH
Oststr. 22
4000 Düsseldorf 1, F.R. Germany
Phone: (211) 369848
Telex: (41) 8588042 DCEL D
FAX: (211) 364429

DAICEL CHEMICAL(ASIA)PTE. LTD.
65 Chulia Street #40-07
OCBC Centre, Singapore 0104
Phone: 5332511
FAX: 5326454

Journal of Chromatography Library, 50

Liquid Chromatography in Biomedical Analysis

edited by **T. Hanai,** *International Institute of Technological Analysis, Health Research Foundation, Kyoto, Japan*

This book presents a guide for the analysis of biomedically important compounds using modern liquid chromatographic techniques. After a brief summary of basic liquid chromatographic methods and optimization strategies, the main part of the book focuses on the various classes of biomedically important compounds: amino acids, catecholamines, carbohydrates, fatty acids, nucleotides, porphyrins, prostaglandins and steroid hormones. The different chapters discuss specialized techniques pertaining to each class of compounds, such as sample pretreatment, pre- and post-column derivatization, detection and quantification.

1991 xii + 296 pages
Price: US $ 154.50 / Dfl. 270.00
ISBN 0-444-87451-8

Contents:

Elsevier Science Publishers

P.O. Box 211, 1000 AE Amsterdam, The Netherlands
P.O. Box 882, Madison Square Station, New York, NY 10159, USA

SPECIAL ISSUE

SEVENTH INTERNATIONAL SYMPOSIUM ON CAPILLARY ELECTROPHORESIS AND ISOTACHOPHORESIS

Tatranská Lomnica (Czechoslovakia), October 2–4, 1990

Guest Editors

PETR BOČEK
(Brno)

DUŠAN KANIANSKY
(Bratislava)

VOL. 545, NO. 2 JOURNAL OF CHROMATOGRAPHY JUNE 7, 1991

CONTENTS

7TH INTERNATIONAL SYMPOSIUM ON CAPILLARY ELECTROPHORESIS AND ISOTACHOPHORESIS, TATRANSKÁ LOMNICA, OCTOBER 2–4, 1990

In articles with more than one author, the name of the author to whom correspondence should be addressed is indicated in the article heading by a 6-pointed asterisk (*)

Journal of Chromatography, 545 (1991) 223
Elsevier Science Publishers B.V., Amsterdam

PREFACE

The *7th International Symposium on Capillary Electrophoresis and Isotachophoresis* was held in Tatranská Lomnica, High Tatras, Czechoslovakia, from October 2nd to 4th, 1990.

The Symposium Chairman was Dr. Dušan Kaniansky and the organizers were the Slovak Chemical Society, the Faculty of Science, Comenius University, Bratislava, the Institute of Radioecology and Applied Nuclear Techniques, Košice, in collaboration with the Faculty of Chemical Technology, Slovak Technical University, Bratislava, the Faculty of Science of Charles University, Prague, the Institute of Analytical Chemistry, Czechoslovak Academy of Science, Brno, and the Institute of Organic Chemistry and Biochemistry, Czechoslovak Academy of Science, Prague.

Eight lecture sessions were devoted to Fundamental aspects of electrophoresis, Theory, Preparative aspects and coupling of analytical methods, Electrokinetic chromatography, Electroosmotic flow and detection in capillary electrophoresis, Zone electrophoresis and coupling of electrophoretic methods and Applications (two sessions). Two poster sessions were organized during late afternoon and provided space and time for direct discussions and exchange of knowledge in small groups.

There were over 110 participants from 12 European countries and Japan, who presented 28 lectures and 45 posters and submitted manuscripts that have led to this special issue.

The High Tatras Symposium continued in the direction introduced in Vienna (6th Symposium, 1988) and brought together experts in capillary isotachophoresis and capillary zone electrophoresis. The presentations on isotachophoresis showed clearly that this technique is a well established one which might even serve as a reference method. The presentations on capillary zone electrophoresis and electrokinetic chromatography demonstrated the high separation potential and expediency of these techniques.

Well organized exhibitions of commercial instrumentation for capillary electrophoresis and presentations of computer-simulated isotachophoresis attracted much attention from participants.

The social programme brought together the participants in the evenings and provided time for informal discussions. Nice weather and the beautiful scenery of the High Tatras also aided the success of the Symposium.

It is my pleasure to congratulate and thank Dr. Dušan Kaniansky and everyone concerned who made the High Tatras Symposium a successful event. Finally, I thank Dr. Karel Macek for his care in producing this special issue.

Brno (Czechoslovakia) PETR BOČEK

Journal of Chromatography, 545 (1991) 225–237
Elsevier Science Publishers B.V., Amsterdam

CHROM. 23 172

Computer-aided simulation of electromigration

BOHUSLAV GAŠ* and JIŘÍ VACÍK

Department of Physical and Macromolecular Chemistry, Faculty of Science, Charles University, Albertov 2030, 128 40 Prague 2 (Czechoslovakia)

and

IMRICH ZELENSKÝ

Department of Analytical Chemistry, Faculty of Science, Komenský University, Mlynská dolina, 84 215 Bratislava (Czechoslovakia)

ABSTRACT

Equations that describe the electrophoretic migration of monovalent ionic substances in solution with a significant presence of H^+ or OH^- ions are formulated. A derivation of the Kohlrausch regulating function for these conditions is presented. The model of electromigration consists of a set of continuity equations, together with a set of algebraic equations describing the chemical equilibria involved, and is implemented on a personal computer. Simulation of some experimental phenomena in electrophoretic methods, *e.g.*, the sharpening effect in capillary zone electrophoresis or anomalous spikes in isotachophoretic systems, is presented.

INTRODUCTION

Considerable attention has been paid to the description of the migration of ions in an electric field. Efforts of theoreticians are directed towards two aspects: first, the use of fundamental laws describing mass transport, chemical equilibria or the electroneutrality principle and the derivation of explicit conclusions useful in a particular application, and second, attempts to solve the basic laws "from the beginning", which leads in practice to the necessity for a solution of partial differential and non-linear algebraic equations. In most instances, these equations are not analytically soluble and therefore are solved numerically using computers. The results are obtained in a numerical or graphical form.

It is not the aim of this paper to attempt a comprehensive review of previous theoretical work, so only a selection will be mentioned. Kohlrausch's study [1] belongs to the first group and established a basis for many subsequent studies. It is possible to refer to, *e.g.*, the *RFQ* method of evaluation of the steady state in isotachophoresis introduced by Beckers and co-workers [2,3] and the work of Mikkers and co-workers dealing with transient states in isotachophoresis [4–6] and some aspects of electrophoresis [7]. A series of papers by Boček and co-workers [8–12] have shown the usefulness of zone existence diagrams in isotachophoresis and introduced the concept

0021-9673/91/$03.50

of the effective mobility of the hydrogen ion. Hirokawa and co-workers described the dynamics of separations in isotachophoresis using a transient state model [13,14] and applied the steady-state theory in isotachophoresis [15,16] to the determination of basic physico-chemical constants.

Many papers by Mosher, Palusinski and co-workers [17–29] belong to the second group. They have developed a general model of electrophoresis of ampholytes in solution and have been able to implement the model on a computer, solve it numerically and simulate many electrophoretic techniques.

Our laboratory has also been engaged in an effort to understand electromigration separation processes. The dynamics of the motion of the boundary between two strong electrolytes was solved on a computer using the net method [30]. The isotachophoretic separation of four strong electrolytes was conveniently simulated on a hybrid computer [31] and later published [32,33].

The purpose of this paper is to present a relatively simple model of migration of weak uni–univalent electrolytes in an electric field. In spite of its simplicity, the model is able to describe or explain many phenomena appearing in electromigration methods. The model is easily implementable on personal computers and is also instructive from a pedagogical point of view.

MATHEMATICAL MODEL

Let us consider a solution of weak uni–univalent electrolytes which are able to migrate in an electric field in one direction, mostly in a capillary tube. The limitation of these considerations to uni–univalent electrolytes is not a serious drawback because most features of electromigration methods could be described in spite of this restriction. It is also known that many important relationships holding in the theory of electromigration can then be easily formulated [20,34]. Let us also neglect the diffusional dispersion. Even this restriction [7,20] will not cause a serious limitation of the model, especially in describing isotachophoresis. Nevertheless, when the presence of H^+ or OH^- ions originating from a solvent and weak electrolytes is significant we shall take these ions into consideration, therefore, we shall use a new term in this context, *viz.*, substance.

By the term substance we shall understand an ionic species together with an eventually related undissociated compound. Three examples of such substances are acetate plus acetic acid, H^+ ions plus propionic acid or OH^- ions plus NH_3.

Concentrations and electrophoretic mobilities are assumed to be positive numbers. The total concentration of substance j is denoted c_j, the relative charge of ionic species j is denoted z_j and can be $+1$ for a cation and -1 for an anion, the concentration of the ionic part of substance j is denoted c_j^z and that of the undissociated compound j is denoted c_j^0. It is then possible to write $c_j = c_j^z + c_j^0$. Further, for simplicity, we shall use the term "weak ion" instead of "ion of a weak electrolyte".

Our aim is to find the time course of the distributions in the capillary tube of all the substances in either the dissociated or the undissociated form. The derivation of the basic equations can start from the mass conservation law in an infinitesimal volume or continuity equation.

First, for simplicity, let us assume a negligible concentration of the H^+ or OH^- ions produced by ionization compared with other substances. These requirements can

be met by performing the separation in the so-called "safe region" [9] at a pH within the range *ca.* 5–10. Fig. 1 shows a system of two weak anions and one weak counter cation. The electric field orientation and consequently the direction of the electric current are assumed to follow the direction of increasing values on abscissa. S_j^z represents the mass flow of j ions. The horizontal arrows denote the mass flow through the depicted volume and the bent arrows symbolize the time changes of the concentration of the substances. The conservation equations can be written as (*cf.*, ref. 20)

$$\frac{\delta c_j}{\delta t} = - z_j \, i \, U_j \frac{\delta}{\delta x}\left(\frac{c_j^z}{\varkappa}\right) \tag{1}$$

and

$$\varkappa = F \sum_{j=1}^{n} c_j^z \, U_j \tag{2}$$

where $j = 1, 2, \ldots, n$, t is time, i is the current density in the capillary tube, $\varkappa$ is the specific conductivity, U_j is the ionic mobility of ion j, x is the length coordinate along the capillary tube, n is the number of substances and F is the Faraday constant.

We assume that ionic mobility U_j (which generally depends on the ionic strength) can be approximated by the limiting ionic mobility in our model. From the set of eqn. 1 we can obtain the regulating function connected with the mass conservation law:

$$\sum_{j=1}^{n} z_j \, c_j = \text{constant } (x) \tag{3}$$

where constant (x) is a function of the length coordinate x, independent of time. If the eletroneutrality condition

$$\sum_{j=1}^{n} z_j \, c_j^z = 0 \tag{4}$$

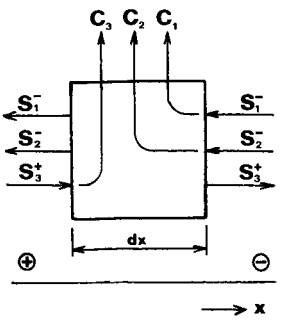

Fig. 1. Graphical illustration of the transport equations for the system of two weak anions and one weak counter cation.

is fulfilled at any length point (it is a good approximation [27]), then the Kohlrausch regulating function holds:

$$\sum_{j=1}^{n} \frac{c_j}{U_j} = \text{constant } (x) \tag{5}$$

Eqns. 3, 4 and 5 are the bonding conditions for the solution of the initial and boundary problem of the set of eqn. 1. Because migration of weak electrolytes is generally considered, we must take into account additional bonding conditions, which are equations describing chemical dissociation equilibria:

$$f(c_1, c_2, \ldots, c_n) = K \tag{6}$$

where f is a non-linear function (the Guldberg–Waage law) and K is the dissociation constant.

For illustration, let us consider a system consisting of five substances: two weak and two strong anions and one common weak counter cation. There are eight unknown variables in this system: two concentrations of the charged and uncharged part of the counter substance, four concentrations of the charged and uncharged part of the weak anionic substances and two concentrations of the strong anionic substances. It follows that we need eight equations to solve this system: three are eqns. 3–5 and two are equations describing dissociation equilibria [of the three original relationships for chemical equilibria (eqn. 6) of the three weak substances, one is cancelled after elimination of the hydrogen ion concentration]. Consequently, three differential equations of the set of eqn. 1 remain.

The situation is more complicated if H^+ or OH^- ions participate in the migration. First, let us assume a significant role of the H^+ ions. For illustration, Fig. 2 shows a system consisting of three substances: acetate (which is composed of acetate anion, $acet^-$, and acetic acid, Hacet), H^+ (which consists of H^+ cation and acetic acid, Hacet) and K^+. The notation of the symbols and arrows is the same as in Fig. 2. An equation describing the transport of hydrogen (either as H^+ ion and hydrogen bonded in acetic acid) can be written in the form

$$\frac{\delta(c_H^+ + c_{Hacet}^0)}{\delta t} = -i\, U_H \frac{\delta}{\delta x}\left(\frac{c_H^+}{\varkappa}\right) \tag{7}$$

The Kohlrausch regulating function is then

$$\frac{c_{Hacet}^0}{U_{acet}} + \frac{c_{acet}^-}{U_{acet}} + \frac{c_K^+}{U_K} + \frac{c_H^+}{U_H} + \frac{c_{Hacet}^0}{U_H} = \text{constant } (x) \tag{8}$$

It can be shown that all the relationships describing the migrating reaction boundary of the zone of H^+ ions in isotachophoresis [8,9,35] can be readily derived from the regulating function in eqn. 8.

The following relationship holds for the general system with significant contribution of H^+ ions:

$$\frac{\delta\left(c_H^+ - \sum_{j=1}^{n} z_j c_j^0\right)}{\delta t} = -i\, U_H \frac{\delta}{\delta x}\left(\frac{c_H^+}{\varkappa}\right) \tag{9}$$

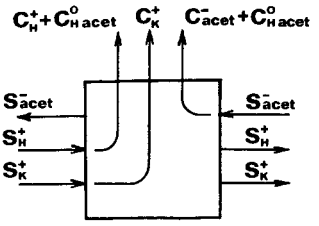

Fig. 2. Graphical illustration of the transport equations for the system potassium acetate–acetic acid.

where n is the number of substances except hydrogen. The Kohlrausch regulating function takes the form

$$\sum_{j=1}^{n} \frac{c_j}{U_j} + \frac{c_H^+}{U_H} - \sum_{j=1}^{n} z_j\, c_j^0/U_H = \text{constant } (x) \tag{10}$$

and the condition of electroneutrality is

$$\sum_{j=1}^{n} c_j^z\, z_j + c_H^+ = 0 \tag{11}$$

There is no simple relationship analogous to eqn. 3.

For the solution of, *e.g.*, a four-substance system containing two weak cations, H^+ cation and weak counter anion, there are seven unknown variables. Three eqn. 6 describe the dissociation equilibria of the weak ions, two equations follow from eqns. 10 and 11 and, consequently, two partial differential equations remain. It is useful to realize that the number of remaining partial differential equations equals the number of boundaries realizable in an isotachophoretic system or the number of peaks in a system modelling zone electrophoresis.

Considering the contribution of the OH^- ions to migration, the following equations can be written:

$$\frac{\delta\left(c_{OH}^- + \sum_{j=1}^{n} z_j\, c_j^0\right)}{\delta t} = i\, U_{OH} \frac{\delta}{\delta x}\left(\frac{c_{OH}^-}{\varkappa}\right) \tag{12}$$

where n is the number of substances except OH^- substance, and the Kohlrausch regulating function,

$$\sum_{j=1}^{n} \frac{c_j}{U_j} + \frac{c_{OH}^-}{U_{OH}} + \sum_{j=1}^{n} z_j\, c_j^0/U_{OH} = \text{constant } (x) \tag{13}$$

is obtained.

It is apparent from the above that a simulation of migration in an electric field (in the framework of the described model) requires the solution of the set of partial differential and linear plus non-linear algebraic equations for various initial and

boundary conditions. These conditions can circumscribe several current electromigration methods, *e.g.*, isotachophoresis or capillary zone electrophoresis.

NUMERICAL METHOD

The same method as in previous work [31] was chosen for the solution of the partial differential equations, namely the CSDT (continuous space, discrete time) method of lines. However, computation was carried out on a personal instead of a hybrid computer.

The CSDT method consists in discretizing the time derivatives at a set of grid points to generate a set of ordinary differential equations instead of partial differential equations with length as the independent variable. The finite-difference approximation is based on the first-order backward difference approximation:

$$\frac{\delta c}{\delta t} = \frac{c_i - c_{i-1}}{\Delta t} \tag{14}$$

where $t = i\Delta t$, $i = 1, 2, \ldots$ and c_0 is the initial concentration distribution in a capillary tube at time $t = 0$.

The Hamming modification of the fourth-order predictor–corrector method [36] was chosen for integration of the set of ordinary differential equations. The method exhibits the same accuracy as the standard fourth-order Runge–Kutta method, but it is almost twice as fast. In addition, the method permits an easy estimation of its error, which is convenient from the numerical point of view.

The numerical method of solution of the differential equations also necessitates discretization of the x-coordinate. The left-hand side of eqn. 1 must be calculated at each point of the x-coordinate; in fact it requires a set of non-linear algebraic equations to be solved at each point for systems including weak electrolytes, because the bonding conditions resulting from the laws of chemical equilibria include products and quotients of the concentrations. The set of non-linear algebraic equations was solved by the Newton–Raphson iteration method [36] and the concentrations computed in the preceding time step are taken as the initial estimates.

All the bonding conditions are linear if only strong electrolytes are considered, and therefore the Gauss elimination method can be used to solve the left-hand side of eqn. 1 in this instance.

EXPERIMENTAL

The computational algorithm for the solution of the whole model was programmed in Pascal language and runs on IBM PC AT computers or other compatible types. The result of computation is a graphical presentation of the time-dependent evolution of the distribution of all the substances and their charged and uncharged parts along the x-coordinate in a capillary tube.

The algorithm allows an "observational window" to be advanced along the capillary tube at the migration rate of a substance of interest and thus enables excessive computer time and memory requirements to be avoided. It was used in simulations of all isotachopherograms, where the window shifts at the migration velocity of the leading ion.

TABLE I

INPUT DATA FOR COMPUTER SIMULATIONS

Substance	pK_a	Ionic mobility (10^{-9} m^2 V^{-1} s^{-1})
Acetate	4.76	42.4
Benzoate	4.20	36.3
Cl^-	–	79.1
Bis–Tris[a]	6.4	26
Aniline	4.8	32.5
Pyridine	5.18	30
TBA	14	18
K^+	–	76.2
H^+	–	363

[a] Bis[tris(hydroxyethylaminomethane)].

Ionic mobilities and pK values of substances used as input data for simulations are listed in Table I.

A CS ZKI 01 isotachophoretic analyser assembled in the column coupling configuration of the separation unit was used for experiments. Chemicals used for the preparation of the leading and terminating electrolytes were of analytical-reagent grade and some were purified by conventional methods.

RESULTS AND DISCUSSION

As pointed out above, the model of electrophoretic migration neglects diffusion of substances. However, during numerical calculation, the first-order approximation eqn. 14 causes an error that imitates the diffusional term in the continuity equations. This error can in principle be decreased by diminishing of Δt in eqn. 14 but it involves more computer time and memory requirements. A reasonable medium value of Δt should always be chosen.

Fig. 3 shows the solution of the isotachophoretic separation of two weak anionic substances in a system of strong leading and terminating anion and a weak buffering counter cation, where the contribution of H^+ or OH^- ions to migration is neglected. A pH inversion occurs between the second weak substance and the terminating anion.

Isotachophoretic systems with a mobility inversion [11] are more interesting. Inversion of mobility can appear in routine practice more often than one might expect, especially in analyses of real samples where related samples could often be present. Anomalies in the conductivity recording of the separation are often considered as artifacts of the contact conductivity detector. The mobility inversion mostly occurs in practice in systems with a low buffering capacity of the counter substance (as, *e.g.*, in the 0.01 M potassium acetate system for cationic separation [11]) or in buffer-free systems [12]. Such systems allow a wide pH swing between subsequent zones. In systems with a maximum buffering capacity of the counter substance, the inversion of the mobilities is a subtle phenomenon observable only within a narrow range of the pH of the leading electrolyte.

A condition for isotachophoretic migration of two weak substances with

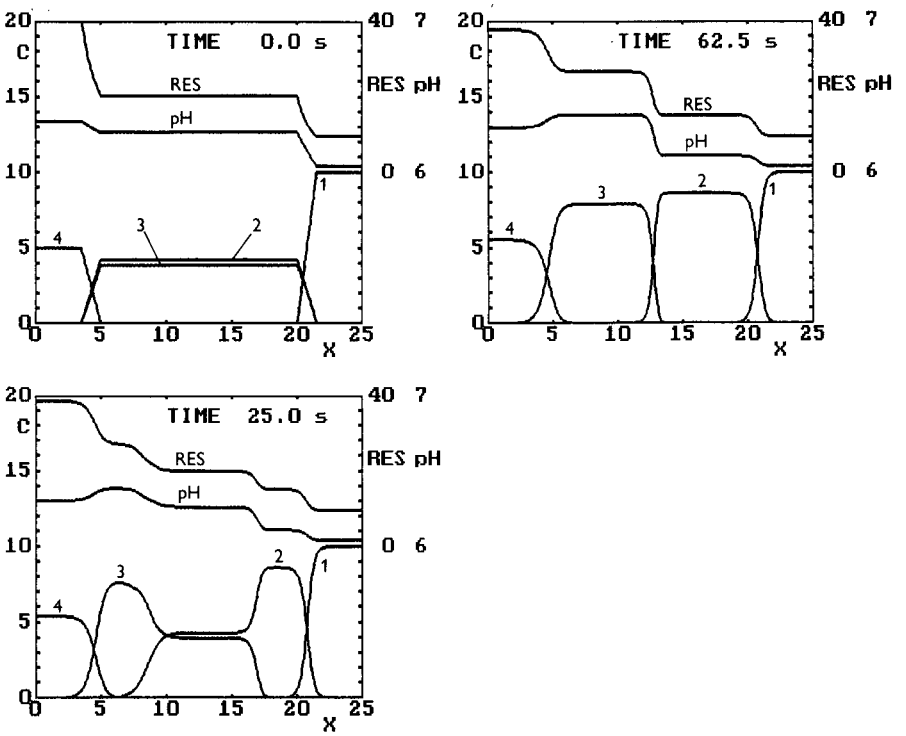

Fig. 3. Simulation of anionic isotachophoresis. 1 = Strong leading anion chloride, $u_1^- = 79.1 \cdot 10^{-9}$ m^2 V^{-1} s^{-1}; 2 = weak anion, $u_2^- = 50 \cdot 10^{-9}$ m^2 V^{-1} s^{-1}, pK = 4; 3 = weak anion, $u_3^- = 40 \cdot 10^{-9}$ m^2 V^{-1} s^{-1}, pK = 6; 4 = strong terminating anion, $u_4^- = 20 \cdot 10^{-9}$ m^2 V^{-1} s^{-1}. Weak counter cation, histidine, $u_5^+ = 29.6 \cdot 10^{-9}$ m^2 V^{-1} s^{-1}, pK = 6.04. Leading electrolyte, 10 mM chloride–20 mM histidine. Current density, 709 A m^{-2}. C = concentration (mM), RES = specific resistance (Ω m), x = coordinate (mm).

mobility inversion is the intersection of their mobility curves. Fig. 4 displays the mobility curves of acetic and benzoic acid, which intersect at pH 5.15, and Fig. 5 shows some parameters of this pair migrating in the system 15 mM chloride as leading anion

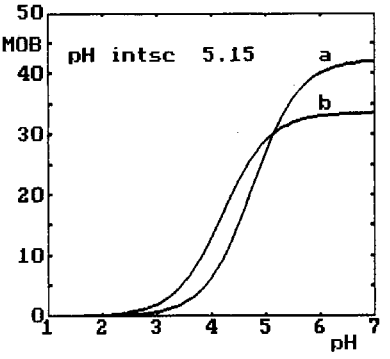

Fig. 4. Mobility curves of (a) acetic acid and (b) benzoic acid. MOB = mobility (10^{-9} m^2 V^{-1} s^{-1}).

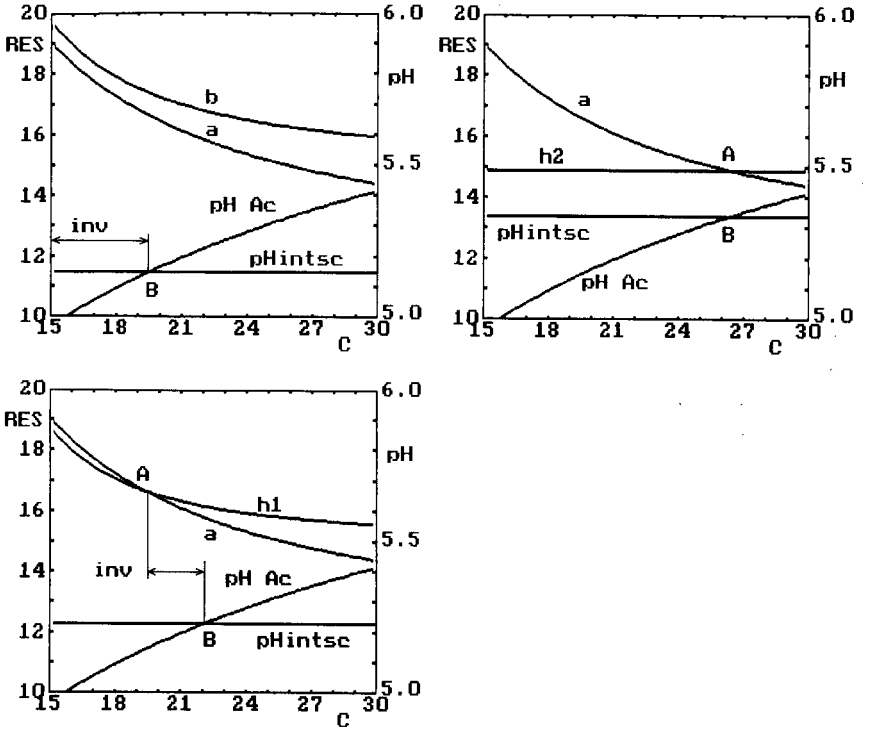

Fig. 5. Influence of pyridine concentration on the specific resistance and pH of zones in the system 15 mM Cl^- plus pyridine. a = Specific resistance of acetate zone; b = specific resistance of benzoate zone; h1 = specific resistance of a hypothetical substance with pK = 4.0; h2 = specific resistance of a hypothetical substance with pK = −1. pH Ac = pH of acetate zone; pHintsc = pH of intersection of mobility curves; inv = interval of mobility inversion; C = concentration of pyridine (mM); RES = specific resistance (Ω m).

and pyridine as buffering counter ion. If instead of benzoic acid with pK = 4.2 another hypothetical acid with pK = 4 is used, migration with mobility inversion can occur in a narrower interval, between the intersection A on the conductivity curves and the intersection B on the pH curves. When a strong acid with pK of, *e.g.*, −1 is used, then, in spite of intersection of the mobility curves, mobility inversion is impossible because there is no space between points A and B. Hence, migration with mobility inversion can occur if the mobility curves intersect but the pK values are not very different. For buffered systems exhibiting a maximum buffering capacity (which are usually employed in practice) this means that the pK difference lies in the range *ca.* 0.3–1 if mobility inversion occurs.

These conclusions are illustrated in Figs. 6 and 7, depicting a computer simulation (see also ref. 11) and an isotachopherogram of the separation of acetic and benzoic acid with a mobility inversion in 15 mM hydrochloric acid + 16 mM pyridine as the leading electrolyte system. Both the computer simulation and the experimental verification on a double-column isotachophoretic analyser have shown that the boundary between benzoate and acetate zones is stable and both are zones of pure substances.

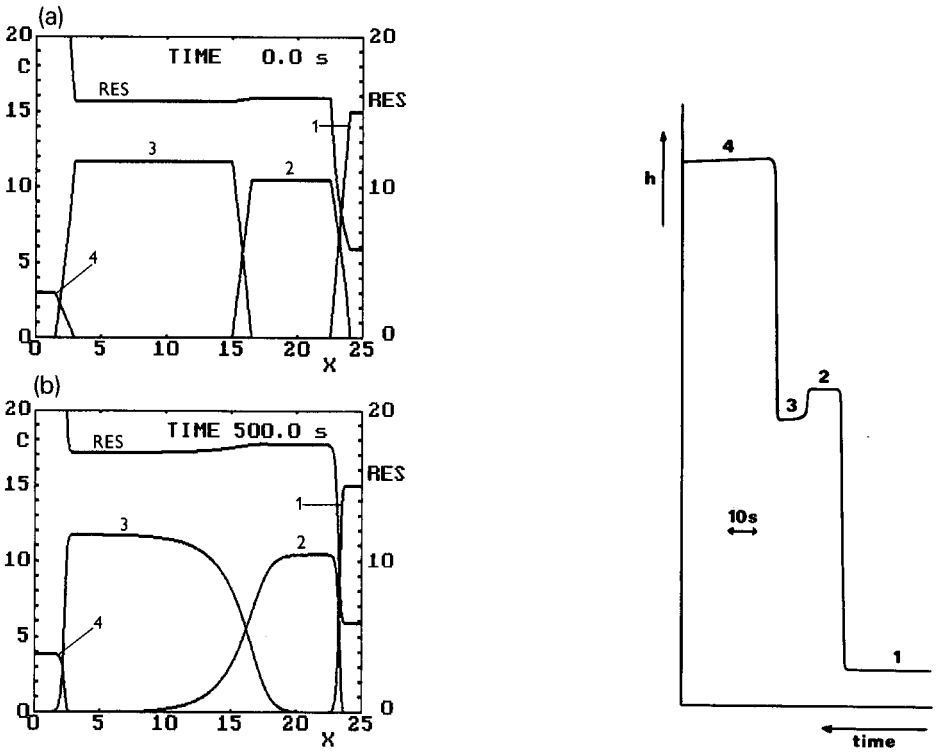

Fig. 6. Simulation of the isotachophoretic system with mobility inversion. 1 = Cl^-; 2 = benzoate; 3 = acetate; 4 = strong terminating anion with $u_4^- = 8 \cdot 10^{-9}$ m^2 V^{-1} S^{-1}. Leading electrolyte, 15 m*M* Cl^-–16 m*M* pyridine. Current density, 1064 A m^{-2}. *C* = concentration (m*M*), RES = specific resistance (Ω m); *x* = coordinate (mm).

Fig. 7. Isotachopherogram of the separation of acetic and benzoic acids with mobility inversion. 1 = Cl^-; 2 = benzoate; 3 = acetate; 4 = caproic acid. Leading electrolyte, 15 m*M* Cl^-–16 m*M* pyridine.

The stable mixed zones can also originate in isotachophoretic systems with intersection of the mobility curves, as already described by Gebauer and Boček [11]. One experiment from this work is simulated in Fig. 8 for a system consisting of potassium acetate + acetic acid with a mixed zone created between aniline and tetrabutylammonium (TBA). It can be seen that the model also depicts a conductivity bump on the boundary between the pure zone of tetrabutylammonium and the mixed zone of tetrabutylammonium + aniline.

Various "irregularities" and "bumps" are often present in conductivity records of isotachopherograms. Mosher *et al.* [22] showed that even the conductivity profile between two pure zones need not always be monotonous but could also exhibit such a bump. This bump can be especially distinct when one of the zones is the zone of hydrogen ions. Fig. 9 shows a simulated conductivity profile of the boundary between zones of aniline and hydrogen ions in the system consisting of 2 m*M* Bis–Tris as the leading cation and different concentrations of acetic acid as the counter anion. Aniline and hydrogen ions migrate in this system with inverted mobilities. Computed

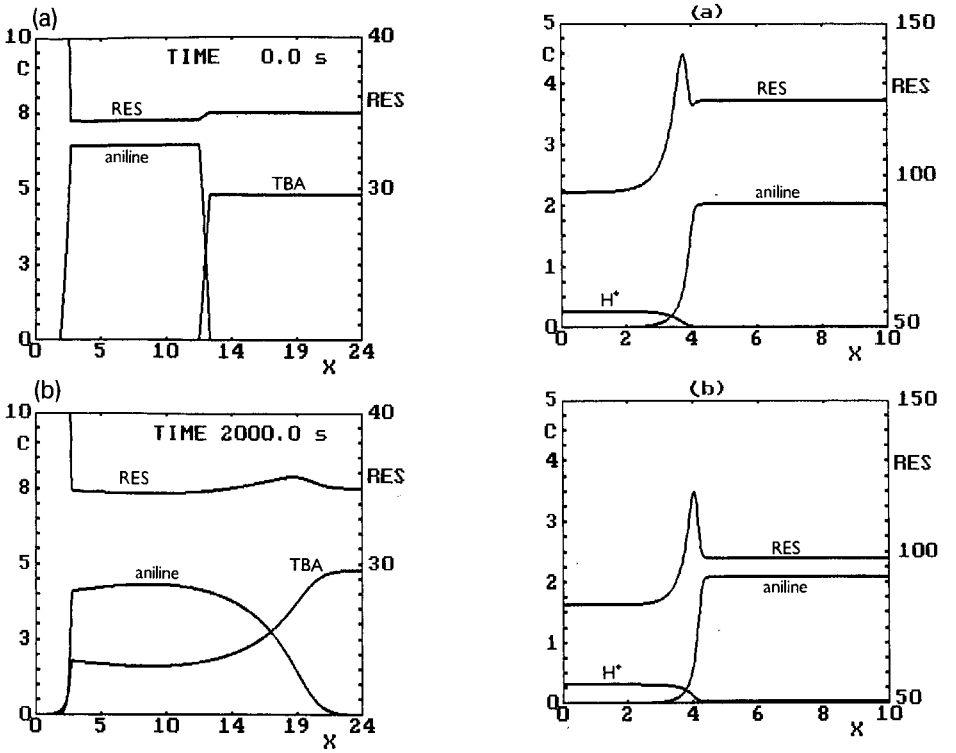

Fig. 8. Simulation of the isotachophoretic system with the stable mixed zone. TBA = tetrabutylammonium. Leading electrolyte, 10 mM potassium acetate–4 mM acetic acid. Current density, 238 A m^{-2}. C = concentration (mM); RES = specific resistance (Ω m); x = coordinate (mm).

Fig. 9. Simulation of the isotachophoretic boundary between aniline and H^+ zone. Leading electrolyte, 2 mM Bis–Tris plus (a) 1.74 mM acetic acid, pH 5.82 or (b) 3 mM acetic acid, pH 5.06. C = concentration (mM); RES = specific resistance (Ω m); x = coordinate (mm).

conductivity profiles for two different pH values of the leading electrolyte are shown. Fig. 10 depicts the results of experimental verification. The strange shape of the conductivity profile at pH 5.8 could cause an incorrect impression that a trace impurity is present in the boundary. Nevertheless, this is the natural shape of the boundary. Similar conductivity profiles of the boundaries between zones have already been published [11].

Models of electromigration that originate from basic physical and chemical laws provide a unifying basis for the description of all electrophoretic processes used in practice [17]. The described model can be employed to explain some phenomena in capillary zone electrophoresis described by Verheggen *et al.* [37]. It has been reported [38] that the method of introducing the sample into the capillary tube is important because only diffusional spreading of the peaks can develop during migration in a homogeneous electric field. It is advantageous if the conductivity of the initial sample area is less than that of the carrier electrolyte because the sample sharpens on the leading edge of the conductivity profile between the sample area and the remainder of

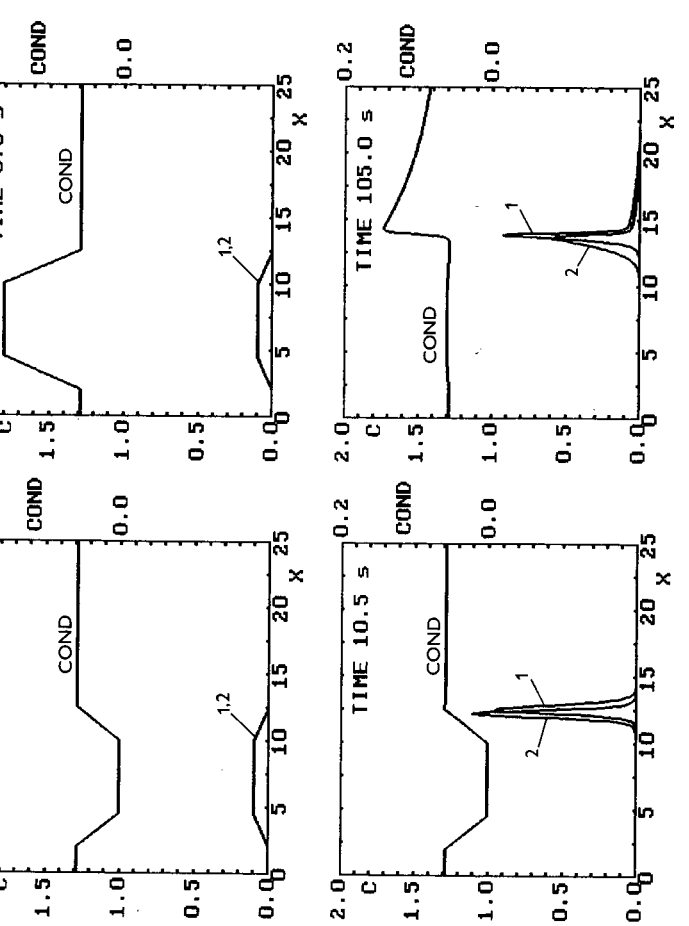

Fig. 10. Registration of the conductivity profile between aniline and H^+ zone. 1 = Aniline; 2 = H^+. Leading electrolyte, 2 m*M* Bis–Tris plus acetic acid: (a) pH 5.8; (b) pH 5.0. Diameter of capillary tube, 0.3 mm; current, 10 μA.

Fig. 11. Simulation of the sharpening and separation of the sample in CZE, with 10 m*M* carrier strong electrolyte, anionic mobility, $u = 30 \cdot 10^{-9}$ m^2 V^{-1} s^{-1}; cationic mobility, $u = 29.6 \cdot 10^{-9}$ m^2 V^{-1} s^{-1}. 1 = First sample, $u = 40 \cdot 10^{-9}$ m^2 V^{-1} s^{-1}; 2 = second sample, $u = 30 \cdot 10^{-9}$ m^2 V^{-1} s^{-1}. COND = specific conductivity (Ω^{-1} m^{-1}). Current density, 200 A m^{-2}. Concentration of Cl^- in sample area: (a) $c_{Cl^-} = 0$; (b) $c_{Cl^-} = 15$ m*M*.

the carrier electrolyte. This is shown in Fig. 11, where the sharpening and separation of two hypothetical anionic substances in a strong electrolyte system is simulated.

Nevertheless, it is possible to use another means of sharpening the sample, namely by addition of an excess of some inactive, fastest or slowest substance. By an inactive substance is meant a substance that does not give a detector response. Fig. 11 shows the separation of the two substances if 15 m*M* chloride is added to the sample. It can be seen that sharpening could also be efficient in this instance. This sharpening effect may explain the very high plate numbers found for some early eluting peaks in Fig. 9 in ref. 37.

REFERENCES

1 F. Kohlrausch, *Ann. Phys. Chem.*, 62 (1897) 209.
2 J. L. Beckers, *Thesis*, Technical University of Eindhoven, Eindhoven, 1973.
3 F. M. Everaerts, J. L. Beckers and Th. P. E. M. Verheggen, *Isotachophoresis—Theory, Instrumentation and Application*, Elsevier, Amsterdam, Oxford, New York, 1976.
4 F. E. P. Mikkers, *Thesis*, Technical University of Eindhoven, Eindhoven, 1980.
5 F. E. P. Mikkers, F. M. Everaerts and J. A. F. Peek, *J. Chromatogr.*, 168 (1979) 293.
6 F. E. P. Mikkers, F. M. Everaerts and J. A. F. Peek, *J. Chromatogr.*, 168 (1979) 317.
7 F. E. P. Mikkers, F. M. Everaerts and Th. P. E. M. Verheggen, *J. Chromatogr.*, 169 (1979) 1.
8 P. Boček, P. Gebauer and M. Deml, *J. Chromatogr.*, 217 (1981) 209.
9 P. Boček, P. Gebauer and M. Deml, *J. Chromatogr.*, 219 (1981) 21.
10 P. Gebauer and P. Boček, *J. Chromatogr.*, 242 (1982) 245.
11 P. Gebauer and P. Boček, *J. Chromatogr.*, 267 (1983) 49.
12 L. Křivánková, F. Foret, P. Gebauer and P. Boček, *J. Chromatogr.*, 390 (1987) 3.
13 T. Hirokawa, K. Nakahara and Y. Kiso, *J. Chromatogr.*, 463 (1989) 51.
14 T. Hirokawa, K. Nakahara and Y. Kiso, *J. Chromatogr.*, 470 (1989) 21.
15 T. Hirokawa, M. Nishino, N. Aoki, Y. Kiso, Y. Sawamoto, T. Yagi and J. Akiyama, *J. Chromatogr.*, 271 (1983) D1.
16 T. Hirokawa, M. Nishino and Y. Kiso, *J. Chromatogr.*, 252 (1982) 49.
17 M. Bier, O. A. Palusinski, R. A. Mosher and D. A. Saville, *Science*, 219 (1983) 1281.
18 W. Thormann and R. A. Mosher, *Trans. Soc. Computer Simulation*, 1 (1984) 83.
19 W. Thormann, R. A. Mosher and M. Bier, *Electrophoresis*, 6 (1985) 78.
20 W. Thormann and R. A. Mosher, *Electrophoresis*, 6 (1985) 413.
21 R. A. Mosher and W. Thormann, *Electrophoresis*, 6 (1985) 477.
22 R. A. Mosher, W. Thormann and M. Bier, *J. Chromatogr.*, 320 (1985) 23.
23 D. A. Saville and O. A. Palusinski, *AIChE J.*, 32 (1986) 207.
24 O. A. Palusinski, A. Graham, R. A. Mosher, M. Bier and D. A. Saville, *AIChE J.*, 32 (1986) 215.
25 W. Thormann, R. A. Mosher and M. Bier, *J. Chromatogr.*, 351 (1986) 17.
26 R. A. Mosher and W. Thormann, *Electrophoresis*, 7 (1986) 395.
27 Y. Su, O. A. Palusinski and P. C. Fife, *J. Chromatogr.*, 405 (1987) 77.
28 R. Kuhn, H. Wagner, R. A. Mosher and W. Thormann, *Electrophoresis*, 8 (1987) 503.
29 R. A. Mosher, D. Dewey, W. Thormann, D. A. Saville and M. Bier, *Anal. Chem.*, 61 (1989) 362.
30 L. Juška, *Thesis*, Charles University, Prague, 1973.
31 B. Gaš, *Diploma Thesis*, Charles University, Prague, 1975.
32 V. Fidler, J. Vacík and Z. Fidler, *J. Chromatogr.*, 320 (1985) 167.
33 Z. Fidler, V. Fidler and J. Vacík, *J. Chromatogr.*, 320 (1985) 175.
34 F. B. Dismukes and R. A. Alberty, *J. Am. Chem. Soc.*, 76 (1954) 191.
35 R. A. Alberty and J. C. Nichol, *J. Am. Chem. Soc.*, 70 (1948) 2297.
36 A. Ralston, *A First Course in Numerical Methods*, McGraw-Hill, New York, 1965.
37 Th. P. E. M. Verheggen, A. C. Schoots and F. M. Everaerts, *J. Chromatogr.*, 503 (1990) 245.
38 F. E. P. Mikkers, F. M. Everaerts and Th. P. E. M. Verheggen, *J. Chromatogr.*, 169 (1979) 11.

Journal of Chromatography, 545 (1991) 239–248
Elsevier Science Publishers B.V., Amsterdam

CHROM. 23 163

Selection of the background electrolyte composition with respect to electromigration dispersion and detection of weakly absorbing substances in capillary zone electrophoresis

VLADIMÍR ŠUSTÁČEK, FRANTIŠEK FORET and PETR BOČEK*
Institute of Analytical Chemistry, Czechoslovak Academy of Sciences, Veveří 97, CS-61142 Brno (Czechoslovakia)

ABSTRACT

A characteristic feature of the migration of sample ions in zone electrophoresis is the formation of either fronting or tailing zones. This so-called electromigration dispersion can generally be suppressed by keeping the sample concentration more than two orders of magnitude below the concentration of the background electrolyte (BGE). In capillary zone electrophoresis the low sample concentration decreases the reliability of on-column UV absorbance detection, especially when substances having low molar absorption coefficients are to be detected. By the proper selection of the electrophoretic mobility of the background electrolyte co-ion, both electromigration dispersion and detection can be optimized. The migration behaviour of phenyllactic acid and four phenyl derivatives of acetic acid was studied in buffered electrolytes with different mobilities and concentrations of the BGE co-ions. For a better understanding of zone broadening, a simplified model of the electromigration together with some model calculations is presented.

INTRODUCTION

On-column UV absorbance detection is the most universal detection method used in capillary zone electrophoresis (CZE). As the optical path length, given by the inside diameter of the separation capillary used, is short (typically 50 μm), it is desirable to keep the concentration of separated ions as high as possible to obtain a good detector response. This requirement concerns especially substances having low molar absorption coefficients. However, an increase in the concentration of the sample ions results in an increase in the electromigration dispersion [1] and, consequently, to a decrease in the separation efficiency.

The electromigration dispersion is related to changes in the local electric field strength in a migrating zone with respect to that in the background electrolyte (BGE). It can be characterized by the electric field strength, which is variable with time and length inside an individual zone. The result is obvious: each part of an individual zone moves with its own velocity and, moreover, the situation changes with time and length. The resulting dispersion may in some instances be so strong that it plays a dominant role among other dispersive factors (for their characterization, see ref. 2).

0021-9673/91/$03.50

In current practice, the electromigration dispersion is frequently suppressed by working under conditions such that the concentration of a solute is lower than that of the BGE by more than two orders of magnitude [1]. Obviously, there are two ways to fulfil such a condition: to inject a small amount of a dilute sample or to use a high-concentration background electrolyte.

Of course, both of the above-mentioned procedures have their limitations. When weakly absorbing solutes are detected by using a UV absorption detector, the sample concentration cannot be reduced below the sensitivity of the detector used. A substantial increase in the concentration of BGE minimizes the electromigration dispersion but simultaneously causes a considerable increase in the BGE conductivity. Then the voltage driving the separation must be decreased to avoid column overheating, which results in a longer analysis time.

The importance of the composition of the BGE for improving the zone sharpness has been already noted by Hjertén *et al.* [3,4]. In this paper, a study of the effect of the difference between the effective mobilities of a solute and of the BGE co-ion on the electromigration dispersion is reported. It is shown theoretically and has been verified experimentally that the electromigration dispersion can be reduced substantially by the proper selection of the composition of the BGE regarding the mobilities of the solute and of the BGE co-ion.

THEORETICAL

The problem of unsteady-state migration (electromigration dispersion) was first solved by Weber [5] for strong electrolytes, and this approach has recently been extended to cover also the migration of a sample pulse (for a review, see ref. 6). Another solution to this problem has been published by Virtanen [7] and Mikkers *et al.* [1].

The core of the calculation presented here is based on Weber's solution, which is modified for weak uni–univalent electrolytes. Absolute values of mobilities are used in all calculations (*i.e.*, $u_i > 0$ for both cations and anions) and both ionic and effective mobilities are assumed to be constants (*i.e.*, both temperature and pH are assumed to be constant at any time and capillary length). The capillary is filled with the background electrolyte AR, the specific conductivity of which is given by the relationship

$$\kappa_0 = Fc_{A,0}(u_A + u_R) = F\bar{c}_{A,0}\bar{u}_A \cdot \frac{u_A + u_R}{u_A} \tag{1}$$

For the specific conductivity in a migrating sample zone, it analogously holds that

$$\kappa_S = F\left(\bar{c}_A\bar{u}_A \cdot \frac{u_A + u_R}{u_A} + \bar{c}_S\bar{u}_S \cdot \frac{u_S + u_R}{u_S}\right) \tag{2}$$

The adjustment of the concentrations in migrating zones may be described by the Kohlrausch regulating function in the forms [8–10]

$$\omega_0 = \bar{c}_{A,0} \cdot \frac{u_A + u_R}{u_A} \tag{3}$$

$$\omega_S = \bar{c}_A \cdot \frac{u_A + u_R}{u_A} + \bar{c}_S \cdot \frac{u_S + u_R}{u_S} \tag{4}$$

The well known condition $\omega_S = \omega_0$ gives the equation

$$\bar{c}_{A,0} \cdot \frac{u_A + u_R}{u_A} = \bar{c}_A \cdot \frac{u_A + u_R}{u_A} + \bar{c}_S \cdot \frac{u_S + u_R}{u_S} \tag{5}$$

The solution of the system of the partial differential transport equations for components A and S is known in the form [5,8]

$$\omega_S/\kappa_S = \sqrt{a/b} \tag{6}$$

where

$$a = \omega_0 l/(F\bar{u}_A\bar{u}_S) \tag{7}$$

and

$$b = jt \tag{8}$$

By combining eqns. 5 and 6, explicit equations for the sample concentration in a migrating sample zone is obtained:

$$\bar{c}_S(l,t) = \frac{\bar{c}_{A,0}}{\bar{u}_S - \bar{u}_A} \cdot \frac{u_S}{u_S + u_R} \cdot \frac{u_A + u_R}{u_A} \left(\frac{1}{F}\sqrt{\frac{b}{a}} - \bar{u}_A \right) \tag{9}$$

Similarly, for the concentration of the BGE co-ion in the sample zone it holds that

$$\bar{c}_A(l,t) = \frac{\bar{c}_{A,0}}{\bar{u}_S - \bar{u}_A} \left(\bar{u}_S - \frac{1}{F}\sqrt{\frac{b}{a}} \right) \tag{10}$$

Eqn. 9 covers both the cases $\bar{u}_S > \bar{u}_A$ and $\bar{u}_S < \bar{u}_A$; characteristic profiles for both cases are depicted in Fig. 1. Obviously, for $\bar{u}_S > \bar{u}_A$ the profile of $\bar{c}_S$ in the capillary is concave and the peak detected is convex, and for $\bar{u}_S < \bar{u}_A$ the opposite apply. In practice, of course, the use of a fixed detector is the most important means of detection and, therefore, the profile of $\bar{c}_S(t)$ at a fixed point $l = L$ will be further described.

Eqn. 9 describes the profile generated by the electromigration between two neighbouring fronts of electrolytes SR and AR [5,8], where the maximum of $\bar{c}_S$ corresponds to the adjusted Kohlrausch value given by eqn. 5 for $\bar{c}_A = 0$:

$$\bar{c}_{S,0} = \bar{c}_{A,0} \cdot \frac{u_S}{u_S + u_R} \cdot \frac{u_A + u_R}{u_A} \tag{11}$$

In practice, however, the maximum $\bar{c}_S$ value seldom reaches the concentration $\bar{c}_{S,0}$ and

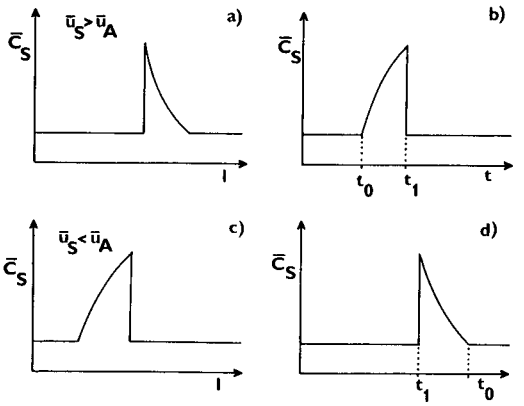

Fig. 1. Scheme of the shapes of the concentration profiles due to electromigration dispersion (see eqn. 9). (a),(b) $\bar{u}_S > \bar{u}_A$; (c),(d) $\bar{u}_S < \bar{u}_A$; (a),(c) $\bar{c}_S = f(l)$, inside the capillary at a given time; (b),(d) $\bar{c}_S = f(t)$, peaks recorded by a fixed-point detector.

is given by the amount injected. To determine the actual maximum $\bar{c}_S$ value in a detected peak, one may integrate the $\bar{c}_S(t)$ profile and compare it with the amount of sample injected.

The calculation of the sample zone profile is started at the time

$$t_0 = L\kappa_0/(\bar{u}_S j) \tag{12}$$

which represents the migration time of a single ion S in the background electrolyte (see scheme in Fig. 1). The profile is then numerically integrated to obtain the amount of substance S in the zone:

$$n_S(\text{calc.}) = \phi \int_{t_0}^{t_1} \bar{c}_S(t) v_S(t) \mathrm{d}t \tag{13}$$

and the calculation is stopped at time t_1 when $n_S(\text{calc.}) \geqslant n_S(\text{injected})$. The velocity of the migration of a concentration $\bar{c}_S(t)$ at the detection time t is given by the expression

$$v_S(t) = \bar{u}_S j/\kappa(t) \tag{14}$$

where $\kappa(t)$ is the specific conductivity in the detection point at the time t given by eqn. 2.

By multiplication of the calculated concentration profile $\bar{c}_S(t)$ with absorption coefficient of species S, one can simulate the record of electrophoretic analysis with UV detection.

To obtain a simple explicit relationship between the peak width and the effective mobilities of A and S, another approximation should be introduced. Let us assume that the solute concentration in the peak maximum, $\bar{c}_{S,max}$ has for a constant amount of sample injected a constant value proportional to $\bar{c}_{S,0}$ (given by eqn. 11):

$$\bar{c}_{S,max} = B\bar{c}_{S,0} \tag{15}$$

where $B < 1$ is a constant. Then the time t_1 when the peak maximum passes through the detector can be expressed as

$$t_1 = t_0 \cdot \frac{[B(\bar{u}_S - \bar{u}_A) + \bar{u}_A]^2}{\bar{u}_A^2} \tag{16}$$

As in capillary electrophoresis the peak width in a time-based record is a function of analysis time (less mobile zone passes through the detection cell for a longer time) [9], the zone widths related to the time in which the peak maximum was detected should be compared instead of the zone widths only. From eqn. 16, the relative sample zone width at the baseline is given by

$$\frac{t_1 - t_0}{t_0} = 2B \cdot \frac{\bar{u}_S - \bar{u}_A}{\bar{u}_A} + B^2\left(\frac{\bar{u}_S - \bar{u}_A}{\bar{u}_A}\right)^2 \tag{17}$$

It is obvious that the relative zone width due to electromigration dispersion is proportional to the difference $\bar{u}_S - \bar{u}_A$. In practice, the actual peak width measured also includes the contributions due to a finite sample pulse at the injection point, due to diffusion, etc., which should be added to the right-hand side of eqn. 17.

EXPERIMENTAL

Apparatus

Experiments were performed in laboratory-made equipment described in detail previously [11]. The separation column was a 46 cm × 75 μm I.D. fused-silica capillary (SGE, Austin, TX, U.S.A.); the inner surface of the capillary was coated with linear polyacrylamide [12] to suppress electroosmotic flow during analysis. Sample introduction was performed by hydrodynamic flow from the sample vial, raised 5 cm above the liquid level in the electrode vessels. The capillary was rinsed with the background electrolyte after each run.

On-column UV detection at 254 nm was used, employing a laboratory-made single–beam detector with an optically stabilized low–pressure mercury lamp. The noise of the detector was *ca.* $3 \cdot 10^{-4}$ absorbance. A fibre-optic detection cell located 41 cm from the injection end of the capillary was described previously [13].

Absorption coefficients at 254 nm were measured by means of a Varian Series 634 spectrophotometer with the use of 1-cm cuvettes and *ca.* $2 \cdot 10^{-4}$ *M* solutions of each compound. All calculations were made on a PMD-85-2 microcomputer (Tesla, Bratislava, Czechoslovakia).

Chemicals

Glutamic acid (Lachema, Brno, Czechoslovakia), 2-hydroxyisobutyric acid (Fluka, Buchs, Switzerland), trichloroacetic acid (Merck, Darmstadt, Germany) and 4-aminobutyric acid (Serva, Heidelberg, Germany), all of analytical-reagent grade, were used for the preparation of the background electrolytes. Phenyl-substituted acids (Fluka), purum grade, served as model sample components. The pH of the sample solution was adjusted to 4.0 with 4-aminobutyric acid.

RESULTS AND DISCUSSION

Phenyllactic acid and four phenyl derivatives of acetic acid were used for the experimental evaluation of the role of the electromigration dispersion on separation and detection in CZE. The electrophoretic mobilities of the sample components are listed in Table I together with their absorption coefficients and concentrations in the sample injected into the capillary. The physico-chemical constants of the substances used for the preparation of the background electrolytes are summarized in Table II.

Based on preliminary experiments, pH 4.0 was selected as the optimum for the separation; at this pH, all sample components are well separated. As no reliable data on mobilities and pK values were available, the effective mobilities were determined experimentally from migration times of single compounds injected, using BGE D (see Table III) and a voltage of 10 kV. No electroosmotic flow was observed under these conditions.

As the molar absorption coefficients ε of all phenyl-substituted acids studied lie in the region of 220–630 l/mol · cm at 254 nm, the absorbance of the zones in the separation capillary was too low and their detection was possible only when high concentrations of solutes in their zones were ensured.

The role of the composition of the BGE on the separation and detection can be explained with the aid of the experimental separation records shown in Fig. 2. Fig. 2a shows the electrophoretic analysis of the model mixture in the background electrolyte containing trichloroacetate as a co-ion, the effective mobility of which is several times higher than those of the sample components (see Tables I and II). Obviously, the analysis is poor, the peaks being very wide and not resolved from one another.

Fig. 2b shows the same electrophoretic analysis in the electrolyte having the same components but ten times higher concentrations. In this instance the peaks of sample substances were still deformed, but their baseline resolution was achieved. As this BGE has a high specific conductivity, the separation voltage had to be decreased to prevent overheating. Excessive heating due to a high current density was observed especially in the low-conductivity sample pulse at the injection end of the capillary. A large temperature rise in this pulse (which took 1.4 cm of the capillary in this experiment) may cause peak broadening during the preconcentration at the sample pulse/BGE

TABLE I

PHENYL-SUBSTITUTED ACIDS USED FOR THE PREPARATION OF THE MODEL SAMPLE

Effective mobilities were determined experimentally from migration data; the ionic mobility of phenylacetic acid was taken from ref. 14 as a mean of reported values; the other ionic mobilities were calculated according to related compounds with the help of ref. 14; ε = absorption coefficient; c = concentration of the substance in the sample.

Substance	Abbreviation	Effective mobility (10^{-5} cm^2/V s)	Ionic mobility (10^{-5} cm^2/V s)	ε (l/mol · cm)	c (mmol/l)
3-Phenyllactic acid	PL	17.4	*ca.* 25	230	4
Phenylacetic acid	PA	10.4	*ca.* 30	220	4
2-Hydroxyphenylacetic acid	2-HPA	8.9	*ca.* 30	630	2
3-Hydroxyphenylacetic acid	3-HPA	9.9	*ca.* 30	480	2
4-Hydroxyphenylacetic acid	4-HPA	8.2	*ca.* 30	350	2

TABLE II

SUBSTANCES USED FOR THE PREPARATION OF THE BACKGROUND ELECTROLYTES

Ionic mobilities and pK_a values were taken from ref. 14; effective mobilities at pH = 4.0 were calculated by multiplying ionic mobilities by the respective degree of ionization.

Substance	pK_a	Ionic mobility (10^{-5} cm^2/V s)	Effective mobility (10^{-5} cm^2/V s)
Trichloroacetic acid	0.64	36.2	36.2
2-Hydroxyisobutyric acid	3.97	33.5	17.3
Glutamic acid	4.32	27.0	8.7
4-Aminobutyric acid (counter ion)	4.0	*ca.* 34	*ca.* 17

boundary and, consequently, deterioration of the analysis. Also, an analysis time several times longer than in the previous instance is a clear disadvantage of such an approach when using capillaries with I.D. greater than *ca.* 10 μm.

Analyses in electrolytes with a lower effective mobility of the BGE co-ion are shown in Fig. 2c and d. In both instances the resolution of zones was sufficient and the analysis time was the same as in that shown in Fig. 2a. The sharpest peaks with the maximum heights are those of components having an effective mobility close to that of the background electrolyte. As the effective mobilities of most sample components are not too different from that of glutamate, the use of electrolyte D is optimum for the separation of the mixture of phenyl-substituted acids.

The use of a low-mobility glutamate co-ion also brings another advantage. The

TABLE III

EXPERIMENTAL CONDITIONS IN CZE ANALYSES OF THE MODEL MIXTURE OF PHENYL-SUBSTITUTED ACIDS

These experimental conditions were applied in CZE analyses shown in Fig. 2a–d and were then used as input data for the simulations, the results of which are shown in Fig. 3a–d.

Fig.	BGE	Sample volume (nl)	Current (μA)	Voltage (kV)
2a, 3a	A	30	16	16
2b, 3b	B	60	40	6
2c, 3c	C	30	15	16
2d, 3d	D	30	12	16

Composition of background electrolytes[a].

BGE	Co-ion constituent	Concentration (mol/l)
A	Trichloroacetic acid	0.01
B	Trichloroacetic acid	0.1
C	2-Hydroxyisobutyric acid	0.02
D	Glutamic acid	0.03

[a] 4-Aminobutyric acid was added to pH 4.0 in all instances.

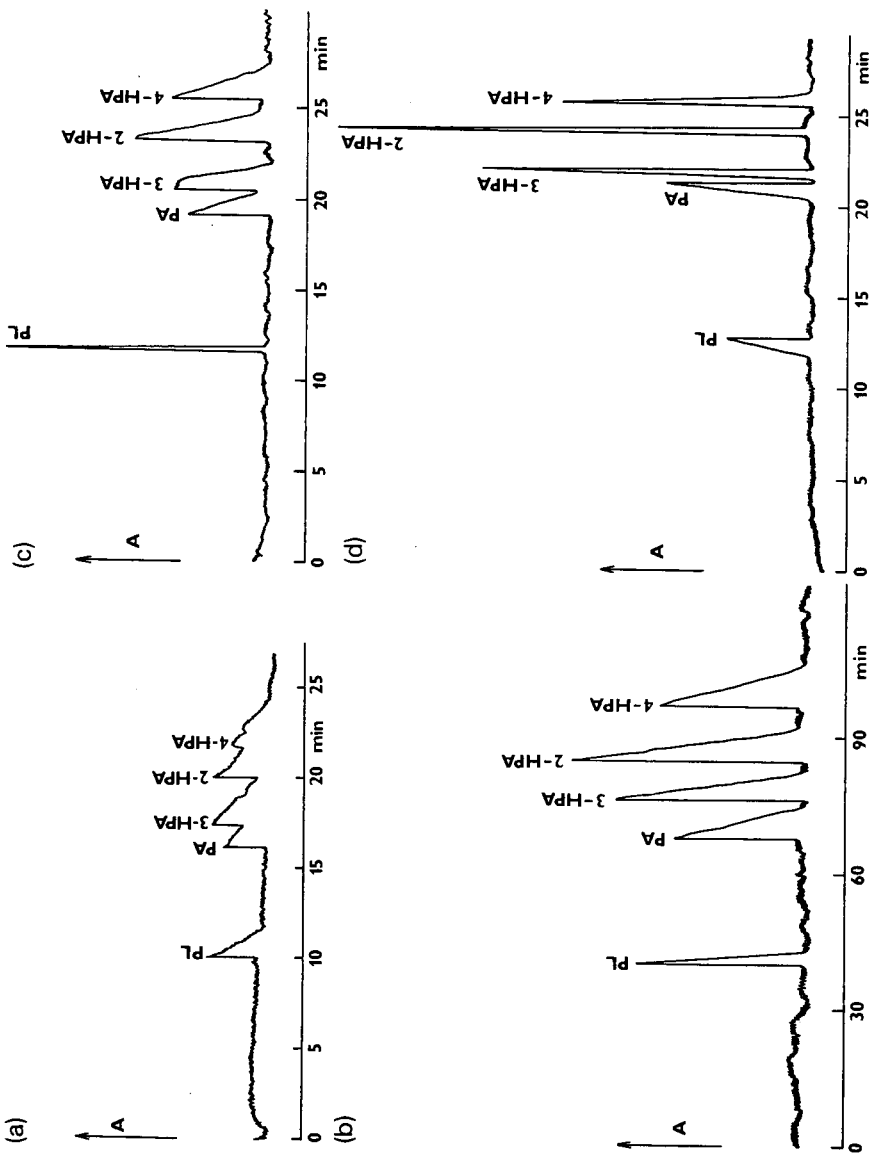

Fig. 2. CZE separation of the mixture of phenyl-substituted acids in electrolytes with different mobilities and concentrations of the BGE co-ions. For abbreviations of solutes, see Table I; for the composition of the background electrolytes and other experimental conditions, see Table III.

BGE can contain a higher concentration of such a co-ion than that of a co-ion with a higher mobility and the specific conductivity of the BGE does not change. A higher co-ion concentration results in decreased electromigration dispersion without increasing thermal effects. In our experiments, the concentrations of electrolytes C and D were higher than that of BGE A to ensure that the specific conductivities of these three electrolytes were approximately the same (*i.e.*, thermal effects in CZE analyses were not too different and the mobilities can be considered to be constant).

Fig. 3 shows simulated electrophoregrams of the analyses shown in Fig. 2, calculated according to the procedure described under Theoretical. If the experimental and simulated records are compared, it is seen that they coincide very well in spite of the fact that many simplifications have been made in the theory presented. Large deviations occur only in the calculated migration times. The differences are caused by neglect of the contribution of H^+ ions to the specific conductivity (which was more than 5% of κ_0 of electrolytes A, C and D), and, especially, by neglecting the increase in

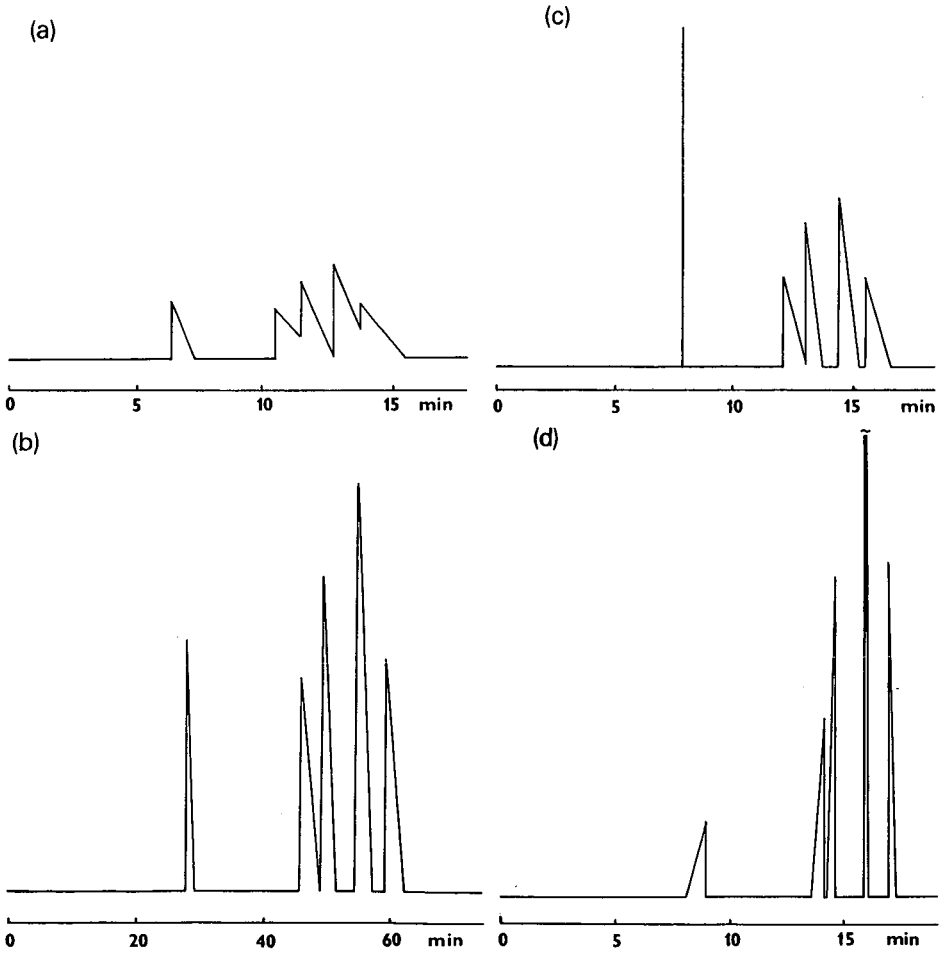

Fig. 3. Simulated records of CZE analyses shown in Fig. 2.

temperature inside the capillary due to Joule heating. It is known that ionic mobilities increase by about 2% if the temperature increases by 1°C. If mobilities of all ions (sample ion, co-ion, counter ion) increase to the same extent, the character of the analysis record does not change and only the migration times vary.

Another large difference between the calculated and experimental records concerns peaks of solutes having effective mobilities almost the same as that of the BGE co-ion. In this instance the other contributions to the peak width, such as a finite length of a sample pulse at the injection point and diffusion, are comparable to the electromigration dispersion and cause additional peak broadening.

It is clear from this study that the selection of the composition of the BGE has a crucial impact on the separation and detection sensitivity in all instances where weakly absorbing substances are to be detected. The simple theoretical model presented here can help one to find optimum separation conditions for analysing such substances.

SYMBOLS

t time
l length coordinate
L length of the separation capillary (from sampling point to detector)
ϕ internal cross-sectional area of the capillary
j current density
F Faraday constant
u_i ionic mobility of species i
$\bar{u}_i$ effective mobility of species i
c_i ionic concentration
$\bar{c}_i$ total (analytical) concentration
$\bar{c}_{A,0}$ analytical concentration of co-ion A in the BGE

Subscripts
S sample component
A BGE co-ion constituent
R BGE counter ion

REFERENCES

1 F. E. P. Mikkers, F. M. Everaerts and Th. P. E. M. Verheggen, *J. Chromatogr.*, 169 (1979) 1.
2 F. Foret, M. Deml and P. Boček, *J. Chromatogr.*, 452 (1988) 601.
3 S. Hjertén, *Top. Bioelectrochem. Bioenerg.*, 2 (1978) 89.
4 S. Hjertén, K. Elenbring, F. Kilár, J. Liao, A. J. C. Chen, C. J. Siebert and M. Zhu, *J. Chromatogr.*, 403 (1987) 47.
5 H. Weber, *Die Partiellen Differential Gleichungen der Mathematischen Physik*, Vol. I, Friedrich Vieweg u. Sohn, Braunschweig, 1910.
6 F. Foret and P. Boček, in A. Chrambach (Editor), *Advances in Electrophoresis*, Vol. 3, VCH, Weinheim, 1989, pp. 271–347.
7 R. Virtanen, *Acta Polytech. Scand.*, 123 (1974) 1.
8 P. Gebauer, M. Deml, J. Pospíchal and P. Boček, *Electrophoresis*, 11 (1990) 724.
9 W. Thormann, R. A. Mosher and M. Bier, *Electrophoresis*, 6 (1985) 78.
10 L. M. Hjelmeland and A. Chrambach, *Electrophoresis*, 3 (1982) 9.
11 S. Fanalli, L. Ossicini, F. Foret and P. Boček, *J. Microcolumn Sep.*, 1 (1989) 190.
12 S. Hjertén, *J. Chromatogr.*, 347 (1985) 191.
13 F. Foret, M. Deml, V. Kahle and P. Boček, *Electrophoresis*, 7 (1986) 430.
14 J. Pospíchal, P. Gebauer and P. Boček, *Chem. Rev.*, 89 (1989) 419.

Journal of Chromatography, 545 (1991) 249–266
Elsevier Science Publishers B.V., Amsterdam

CHROM. 23 144

Optimization of isotachophoretic analysis: use of the charge-based transient-state model

VLADISLAV DOLNÍK*, MIRKO DEML, PETR GEBAUER and PETR BOČEK
Institute of Analytical Chemistry, Czechoslovak Academy of Sciences, Veveří 97, 611 42 Brno (Czechoslovakia)

ABSTRACT

A charged-based transient-state model of the isotachophoretic separation of a multi-component mixture is described. The model enables both the column hold-up required for the full separation of a multi-component sample and the analysis time to be calculated. The optimum pH of the leading electrolyte can be found by plotting the analysis time *vs.* the pH of leading electrolyte. The method was applied to the separation of a three-component mixture (acetate, lactate, butyrate) and the theoretical values of the required column hold-up were compared with those obtained experimentally. Good agreement between the theoretical and experimental values was found.

INTRODUCTION

In analytical isotachophoresis, there are several parameters (*e.g.*, analysis time, cost of analysis, sample volume) which are optimized during the elaboration of an analytical procedure. Because of its practical importance, the analysis time is the parameter that is optimized most frequently.

To achieve the complete separation of all sample components during isotachophoretic analysis, the separation capillary has to provide a sufficient separation capacity. This leads to the necessity to express the grade of the separation achieved quantitatively; until now, the separation of binary mixed zones was treated most frequently.

Capillary length [1], separation time [2–4] and electric charge passed through the column [5,6] have been used as quantitative parameters expressing the level of separation achieved. As far as a multi-component mixture is concerned, its separation should be solved as the separation of the binary mixture containing the pair of components that are the most difficult to separate [1,2]. Recently, Hirokawa *et al.* [7] described a transient-state model for a three-component system.

The optimum separation conditions, especially the pH of the leading electrolyte, have been determined typically by plotting the effective mobilities of the separated compounds in their pure isotachophoretic zones *vs.* the pH of the leading electrolyte. The values of the effective mobilities were obtained experimentally [8] or by calculation [9–11]. At the optimum pH of the leading electrolyte, the minimum mobility difference

0021-9673/91/$03.50

between two adjacent zones for a given multi-component mixture reaches the maximum value in the tested pH interval.

This paper offers a possible solution of the optimization problem of the isotachophoretic separation of a multi-component sample. It is based on mathematical modelling of the separation process and the optimization is performed by using the pH of the leading electrolyte, pH_L as the variable parameter. We assume a constant detection sensitivity (which determines the given sample amount which is necessary to obtain sufficient quantification of all minor sample components). For each pH_L, the calculation provides the following output parameters: the column hold-up necessary for the separation of the sample, the effective mobility of the terminator (which should be as mobile as possible), the conductivity of its zone and the resulting maximum electric driving current (with constant cooling properties of the capillary) and the analysis time. The solution is then the pH_L at which the minimum analysis time is achieved.

THEORETICAL

Optimization of isotachophoretic analysis

The goal of the optimization of an isotachophoretic analysis can be stated as the establishment of conditions under which the necessary sample amount is separated (analysed) within a minimum time. The necessary sample amount is given by the requirement that all minor sample components must be determined with sufficient precision and accuracy.

Such time-based optimization is necessary especially if a routine analytical method is worked out, *i.e.*, if a large number of samples have to be analysed over a long time period. There are two ways to perform such an optimization: by experiment or by calculation. The former is very time consuming, which is why the latter is of special interest. The computational optimization must be based on knowledge of the sample as detailed as possible: one must know all ionogenic components of the sample, their ionic mobilities and pK_a values and the ranges of their possible concentrations. The determination of the necessary sample amount is then based on the minimum amount of the minor components that is necessary for good quantification. The estimated sample amount and the maximum expected concentration of the sample components serve as inputs for the mathematical modelling of the isotachophoretic separation.

The minimum analysis time of an n-component sample can be expressed as

$$t_{\min} = \frac{Q_{L,req} + \sum_{i=1}^{n} Q_i}{I_{max}} \tag{1}$$

where I_{max} is the maximum electric driving current that can be used without danger of overheating, $\sum_{i=1}^{n} Q_i$ is the sum of zone passage charges of the individual sample components and $Q_{L,req}$ is the column hold-up required for the complete separation of the given sample. Note that both the sample amount and the separation capabilities of the system are expressed in terms of electric charge (the zone passage charge is the

electric charge required for the passage of an isotachophoretic zone through, *e.g.*, the detection cell; the column hold-up is the electric charge which transfers the rear boundary of the zone of leading electrolyte from the starting point to the detection cell [5,12]); this proved to be useful by providing a more general description than is possible with other quantities. Eqn. 1 may be rewritten in the form

$$t_{\min} = \frac{Q_{\mathrm{L,req}} + \sum_{i=1}^{n} Q_i}{\sqrt{\kappa_{\mathrm{T}}}} \cdot \text{const.} \qquad (2)$$

where κ_{T} is the conductivity of the terminating zone (of the zone with the lowest conductivity).

The optimization procedure may then be as follows. We assume we have an isotachophoretic column the hold-up of which can be varied in order to keep it always at the minimum necessary value, $Q_{\mathrm{L,req}}$. If now, *e.g.*, the pH of the leading electrolyte, $\mathrm{pH_L}$, is taken as the parameter, the values of all quantities in eqn. 2 may be calculated; by plotting the resulting $t_{\min}$ *vs.* $\mathrm{pH_L}$, the optimum (minimum) value of $t_{\min}$ can be found.

Separation scheme for a multi-component mixture

When calculating the value of $t_{\min}$ from eqn. 2, the most difficult step is to obtain the necessary value of $Q_{\mathrm{L,req}}$, especially for multi-component samples. In order to be able to calculate $Q_{\mathrm{L,req}}$, it is useful to make some simplifications in the description of the system (which apply also to eqns. 1 and 2): (i) the sample is assumed to have the composition of an adjusted isotachophoretic mixed zone; (ii) the separation is assumed to proceed at constant temperature; (iii) we neglect diffusion, interactions between ions and other disturbing effects such as electroosmosis.

For the complete description of the separation process of an n-component sample, all partial Q_{L} values must be calculated which correspond to the extinction of all various mixed zones containing from 2 to n components. The symbol $Q_{\mathrm{L},i\ldots j}$, *e.g.*, corresponds to the column hold-up necessary for the extinction of the transient mixed zone containing $j-i+1$ components, *viz.*, i, $i+1$, ..., $j-1$, j.

Fig. 1a, b and c show the schemes of the isotachophoretic separation of samples containing two, three and four components, respectively. The schemes are drawn as plots of the electric charge that passed through the column, Q, *vs.* the column hold-up, Q_{L}. The position of a point on the diagram may be understood as follows: its x-coordinate indicates the actual position in the isotachophoretic column (expressed in the term of Q_{L}) and its y-coordinate refers to a given point of the separation process (expressed in terms of Q). The scheme shows the composition of the stack of isotachophoretic (steady-state and transient) zones in each location in the column after electric charge Q has passed through the column. The lines in the scheme represent the boundaries between neighbouring zones, *i.e.*, for given Q and Q_{L} we obtain information on the location and size of the individual zones (including information on which zone is just in the detection cell). The slopes of these lines are equivalent to the reciprocal relative velocities of the respective boundaries (see eqns. 18 and 19 in the Appendix). The line parallel to the x-axis at a distance Q crosses the network

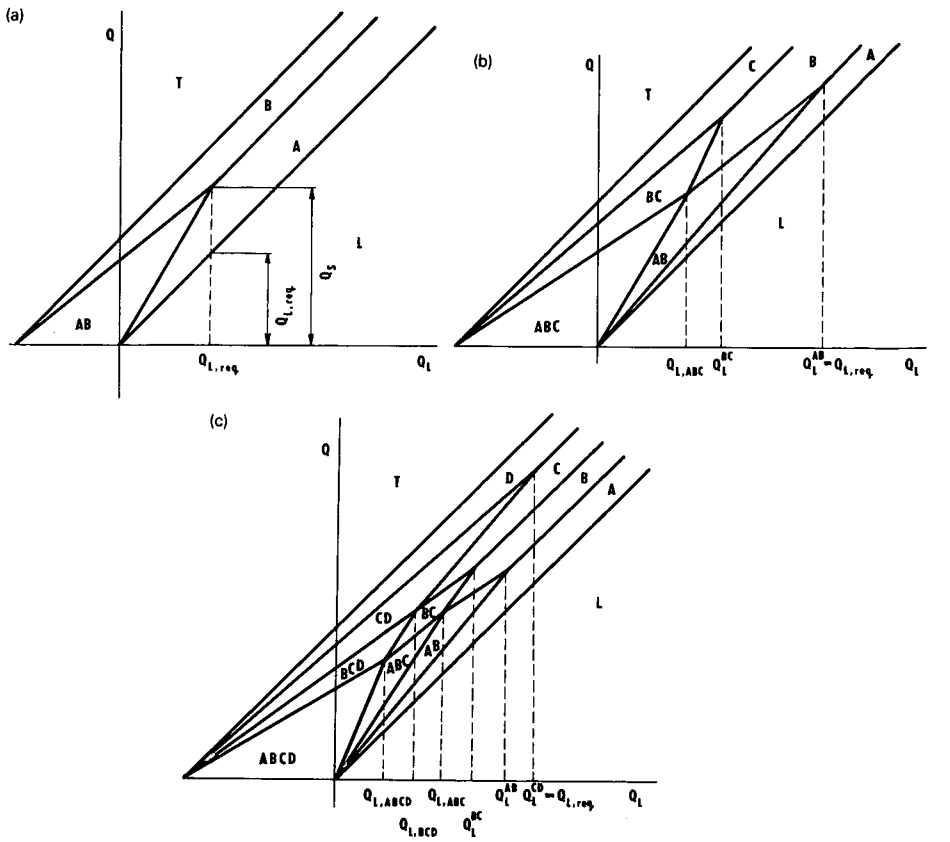

Fig. 1. Scheme of isotachophoretic separation of multi-component sample containing (a) two components A and B, (b) three components A, B and C and (c) four components A, B, C and D.

representing the zone boundaries showing the state of separation after charge Q has passed through the column. Similarly, the line parallel to the y-axis at a distance Q_L shows by its crossing the network how zones pass through the detection cell if the column hold-up is equal to Q_L.

From the viewpoint of the description of the separation process, the points of intersection of the lines corresponding to the zone boundaries are important: they are the points of extinction of mixed zones. The x-coordinate of such a point represents the column hold-up required for the disappearance of the respective mixed zone; the corresponding y-coordinate represents the appropriate separation charge. The largest of the Q_L^{XY} values (corresponding to the extinction of binary mixed zones) is then equal to the $Q_{L,req}$ value required for the complete separation of the sample.

It is obvious that in an optimum case the isotachophoretic column has a hold-up just equal to the value $Q_{L,req}$. If the actual Q_L is lower, then only incomplete separation is achieved. If the column has a higher Q_L value, complete separation is obtained but an additional electric charge is required to transfer the separated zones to the detection

cell. We can say that in an optimum case the binary mixture the separation of which is the most crucial is separated just when it reaches the detection cell.

The calculation of the $Q_{L,req}$ value depends on the number of the sample components. For a two-component sample, this value can be determined simply from (*cf.*, eqn. 25 in the Appendix)

$$Q_{L,req} = (Q_A + Q_B)\frac{\bar{u}_{B,AB}}{\bar{u}_{A,AB} - \bar{u}_{B,AB}} \tag{3}$$

where $\bar{u}_{i,j}$ is the effective mobility of substance i in zone j.

If the sample contains three or more components, it is necessary to calculate the Q_L^{XY} values for each pair of neighbouring components and to find the maximum value of them to obtain $Q_{L,req}$. For the simplest case of a three-component sample (containing substances A, B and C) we have to calculate Q_L^{AB} and Q_L^{BC}. According to eqns. 37 and 38 (see Appendix) their values can be obtained from

$$Q_L^{AB} = \frac{Q_A}{\frac{\bar{u}_{L,L}\kappa_{AB}}{\kappa_L \bar{u}_{B,AB}} - 1} \tag{4}$$

$$Q_L^{BC} = \frac{Q_C}{\frac{\bar{u}_{B,BC}\kappa_L}{\kappa_{BC}\bar{u}_{L,L}} - 1} - Q_A - Q_B \tag{5}$$

The column hold-up required for the complete separation of the sample is then given by the higher value of Q_L^{AB} and Q_L^{BC}.

The determination of $Q_{L,req}$ if the sample contains more than three components is analogous. A detailed mathematical description of the problem is given in the Appendix.

EXPERIMENTAL

All chemicals were of analytical-reagent grade from Lachema (Brno, Czechoslovakia).

The isotachophoretic experiments were carried out in an Agrofor instrument (JZD Odra, Krmelín, Czechoslovakia) at room temperature. For calculations, a PMD-85-2 computer (Tesla Piešťany, Czechoslovakia) was used.

Published ionic mobilities and dissociation constants [13] were used in the calculations.

RESULTS AND DISCUSSION

For the determination of the optimum pH of the leading electrolyte, a computer program was written that enables the separation of a three-component sample to be solved. The amount of separated components and their physico-chemical constants (ionic mobilities and dissociation constants have to be known for the use of the

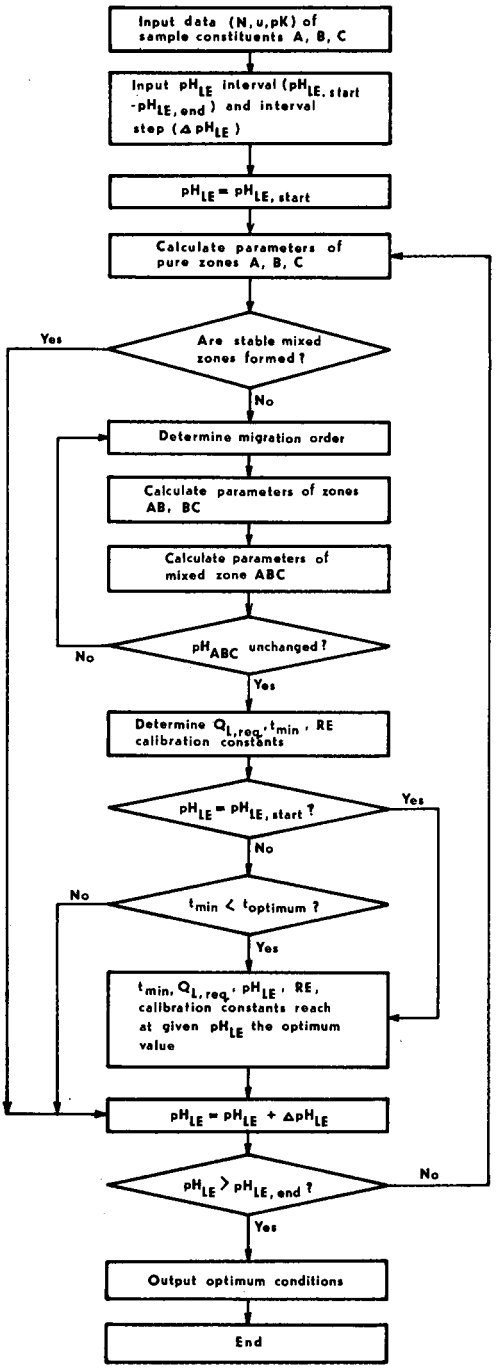

Fig. 2. Flow chart of optimization of isotachophoretic separation.

computer program). The program provides the composition of the optimum leading electrolyte, the required column hold-up, the recommended driving current and the time of analysis and further qualitative and quantitative parameters of the particular isotachophoretic zones (relative effective mobilities or *RE* values and calibration constants). A flow chart of the computer program is shown in Fig. 2.

To test the applicability of the computer program, the separation of lactate, acetate and butyrate in silages was selected [14]. To simulate a silage extract, a mixture of 37 m*M* acetate, 25 m*M* lactate and 22 m*M* butyrate was used [8]. The computer output is shown in Fig. 3. For the calculation of the time of analysis the parameters of the LKB Tachophor were used [15].

The minimum required column hold-up, 30.5 mC, was found at $pH_L = 3.4$, but the optimum, *i.e.*, minimum, analysis time (2.74 min) was found at $pH_L = 4.5$, when a column hold-up of 33.2 mC was required.

The plot of analysis time *vs.* pH_L can be only partly verified experimentally.

```
SEPARATION OF ANIONS A,B,C


A: N= 3.7E-08 mol
   pK(1)= 4.756   pK(2)= 0     pK(3)= 0
   u(1)=-42.4     u(2)= 0      u(3)= 0

B: N= 2.5E-08 mol
   pK(1)= 3.86    pK(2)= 0     pK(3)= 0
   u(1)=-36.5     u(2)= 0      u(3)= 0

C: N= 2.2E-08 mol
   pK(1)= 4.82    pK(2)= 0     pK(3)= 0
   u(1)=-33.8     u(2)= 0      u(3)= 0


pH(LE)     Q(L)          TIME          pH(ABC)
           [C]           [MIN]

 3         .0357017      5.5999        3.86286
 3.5       .0304899      3.71887       4.24143
 4         .0318718      3.25428       4.50266
 4.5       .0332153      2.74921       4.8715
 5         .126952       6.97172       5.25818
 5.5       .245324       11.8057       5.67292
 6         .0981953      5.06607       6.13667
 6.5       .103402       5.2247        6.61783

RECOMMENDED LEADING ELECTROLYTE: 10 mmol/HCl
+ 6-AMINOCAPROIC ACID, pH(LE)= 4.5
REQUIRED COLUMN HOLD-UP Q(L)= .0332153 C
RECOMMENDED DRIVING CURRENT I= 375 /uA
ANALYSIS TIME t= 2.74921 min
RE(A)= 3.15652
RE(B)= 2.47397
RE(C)= 4.03037
1 mC= 6.09947 nmol A
1 mC= 5.7073 nmol B
1 mC= 5.52044 nmol C
```

Fig. 3. Computer output of optimization program.

However, the model can be tested by comparing theoretical and experimental values of the required column hold-up.

Calculated values of the required column hold-up and experimentally measured values are shown in Fig. 4. There is good agreement between the theoretical and experimental values. The differences are insignificant and are probably caused by the deviations from the introductory presumptions that the sample has the composition of an adjusted mixed isotachophoretic zone and that the ionic mobilities and dissociation constants do not depend on temperature.

The sufficient agreement between the theoretical and experimental values of the required column hold-up confirmed that the separation conditions of isotachophoretic analysis can be easily optimized by computer simulation using the charge-based transient-state model. If the sample contains only several identified compounds, the ionic mobilities, dissociation constants and concentration range of which are known, the labourious experimental determination of suitable separation conditions can be omitted and only optimization of the separation based on the theoretical model needs to be performed.

APPENDIX

Zone passage charge

The zone passage charge [6,8,12] is a general quantitative parameter of isotachophoretic analysis that is suitable for the quantitative description of an isotachophoretic zone. It is the electric charge that has to be passed through the isotachophoretic column to shift the rear boundary of an isotachophoretic zone to reach the position where the front boundary of that zone was prior to the passage of electric current. The expression of the zone passage charge can be derived by

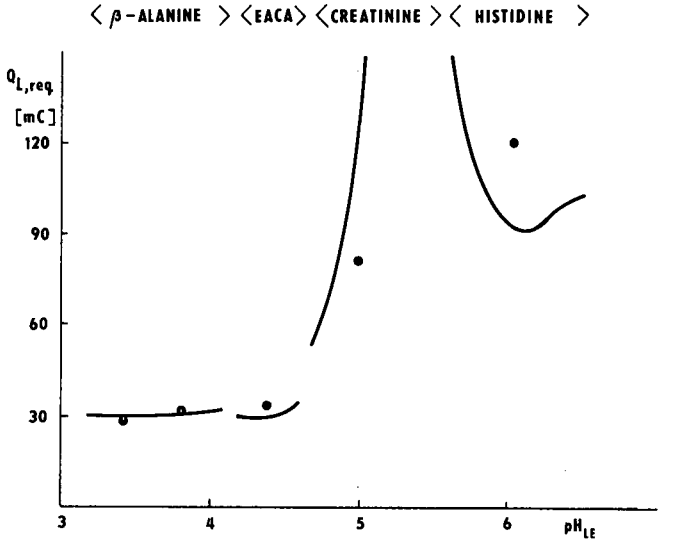

Fig. 4. Dependence of column hold-up required for separation of a sample containing 37 nmol acetic acid, 25 nmol lactic acid and 22 nmol butyric acid. Solid lines, calculated results; ●, experimental data. < > show the pH_{LE} regions of the used counterions. EACA = ε-aminocaproic acid.

combination of the modified Ohm's law (eqn. 6), the expression for the migration velocity of a substance (eqn. 7), electric charge (eqn. 8) and effective mobility (eqn. 9).

$$E_i = \frac{I}{S\kappa_i} \tag{6}$$

$$v_i = \frac{l_i}{t} = |\bar{u}_i|E_i \tag{7}$$

$$Q = It \tag{8}$$

$$\bar{u}_i = \frac{\sum_{j=1}^{m} c_j u_j}{\bar{c}_i} \tag{9}$$

where I = electric current, S = cross-section of separation capillary, t = time, Q = electric charge, E_i = electric field strength in the ith zone, v_i = isotachophoretic velocity, l_i = migration path of substance i, $\bar{u}_i$ = effective mobility of substance i in its isotachophoretic zone, $\bar{c}_i$ = analytical concentration of substance i in its isotachophoretic zone, c_j = concentration of jth species of substance i dissociating into m ionic species and κ_i = conductivity of ith zone.

For the zone passage charge of substance i, we obtain by combination of eqns. 6–9

$$Q_i = N_i \cdot \frac{\kappa_i}{\sum_{j=1}^{m} c_j|u_j|} \tag{10}$$

where $N_i = \bar{c}_i l_i S$ is the molar amount of substance i.

Concentration of counter ion in an n-component mixed zone

The counter-ion mass balance can be expressed for both front and rear boundaries of an isotachophoretic zone containing n components (see Fig. 5) by the equations

$$\bar{c}_{R,1\ldots n-1}(\bar{u}_{R,1\ldots n-1}E_{1\ldots n-1} - v_{1\ldots n\to 1\ldots n-1}) = \bar{c}_{R,1\ldots n}(\bar{u}_{R,1\ldots n}E_{1\ldots n} - v_{1\ldots n\to 1\ldots n-1}) \tag{11}$$

$$\bar{c}_{R,2\ldots n}(\bar{u}_{R,2\ldots n}E_{2\ldots n} - v_{2\ldots n\to 1\ldots n}) = \bar{c}_{R,1\ldots n}(\bar{u}_{R,1\ldots n}E_{1\ldots n} - v_{2\ldots n\to 1\ldots n}) \tag{12}$$

where the subscripts R, 1 and n refer to counter ion, component with the highest effective mobility and component with the lowest mobility in the mixed zone, respectively, v_1 and v_n are the migration velocities of the rear and front boundaries, for which

$$v_{2\ldots n\to 1\ldots n} = |\bar{u}_{1,1\ldots n}|E_{1\ldots n} \tag{13}$$

$$v_{1\ldots n\to 1\ldots n-1} = |\bar{u}_{n,1\ldots n}|E_{1\ldots n} \tag{14}$$

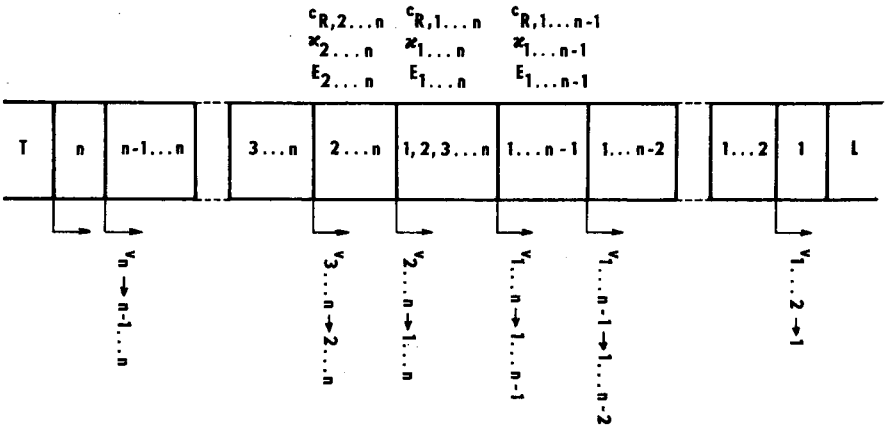

Fig. 5. Scheme of separation of an n-component mixed zone.

If eqns. 6 and 11–14 are combined, the following expressions for the concentration of the counter ion in the n-component mixed zone and the conductivity of this zone are obtained:

$$\bar{c}_{R,1\ldots n} = \frac{\bar{u}_{R,1\ldots n-1}\kappa_{2\ldots n}\bar{u}_{1,1\ldots n} - \bar{u}_{R,2\ldots n}\kappa_{1\ldots n-1}\bar{u}_{n,1\ldots n}}{\frac{\kappa_{2\ldots n}\bar{u}_{R,1\ldots n-1}}{\bar{c}_{R,2\ldots n}}(\bar{u}_{R,1\ldots n} - \bar{u}_{1,1\ldots n}) - \frac{\kappa_{1\ldots n-1}\bar{u}_{R,2\ldots n}}{\bar{c}_{R,1\ldots n-1}}(\bar{u}_{R,1\ldots n} - \bar{u}_{n,1\ldots n})} \tag{15}$$

$$\kappa_{1\ldots n} = \frac{\bar{c}_{R,1\ldots n-1}\bar{u}_{n,1\ldots n}(\bar{u}_{R,1\ldots n} - \bar{u}_{1,1\ldots n}) - \bar{c}_{R,2\ldots n}\bar{u}_{1,1\ldots n}(\bar{u}_{R,1\ldots n} - \bar{u}_{n,1\ldots n})}{\frac{\bar{c}_{R,1\ldots n-1}\bar{u}_{R,1\ldots n-1}}{\kappa_{1\ldots n-1}}(\bar{u}_{R,1\ldots n} - \bar{u}_{1,1\ldots n}) - \frac{\bar{c}_{R,2\ldots n}\bar{u}_{R,2\ldots n}}{\kappa_{2\ldots n}}(\bar{u}_{R,1\ldots n} - \bar{u}_{n,1\ldots n})} \tag{16}$$

General isotachophoretic condition for an n-component mixed zone

Let us consider the isotachophoretic system shown in Fig. 5. The general isotachophoretic condition for pure isotachophoretic zones can be expressed as [16]

$$W = \frac{|\bar{u}_{i,i}|}{\kappa_i} = \text{constant} \tag{17}$$

If we consider the migration of a mixed zone containing n components, the linear velocities of the front and rear boundaries are expressed by eqns. 13 and 14. If these are related to the linear velocity of the leading zone (eqn. 7), relative velocities of the boundaries, R, are obtained:

$$R_n = \frac{\bar{u}_{n,1\ldots n}\kappa_L}{\kappa_{1\ldots n}\bar{u}_{L,L}} \tag{18}$$

$$R_1 = \frac{\bar{u}_{1,1\ldots n}\kappa_L}{\kappa_{1\ldots n}\bar{u}_{L,L}} \tag{19}$$

The total zone passage charge of the components that passed through the front and rear boundaries of the n-component mixed zone until its extinction can be expressed as

$$Q_{\text{front},1\ldots n} = \sum_{i=1}^{n} Q_{i,1\ldots n} \frac{\bar{u}_{i,1\ldots n} - \bar{u}_{n,1\ldots n}}{\bar{u}_{1,1\ldots n} - \bar{u}_{n,1\ldots n}} \tag{20}$$

$$Q_{\text{rear},1\ldots n} = \sum_{i=1}^{n} Q_{i,1\ldots n} \frac{\bar{u}_{1,1\ldots n} - \bar{u}_{i,1\ldots n}}{\bar{u}_{1,1\ldots n} - \bar{u}_{n,1\ldots n}} \tag{21}$$

The separation charge that has to pass through the column to reach the extinction of zone $1\ldots n$ can be expressed (see Fig. 1) as

$$Q_{\text{S},1\ldots n} = \frac{\sum_{i=1}^{n} Q_{\text{i},1\ldots n}}{R_1 - R_n} = \frac{Q_{\text{front},1\ldots n}}{1 - R_n} = \frac{Q_{\text{rear},1\ldots n}}{R_1 - 1} \tag{22}$$

By combining eqns. 18, 19 and 22, the isotachophoretic condition related to mixed zone $1\ldots n$ is obtained:

$$W = \frac{\sum_{i=1}^{n} Q_{i,1\ldots n}\bar{u}_{i,1\ldots n}}{\kappa_{1\ldots n} \sum_{i=1}^{n} Q_{i,1\ldots n}} = \frac{\bar{u}_{i,i}}{\kappa_i} \tag{23}$$

Required column hold-up $Q_{\text{L},1\ldots n}$

Let us consider the separation of the n-component mixed zone shown in Fig. 5. The front boundary migrates with relative velocity R_n and the rear boundary with relative velocity R_1. The zone passage charge of each component i is $Q_{i,1\ldots n}$. Comparing the path (expressed as the electric charge) through which both front and rear boundaries migrate from the start of the analysis to the extinction of zone $1\ldots n$, we obtain

$$R_1(Q_{\text{L},1\ldots n} + \sum_{i=1}^{n} Q_{i,1\ldots n}) = R_n Q_{\text{L},1\ldots n} \tag{24}$$

By arrangement and combination with eqns. 18 and 19 we can write

$$Q_{\text{L},1\ldots n} = \frac{\bar{u}_{n,1\ldots n}}{\bar{u}_{1,1\ldots n} - \bar{u}_{n,1\ldots n}} \sum_{i=1}^{n} Q_{i,1\ldots n} \tag{25}$$

Eqn. 25 is a general expression for the column hold-up required for the extinction of an n-component mixed zone. If $n = 2$ the expression also describes the column hold-up required for the full separation of the sample.

Separation charge

Separation charge is another important parameter of isotachophoretic separation [5]. It is the electric charge that has to pass across the isotachophoretic column to achieve extinction of the appropriate mixed zone. Let us consider the separation of the n-component mixed zone shown in Fig. 5. If the hold-up of the column between the n-component sample and the detection cell is $Q_{L,1\ldots n}$, the n-component mixed zone disappears just in the detection cell. However, the electric charge that has to pass through the column to reach this situation is higher because not only leading zone but also all zones that are generated in front of the n-component mixed zone has to pass the detection cell, *i.e.*, it holds that

$$Q_{S,1\ldots n} = Q_{L,1\ldots n} + Q_{front,1\ldots n} = \frac{\sum_{i=1}^{n} Q_{i,1\ldots n}\bar{u}_{i,1\ldots n}}{\bar{u}_{1,1\ldots n} - \bar{u}_{n,1\ldots n}} \tag{26}$$

Column hold-up required for the full separation of an n-component sample $Q_{L,req}$

There is no general equation describing the column hold-up required for the full separation of an n-component sample. Calculation of the required column hold-up, $Q_{L,req}$, depends on the number of sample components.

If the sample contains only two components (Fig. 1a), the required column hold-up can be determined in a simple way (see eqn. 3).

Solving the separation of a multi- component sample containing three and more components, the procedure for the calculation of the required column hold-up can be formulated as a parallel calculation of the column hold-up required for the extinction of all individual mixed zones and, as a result, binary-mixed-zone column hold-ups Q_L^{XY} are obtained. The Q_L^{XY} which reaches the largest value is then the final resulting $Q_{L,req}$.

If the sample contains three components, A, B and C, the column hold-ups required for the extinction of the mixed zone ABC and of the remaining binary mixed zones AB and BC have to be determined. According to eqns. 25 and 26, the column hold-up $Q_{L,ABC}$ and corresponding separation charge $Q_{S,ABC}$ can be calculated from the equations

$$Q_{L,ABC} = \frac{\bar{u}_{C,ABC}}{\bar{u}_{A,ABC} - \bar{u}_{C,ABC}}(Q_A + Q_B + Q_C) \tag{27}$$

$$Q_{S,ABC} = \frac{Q_A\bar{u}_{A,ABC} + Q_B\bar{u}_{B,ABC} + Q_C\bar{u}_{C,ABC}}{\bar{u}_{A,ABC} - \bar{u}_{C,ABC}} \tag{28}$$

If the column hold-up required for the separation of zone ABC is applied, parts of zone AB and BC remain unseparated. Their zone passage charges $Q'_{A,AB} + Q'_{B,AB}$ and $Q'_{B,BC} + Q'_{C,BC}$ can be calculated by the sumation of the appropriate contributions of individual constituents. For the content of component B in both zones it holds, according to eqns. 20 and 21, that

$$Q'_{B,AB} = \frac{\bar{u}_{B,ABC} - \bar{u}_{C,ABC}}{\bar{u}_{A,ABC} - \bar{u}_{C,ABC}} \cdot Q_B \tag{29}$$

$$Q'_{B,BC} = \frac{\bar{u}_{A,ABC} - \bar{u}_{B,ABC}}{\bar{u}_{A,ABC} - \bar{u}_{C,ABC}} \cdot Q_B \tag{30}$$

After passing electric charge $Q_{S,ABC}$ through the column, the zone passage charge of pure zone A is equal to the product of the difference in relative velocities of both boundaries of zone A and of charge passed:

$$Q'_{A,A} = Q_{S,ABC}\left(1 - \frac{\kappa_i \bar{u}_{B,AB}}{\kappa_{AB}\bar{u}_{i,i}}\right) \tag{31}$$

By rearrangement and combination, we obtain

$$Q'_{A,AB} = Q_A - Q_{S,ABC} \cdot \frac{Q_A(\bar{u}_{A,AB} - \bar{u}_{B,AB})}{Q_A\bar{u}_{A,AB} + Q_B\bar{u}_{B,AB}} \tag{32}$$

Analogously, it holds that

$$Q'_{C,BC} = Q_C - Q_{S,ABC} \cdot \frac{Q_C(\bar{u}_{B,BC} - \bar{u}_{C,BC})}{Q_B\bar{u}_{B,BC} + Q_C\bar{u}_{C,BC}} \tag{33}$$

The column hold-up Q_L^{AB} consists of three parts: (i) $Q_{L,ABC}$, (ii) zone passage charge $(Q'_{A,AB} + Q'_{B,AB})$ and (iii) $Q_{L,AB}$. By combining eqns. 25 and 27–30 we obtain

$$Q_L^{AB} = (Q_A + Q_B + Q_C) \cdot \frac{\bar{u}_{C,ABC}}{\bar{u}_{A,ABC} - \bar{u}_{C,ABC}} + \left[Q_A - \frac{Q_A\bar{u}_{A,ABC} + Q_B\bar{u}_{B,ABC} + Q_C\bar{u}_{C,ABC}}{\bar{u}_{A,ABC} - \bar{u}_{C,ABC}} \cdot \right.$$

$$\left. \frac{Q_A(\bar{u}_{A,AB} - \bar{u}_{B,AB})}{Q_A\bar{u}_{A,AB} + Q_B\bar{u}_{B,AB}} + Q_B \cdot \frac{\bar{u}_{B,ABC} - \bar{u}_{C,ABC}}{\bar{u}_{A,ABC} - \bar{u}_{C,ABC}} \right] \frac{\bar{u}_{A,AB}}{\bar{u}_{A,AB} - \bar{u}_{B,AB}} \tag{34}$$

The column hold-up Q_L^{BC} consists of two parts, (i) $Q_{L,ABC}$ and (ii) $Q_{L,BC}$, and can be expressed as

$$Q_L^{BC} = (Q_A + Q_B + Q_C) \cdot \frac{\bar{u}_{C,ABC}}{\bar{u}_{A,ABC} - \bar{u}_{C,ABC}} + \left[Q_B \cdot \frac{\bar{u}_{A,ABC} - \bar{u}_{B,ABC}}{\bar{u}_{A,ABC} - \bar{u}_{C,ABC}} + Q_C - \right.$$

$$\left. \frac{Q_A\bar{u}_{A,ABC} + Q_B\bar{u}_{B,ABC} + Q_C\bar{u}_{C,ABC}}{\bar{u}_{A,ABC} - \bar{u}_{C,ABC}} \cdot \frac{Q_C(\bar{u}_{B,BC} - \bar{u}_{C,BC})}{Q_B\bar{u}_{B,BC} + Q_C\bar{u}_{C,BC}} \right] \frac{\bar{u}_{C,BC}}{\bar{u}_{B,BC} - \bar{u}_{C,BC}} \tag{35}$$

If the separation of a multi-component sample is to be solved, another approach is suitable; however, the resulting Q_L^{XY} values are then expressed by more parameters than only zone passage charges and effective mobilities. In this approach general expressions for $Q_L^{1,2}$, $Q_L^{2,3} \ldots Q_L^{n-2,n-1}$, $Q_L^{n-1,n}$ can be derived. Let us consider the separation of the n-component sample shown in Fig. 5 (compare, *e.g.*, Fig. 1c). The zone passage charge of the pure zone 1 can be expressed as the product of the charge

passed through the column until the complete separation of zones 1 and 2 and the difference in relative velocities of the front and rear boundaries of zone 1:

$$Q_1 = (Q_L^{1,2} + Q_1)\left(1 - \frac{\bar{u}_{2,1\ldots2}\kappa_L}{\kappa_{1\ldots2}\bar{u}_{L,L}}\right) \tag{36}$$

By rewriting eqn. 36 we obtain

$$Q_L^{1,2} = \frac{Q_1}{\dfrac{\bar{u}_{L,L}\kappa_{1\ldots2}}{\kappa_L\bar{u}_{2,1\ldots2}} - 1} \tag{37}$$

Analogously, the expression for $Q_L^{n-1,n}$ can be derived:

$$Q_L^{n-1,n} = \frac{Q_n}{\dfrac{\bar{u}_{n-1,n-1\ldots n}\kappa_L}{\kappa_{n-1\ldots n}\bar{u}_{L,L}} - 1} - \sum_{i=1}^{n-1} Q_i \tag{38}$$

The expression for $Q_L^{2,3}$, $Q_L^{n-1,n}$ and other Q_L^{XY} can be derived in a similar way, but the derivation and the resulting expressions are more complicated.

The required column hold-up is then obtained as the largest value of Q_L^{XY}.

Calculation of the composition of n-component mixed zone

The method of calculation of the composition of a mixed zone is very similar to that used for the calculation of individual isotachophoretic zones [17,18]. The isotachophoretic condition can be written in the form

$$Q_i^* = \frac{\kappa_i}{F|\bar{u}_{i,i}|} = \text{constant} \tag{39}$$

where F is the Faraday constant. By iteration, the pH of any mixed zone can be calculated by the method the algorithm of which is based on finding the roots of the function *RFQ* [17], defined as

$$RFQ = \frac{Q_L^*}{Q_i^*} - 1 = 0 \tag{40}$$

The pH at which *RFQ* equals zero can be found by finding the pH range in which the function *RFQ* changes its sign and further by the method of interval bisection. A detailed description of the method can be found elsewhere [8].

For a mixed zone that contains n components we define the *RFQ* function as

$$RFQ = \frac{\kappa_L \sum_{i=1}^{n} Q_{i,1\ldots n}\bar{u}_{i,1\ldots n}}{\bar{u}_{L,L}\kappa_{1\ldots n}\sum_{i=1}^{n} Q_{i,1\ldots n}} - 1 = 0 \tag{41}$$

To find the roots of the *RFQ* function, $\kappa_{1\ldots n}$ has to be determined. For the use of eqn. 16 it is necessary to know the parameters of partially mixed zones which are calculated in the same way: first, binary mixed zones are calculated from the pure isotachophoretic zones, then ternary mixed zones from the binary mixed zones, etc. However, in partially mixed zones, the content of individual components expressed as $Q_{i,1\ldots n}$ cannot be directly determined and has to be calculated by another iteration.

By using parameters of an n-component mixed zone, the binary zones have to be calculated and the composition of the n-component zone is recalculated using new values of the binary mixed zones. The procedure of both combined iteration steps is repeated as long as values of all mixed zones do not differ from those obtained in the previous step. For example, the composition of binary zones in the case of a three-component sample can be calculated from eqns. 29–33 and zone passage charges of individual components in the binary zones are obtained. Those are then substituted for $Q_{i,1\ldots n}$ in eqn. 41 and used in the *RFQ* method. The procedure is repeated as described above.

Calculation of required column hold-up from experimental data

Let us consider the separation of a sample containing components A, B and C when complete separation is not achieved with column hold-up Q_L and the mixed zone BC can be observed in the isotachopherogram (see Fig. 6). The sampling ratio of components B and C expressed as the ratio of zone passage charges is q:

$$q = Q_C/Q_B \tag{42}$$

The separation charge of the partial separation of the mixed zone BC is, according to eqn. 26, equal to

$$Q'_S = Q_L + \bar{Q}_A + \bar{Q}_B = \frac{\bar{Q}_B\bar{u}_{B,BC} + \bar{Q}_B q\bar{u}_{C,BC}}{\bar{u}_{B,BC} - \bar{u}_{C,BC}} \tag{43}$$

when $\bar{Q}_i$ is the zone passage charge of the ith zone taken from the isotachopherogram. During passage of mixed zone BC through the detection cell, zone BC is further

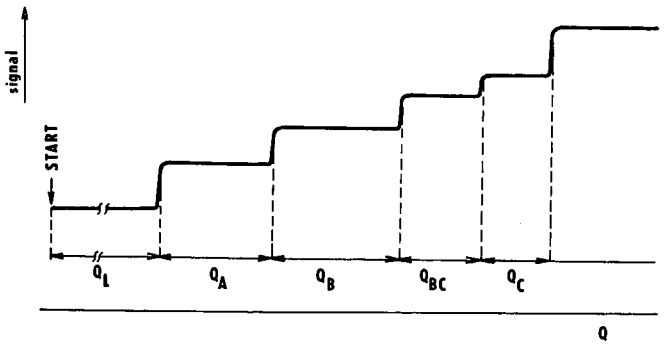

Fig. 6. Isotachopherogram of analysis of a sample with components A, B and C when only partial separation of components B and C is obtained.

separated so that zone C has at its passage through the detection cell zone passage charge Q_C. For the separation charge of this partial separation it holds that

$$Q''_S = Q_L + \bar{Q}_A + \bar{Q}_B + \bar{Q}_{BC} = \frac{\bar{Q}_C \bar{u}_{C,BC} + \bar{Q}_C \bar{u}_{B,BC}/q}{\bar{u}_{B,BC} - \bar{u}_{C,BC}} \tag{44}$$

For the column hold-up Q_L and column hold-up $Q_{L,req}$ required for the complete separation, it holds according to eqn. 25 that

$$Q_L = (\bar{Q}_B + \bar{Q}_B q)\frac{\bar{u}_{C,BC}}{\bar{u}_{B,BC} - \bar{u}_{C,BC}} - \bar{Q}_A \tag{45}$$

$$Q_{L,req} = (\bar{Q}_B + \bar{Q}_{BC} + \bar{Q}_C)\frac{\bar{u}_{C,BC}}{\bar{u}_{B,BC} - \bar{u}_{C,BC}} - \bar{Q}_A \tag{46}$$

The zone passage charge of the zone A is subtracted from the column hold-up because also during migration of zone A through the detection cell the mixed zone BC is separated.

By combination of eqns. 43–46, an expression is obtained for the column hold-up required for the complete separation of sample ABC:

$$Q_{L,req} = \frac{(Q_L + \bar{Q}_A)(\bar{Q}_B + \bar{Q}_{BC} + \bar{Q}_C)(Q_L + \bar{Q}_A + \bar{Q}_B + \bar{Q}_{BC})}{(Q_L + \bar{Q}_A + \bar{Q}_B)(\bar{Q}_B + \bar{Q}_C) + \bar{Q}_B \bar{Q}_{BC}} - \bar{Q}_A \tag{47}$$

If the first substance forms a transient mixed zone, eqn. 47 can be rewritten by omitting $\bar{Q}_A$ and the equation already published [8] is obtained.

SYMBOLS AND ABBREVIATIONS

A	separated component of sample (separand)
B	separated component of sample (separand)
C	separated component of sample (separand)
$\bar{c}_i$	analytical concentration of substance i
c_j	concentration of jth ion of substance i
$\bar{c}_{R,1\ldots n}$	total concentration of counter ion in mixed zone containing components 1,2,...n
$\bar{c}_{1,1\ldots n}$	total concentration of substance 1 in mixed zone containing components 1,2,...n
E_i	electric field strength in ith zone
$E_{1\ldots n}$	electric field strength in mixed zone containing components 1,2,...n
F	Faraday constant
I	electric driving current
I_{max}	maximum electric driving current
l_i	migration path of substance i
N_i	amount of substance i
pH_L	pH of leading electrolyte

Q	electric charge
Q_i	zone passage charge of substance i
$Q'_{i,1\ldots n}$	zone passage charge of substance i in partially separated zone $1\ldots n$
$Q_{\text{front},1\ldots n}$	total zone passage charge of substances that passed the front boundary of mixed zone $1\ldots n$
Q_L	column hold-up
$Q_{L,\text{req}}$	column hold-up required for complete separation of sample
$Q_{L,1\ldots n}$	column hold-up required for extinction of mixed zone containing $1,2\ldots n$ components
Q_L^{AB}	column hold-up required for the complete separation of sample when zone AB is separated last
$Q_{\text{rear},1\ldots n}$	total zone passage charge of substances that passed the rear boundary of mixed zone
Q_S	separation charge
$Q_{S,1\ldots n}$	separation charge corresponding to extinction of mixed zone containing components $1,2\ldots n$
Q'_S	quasi-separation charge if only incomplete separation is achieved
Q''_S	quasi-separation charge if incomplete separation is obtained and mixed zone contributes to it
$\bar{Q}_i$	zone passage charge of ith zone taken from the isotachopherogram
Q_i^*	Q_i/V_iF
$Q^*_{1\ldots n}$	$\sum_{i=1}^{n} Q_i/V_iF$
$\sum_{i=1}^{n} Q_i$	zone passage charge of mixed zone partially separated
q	sampling ratio
R_n	relative velocity of boundary between zones $1\ldots n$ and $1\ldots n-1$
S	cross-section of separation capillary
ΔT	difference between mean temperature of isotachophoretic zone and thermostating temperature
t	time
$t_{\min}$	minimum time of analysis
$\bar{u}_{i,1\ldots n}$	effective mobility of substance i in mixed zone containing components $1,2\ldots n$
u_j	ionic mobility of jth subspecies of substance i
$\bar{u}_{R,1\ldots n}$	effective mobility of counter ion in mixed zone containing components $1,2,\ldots n$
v_i	migration velocity of ith substance
$v_{1\ldots n\to 1\ldots n-1}$	velocity of boundary between zones $1\ldots n$ and $1\ldots n-1$
W	charge-related volume velocity
κ_T	conductivity of the zone with the lowest conductivity in the system
κ_i	conductivity of zone of ith substance
$\kappa_{1\ldots n}$	conductivity of mixed zone containing substances $1,2,\ldots n$

REFERENCES

1 A. J. P. Martin and F. M. Everaerts, *Proc. R. Soc. London, Ser. A*, 316 (1970) 493.

2 G. Brouwer and G. A. Postema, *J. Electrochem. Soc.*, 117 (1970) 874.
3 F. E. P. Mikkers, F. M. Everaerts and J. A. F. Peek, *J. Chromatogr.*, 168 (1979) 293.
4 T. Hirokawa, K. Nakahara and Y. Kiso, *J. Chromatogr.*, 463 (1989) 51.
5 P. Boček, M. Deml, B. Kaplanová and J. Janák, *J. Chromatogr.*, 160 (1978) 1.
6 V. Dolník, M. Deml and P. Boček, *J. Chromatogr.*, 320 (1985) 89.
7 T. Hirokawa, K. Nakahara and Y. Kiso, *J. Chromatogr.*, 470 (1989) 21.
8 P. Boček, M. Deml, P. Gebauer and V. Dolník, *Analytical Isotachophoresis*, VCH, Weinheim, 1988.
9 T. Hirokawa and Y. Kiso, *J. Chromatogr.*, 257 (1983) 197.
10 T. Hirokawa, H. Takemi and Y. Kiso, *J. Chromatogr.*, 305 (1984) 429.
11 T. Hirokawa, T. Gojo and Y. Kiso, *J. Chromatogr.*, 390 (1987) 201.
12 P. Gebauer, V. Dolník, M. Deml and P. Boček, *Adv. Electrophoresis*, 1 (1987) 281.
13 T. Hirokawa, M. Nishino, N. Aoki, Y. Kiso, Y. Sawamoto, T. Yagi and J. Akiyama, *J. Chromatogr.*, 271 (1983) D1.
14 P. Boček, S. Pavelka, K. Grígelová, M. Deml and J. Janák, *J. Chromatogr.*, 154 (1978) 356.
15 Z. Ryšlavý, P. Boček, M. Deml and J. Janák, *J. Chromatogr.*, 144 (1977) 17.
16 P. Gebauer and P. Boček, *J. Chromatogr.*, 320 (1985) 49.
17 J. L. Beckers and F. M. Everaerts, *J. Chromatogr.*, 68 (1972) 207.
18 P. Boček and P. Gebauer, *Electrophoresis*, 5 (1984) 338.

Journal of Chromatography, 545 (1991) 267–281
Elsevier Science Publishers B.V., Amsterdam

CHROM. 23 170

Effect of sample composition on the separation efficiency of isotachophoresis

TAKESHI HIROKAWA*, YASURO YOKOTA[a] and YOSHIYUKI KISO
Applied Physics and Chemistry, Faculty of Engineering, Hiroshima University, Kagamiyama 1, Higashi-hiroshima 724 (Japan)

ABSTRACT

In order to clarify the effect of the sample composition on the separation efficiency of isotachophoresis, approximate equations expressing the resolution time of strong electrolytes were derived. The transient two-component mixed zone formed in the separation process of a three-component mixture was simulated by varying the molar amount and the mobility of the third component. It was apparent that the resolution time of two components of interest was increased with the addition of the other components, owing to the change in the potential gradient of the two-component mixed zone. The magnitude of the delay was especially large when the mobility of the added component was close to that of the two components of interest. The increase in resolution time was evaluated for the separation of mixtures of up to six equimolar components. The present simulation was confirmed by analysing the actual separation process using a scanning ultraviolet spectrophotometric detector.

INTRODUCTION

The driving force of isotachophoretic separation is the different migration velocities of separands in the transient mixed zones [1,2]; a large difference in these migration velocities means efficient separation. As the electrophoretic velocity is expressed by the product of the effective mobility of an ion and the potential gradient of its zone, the resolution time of the mixed zone must depend on both factors.

In the optimization of isotachophoretic separations, however, the effect of effective mobility on the separation efficiency has been emphasized [1–3]. In fact, the optimization of the pH of the leading electrolyte is undoubtedly very important, and this is obtained straightforwardly from the pH dependence of the effective mobility of weak electrolytes. Mikkers *et al.* [4,5] have given a theoretical elucidation of the effect of pH on the separation efficiency of two-component mixtures. The separability of a two-component mixture was discussed in relation to the pH of the operational system considering zone stability by Bocek and Gebauer [6]. It was also reported that the pH of the sample solution affects the separation efficiency [4,5], although not so seriously

[a] Present address: Mitsubishi Paper Mills Ltd., Tsukuba Research Laboratories, Tsukuba, Ibaraki, Japan.

0021-9673/91/$03.50

[7]. The dynamics of the isotachophoretic separation of two-component mixtures was reviewed by Thormann [8].

In addition to straightforward factors such as effective mobility, however, we have suggested another important factor that affects the separation efficiency, namely the composition of the sample solution [9]. This was based on the fact that the resolution time of a two-component mixed zone formed in the isotachophoretic separation process of a three-component mixture was longer than that of the equivalent two samples being separated independently. Although this phenomenon has been confirmed experimentally [9], it was not apparent how the separation efficiency was affected by the addition of other separands to the original two-component mixture. This is an important problem for practical samples, especially from the viewpoint of the optimization of their separation.

In order to elucidate this phenomenon, several equations were derived to express the resolution time of strong electrolytes, which are free from dependence of the effective mobility on pH. The separation process of a mixture of SPADNS, monochloroacetic acid, picric acid and 2,4-dihydroxybenzoic acid was analysed to examine our conclusions based on computer simulation. A new scanning ultraviolet (UV) spectrophotometric detection system was utilized for the direct observation of the separation process [10]. The observed tendency of the separation efficiency was compared with the simulated data.

THEORETICAL

Assume a two-component mixture consisting of strong electrolytes. The separand ions, A and B, are monovalent and ion A is more mobile than ion B. The resolution time of the mixed zone AB can be expressed as follows [4,5]:

$$t_{res,AB} = \frac{l_A}{V_{ITP} - V_{A/AB}} = \frac{l_A}{E_A\bar{m}_A - E_{AB}\bar{m}_{B,AB}} \tag{1}$$

where l_A is the zone length of the separand A in a separation tube at the steady state, V_{ITP} the isotachophoretic velocity, $V_{A/AB}$ the velocity of the boundary between zones A and AB, E_A the potential gradient of zone A at the steady state, $\bar{m}_A$ the effective mobility of ion A in zone A at the steady state, E_{AB} the potential gradient of the mixed zone AB and $\bar{m}_{B,AB}$ the effective mobility of ion B in zone AB. The zone length l_A is linearly proportional to the sample amount [1–3], which is expressed as follows using the time-based zone length t_A [3,11] and the isotachophoretic velocity $E_A\bar{m}_A$:

$$l_A = t_A E_A \bar{m}_A = \frac{Fn_A}{i}(1 + m_Q/m_A)E_A\bar{m}_A \tag{2}$$

where F is the Faraday constant, n_A the molar amount of component A, i the migration current and m_Q the mobility of the counter ion as the pH buffer in the steady zone of A. Combination of eqns. 1 and 2 yields

$$t_{res,AB} = \frac{Fn_A}{i}(1 + m_Q/m_A)\frac{E_A\bar{m}_A}{(E_A\bar{m}_A - E_{AB}\bar{m}_{B,AB})} \tag{3}$$

As E_A and $\bar{m}_A$ are quantities at the steady state, they are independent of coexisting components. Also, in this particular case of a strong electrolyte, $\bar{m}_{B,AB}$ will have almost the same value as the effective mobility of ion B[a] at the steady state and will not be affected by the sample composition. Therefore, the possibility of causing a change in $t_{res,AB}$ must result from a change in E_{AB} or the specific conductivity of the mixed zone. These values may be affected by the molar amount and the mobility of the coexisting ionic components in a sample. Our purpose in this section is to derive the equations that express how E_{AB} and the resolution time are affected by the sample composition.

From the moving boundary equation [12], E_{AB} is exactly correlated with E_A as follows:

$$E_{AB} = \frac{\bar{m}_A C_A^t}{\bar{m}_{A,AB} C_{A,AB}^t + \bar{m}_{B,AB}(C_A^t - C_{A,AB}^t)} \cdot E_A \tag{4}$$

where $\bar{m}_{A,AB}$ is the effective mobility of the separand A in the zone AB, C_A^t the total molar concentration of A in the partly separated steady-state zone and $C_{A,AB}^t$ is that in the mixed zone AB.

The potential gradient of the mixed zone is closely related to the composition of the zone. The concentration ratio of the two components in the mixed zone is expressed as follows using the concentration and mobility in the injected solution (I) [13]:

$$\frac{C_{B,AB}^t}{C_{A,AB}^t} = \frac{\bar{m}_{A,AB}\bar{m}_{B,I} C_{B,I}^t}{\bar{m}_{B,AB}\bar{m}_{A,I} C_{A,I}^t} \tag{5}$$

In the present equimolar case for strong electrolytes, the ratio is regarded as unity. Further, as a first approximation, the following equation is valid for the two-component mixed zone AB:

$$C_{A,AB}^t + C_{B,AB}^t = C_A^t \tag{6}$$

$$C_{A,AB}^t = C_A^t/2 \tag{7}$$

As the separands are strong electrolytes, the effective mobilities of ions A and B in the mixed zone may be regarded as being equal to those at the steady state, $\bar{m}_A$ and $\bar{m}_B$, if we neglect the difference in the ionic strength:

$$\bar{m}_{A,AB} = \bar{m}_A;\ \bar{m}_{B,AB} = \bar{m}_B \tag{8}$$

By inserting eqns. 5–8 into eqn. 4, one can obtain a very simplified expression for the potential gradient of the mixed zone for the two-component mixture:

$$E_{AB}(2) = \frac{2\bar{m}_A}{\bar{m}_A + \bar{m}_B} \cdot E_A \tag{9}$$

---

[a] In anionic analysis, the relation $pH_L < pH_A < pH_{AB} < pH_B$ is usually valid, while the separands are monovalent strong electrolytes. Therefore, this relationship is no longer a good approximation for weak electrolytes.

where the number 2 in parentheses is the number of components in the sample mixture. Then eqn. 3 is reduced to the following form:

$$t_{res,AB}(2) = \frac{Fn_A}{i}(1 + m_Q/m_A)\frac{\bar{m}_A + \bar{m}_B}{\bar{m}_A - \bar{m}_B} \quad (10)$$

Apparently from eqn. 10, the resolution time is the time-based zone length multiplied by the ratio of the sum to the difference of the mobilities of separands. With strong electrolytes, the effective mobility in eqn. 10 can be replaced with the absolute mobility. Mikkers *et al.* [4] concluded that the ratio of the separand mobilities is one of the most important factors affecting the separation efficiency. The same conclusion can be derived from eqn. 10. We left eqn. 10 as it was, because it seemed to be straightforward.

Table I gives the resolution times of several model anions evaluated by the approximate eqn. 10, together with those simulated exactly. The mobility of ion A was $60 \cdot 10^{-5}$ and $30 \cdot 10^{-5}$ $cm^2\ V^{-1}\ s^{-1}$ and the mobility difference between ions A and B was in the range $1 \cdot 10^{-5}$–$10 \cdot 10^{-5}$ $cm^2\ V^{-1}\ s^{-1}$. The leading ion was 10 m*M* chloride and the mobility was $79.08 \cdot 10^{-5}$ $cm^2\ V^{-1}\ s^{-1}$. The pH of the leading electrolyte was 6 and the pH buffer used was histidine ($m_Q = 29.6 \cdot 10^{-5}$ $cm^2\ V^{-1}\ s^{-1}$, $pK_a = 6.04$). The validity of eqn. 10 as a first approximation is obvious from Table I, as the deviation is less than 10%.

Figs. 1 and 2 were plotted for convenience of a rapid calculation of the resolution time of a two-component mixed zone, where the mobility of the first appearing separand (m_A) was varied in the range $15 \cdot 10^{-5}$–$75 \cdot 10^{-5}$ $cm^2\ V^{-1}\ s^{-1}$ and the mobility difference in the range 0–$10 \cdot 10^{-5}$ $cm^2\ V^{-1}\ s^{-1}$. Fig. 1 shows the exactly simulated resolution time in the range 0–2000 s. In Fig. 2, time scale was expanded. The other operational conditions for Figs. 1 and 2 were the same as those in Table I. Apparently from Figs. 1 and 2, the resolution time decreased with decrease in the

TABLE I

EXACTLY SIMULATED AND APPROXIMATELY EVALUATED RESOLUTION TIMES OF TWO-COMPONENT MIXTURES OF SEVERAL MODEL ANIONS

m_A, m_B = Absolute mobilities of model anions (A and B) ($\times 10^5$ $cm^2\ V^{-1}\ s^{-1}$). Amount of separands = 10 nmol. Migration current = 100 μA. Approximate resolution time was evaluated using eqn. 10. Leading electrolyte: 10 m*M* HCl–histidine (pH 6).

m_A/m_B	Resolution time (s)		
	Exact	Approximate	Difference (%)
60/59	1614	1715	6.3
60/58	803	850	5.9
60/55	316	331	4.7
60/50	153	158	3.3
30/29	1050	1131	7.7
30/28	521	556	6.7
30/25	203	211	3.9
30/20	97	96	−1.0

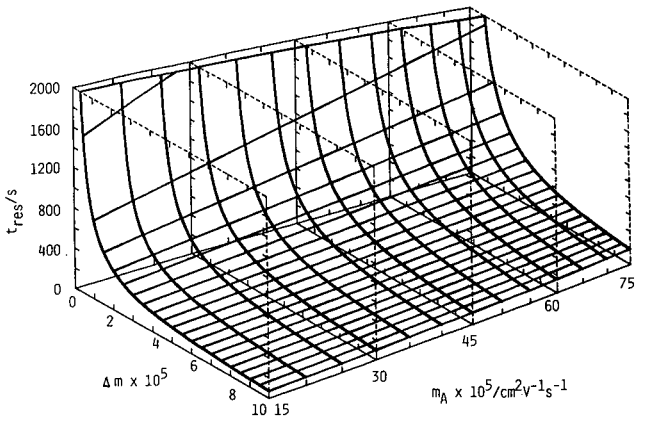

Fig. 1. Resolution time of an equimolar two-component mixture of model anions, A and B. m_A = Mobility of the first appearing ion; Δm = mobility difference between the separands; t_{res} = resolution time of the mixed zone. The amount of each separand was 10 nmol. Leading electrolyte, 10 m*M* HCl–histidine (pH 6); migration current, 100 μA.

mobility of the first appearing separand, when the mobility difference of the separands was constant.

We shall now consider a three-component mixture in order to establish the effect of a third component added to a two-component mixture. It should be borne in mind that the analytical amount of the original two components is equimolar and it is kept constant during the following treatment. There are two cases concerning the mobility order: $m_A > m_B > m_C$ or $m_C > m_A > m_B$. In the former the resolution time is expressed by eqn. 1 and in the latter it is expressed as follows [9]:

$$t_{res,AB} = \frac{l_B}{E_{AB}\bar{m}_{A,AB} - E_B\bar{m}_B} \qquad (1')$$

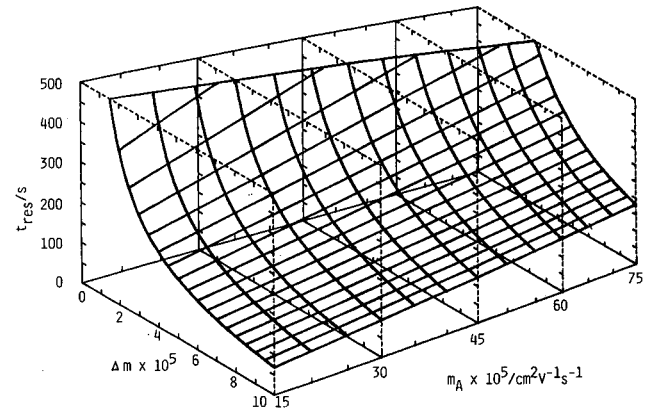

Fig. 2. Resolution time of an equimolar two-component mixture of model anions, A and B. Operational conditions as in Fig. 1.

As shown later, the extent of the increase in the resolution time with the addition of the third component was similar in both cases. However, it should be noted that the direction of the change of E_{AB} that causes the increase is different in the two cases.

The concentration ratio of separands A and B in the mixed zone AB is exactly expressed as follows in both cases [9]:

$$\frac{C^t_{B,AB}}{C^t_{A,AB}} = \frac{F_1 \bar{m}_{A,AB} \bar{m}_{B,I} C^t_{B,I}}{F_2 \bar{m}_{B,AB} \bar{m}_{A,I} C^t_{A,I}} \tag{11}$$

$$F_1 = \frac{(\bar{m}_{C,ABC} - \bar{m}_{B,ABC})}{\bar{m}_{C,ABC} E_{ABC} - \bar{m}_{B,AB} E_{AB}} \tag{12}$$

$$F_2 = \frac{(\bar{m}_{C,ABC} - \bar{m}_{A,ABC})}{m_{C,ABC} E_{ABC} - \bar{m}_{A,AB} E_{AB}} \tag{13}$$

where the subscript ABC denotes the three-component mixed zone. The only possibility of changing E_{AB} is to change the ratio $C^t_{B,AB}/C^t_{A,AB}$ from the value for the two-component mixture, because it causes a change in the conductivity of the mixed zone ($m_A \neq m_B$). Combining eqns. 11–13 and the following relationship between E_{ABC} and E_{AB} obtained from the moving boundary equation:

$$E_{ABC} = \frac{\bar{m}_{A,AB} C^t_{A,AB}}{\bar{m}_{C,ABC} C^t_{A,AB} + (\bar{m}_{A,ABC} - \bar{m}_{C,ABC}) C^t_{A,ABC}} \cdot E_{AB} \tag{14}$$

one can rewrite eqn. 11, inserting eqn. 14 into eqns. 12 and 13, as follows:

$$\frac{C^t_{B,AB}}{C^t_{A,AB}} = \frac{\bar{m}_A(\bar{m}_B - \bar{m}_C) C^t_{A,ABC}}{\bar{m}_C(\bar{m}_B - \bar{m}_A) C^t_{A,AB} + \bar{m}_B(\bar{m}_A - \bar{m}_C) C^t_{A,ABC}} \tag{15}$$

This non-linear equation can be solved by combination with eqn. 5 and the following assumption for an equimolar three-component mixture:

$$C^t_{A,ABC} = C^t_A/3 \tag{16}$$

Consequently, the following equation is obtained for the ratio of the concentrations:

$$\frac{C^t_{B,AB}}{C^t_{A,AB}} = \frac{C^t_A - C^t_{A,AB}}{C^t_{A,AB}} \equiv R_C \tag{17}$$

$$C^t_{A,AB} = \frac{-Q + SG(Q^2 - 4PR)^{1/2}}{2P} \tag{18}$$

$SG = 1$ for $\bar{m}_A > \bar{m}_B > \bar{m}_C$; $SG = -1$ for $\bar{m}_C > \bar{m}_A > \bar{m}_B$

$$P = 3\bar{m}_C(\bar{m}_B - \bar{m}_A) \tag{19}$$

$$Q = 2(\bar{m}_A\bar{m}_B - 2\bar{m}_B\bar{m}_C + \bar{m}_A\bar{m}_C)C_A^t \tag{20}$$

$$R = -\bar{m}_B(\bar{m}_A - \bar{m}_C)C_A^{t\,2} \tag{21}$$

This ratio is referred to as R_C hereafter. The value of R_C was larger than 1 when $m_A > m_B > m_C$ and less than 1 when $m_C > m_A > m_B$.

Eqn. 4 is also valid for a three-component mixture. C_{AB}^t in eqn. 4 is expressed using the concentration ratio as follows:

$$C_{A,AB}^t = C_A^t/(R_C + 1) \tag{22}$$

Combination of eqns. 4 and 22 gives the potential gradient of the mixed zone AB formed in the separation process of the three-component mixture, $E_{AB}(3)$, as follows:

$$E_{AB}(3) = \frac{\bar{m}_A(R_C + 1)}{\bar{m}_A + \bar{m}_B R_C} \cdot E_A \qquad m_A > m_B > m_C \tag{23}$$

$$= \frac{\bar{m}_B(R_C + 1)}{\bar{m}_A + \bar{m}_B R_C} \cdot E_B \qquad m_C > m_A > m_B \tag{23'}$$

$E_{AB}(3)$ is larger than $E_{AB}(2)$ in eqn. 9 when $m_A > m_B > m_C$ and smaller than $E_{AB}(2)$ when $m_C > m_A > m_B$. Consequently, the resolution time of the mixed zone formed in the separation process of the three-component mixture can be expressed as follows:

$$t_{res,AB}(3) = \frac{Fn_A}{i}(1 + m_Q/m_A)\frac{\bar{m}_A + R_C\bar{m}_B}{\bar{m}_A - \bar{m}_B} \qquad m_A > m_B > m_C \tag{24}$$

$$= \frac{Fn_B}{i}(1 + m_Q/m_B)\frac{\bar{m}_A/R_C + \bar{m}_B}{\bar{m}_A - \bar{m}_B} \qquad m_C > m_A > m_B \tag{24'}$$

As R_C for the three-component mixture was larger than 1 when $m_A > m_B > m_C$ and less than 1 when $m_C > m_A > m_B$, it is apparent that $t_{res,AB}(3)$ was always larger than $t_{res,AB}(2)$. The ratio of the resolution time, R_t, is expressed as follows:

$$R_t = \frac{t_{res,AB}(3)}{t_{res,AB}(2)}$$

$$= \frac{\bar{m}_A + R_C\bar{m}_B}{\bar{m}_A + \bar{m}_B} \qquad m_A > m_B > m_C \tag{25}$$

$$= \frac{\bar{m}_A/R_C + \bar{m}_B}{\bar{m}_A + \bar{m}_B} \qquad m_C > m_A > m_B \tag{25'}$$

For a sample mixture consisting of four or more separands, the resolution time of the mixed zone AB is also given by eqn. 24, although the mathematical expression of R_C

become complicated. The essential fact is that the effect of the addition of the fourth component is smaller than that of the third component, as shown later.

The separation efficiency in isotachophoresis is defined as the current efficiency in the separation. Therefore, it is closely related to the molar amount of separated sample/electric charges in coulombs. Mikkers *et al.* [4,5] defined the separation number (S) to discuss the separation efficiency as follows:

$$S = \frac{F}{i} \cdot \frac{n_A}{t} = \frac{F}{i} \cdot \frac{n_A}{t_{res,AB}} \tag{26}$$

Inserting eqn. 24 into eqn. 26 gives the following different expression for S for the case when $m_A > m_B > m_C$:

$$S = \frac{m_A}{m_A + m_Q} \cdot \frac{\bar{m}_A - \bar{m}_B}{\bar{m}_A + R_C \bar{m}_B} \tag{27}$$

S decreases with the addition of the other components. It should be noted that S is independent of the migration current.

EXPERIMENTAL

Samples

The samples used were 4,5-dihydroxy-3-(*p*-sulphophenylazo)-2,7-naphthalene-disulphonic acid (SPADNS), monochloroacetic acid (MCA), picric acid (PA) and 2,4-dihydroxybenzoic acid (DBA). Except for MCA, these samples absorb visible light (SPADNS and PA) and UV radiation (SPADNS, PA and DBA). The sodium salt of SPADNS was purchased from Dojin (Tokyo, Japan) in the purest form and the other compounds were obtained from Tokyo Kasei (Tokyo, Japan) (extra-pure grade), and were used as received. Stock sample solutions (10 mM) were prepared by dissolving the compounds in distilled water.

In order to confirm the above estimation, the separation processes of the following three equimolar mixtures were observed individually and the resolution times were compared with each other: (1) SM = SPADNS–MCA, (2) SMP = SPADNS–MCA–PA and (3) SMPD = SPADNS–MCA–PA–DBA. The pH of these solutions was adjusted to 3.6 by adding β-alanine.

Apparatus

Instead of a fixed detection system with an array of 32 equidistant UV detectors arranged along a separation tube [13], an isotachophoretic analyser with a scanning UV spectrophotometric detection system was used [10]. A fused-silica capillary of O.D. 0.66 mm and I.D. 0.53 mm (Gasukuro Kogyo, Tokyo, Japan) as the separation tube was scanned repeatedly over a length of 32 cm and the UV signals (position spectra of migrating zones) were acquired. A linear head equipped with a stepping motor was used to move the assembly of a deuterium UV lamp and a silicon photodiode detector. The UV radiation from the deuterium lamp was passed through a UV glass filter (λ_{max} = 330 nm). A single cycle of scanning took 7.025 s and 5333

photometric signals were acquired through an analogue-to-digital converter. The resolution was 0.06 mm per data point, which was sufficient to trace the separation process accurately. For data acquisition, an NEC (Tokyo, Japan) PC9801VX microcomputer was used (80286–80287, clock 10 MHz). All experiments were carried out at 25°C. The details of this apparatus have been described previously [10].

Operational electrolyte system

The concentration of the leading electrolyte (hydrochloric acid) was 5 m*M*. The pH was adjusted to 3.6 by adding β-alanine. The terminator was 10 m*M* caproic acid. Hydroxypropylcellulose (HPC, 0.2%) was added to the leading and terminating electrolytes to suppress electroendosmosis. The viscosity of the 2% aqueous solution is 1000–4000 cP at 20°C according to the specification. The sample solution was injected into the terminating electrolyte near the boundary between the leading and terminating electrolytes. The pH of the terminating electrolyte was also adjusted to 3.6 by adding β-alanine to ensure that the pH of the sample solution at the initial stage of migration was equal to the prepared value. The pH measurements were carried using a Horiba (Tokyo, Japan) Model F7ss expanded pH meter.

Simulation

Two different methods for the simulation of the transient state have been reported [8]. One is based on solving a set of partial differential equations applying a suitable approximation [14–17] and the other is a direct analytical method to solve several simultaneous equations which should be satisfied in the mixed zones [4,5,7,18]. Using the latter approach, we have recently established a calculation method for the simulation of the isotachophoretic transient state of a sample mixture consisting of up to six separands. Although the complexity of the computational procedure increased considerably with increase in the number of separands, the concept of the simulation on the basis of the MSPR model was essentially the same as that reported for a three-component mixture [9]. In the analysis of a six-component mixture consisting of ions A, B, C, D, E and F, for example, iterative calculations were made until the *RFQ* functions [1,7] of the mixed zones AB, ABC, ABCD, ABCDE and ABCDEF were less than 10^{-5} simultaneously, and the other zones were analysed successively.

Appropriate initial properties of the mixed zones such as the separand concentrations were necessary for the smooth convergence of the iterative calculation. For example, when the transient zones of six separands are analysed, the calculation starts from the analysis for the two-component mixture, next the three component mixture, and so on until finally the six-component mixture was analysed using the results for the five-component mixture as the initial values. Therefore, the time needed for calculation increased progressively with increase in the number of separands. The previous computer code SIPSR was rewritten in Microsoft QUICK BASIC (the program size was 400 kB, the essential part being 150 kB). By use of an NEC PC-9801RA2 microcomputer (CPU 80386, coprocessor 80387, clock 16 MHz), it took several seconds for the two-separand analysis and about 6 min for the six-separand analysis.

RESULTS AND DISCUSSION

Simulation

The resolution time of a two-component mixed zone in a three-component mixture was evaluated for model anions by varying the mobility and the molar amount of the third component. The mobilities of two of the three separands, A and B, were fixed at $50 \cdot 10^{-5}$ and $45 \cdot 10^{-5}$ cm^2 V^{-1} s^{-1}. The sample amount was equimolar (50 nmol). The mobilities and the amounts were fixed throughout this study. The leading electrolyte used for the simulation was 10 m*M* hydrochloric acid buffered at pH 6 by adding histidine. According to the simulation of the separation process for a two-component mixture, the concentration ratio R_C was unity (*i.e.*, $C^t_{A,AB} = C^t_{B,AB}$), the potential gradient E_{AB} was 88.80 V cm^{-1} and the resolution time ($t_{res,AB}$) was 1387s (I.D. of the separation tube = 0.5 mm, migration current = 100 μA). As discussed above, these characteristics of the mixed zone AB were affected by the addition of the third component. The mobility of the third component, ion C, was assumed to be in the range $70 \cdot 10^{-5}$–$51 \cdot 10^{-5}$ cm^2 V^{-1} s^{-1} ($m_C > m_A > m_B$) and $44 \cdot 10^{-5}$–$10 \cdot 10^{-5}$ cm^2 V^{-1} s^{-1} ($m_A > m_B > m_C$). It should be noted the formulation in this paper is limited to the latter case. The amount of ion C was varied as 25, 50, 100 and 200 nmol.

Figs. 3 and 4 show the simulated values of the concentration ratio R_C (eqn. 17) and the potential gradient of the mixed zone, E_{AB}(3), in the mixed zone AB. As expected, the ratio R_C depended significantly on the mobility and the amount of the third component C. When $m_A > m_B > m_C$, R_C was always greater than 1, *i.e.*, $C^t_{A,AB} < C^t_{B,AB}$, and less than 1 when $m_C > m_A > m_B$. In both cases, the deviation of R_C from unity was large when C was large and m_C was close to m_A or m_B. The change in R_C led to a change in the specific conductivity of the mixed zone AB. As the migration current was kept constant (100 μA), the potential gradient E_{AB} varied with the conductivity of the zone. The curves in Fig. 3 and 4 are the best-fitted functions using tanh functions.

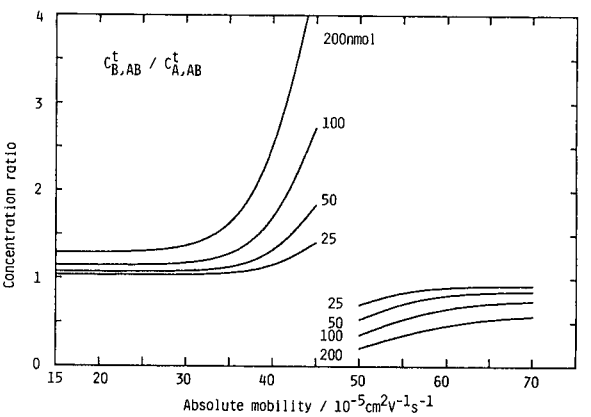

Fig. 3. Simulated dependence of concentration ratio $R_C = C^t_{B,AB}/C^t_{A,AB}$ on the molar amount and the mobility of the third component. The mobilities of two of the three separands, A and B, were fixed at $50 \cdot 10^{-5}$ and $45 \cdot 10^{-5}$ cm^2 V^{-1} s^{-1} and the sample amount was equimolar (50 nmol). m_C = Mobility of the added third component, ion C. The I.D. of the separation tube was assumed to be 0.5 mm. Operational conditions as in Fig. 1.

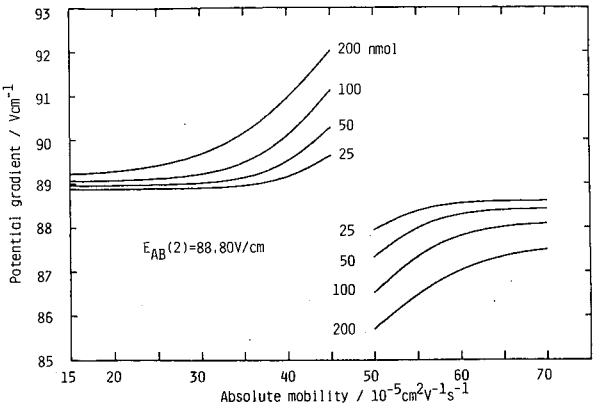

Fig. 4. Simulated dependence of the potential gradient of the mixed zone, E_{AB}, on the molar amount and the mobility of the third component. The I.D. of the separation tube was assumed to be 0.5 mm and the migration current was 100 μA. For other conditions see Fig. 3.

Fig. 5 shows the dependence of the increase in resolution time on mobility in terms of the ratio of resolution time R_t (eqn. 25). It should be noted that the increase was linear with respect to the molar amount of the third separand but not with respect to the mobility. Thus a large increase in the resolution time was observed when the mobility of the third separand was close to that of the original components. When 50 nmol of a component with a mobility of $51 \cdot 10^{-5}$ cm^2 V^{-1} s^{-1} and $46 \cdot 10^{-5}$ cm^2 V^{-1} s^{-1} was added to the original pair, respectively, the resolution time of the original pair was increased to 1943 s (R_t = 1.40) and 1884 s (R_t = 1.36). On the other hand, if the mobility of the third separand was far from that of the original sample, the increase in the resolution time was not as great.

Fig. 6 shows the separation diagrams simulated for the two- to six-component mixtures, which obey the separation diagram proposed by Brouwer and Postema [18].

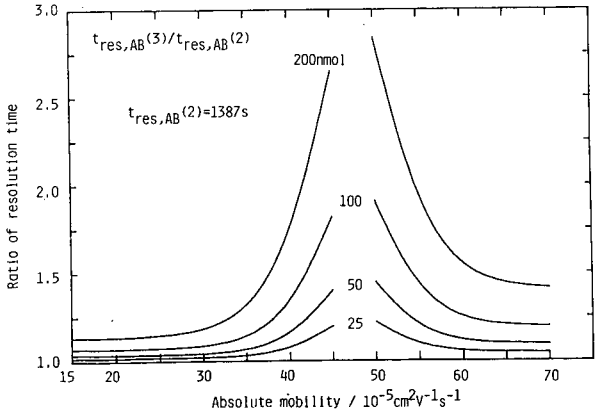

Fig. 5. Dependence of mobility on the ratio of resolution time, R_t = ($t_{res,AB}$ of the three-component mixture)/$t_{res,AB}$ of the two-component mixture). See caption to Fig. 3. Operational conditions as in Fig. 1.

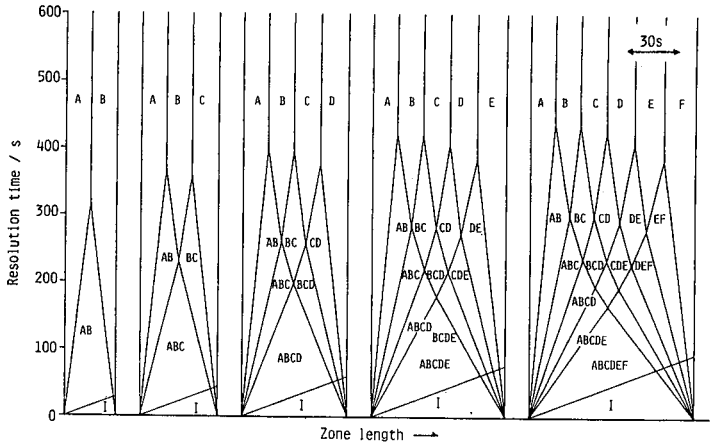

Fig. 6. Separation diagrams simulated for equimolar anions (A–F) with mobilities of $60 \cdot 10^{-5}$, $55 \cdot 10^{-5}$, $50 \cdot 10^{-5}$, $45 \cdot 10^{-5}$, $40 \cdot 10^{-5}$ and $35 \cdot 10^{-5}$ cm^2 V^{-1} s^{-1}. The pK_a values were assumed to be -1. The amount of each separand was 10 nmol. I represents the injected sample zone.

The mobilities of the model anions (A–F) were $60 \cdot 10^{-5}$, $55 \cdot 10^{-5}$, $50 \cdot 10^{-5}$, $45 \cdot 10^{-5}$, $40 \cdot 10^{-5}$ and $35 \cdot 10^{-5}$ cm^2 V^{-1} s^{-1}. The pK_a values were assumed to be -1. The concentration of the separands in the sample solution was 2 mM, the pH was 6 and the amount of the separands was 10 nmol. The operational electrolyte system was the same as that given in Table I. In Fig. 6, the leading and terminating zones are not shown and no mixing with samples was assumed. The potential gradients, the separand

TABLE II

RESOLUTION TIME OF SEVERAL MODEL ANIONS FOR TWO- TO SIX-COMPONENT MIXTURES

A–F = model anions with absolute mobilities of $60 \cdot 10^{-5}$, $58 \cdot 10^{-5}$, $53 \cdot 10^{-5}$, $48 \cdot 10^{-5}$, $43 \cdot 10^{-5}$ and $38 \cdot 10^{-5}$ cm^2 V^{-1} s^{-1}. The pK_a values are assumed to be -1. t_{res} = resolution time; $R_t = (t_{res}$ of two-component mixed zone in multi-component mixture)$/t_{res}(2)$. Leading electrolyte: 10 mM HCl–histidine (pH 6).

Parameter	Mixed zone	No. of separands				
		2	3	4	5	6
t_{res}	AB	803	868	904	928	945
	BC	308	407	445	469	485
	CD	289		403	432	452
	DE	270			406	430
	EF	251				404
R_t	AB	1.00	1.08	1.13	1.16	1.18
	BC	1.00	1.32	1.44	1.52	1.57
	CD	1.00		1.39	1.49	1.56
	DE	1.00			1.50	1.59
	EF	1.00				1.61

concentrations, the resolution time, etc., of the two-component mixed zones are summarized in Table II together with those of the zones at the steady state.

Apparently from Fig. 6 and Table II, the resolution time of each two-component mixed zone increased with increase in the number of components in the mixture. Although this simulation is a special case for an equimolar mixture, the dependence of the resolution time on the number of components is easily calculated from the behaviour of R_t in Fig. 5. Thus, the perturbation of the separation efficiency of the two components of interest caused by the addition of the other components can be discussed from the viewpoint of the number of separands in the mixture if the mixture is equimolar. When the mobility difference of neighbouring separands is appropriate, a considerable number of equimolar separands can be separated by isotachophoresis. For example, when the mobility of the terminating ion is $10 \cdot 10^{-5}$ cm^2 V^{-1} s^{-1}, that of the most mobile ion is $75 \cdot 10^{-5}$ cm^2 V^{-1} s^{-1} and the mobility differences among the adjacent ions are $1 \cdot 10^{-5}$ cm^2 V^{-1} s^{-1}, a mixture of 65 anions (each 10 nmol) can be separated within 3200 s (migration current = 100 μA).

Observation of separation process

In order to confirm the present estimation, the resolution time of the two-separand mixed zone of SPADNS and monochloroacetic acid was measured for SPADNS, monochloroacetic acid, picric acid and 2,4-dihydroxybenzoic acid, and was compared with the results of simulation. Fig. 7 shows the transient isotachopherogram obtained with the scanning UV detector [10]. Fig. 7A shows the separation of SPADNS and monochloroacetic acid (concentration = 5 mM, volume injected = 5 μl), Fig. 7B that of SPADNS, monochloroacetic acid and picric acid (3.3 mM, 7.5 μl) and Fig. 7C that of SPADNS, monochloroacetic acid, picric acid and 2,4-dihydroxybenzoic acid (2.5 mM, 10 μl), referred to hereafter as SM, SMP and SMPD, respectively. The amount of each separand was the same (25 nmol). In these experiments, SPADNS and monochloroacetic acid corresponded to the model anions A and B.

The leading electrolyte was 5.00 mM hydrochloric acid–β-alanine (pH 3.6) and the migration current was 49.5 μA. In Fig. 7 one can see the increase in the resolution time of the SM zone: the observed resolution time for sample SM was 1030 s, that for SMP was 1141 s and that for SMPD was 1199 s. Table III summarizes the observed resolution times for the mixed zones formed in the separation process and the ratio with respect to two-separand mixed zones. Good agreement was obtained, confirming the present estimation. The method of evaluation of the resolution time and the boundary velocity was detailed in ref. 7.

In conclusion, the composition of the sample has a considerable effect on the separation efficiency of the two-component mixed zone of interest. To increase the separation efficiency, the amount of the coexisting components should be minimized, especially coexisting components having a similar mobility to the components of interest.

In the isotachophoretic analyser, a sample mixture is injected into the leading electrolyte or the terminating electrolyte. Apparently from Fig. 5, the mixing between the sample solution and the operational electrolyte should be minimized for a good separation efficiency. The present simulation was carried out on the assumption that the sample solution was injected ideally between the leading and terminating electrolytes, *i.e.*, the formation of a mixed zone between the samples and the leading

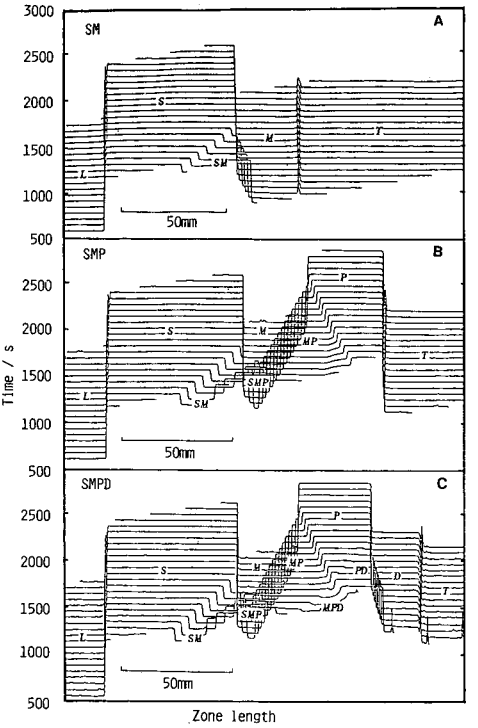

Fig. 7. Observed separation process of (A) SPADNS and monochloroacetic acid (concentration = 5 m*M*, volume injected = 5 μl), (B) SPADNS, monochloroacetic acid and picric acid (3.3 m*M*, 7.5 μl) and (C) SPADNS, monochloroacetic acid, picric acid and 2,4-dihydroxybenzoic acid (2.5 m*M*, 10 μl) using the scanning UV detector. Leading electrolyte, 5.00 m*M* HCl–β-alanine (pH 3.6); terminating electrolyte, 10 m*M* caproic acid; migration current, 49.5 μA.

TABLE III

RESOLUTION TIMES OF MIXED ZONES OBSERVED WITH THE UV SCANNING DETECTOR AND SIMULATED VALUES

S,M,P,D = sample anions: S = SPADNS; M = monochloroacetic acid; P = picric acid; D = 2,4-dihydroxybenzoic acid. The amount of each was 25 nmol. t_{res} = resolution time (s); figures in parentheses are simulated values; R_t = (t_{res} of two-component mixed zone in multi-component mixture)/t_{res}(2). Leading electrolyte: 5.00 m*M* HCl–β-alanine (pH 3.6). Migration current: 49.5 μA.

Parameter	Mixed zone	Sample system		
		SM	SMP	SMPD
t_{res}	SM	1030 (1156)	1141 (1265)	1199 (1306)
	MP	–	1860 (1975)	1896 (1915)
	PD	–	–	1469 (1514)
	SMP	–	955 (1035)	1014 (1075)
	MPD	–	–	1110 (1153)
R_t	SM	1.00 (1.00)	1.11 (1.09)	1.16 (1.13)
	MP	–	1.00 (1.00)	1.02 (1.03)

electrolyte and a mixed zone between the samples and the terminating electrolyte was not taken into account. In an actual analysis, this will lower the separation efficiency.

In the separation of a multi-component mixture, it should be noted that the differences between the potential gradients of the separated adjacent zones were small (*ca.* 1 V cm^{-1} for the previous 65 model anions), and the difference may be much smaller in the separation process. This suggests that the self-restoring capability is low. Hence such a complex sample mixture may be easily perturbed by a flow along the capillary axis due to, for example, electroendosmosis.

ACKNOWLEDGEMENT

T.H. expresses his thanks to the Ministry of Education, Science and Culture of Japan for support of part of this work under a Grant-in-Aid for Scientific Research (No. 1540482).

REFERENCES

1 F. M. Everaerts, J. L. Beckers and Th. P. E. M. Verheggen, *Isotachophoresis—Theory, Instrumentation and Applications* (*Journal of Chromatography Library*, Vol. 6), Elsevier, Amsterdam, 1976.
2 P. Bocek, M. Deml, P. Gebauer and V. Dolnik, *Analytical Isotachophoresis*, VCH, Weinheim, 1988.
3 T. Hirokawa, M. Nishino, N. Aoki, Y. Kiso, Y. Sawamoto, T. Yagi and J. Akiyama, *J. Chromatogr.*, 271 (1983) D1.
4 F. E. P. Mikkers, F. M. Everaerts and J. A. F. Peek, *J. Chromatogr.*, 168 (1979) 293.
5 F. E. P. Mikkers, F. M. Everaerts and J. A. F. Peek, *J. Chromatogr.*, 168 (1979) 317.
6 P. Bocek and P. Gebauer, *Electrophoresis*, 5 (1984) 338.
7 T. Hirokawa, K. Nakahara and Y. Kiso, *J. Chromatogr.*, 463 (1989) 51.
8 W. Thormann, *Sep. Sci. Technol.*, 19 (1984) 455.
9 T. Hirokawa, K. Nakahara and Y. Kiso, *J. Chromatogr.*, 470 (1989) 21.
10 T. Hirokawa, Y. Yokota and Y. Kiso, *J. Chromatogr.*, 538 (1991) 403.
11 T. Hirokawa and Y. Kiso, *J. Chromatogr.*, 260 (1983) 225.
12 R. A. Alberty, *J. Am. Chem. Soc.*, 72 (1950) 2361.
13 T. Hirokawa, K. Nakahara and Y. Kiso, *J. Chromatogr.*, 463 (1989) 39.
14 G. T. Moore, *J. Chromatogr.*, 106 (1975) 1.
15 M. Bier, O. A. Palusinski, R. A. Mosher and D. A. Saville, *Science*, 219 (1983) 1281.
16 V. Fidler, J. Vacik and Z. Fidler, *J. Chromatogr.*, 320 (1985) 167.
17 P. Radi and E. Schumacher, *Electrophoresis*, 6 (1985) 195.
18 G. Brouwer and G. A. Postema, *J. Electrochem. Soc.*, 117 (1970) 874.

Journal of Chromatography, 545 (1991) 283–297
Elsevier Science Publishers B.V., Amsterdam

CHROM. 23 145

Isotachophoresis in open systems

Problems in quantitative analysis

M. T. ACKERMANS*, F. M. EVERAERTS and J. L. BECKERS
Laboratory of Instrumental Analysis, Eindhoven University of Technology, P.O. Box 513, 5600 MB Eindhoven (The Netherlands)

ABSTRACT

So far, isotachophoretic (ITP) analyses have been carried out in commercially available or laboratory-made ITP instruments, generally in closed systems. At present several instruments are commercially available, originally designed for capillary zone electrophoresis with open capillaries, and these instruments can also be used for ITP. If ITP experiments are carried out using such apparatus, however, an electroosmotic flow (EOF) will act on the ITP system. The velocity of the EOF strongly varies with the choice of the leading electrolyte and terminating electrolyte and also the composition of the sample. Hence the reproducibility in quantitative analyses is a serious problem. For quantitative experiments at least an internal standard must be used to correct for undesirable fluctuations in the EOF and irreproducible injections. Better results can be obtained by effectively suppressing the EOF by using additives such as methylhydroxyethylcellulose. Results of quantitative experiments using the Beckman P/ACE System 2000 HPCE are presented, showing some of the problems in quantitative analyses with ITP in open capillaries.

INTRODUCTION

Generally, electrophoretic equipment can be used for all electrophoretic modes, *viz.*, for isotachophoresis (ITP), zone electrophoresis (ZE), moving boundary (MB) and isoelectric focusing (IEF). The choice of the electrolytes in the capillary and electrode compartments determines which electrophoretic mode is applicable, *e.g.*, for the ZE mode a background electrolyte and for ITP a leading and terminating electrolyte will be used.

So far, ITP has usually been carried out in laboratory-made [1] or commercially available apparatus with closed systems, *i.e.*, no electroosmotic flow (EOF) acts. At present, commercial apparatus for CZE is available, generally with open capillaries. Because this equipment can also be used for ITP, it is of interest to investigate the possibilities of ITP in open systems.

Hjerten *et al.* [2] carried out displacement electrophoresis experiments in glass capillaries, which were coated to suppress the EOF and adsorption of the solutes on the tube wall. Udseth *et al.* [3] reported experiments with tandem ITP–mass spectrometry and showed that the separation was not disturbed by the EOF. They recog-

0021-9673/91/$03.50

nized that during the analysis the velocity of the EOF is not constant and is first determined by the composition of the leading electrolyte and finally by that of the terminating solution. Thormann [4] studied the impact of electroosmosis on zone formation and displacement and described anionic and cationic separations in open capillary systems. Recently Beckers *et al.* [5] adapted a mathematical model for the calculation of parameters for the different zones in ITP without EOF, for application to ITP with EOF, and it was concluded that these models are identical because the effects of the EOF cancel each other in all equations.

Four modes can be distinguished in ITP with EOF, *viz.*, the anionic (AM) and cationic modes (CM) and the reversed-anionic (RAM) and reversed-cationic modes (RCM). For the reversed modes the isotachophoretic velocity is directed away from the detector but the isotachophoretic system has a net velocity in the direction of the detector owing to the large velocity of the EOF. In the reversed modes the components are detected in a reversed order, *i.e.*, first the terminator, then the sample components with increasing mobilities and finally the leading zone [4,5].

Whether a specific mode can be applied depends on the velocity of the ITP system and of the EOF. Generally, the velocity of the EOF changes during ITP analyses because the capillary is filled more and more with the terminating solution, which has an EOF different from that of the leading electrolyte. Therefore, the ITP system sometimes comes to a standstill if during the analyses the velocity of the EOF counteracts the isotachophoretic velocity and increases until the net migration of the ITP system becomes zero.

In this paper we present data concerning quantitative experiments and discuss some problems in quantitative analyses.

EXPERIMENTAL

For all ITP experiments in open systems the Beckman P/ACE System 2000 HPCE (Palo Alto, CA, U.S.A.) was used, applying UV detection at 254 nm for all cationic and at 214 nm for all anionic analyses. All experiments were carried out at 25°C applying a constant direct current, using an original Beckman capillary of 57 cm, with a distance between injection and detection of 50 cm and an I.D. of 75 μm. For further information concerning the apparatus, see ref. 6.

For ITP experiments in the cationic mode (CM) the capillary is filled with the leading electrolyte L, while the terminating solution T must be present at the inlet of the apparatus. The sample solution is introduced between L and T by pressure injection. The detector and cathode are placed at the outlet and the anode at the inlet. For ITP experiments in the anionic mode (AM) the cathode is placed at the inlet side and the anode at the outlet. The capillary is filled with the leading electrolyte and the terminator is present at the inlet.

For all ITP experiments with closed systems, a laboratory-built apparatus, with conductivity and UV detectors, was used as described previously [1]. In this apparatus, the closed system is obtained by shielding the separation capillary from the open electrode compartments with semipermeable membranes. Note that a PTFE capillary tube (0.2 mm I.D.) is used, in contrast to the fused-silica capillaries used in the Beckman apparatus.

RESULTS AND DISCUSSION

On applying ITP in closed systems, all ITP zones move with an equal velocity if the steady state is reached. As all zone concentrations are adapted to that of the leading zone, according to the Kohlrausch condition, a linear relationship is obtained between zone length and amount of sample injected. Another approach in quantitative determinations is to use the response factor [7], *RF* (C/mol), representing the slope of the calibration graph of the product of the zone length *l* (s) and applied constant electric current (A) *versus* the amount of sample (mol).

When using ITP in open systems, an EOF acts on the ITP system. Generally, the velocity of the EOF changes during ITP analyses because the capillary is filled with different electrolytes during the analyses as the terminator is migrating into the capillary. Thus the zones do not have the same velocity passing the detector and the detected zone length depends on the velocity of the EOF at the moment of detection. Non-linear calibration graphs are the result. In order to work quantitatively in ITP in open systems, the behaviour of the EOF must be understood.

Velocity of the electroosmotic flow

To obtain an impression of the velocity of the EOF we can fill, by pressure injection, the capillary alternately with the chosen electrolyte and a mixture of this electrolyte and a UV-absorbing component, without electrophoretic mobility, such as mesityl oxide (MO). Monitoring the absorbance of the equidistant EOF marker bands in the chosen electrolyte during the ITP experiment gives an idea of changes in the EOF velocity.

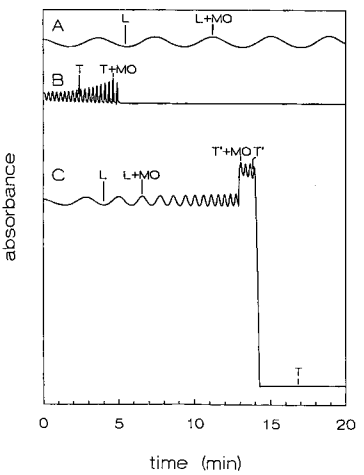

Fig. 1. Part of the electropherograms obtained by applying a constant electric current of 1.5 μA for (A) a leading electrolyte of 0.01 *M* sodium nicotinate at pH 5.4, (B) a terminating electrolyte of 0.01 *M* GABA–nicotinate at pH 5 and (C) an ITP system with a leading electrolyte L of 0.01 *M* sodium nicotinate at pH 5.4 and a terminating electrolyte T of 0.01 *M* GABA–nicotinate at pH 5. The terminating solution T′ is the modified terminating solution according to Kohlrausch's law. The electrolyte in the capillary was alternately mixed with equidistant bands of mesityl oxide (MO) in order to indicate variations in the velocity of the EOF.

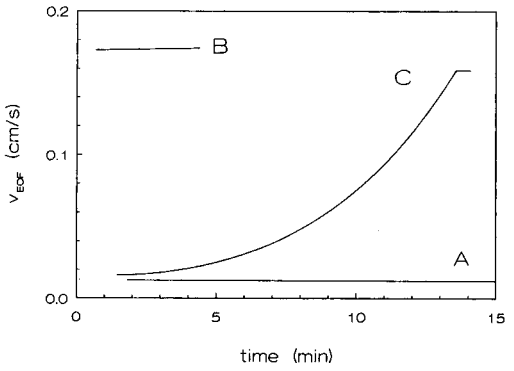

Fig. 2. Calculated velocities of the EOF, using the time intervals between the MO peaks, for the electropherograms in Fig. 1 as a function of time. The EOF velocity of (C) the ITP system varies between the values of (A) the leading and (B) the terminating electrolyte, although not linearly.

As an example to demonstrate the change in EOF during ITP experiments, in Fig. 1 the electropherograms are given for the migration in the cationic mode of (A) the leading electrolyte of 0.01 *M* NaOH at pH 5.4 adjusted by adding nicotinic acid, (B) the terminating electrolyte of 0.01 *M* γ-aminobutyric acid (GABA) at pH 5 adjusted by adding nicotinic acid and (C) the ITP experiment with the leading electrolyte sodium nicotinate and terminator GABA–nicotinate. The three experiments were carried out at a constant electric current of 1.5 μA. To visualize the change in the velocity of the EOF, we filled the capillary alternately with sodium nicotinate or GABA–nicotinate (22 s, pressure injection) and a mixture of sodium nicotinate (or GABA–nicotinate) with 0.001 *M* MO (3 s, pressure injection). From the number of MO peaks over the separation length from the inlet to the detector the distance between the equidistant peaks can be calculated and using the differences in time between the adjacent peaks the average velocity at that time can be calculated.

In Fig. 2 the calculated velocities of the EOF as function of time are given for the situations in Fig. 1. It can be clearly seen that if the capillary is filled with one electrolyte (A and B) the velocity is constant, although this velocity is much greater with GABA–nicotinate because the voltage gradient is higher at the same electric

TABLE I

VOLTAGE *V*, MIGRATION TIMES *t*, VELOCITIES *v* AND MOBILITIES $m \cdot 10^5$ OF THE EOF FOR THE LEADING ELECTROLYTE SODIUM NICOTINATE AND SEVERAL TERMINATING SOLUTIONS

Electrolyte	pH	Counter ion	*V* (kV)	*t* (min)	*v* (cm/s)	*m* (cm^2/V s)
0.01 *M* NaOH	5.4	Nicotinic acid	2.24	80.64	0.010	26.30
0.01 *M* GABA	5.0	Nicotinic acid	23.44	5.23	0.159	38.75
0.01 *M* GABA	3.5	Formic acid	2.37	119.05	0.007	16.84
0.01 *M* HIS	5.0	Nicotinic acid	3.41	59.52	0.014	23.40
0.01 *M* HIS	6.7	MES	13.89	6.46	0.129	52.94

current and the mobility of the EOF is larger owing to the low ionic concentration of the terminating solution at pH 5 (the pK value of GABA is 4.03).

If an ITP experiment is carried out (Fig. 2C) in the first instance, the velocity of the EOF is comparable to that of the original leading electrolyte L. During the analysis the terminator T is migrating into the capillary behind the leading electrolyte and the velocity of the EOF varies strongly with time until a value is reached that is comparable to that of the original terminating solution of the whole capillary if filled with that solution T. The velocity of the EOF varies during the ITP experiment, between the values for the pure leading and the terminating solutions, but this relationship is not linear. Between the leading and terminating solutions we can see the adapted terminating solution T′ according to Kohlrausch's law (Fig. 1C). The last MO peak coincides with the concentration boundary between adapted terminating T′ and original terminating T solution.

In Table I the applied voltages and migration times, velocities and calculated mobilities of the EOF are given for the leading electrolyte sodium nicotinate and several terminating solutions applied with a constant electric current of 1.5 μA. In fact the mobility of the EOF does not differ much for sodium nicotinate and GABA–nicotinate, but it must be remembered that the voltage gradients in the ITP system differ considerably between the leading and terminating solutions so that the velocity of the EOF increases very rapidly if the terminating solution fills the capillary.

From Figs. 1 and 2, it can be concluded that the velocity of the EOF changes

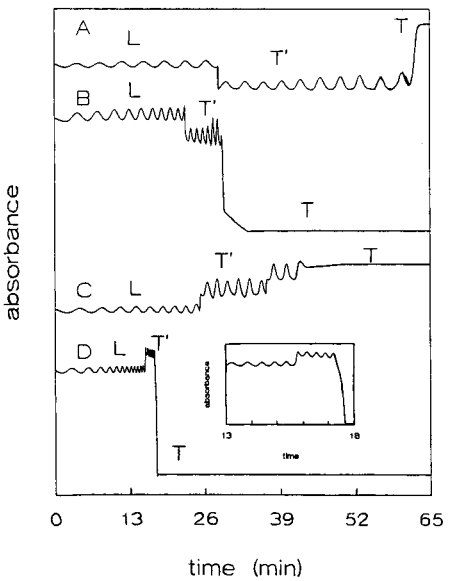

Fig. 3. Electropherograms for a leading electrolyte of sodium nicotinate at pH 5.4 applying as terminating solutions (A) 0.01 M HIS–nicotinate at pH 5, (B) 0.01 M HIS–MES at pH 6.7, (C) 0.01 M GABA–formate at pH 3.5 and (D) 0.01 M GABA–nicotinate at pH 5. Electric current, 1.5 μA. The inset shows part of the electropherogram D from 13 to 18 min. It can be clearly seen that different terminating solutions in ITP experiments can cause strong variations in the velocity of the EOF (note the varying time intervals between the MO bands), resulting in different times of analysis.

during ITP experiments because the capillary contains more than one electrolyte. Because it is essential that the EOF is constant during detection in order to carry out quantitative ITP, we considered further the influence of both the effect of the composition of the terminating and sample solutions and the effect of an EOF-suppressing additive, in order to choose an optimum ITP system.

Effect of different terminators. The variation in EOF is caused by the presence of more than one solution migrating in the capillary. To demonstrate what the effect of different terminating solutions is, in Fig. 3 the electropherograms (CM) are given for a leading electrolyte of 0.01 *M* sodium nicotinate at pH 5.4, alternately mixed with 0.001 *M* MO, and applying as the terminator (A) 0.01 *M* histidine (HIS) at pH 5 adjusted by adding nicotinic acid, (B) 0.01 *M* histidine at pH 6.7 adjusted by adding 2-(N-morpholino)ethanesulphonic acid (MES), (C) 0.01 *M* GABA at pH 3.5 adjusted by adding formic acid and (D) 0.01 *M* GABA at pH 5 adjusted by adding nicotinic acid. In Fig. 4 all calculated velocities of the EOF as a function in time are given.

It can be clearly seen that by applying (A) a terminating solution of histidine (pK = 6.04) with a relatively high mobility at a pH at which a high ionic concentration is present (pH < pK), a nearly constant velocity of the EOF can be obtained during the ITP experiment (see Fig. 4A). For (B) with the same terminator at low ionic concentration (pH > pK), the voltage gradient in the original solution will be very high, causing a high end-velocity of the EOF and thus a strong variation in the velocity of the EOF during the analysis (see Fig. 4B). On carrying out similar experiments with the terminator GABA (pK = 4.03) at pH (C) 3.5 (pH < pK) and (D) 5 (pH > pK), similar effects can be obtained as with histidine as the terminator. On applying the terminator GABA–formate at pH 3.5, a step in the T′ zone could be observed. Repeating this experiment applying GABA–nicotinate at pH 3.5 also gave a double T′ zone. Although not understandable, it might be a moving pH boundary between

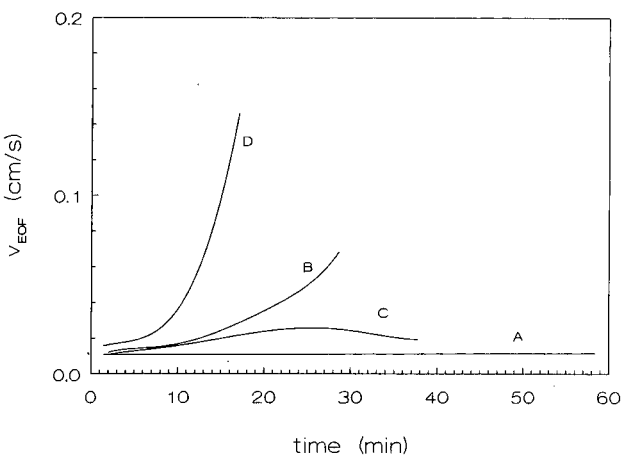

Fig. 4. Calculated velocities of the EOF, using the time intervals between the MO peaks, for the electropherograms in Fig. 3 as a function of time. The (B,D) EOF velocity of the ITP system varies strongly if the pH of the terminator is higher than the pK value of the terminator (low ionic concentrations and thus a high EOF) compared with (A,C) terminator solutions at a pH < pK.

the adapted T′ zone and the original terminating solution T as suggested by Hirokawa *et al.* [8].

From Fig. 3 it can clearly be concluded that using terminators with a low effective mobility and/or at low ionic concentration, strongly varying values of the EOF are the result. It should be remembered that sample ionic species will be found between the L and T′ zones, and that EOF velocities at that moment determine whether reproducible quantitative determinations are possible. The time of analysis also varies strongly depending on the terminator applied.

Effect of sample solutions. To demonstrate the effect of sample solutions on the velocity of the EOF during ITP experiments, we used the leading electrolyte 0.01 *M* sodium nicotinate at pH 5.4 and the terminating electrolyte 0.01 *M* HIS–nicotinate at pH 5, for which a fairly constant EOF can be expected.

In Fig. 5 the electropherograms (CM) obtained by injecting a sample of 0.0025 *M* lithium nitrate with increasing pressure injection times are given. It is clear that the injection of large sample zones causes strongly increasing EOF velocities, so that the migration times decrease substantially and the results of quantitative analyses are erroneous. This effect will be much greater when using sample solutions at a lower ionic strength. It should be remembered that the velocity of the EOF increases strongly because the mobility of the EOF is larger at low ionic strength and the voltage gradient over the original diluted sample zone is much larger.

Suppressed EOF. From the foregoing, it can be concluded that the velocity of the EOF varies strongly with the compositions of the terminating and sample solutions. Varying EOF velocities cause irreproducible migration times and zone lengths and hence the results of quantitative determinations are erroneous. To work quantitatively with ITP in open systems in an appropriate way, the velocity of the EOF must be controlled or eliminated.

It is well known that the EOF can be suppressed by adding surface-active substances to the electrolyte system, such as methylhydroxyethylcellulose (MHEC). A problem is that if MHEC is used as an EOF suppressor, the MO peaks in the leading electrolyte cannot be used as an EOF indicator as they no longer move.

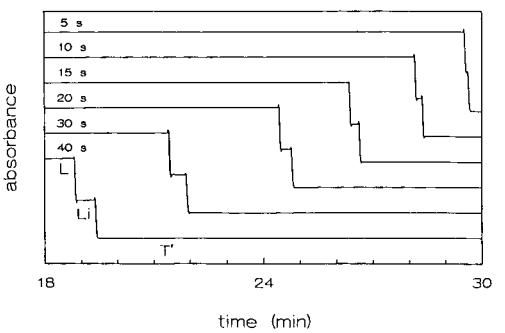

Fig. 5. Electropherograms with a leading electrolyte (L) of 0.01 *M* sodium nicotinate at pH 5.4 and a terminator of 0.01 *M* HIS–nicotinate at pH 5 for several pressure injection times of a solution of 0.0025 *M* lithium nitrate (Li). Increasing zone lengths of the introduced sample result in decreasing times of analysis owing to an increasing velocity of the EOF. Electric current, 1.5 μA.

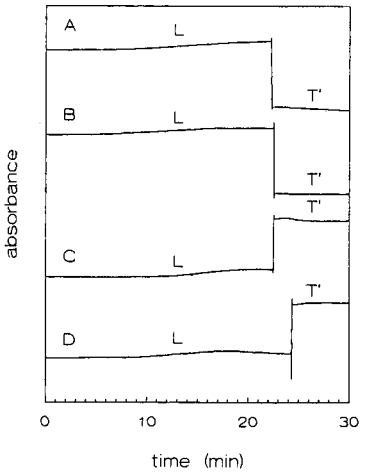

Fig. 6. Electropherograms for a leading electrolyte of sodium nicotinate at pH 5.4 applying as terminating solutions (A) 0.01 *M* HIS–nicotinate at pH 5, (B) 0.01 *M* HIS–MES at pH 6.7, (C) 0.01 *M* GABA–formate at pH 3.5 and (D) 0.01 *M* GABA–nicotinate at pH 5. To all solutions 0.05% of MHEC was added. It can be clearly seen that, compared with the electropherograms in Fig. 3, different terminating solutions in ITP experiments with suppressed EOF show a fairly constant velocity of the EOF, resulting in reasonably constant migration times. Electric current, 3 μA.

However, the migration times for a leading electrolyte in ITP should be constant, independent of the choice of the terminator. In Fig. 6 the electropherograms for the same electrolyte systems as used in Fig. 3 are given, but 0.05% of MHEC was added to all solutions. Although the migration times are not identical they are fairly similar, indicating that the EOF is nearly suppressed, *i.e.*, the velocity of the EOF must be constant, resulting in, however, longer times of analysis (note that only the adapted T′ zones are detected).

Another possibility to check the effect of MHEC on the EOF is the relationship between the voltage over the capillary and time of analysis. These relationships are given in Fig. 7A for the electrolyte systems used for Fig. 3 (different terminators without MHEC) and in Fig. 7B for the electrolytes systems used for Fig. 6 (the same terminators with MHEC).

It can be clearly seen that with addition of MHEC (Fig. 7B) linear relationships are obtained, in contrast to those obtained without MHEC (Fig. 7A), especially for cases B and D. The decrease in case C (Fig. 7A) corresponds to the migration of the unmodified terminator solution into the capillary. In the next section, the results of quantitative experiments, applying several electrolyte systems, are compared with and without the addition of MHEC.

Quantitative analysis

Although the UV detector of the Beckman apparatus is not a universal detector, it can be used in a reasonably universal way in ITP by applying a UV-absorbing counter ionic species because the concentration of the sample ions differ considerably according to Kohlrausch's law. Owing to the electroneutrality equation the concen-

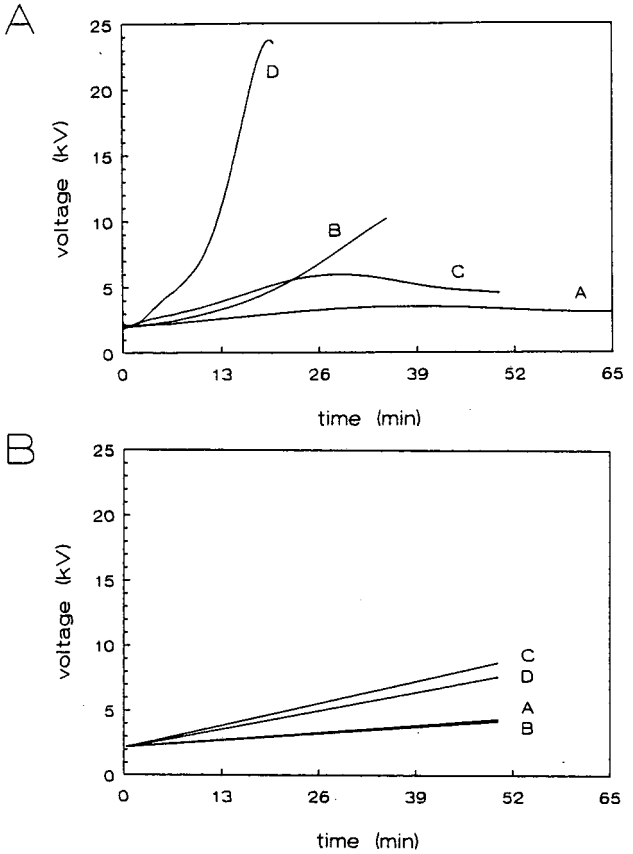

Fig. 7. Relationship between voltage drop over the capillary tube and time of analysis (A) for the electrolyte systems used for Fig. 3, without MHEC, and (B) the same electrolyte systems with MHEC as used in Fig. 6. All data are recalculated to an electric current of 1.5 μA. With the additive MHEC linear relationships are obtained in all instances.

tration of the buffering counter ions also varies from zone to zone, causing different UV absorbances. The same principle can be used in CZE applying a UV-absorbing carrier ion [9].

In Fig. 8 the electropherograms (CM) obtained using a laboratory-made ITP apparatus with (A) a conductivity and (B) a UV detector and (C) using the Beckman apparatus with a UV detector are given. The leading electrolyte was 0.01 *M* sodium nicotinate at pH 5.4 and the terminating electrolyte was 0.01 *M* GABA–nicotinate at pH 5. These electropherograms show clearly that generally the UV detector is applicable for non-UV-absorbing components. Note the similarity between the two UV signals.

Effect of suppressed EOF in quantitative ITP. In order to study the effect of suppressing EOF in ITP in open systems, we measured the zone lengths *versus* the amount of sample by varying the pressure injection time for a concentration of $2.5 \cdot 10^{-3}$ and $1 \cdot 10^{-2}$ *M* of histidine with the leading electrolyte 0.01 *M* sodium nicotin-

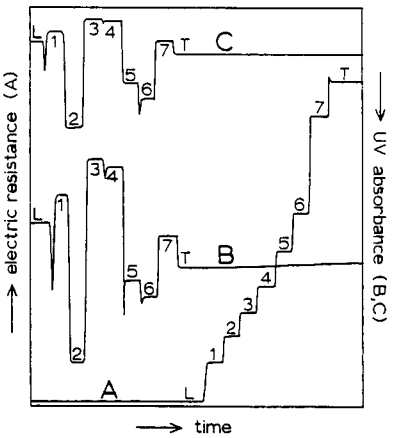

Fig. 8. Electropherograms obtained with (A) a conductivity detector and (B) a UV detector with a laboratory-made ITP apparatus with a closed system and (C) a UV detector with the Beckman P/ACE System 2000 HPCE. The leading electrolyte was 0.01 *M* sodium nicotinate at pH 5.4 and the terminator was 0.01 *M* GABA–nicotinate at pH 5. The electric current was 1.5 μA for the Beckman and 5.5 μA for the laboratory-made ITP instrument. Note the similarity between the two UV signals. The sample composition was 0.00125 *M* of (1) lithium, (2) Girard reagent P, (3) TRIS, (4) HIS, (5) creatinine, (6) *o*-phenylenediamine and (7) ε-aminocaproic acid. Injection, 1 μl for the laboratory made ITP instrument and 5 s pressure injection for the Beckman apparatus.

ate at pH 5.4 using the terminators 0.01 *M* GABA–formate and 0.01 *M* GABA–nicotinate at pH 3.5 and 5, respectively, without and with the addition of 0.05% of MHEC to all electrolyte solutions. All experiments were carried out with an electric current of 1.5 μA.

In Fig. 9A all measured zone lengths as a function of the sample amount (in *M* s units, *i.e.*, molarity multiplied by injection time in seconds) are given without the addition of MHEC. The zone lengths using the terminator GABA–nicotinate at pH 5 are much shorter than those of GABA–formate at pH 3.5 owing to its higher EOF velocity (effect of the low ionic concentration in the original terminating solution). For both terminating solutions the zone lengths decrease considerably with the low concentrations of histidine applying longer injection times, owing to the sample solution effect on the EOF velocity.

It can be concluded that the influence of the composition of both the terminating solutions and the sample solutions on the EOF velocity makes quantitative analyses difficult.

In order to compare the effect of the EOF *versus* the suppressed EOF in quantitative ITP, we repeated all experiments after adding 0.05% of MHEC to all electrolyte solutions. In Fig. 9B the measured zone lengths as a function of the amount of sample are given for these experiments.

A comparison between Fig. 9A and B shows that the zone lengths for $1 \cdot 10^{-2}$ *M* histidine for both terminators with MHEC are much longer than those for the systems without MHEC. The zone lengths for $2.5 \cdot 10^{-3}$ *M* histidine are longer than those for the systems without MHEC, although for GABA at pH 5 not quite a linear relationship could be obtained, identical with those for the $1 \cdot 10^{-2}$ *M* solutions.

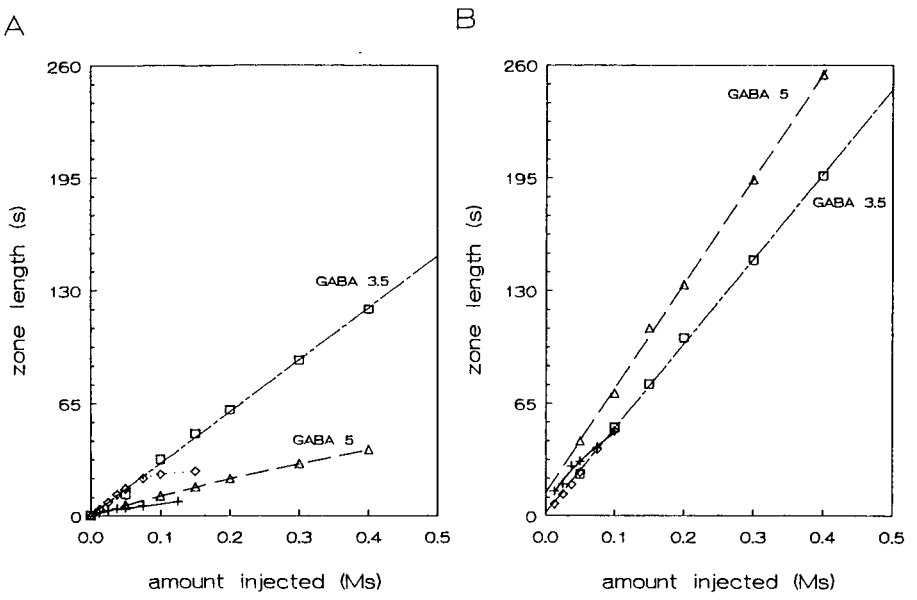

Fig. 9. Relationship between measured zone length (s) and injected amount of histidine (M s) using the terminator 0.01 M GABA at pH 3.5 by adding formic acid and a sample of (□) 0.01 M and (◇) 0.0025 M histidine and the terminator 0.01 M GABA at pH 5.0 by adding nicotinic acid with a sample of (△) 0.01 M and (+) 0.0025 M histidine, (A) without and (B) with the addition of 0.05% of MHEC to all electrolyte solutions.

From Figs. 9A and B it can be concluded that although the effect of the composition of the terminating solutions on the EOF by the addition of MHEC can be suppressed for the greater part, the influence of the ionic strength of the sample solution cannot be eliminated completely.

Reproducibility in quantitative ITP in open systems. In order to demonstrate the reproducibility of quantitative ITP in open systems, we determined five times a calibration graph (CM) for lithium, tris(hydroxymethyl)aminomethane (TRIS), HIS and ε-aminocaproic acid (EAC) in sodium nicotinate at pH 5.4, applying three different terminators, *viz.*, (A) GABA–nicotinate at pH 5, (B) GABA–formate at pH 3.5 and (C) acetic acid at pH 3, injecting six different amounts of the mixture of the sample components with pressure injection times of 5, 10, 15, 20, 30 and 40 s. To all solutions 0.05% of MHEC was added. Data for the calibration graphs are given in Table II.

Although all the calibration graphs were fairly linear (the average regression coefficient is 0.9989), the absolute values of the slopes differ by up to about 12%, and large differences arise for the systems with different terminators. If we calculate the slope relative to that of histidine, the differences are much smaller. For example, the first two values of the slope of the calibration graph for lithium in system A are 870.94 and 934.11 whereas the relative slopes are 1.263 and 1.264.

Two important conclusions can be drawn from Table II. First, by applying ITP in open systems absolute values of zone lengths can never be handled and it is essential to work with at least an internal standard. An extra advantage is that by applying an internal standard, the fluctuations in injected volume are eliminated. Second, the

TABLE II

SLOPES OF CALIBRATION GRAPHS FOR LITHIUM, TRIS, HIS AND EAC AND AVERAGE SLOPE AND STANDARD DEVIATIONS OF THESE VALUES AND THOSE FOR SLOPES RELATIVE TO HISTIDINE

Leading electrolyte, 0.01 *M* sodium nicotinate (pH 5.4); terminating electrolyte, (A) 0.01 *M* GABA–nicotinate (pH 5.0), (B) 0.01 *M* GABA–formate (pH 3.5), (C) acetic acid (pH 3). To all electrolytes 0.05% of MHEC was added. Constant current, 1.5 μA. All calibration graphs were determined by pressure injection of 5, 10, 15, 20, 30 and 40 s of the sample solution (all ionic concentrations were 0.002 *M*).

Sample	Slope (arbitrary units)			Relative slope		
	A	B	C	A	B	C
Lithium	870.94	442.50	464.03	1.263	0.833	0.861
	934.11	435.44	477.18	1.264	0.854	0.850
	911.06	458.32	454.26	1.279	0.839	0.846
	946.03	461.53	459.68	1.360	0.860	0.872
	876.85	456.56	452.03	1.320	0.860	0.854
Average	907.80	450.87	461.44	1.297	0.849	0.857
S.D.	29.90	10.10	8.92	0.038	0.011	0.009
TRIS	730.82	509.18	530.38	1.060	0.959	0.984
	789.47	499.03	544.62	1.068	0.979	0.970
	754.09	525.41	507.03	1.059	0.962	0.944
	769.82	501.53	491.59	1.106	0.934	0.932
	707.29	518.09	505.50	1.065	0.975	0.955
Average	750.73	510.65	515.82	1.072	0.962	0.957
S.D.	28.84	9.94	19.04	0.018	0.016	0.019
HIS	689.47	531.06	538.82	1.000	1.000	1.000
	739.18	509.79	561.32	1.000	1.000	1.000
	712.38	546.12	537.24	1.000	1.000	1.000
	695.79	536.82	527.41	1.000	1.000	1.000
	664.12	531.15	529.24	1.000	1.000	1.000
Average	700.19	530.99	538.81	1.000	1.000	1.000
S.D.	24.92	11.93	12.09			
EAC	678.79	540.21	563.38	0.985	1.017	1.046
	723.06	505.94	577.24	0.978	0.992	1.028
	690.62	569.32	574.59	0.969	1.042	1.070
	681.91	540.44	550.06	0.980	1.007	1.043
	657.74	561.35	551.68	0.990	1.057	1.042
Average	686.42	543.45	563.39	0.981	1.023	1.046
S.D.	21.27	21.98	11.24	0.007	0.023	0.013

use of different terminators can give totally different relative slopes, although reproducible with time. For further experiments we used as the terminator acetic acid at pH 3.

Quantitative ITP in open systems. In order to study the usefulness of the relative slopes in quantitative ITP, we determined the relative slopes for several ionic species in both a cationic and an anionic ITP system. Further, we compared the determined relative slopes in open systems with those in closed systems and theoretical values.

TABLE III

THEORETICAL VALUES OF SLOPES AND EXPERIMENTALLY DETERMINED VALUES FOR ITP IN CLOSED SYSTEMS AND OPEN SYSTEMS (IN DUPLICATE) FOR SEVERAL CATIONIC COMPONENTS IN COMPLEX MIXTURES RELATIVE TO HISTIDINE

Leading electrolyte 0.01 *M* KOH at pH 5.4 adjusted by adding nicotinic acid; terminator, acetic acid at pH 3; both containing 0.05% of MHEC; constant current, 3 μA.

Sample	Theoretical	Closed	Open (1)	Open (2)
Barium	1.377	1.321	1.349	1.315
Creatinine	0.888	0.888	0.897	0.881
EAC	1.084	1.066	1.025	1.006
GABA	1.135	1.000	1.019	1.039
HIS	1.000	1.000	1.000	1.000
Lithium	0.836	0.863	0.866	0.855
OPDA[a]	–	0.940	0.906	0.922
Sodium	0.740	0.713	0.685	0.643
TRIS	1.005	0.993	0.986	0.976

[a] *o*-Phenylenediamine.

In Table III all values are given for cationic species determined with a leading electrolyte of 0.01 *M* KOH at pH 5.4 adjusted by adding nicotinic acid and the terminator acetic acid at pH 3, both containing 0.05% of MHEC. MHEC was also added to all sample solutions. The calibration graphs were measured by injecting five different amounts of the sample components with pressure injection times of 10, 20, 30, 40 and 50 s and an applied direct current of 3 μA.

From Table III, it can be concluded that ITP in open systems can be applied in a reproducible way for cations, although special care must be taken in the choice of the electrolyte system. We also carried out numerous experiments with GABA at pH 5 and 3.5 as terminator and here the relative slopes varied much more with time, although the regression coefficients were good.

More problems with the reproducibility were encountered on applying an anionic system, because the systems in the AM seem to be much more sensitive to fluctuations in EOF.

In Table IV all values are given for anionic species with the leading electrolyte 0.01 *M* HCl at pH 6 adjusted by adding histidine and the terminator 0.02 *M* HIS at pH 6.43 adjusted by adding MES, both containing 0.05% of MHEC. With the addition of MHEC the anionic species could be measured in the normal AM. We already discussed earlier [5] that without the addition of MHEC most anionic systems do not move in the anionic mode owing to the counter action of the EOF.

To illustrate the importance of suppression of the EOF caused by the sample composition, we give in Table IV the theoretical relative slopes, the experimentally determined relative slopes in closed systems and those for open systems (in duplicate) for (A) an anion mixed with the standard without MHEC, (B) mixtures of several anions without MHEC and (C) mixtures of anions with MHEC. The calibration graphs were measured by injecting five different amounts of the sample components with pressure injection times of 10, 20, 30, 40 and 50 s.

From Table IV, it can be concluded that most values for the closed system fit

TABLE IV

THEORETICAL VALUES OF SLOPES AND EXPERIMENTALLY DETERMINED VALUES FOR ITP IN CLOSED SYSTEMS AND OPEN SYSTEMS (IN DUPLICATE) FOR SEVERAL ANIONIC COMPONENTS (A) MIXED WITH THE STANDARD AND (B) IN COMPLEX MIXTURES AND (C) IN COMPLEX MIXTURES WITH MHEC RELATIVE TO FORMATE

Leading electrolyte, 0.01 *M* HCl at pH 6.0 adjusted by adding histidine + 0.05% MHEC; terminating electrolyte, 0.01689 *M* histidine at pH 6.43 adjusted by adding MES + 0.05% MHEC. Constant current, 3μA; wavelength of UV detector, 214 nm.

Sample	Theoretical	Closed	Open					
			A	A	B	B	C	C
Acetate	1.12	1.16	1.16	1.08	1.06	1.06	0.97	1.01
Adipate	2.09	2.06	1.94	1.98	2.16	2.16	2.20	2.07
Benzoate	1.25	1.28	1.34	1.35	1.37	1.49	1.28	1.28
Benzylaspartate	1.44	1.58	1.77	1.78	2.03	2.29	1.79	1.71
Chlorate	0.95	0.99	0.99	1.01	1.15	1.19	0.99	0.99
Enanthate	1.37	1.41	1.40	1.54	1.42	1.68	1.47	1.55
Formate	1.00	1.00	1.00	1.00	1.00	1.00	1.00	1.00
Malonate	1.80	1.80	1.82	1.89	1.90	2.02	1.88	1.54
Propionate	1.19	1.21	1.26	1.29	1.09	0.98	1.14	1.18

the theoretical values reasonably well. The measured values (A) for anionic components mixed with the standard formate are not too bad, although that for benzyl aspartate is too high. The measured values (B) for mixtures of several anionic components are often too high. It must be remembered that although 0.05% of MHEC was added to the leading and terminating electrolytes in order to suppress the EOF, no MHEC was added to the sample mixtures. For small injected amounts it can be expected that the effect of the sample on EOF will be minor but especially long injection times with dilute samples can cause serious variations in the EOF. Because the EOF is oppositely directed to the ITP migration velocity, longer sample zones can be expected. The measured values (C) for mixtures with MHEC are much better.

CONCLUSIONS

It is concluded that although the UV detector is a selective detector, it can also be used for non-UV-absorbing components using a UV-absorbing counter ion. In contrast to ITP in closed systems, in open systems an EOF will act on the ITP system causing an extra displacement of the system. The velocity of the EOF changes continuously if the capillary contains more than one electrolyte. Terminating and sample ions with low mobility, especially at a low ionic concentration, accelerate the EOF considerably, so that quantitative analyses are meaningless.

The addition of MHEC to the electrolyte solutions suppresses the EOF for the greater part, so that linear relationships between sample amounts and zone lengths can be obtained. In spite of the addition of MHEC, the reproducibility of the zone lengths with time is poor and depends on the 'state' of the capillary, an internal standard is necessary for quantitative analyses. Different terminating electrolytes can cause differences in relative slopes.

It can be stated that quantitative ITP in open systems is only possible if precautions are taken to suppress the EOF in an effective way. The addition of, *e.g.*, MHEC to the sample solution is very important, especially in the AM. In the AM the reproducibility seems to be more troublesome. The use of other EOF-suppressing agents can probably give better results. Generally, closed systems are to be preferred to open systems for quantitative ITP.

ACKNOWLEDGEMENT

The authors express their gratitude to the State Institute for Quality Control of Agricultural Products (RIKILT, The Netherlands) for financial support of this investigation.

REFERENCES

1 F. M. Everaerts, J. L. Beckers and Th. P. E. M. Verheggen, *Isotachophoresis–Theory, Instrumentation and Applications* (*Journal of Chromatography Library*, Vol. 6), Elsevier, Amsterdam, 1976.
2 S. Hjerten, K. Elenbring, F. Kilar, J. Liao, A. J. C. Chen, C. J. Siebert and M. Zhu, *J. Chromatogr.*, 403 (1987) 47.
3 H. R. Udseth, J. A. Loo and R. D. Smith, *Anal. Chem.*, 61 (1989) 228.
4 W. Thormann, *J. Chromatogr.*, 516 (1990) 211.
5 J. L. Beckers, F. M. Everaerts and M. T. Ackermans, *J. Chromatogr.*, 537 (1991) 429.
6 V. P. Burolla, S. L. Pentoney and R. Zare, *Am. Biotechnol. Lab.*, 7(10) (1989) 20.
7 J. L. Beckers and F. M. Everaerts, *J. Chromatogr.*, 470 (1989) 277.
8 T. Hirokawa, K. Nakahara and Y. Kiso, *J. Chromatogr.*, 463 (1989) 51.
9 J. L. Beckers, F. M. Everaerts and M. T. Ackermans, *J. Chromatogr.*, 537 (1991) 407.

Journal of Chromatography, 545 (1991) 299–305
Elsevier Science Publishers B.V., Amsterdam

CHROM. 23 179

Isotachophoresis in open-tubular fused-silica capillaries with on-column multi-wavelength detection

PETR GEBAUER[a] and WOLFGANG THORMANN*
Department of Clinical Pharmacology, University of Berne, Murtenstrasse 35, CH-3010 Berne (Switzerland)

ABSTRACT

The use of a fast-scanning multi-wavelength detector for isotachophoresis in open-tubular fused-silica capillaries is described. It is demonstrated that it allows sophisticated characterization of isotachophoretic sample zones, identification of compounds in isotachophoretic zones, investigation of zone purity and confirmation of separation in isotachophoresis.

INTRODUCTION

Photometric detection has been employed for many years in isotachophoresis (ITP) with capillary tubes of 200–500 μm I.D. The combination of this selective detection technique with conductance or electric field measurements has been demonstrated to be extremely helpful for the evaluation of complex isotachopherograms [1]. Two sensors placed in series at the end of the separation column were employed and implemented in commercial capillary-type instruments. Although the application of dual-wavelength detection [2] and photodiode-array sensing [3] has been discussed, fixed-wavelength detectors have been primarily used. This is a major limitation, as only one or two wavelength resolution elements are registered at a time, which is insufficient for the identification of the components of an ITP zone. The gathering of complete absorption spectra in times of the order of milliseconds, *i.e.*, the simultaneous detection of a large number of spectral resolution elements, adds an additional dimension of information. The data in digital form can be readily stored, manipulated and presented in any desired format, making it possible to obtain three-dimensional pherograms within the time needed for a single run.

In a recent paper [4], it was shown that anionic and cationic ITP analyses can be performed in untreated and coated open-tubular fused-silica capillaries with very small inside diameters. In this paper the use of a fast-scanning detector for solute monitoring and confirmation of the ITP steady state via comparison of absorption

[a] Permanent address: Institute of Analytical Chemistry, Czechoslovak Academy of Sciences, CS-611 42 Brno, Czechoslovakia.

0021-9673/91/$03.50

spectra is discussed in conjunction with ITP analyses in an untreated, open-tubular fused-silica capillary, *i.e.*, in the presence of an electroosmotic flow.

EXPERIMENTAL

Chemicals

All chemicals were of analytical-reagent or research grade.

Electrolyte system

For all the experiments presented here, a cationic model system was employed, consisting of 0.01 *M* potassium acetate and acetic acid (pH_L = 4.75) as the leading electrolyte (catholyte) and 0.01 *M* acetic acid as the terminating electrolyte (anolyte). No additives were used.

Instrumentation and running conditions

The instrument used featured a 75 μm I.D. fused-silica capillary of about 90 cm length (Product TSP/075/375; Polymicro Technologies, Phoenix, AZ, U.S.A.) together with a Model UVIS 206 PHD fast-scanning multi-wavelength detector [5] with an on-column capillary detector cell No. 9550-0155 (both from Linear Instruments, Reno, NV, U.S.A.) towards the capillary end. The effective separation distance was 70 cm. Two 50-ml plastic bottles served as electrode vessels and a Model VacTorr 150 vacuum pump (CGA/Precision Scientific, Chicago, IL, U.S.A.) was used to rinse the capillary with cleaning solution (0.1 *M* sodium hydroxide) and leading electrolyte. Current was applied at a constant voltage (20 kV) with a Model HCN 14-20000 power supply (FUG Elektronik, Rosenheim, Germany). The cathode was on the detector side. Samples were applied manually via gravity by lifting the anodic capillary end, dipped into the sample vial, by *ca.* 34 cm for a specified time interval. Multi-wavelength data were read, evaluated and stored employing a Mandax AT 286 computer system and running the Model 206 detector software package version 2.0 (Linear Instruments) with windows 286 version 2.1 (Microsoft, Redmont, WA, U.S.A.). Conditioning for each experiment was effected by rinsing the capillary with 0.1 *M* sodium hydroxide solution for 3 min and with leading electrolyte for 5 min. Throughout this work the Model 206 detector was employed in the high-speed polychrome mode by scanning from 195 to 320 nm at 5-nm intervals (26 wavelengths). With these settings the sampling rate for each wavelength was 3.69 data points/s.

For comparison, experiments were also performed on a Tachophor 2127 analyser (LKB, Bromma, Sweden). This instrument was equipped with a 28-cm × 0.5 mm I.D. PTFE capillary and a conductivity and a UV detector (277-nm filter) at the column end. The measurements were performed at a constant current of 150 μA. Samples were injected with a 10-μl syringe (Hamilton, Bonaduz, Switzerland). The data were registered with a Model PM8252A two-channel strip chart recorder (Philips, Eindhoven, The Netherlands).

RESULTS AND DISCUSSION

As a first example, the cationic ITP analysis of ephedrine, procaine and cycloserine was studied. Data obtained on the Tachophor analyser (Fig. 1) illustrate that the

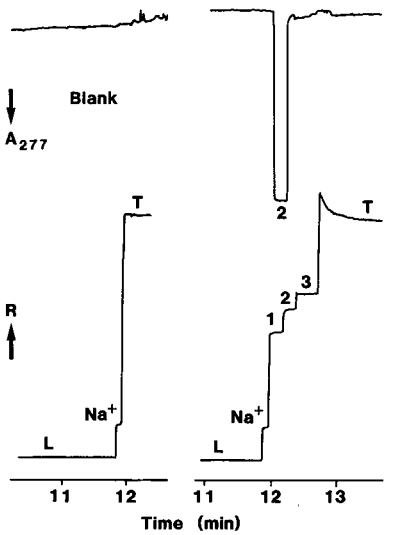

Fig. 1. Blank and cationic ITP analysis of (1) ephedrine, (2) procaine and (3) cycloserine using the Tachophor analyser. A 1-μl volume of an aqueous sample solution containing 10 mM of each compound was injected. Tracings of the conductivity expressed as increase in resistance R (lower graph) and the absorbance measurement at 277 nm (upper graph) are shown. L and T refer to leading and terminating electrolyte, respectively.

three compounds are well separated under the given conditions. With a PTFE column ephedrine (1) migrated ahead of procaine (2), as reported previously by Fanali *et al.* [6] using a similar electrolyte system, and cycloserine (3) was the slowest. Together with a sodium impurity, the three compounds were readily detected via the stepwise response of the conductivity probe. With UV absorbance detection at 277 nm, however, only procaine could be monitored. With these modes of detection and performing a single experiment only, identification of zones and confirmation of complete separation are not achieved [7]. Time-consuming procedures of running single substances and/or various sample loads of the mixture may help in the identification problem and in the recognition of complete separation [8]. The former problem can, however, be solved only for a known sample composition and if all sample components are available as standard substances.

The use of a multi-wavelength detector permits the gathering of three-dimensional isotachopherograms and identification of the sample zones. Fig. 2 depicts such data for the analysis in Fig. 1 performed with a 75 μm I.D. fused-silica capillary in the presence of electroosmosis. The three sample components migrated in the same order as in the Tachophor analyses. All three panels were generated from the data of a single run, illustrating the versatility of data presentation. The projection plot of absorbance *vs.* time relationships between 195 and 320 nm permits the selection of a suitable wavelength for the detection of all three compounds (bottom panel in Fig. 2), the extraction of a complete absorption spectrum for each zone as a so-called time slice (Fig. 3), and thus unambiguous characterization of all three zones. With such data, a computer library of reference spectra can be established, thus allowing qual-

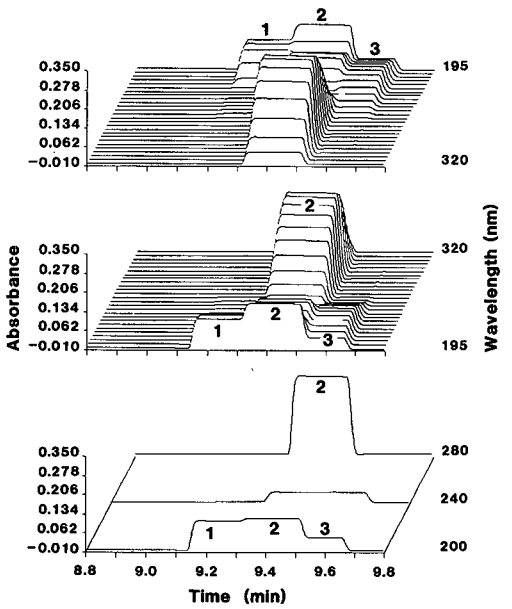

Fig. 2. Three-dimensional isotachopherogram of the cationic analysis of (1) ephedrine, (2) procaine and (3) cycloserine using the fused-silica capillary instrument. The sample solution was the same as in Fig. 1 and the sample application time was 15 s. The initial and final (at detection time) currents were 11 and 3 μA, respectively.

itative studies, such as the identification of substances in steady-state zones, the investigation of the purity of ITP zones and the attainment of the ITP steady state, *i.e.* whether or not the ITP separation process is terminated at the time of detection.

An analysis of the same three compounds with a 3.7-fold higher sample load is shown in Fig. 4. A four-zone structure is monitored, which is clearly seen in the three-dimensional data plot in panel A. The normalized absorption spectra of zones 1, 2 and 3 from Fig. 3 are in complete agreement with those obtained from the data in Fig. 4 (panel B). This proves the identity of the composition of these zones in the two experiments. The normalized time slice of the zone denoted by M was found to be

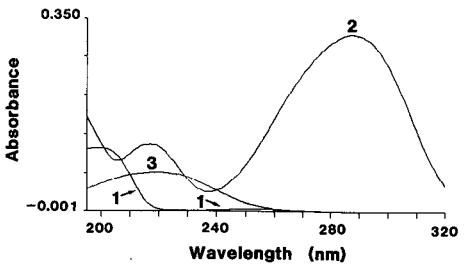

Fig. 3. Absorption spectra of (1) ephedrine, (2) procaine and (3) cycloserine obtained as time slices from the data in Fig. 2.

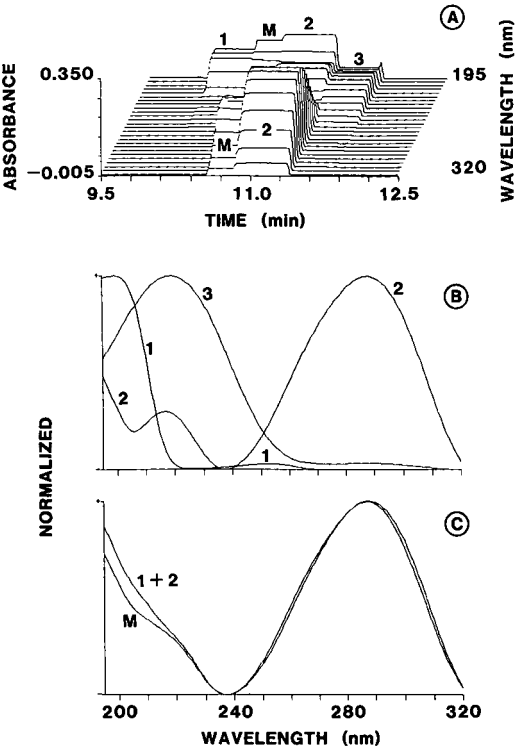

Fig. 4. Three-dimensional isotachopherogram of the same analysis as shown in Fig. 2 but with a sample application time of 55 s. For further details, see text. Note that the normalized spectra in panel B represent an overlay of the data of two different experiments (Figs. 2 and 4).

almost identical with the sum of those of zones 1 and 2 (panel C). In this way we can easily and unambiguously identify zone M as a mixed zone composed of ephedrine and procaine which was not completely resolved before reaching the location of detection. Experiments with 50- and 60-s injection times showed similar patterns having a shorter and longer mixed zone, respectively, than monitored in Fig. 4, whereas with an 80-s injection a five-zone structure containing two different mixed zones was obtained (data not shown). With this sample, the load capacity of the column was reached with an injection time of about 45 s.

Another example illustrating the superiority of multi-wavelength detection over monitoring at one wavelength only is shown in Fig. 5, depicting the purity control of a synthetic peptide, L-histidyl-L-phenylalanine (L-His-L-Phe). Again, all the graphs can be generated from the data from one experiment. The single-wavelength data at 255 nm (panel A) are comparable to those obtained on the Tachophor analyser [9]. Zones 1 and 3 represent impurities and zone 2 the dipeptide. The spectra of the three zones are very different, as is shown in the three-dimensional data plot in panel B and the time slices at (1) 12.174, (2) 12.818 and (3) 13.745 min in panel C. It is interesting that with monitoring at 200 nm (inset in panel A) the impurities are not readily recognized. This is important, as purity control of peptides is typically performed

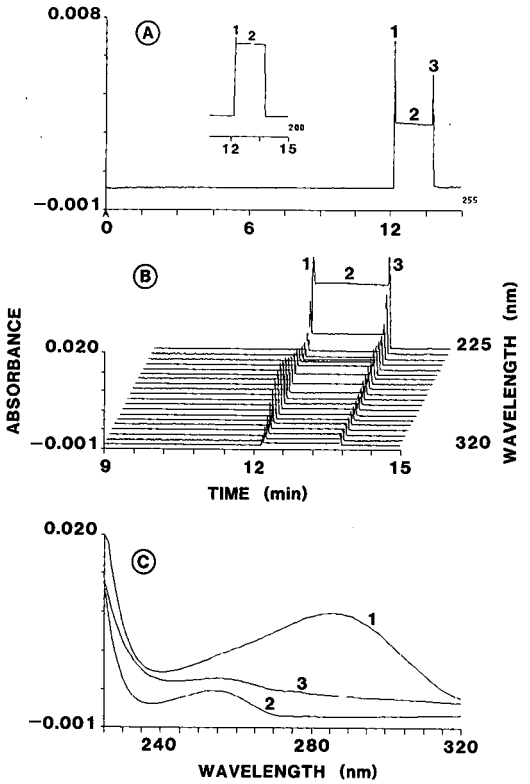

Fig. 5. Cationic analysis of L-His-L-Phe (zone 2) in the fused-silica capillary apparatus with multi-wavelength detection. A *ca.* 100 m*M* sample solution in the leading electrolyte was introduced during 5 s. The current dropped from 10 to 3 μA. Single-wavelength data at 255 and 200 nm (inset with 50-fold larger absorbance scale) are depicted in panel A, a three-dimensional data plot between 225 and 320 nm in panel B and the absorbance spectra of the three zones in panel C. Zones 1 and 3 represent impurities.

around 200 nm [9]. Data reduction on the basis of the ratio of absorption at any two measured wavelengths (as was described for dual-wavelength detection [2]) is not shown here but is easily performed with the Model 206 software.

In conclusion, the use of multi-wavelength detection over a relatively wide range of wavelengths allows a sophisticated characterization of ITP sample zones, the identification of compounds in ITP zones if complete separation is attained, the investigation of zone purity and the confirmation of separation in ITP. Having more than one such detector along the capillary permits the attainment of the ITP steady state to be followed as described previously for sensors measuring a universal sample property [7].Thus, capillary instruments featuring multi-wavelength detectors do not require a second sensor, such as a conductivity or electric field probe, for proper zone assignement in most ITP work. The requirement for optical absorption represents the only limitation to employing this technology as a general and versatile detection principle in ITP.

ACKNOWLEDGEMENTS

The authors acknowledge the valuable experimental assistance of Frank Binder. The generous loan of the Model UVIS 206 detector by Linear Instruments and of the HCN power supply by Mettler–Toledo (Greifensee, Switzerland) is gratefully acknowledged. This work was supported in part by the Swiss National Science Foundation.

REFERENCES

1 F. M. Everaerts, J. L. Beckers and Th. P. E. M. Verheggen, *Isotachophoresis–Theory, Instrumentation and Applications,* Journal of Chromatography Library, Vol. 6, Elsevier, Amsterdam 1976.
2 J. C. Reijenga, Th. P. E. M. Verheggen and F. M. Everaerts, *J. Chromatogr.*, 267 (1983) 75.
3 M. Goto, K. Irino and D. Ishii, *J. Chromatogr.*, 346 (1985) 167.
4 W. Thormann, *J. Chromatogr.*, 516 (1990) 211.
5 K. Weinberger, *Am. Lab.*, December (1989), 12.
6 S. Fanali, F. Foret and P. Boček, *J. Chromatogr.*, 330 (1985) 436.
7 W. Thormann, *J. Chromatogr.*, 334 (1985) 83, and references cited therein.
8 P. Boček, M. Deml, P. Gebauer and V. Dolník, *Analytical Isotachophoresis*, VCH, Weinheim, 1988.
9 M. A. Firestone, J. Michaud, R. H. Carter and W. Thormann, *J. Chromatogr.*, 407 (1987) 363.

Journal of Chromatography, 545 (1991) 307–313
Elsevier Science Publishers B.V., Amsterdam

CHROM. 23 154

Determination of halofuginone in feedstuffs by the combination of capillary isotachophoresis and capillary zone electrophoresis in a column-switching system

LUDMILA KŘIVÁNKOVÁ*, FRANTIŠEK FORET and PETR BOČEK
Institute of Analytical Chemistry, Czechoslovak Academy of Sciences, Veveří 97, 611 42 Brno (Czechoslovakia)

ABSTRACT

A method has been developed for the determination of the coccidiocidic drug halofuginone in feedstuff concentrates which is based on the combination of capillary isotachophoresis and capillary zone electrophoresis in the column-switching mode. The high load capacity of the isotachophoretic step and high sensitivity of the zone electrophoretic step enabled analysis of up to 25 μl of sample solution containing as little as 10^{-8} *M* halofuginone with excellent reproducibility (R.S.D. about 1%). Attention was paid to the possibility of the existence of transient local isotachophoresis in the zone electrophoretic step, and experimental and theoretical methods of revealing zones migrating isotachophoretically in the background electrolyte were shown.

INTRODUCTION

Halofuginone (HFG), DL-*trans*-7-bromo-6-chloro-3-[3-(3-hydroxy-2-piperidyl)-2-oxopropyl]-4-[3H]quinazoline (Fig. 1), is included in the category of full broad-spectrum coccidiocides [1] that is added together with minerals, vitamins, amino acids, protectives, stimulants and antioxidants to industrially prepared feedstuffs for poultry. HFG levels in feedstuffs must not exceed the authorized limits, and analytical control is of great importance in order to prevent economic losses due to over- or under-dosage. For the determination of HFG, spectrophotometric methods [2], gas chromatography [3–5] and column liquid chromatography [6] were used, giving results as discussed in the survey [6]. As HFG can easily be protonated on forming cations in aqueous solution, capillary electrophoresis offering high speed, high sensitivity and

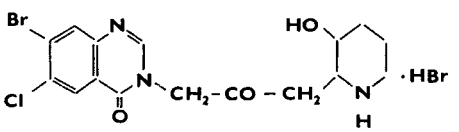

Fig. 1. Structure of halofuginone.

0021-9673/91/$03.50

simple operation may be very useful in its detection [7–10]. Recently, it has been shown that the combination of capillary isotachophoresis (CITP) and capillary zone electrophoresis (CZE) [11,12] offers the advantages of both methods. Isotachophoresis (ITP) offers the ability to inject large amounts of a sample, *e.g.* 30 μl, and thus to analyse trace components below the 10^{-6} *M* level. Column-switching technique offers the ability to cut-off bulk components. Finally, the CZE step offers high resolution and aids the identification of sample components using migration times.

In this paper we show that the combination of CITP and CZE performed using commercial column-switching instrumentation for ITP may be routinely used for analyses of additives in feedstuffs for poultry. Further, we show that the process of switching from ITP to CZE, due to the change of the electrolyte system, is a transient one and may be accompanied by a local existence zones showing self-sharpening boundaries.

EXPERIMENTAL

Instrumentation

A CS isotachophoretical analyzer (ÚRVJT, Spišská Nová Ves, Czechoslovakia) equipped with a column-switching system was used. Pre-separation and analytical capillaries (0.8 and 0.3 mm I.D., respectively) are made of polytetrafluorinated ethylene (PTFE). The distance between the injection port and the conductivity detector is 17 cm. The analytical capillary is equipped with conductivity and UV (254 nm) detectors which are positioned at 17 and 13.5 cm from the starting and bifurcation points, respectively. Solution pH was measured with a Model MS-20 ion activity meter (Laboratorní přístroje, Prague, Czechoslovakia) with glass and silver chloride electrodes.

Absorption spectrum of HFG was measured with a Jasco 875-UV detector.

Chemicals

2-Morpholinoethanesulfonic acid (MES) p.a. and Triton X-100 were from Fluka (Buchs, Switzerland). Other chemicals of analytical grade were from Lachema (Brno, Czechoslovakia). Distilled water was deionized with a mixed-bed ion exchanger Ostion AD and KS (Spolchemie, Ústí n.L., Czechoslovakia). Halofuginone bromohydrate was obtained from Roussel UCLAF (Romainville, France). Vitamin B_1 was a product of Spofa (Prague, Czechoslovakia).

Working procedures

Extraction of halofuginone from feedstuffs. About 10 g of the concentrated mixture of additives are mixed with 5–7 ml of concentrated acetic acid and sonicated for 5 min. Then 50 ml of water are added and the sonication is repeated. Finally, the volume is made up to 100 ml with water. Supernatant obtained after centrifugation or filtration was used as the sample for injection.

ITP or ITP–CZE analysis. The sample was introduced via a sampling valve (24.5 μl) or with a 10-μl Hamilton microsyringe. For ITP measurements, pre-separation and analytical capillaries of the instrument were filled with electrolyte system I and the appropriate current was set (Table I). For the ITP–CZE combination, electrolyte system II and the current given in Table I were used. In this case, current I_1 was

TABLE I

WORKING CONDITIONS

Electrolyte system			Capillary	Current
I	L_1:	10 m*M* KOH + MES[a], pH 6.0, 0.2% Triton X-100	Pre-separation	I_1 = 150 μA
	L_2:	5 m*M* KOH + MES, pH 5.7	Analytical	I_2 = 20 μA
	T:	10 m*M* EACA		
II	L_1:	5 m*M* KOH + MES, pH 5.7, 0.2% Triton X-100	Pre-separation	I_1 = 150 μA
	L_2:	25 m*M* EACA + acetic acid, pH 4.0, 0.2% Triton X-100	Analytical	I_2 = 20 μA
	T:	25 m*M* EACA + acetic acid, pH 4.0, 0.2% Triton X-100		

[a] 2-(N-Morpholino)ethanesulphonic acid.

switched to I_2 exactly 3 s before the bifurcation point. For ITP analysis the timing of column switching is not so critical and a longer period can be chosen.

RESULTS AND DISCUSSION

By orientation experiments, the effective mobility of HFG was found to be $19 \cdot 10^{-9}$ m^2 V^{-1} s^{-1} at pH 4. Hence, electrolyte system I (Table I) was selected where the adjusted pH of the terminating electrolyte was 4.0, ensuring sufficient protonation of HFG and sufficiently low effective mobility of H^+ as a potential terminating electrolyte (TE). To speed up the analysis, ε-aminocaproic acid (EACA) was used as the actual terminator. Analysis of a model mixture of HFG and B_1 carried out by column-switching technique in the ITP + ITP mode is shown in Fig. 2. Obviously,

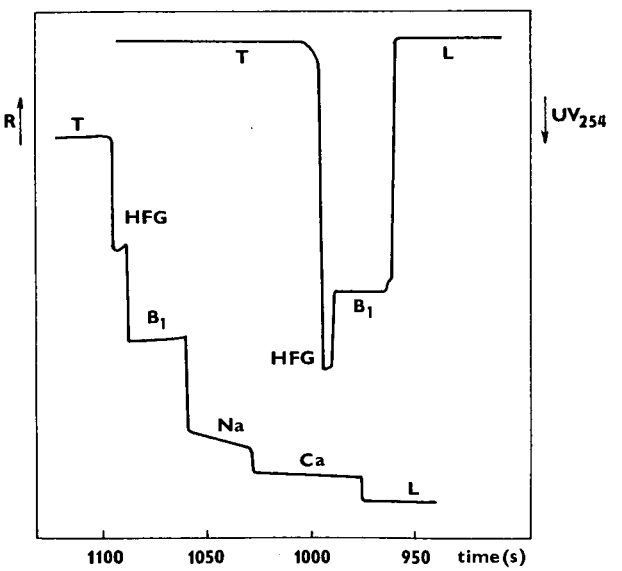

Fig. 2. Isotachophoresis of a model mixture of 2 μl of 2 m*M* HFG and 5 μl of 0.76 m*M* vitamin B_1 in electrolyte system I. R = resistance.

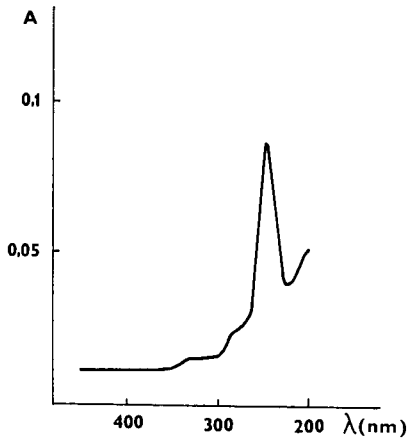

Fig. 3. Absorption spectrum of 0.1 m*M* halofuginone. Optical pathway 10 mm.

good separation of all species was obtained and distinct well developed zones are present in the conductivity detector record. UV detection was carried out at 254 nm which corresponds closely to the absorbance maximum of HFG at 243 nm (see the absorption spectrum in Fig. 3).

Analysis of an extract of the feedstuffs performed in ITP + ITP mode is shown in Fig. 4. Only short zones of HFG and B_1 were obtained, even when full load capacity was utilized. These zones were difficult not only to quantify but also to identify. Even the UV detector gave no unequivocal responses since there were other absorbing compounds in the sample with concentrations and mobilities close to those of HFG.

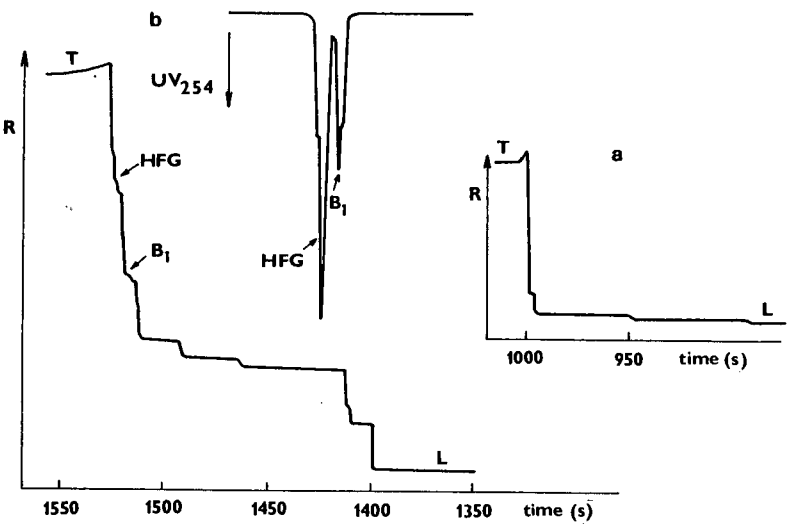

Fig. 4. Isotachophoresis of the extract of feedstuffs supplement. A 10-μl volume of water extract (1.8 g of biofactor supplement per 100 ml of water) was analysed in electrolyte system I. (a) Pre-separation run; (b) analytical run. R = Resistance.

The concentration of HFG in the sample was too low for evaluation from step length in the UV trace, and the presence of other UV absorbing compounds accompanying HFG did not allow use of the spike method for quantification.

The analysis of an extract of the feedstuffs carried out by the combination ITP–CZE is shown in Fig. 5. The first stage was ITP and the electrolyte system was the same as in Fig. 4. The surplus of sodium and calcium was directed towards the auxiliary electrode of the pre-separation capillary, and when the portion of interest appeared close to the bifurcation point the voltage was switched across the analytical capillary. This capillary was filled with TE adjusted to pH 4.0 (electrolyte system II, Table I), which corresponded to the adjusted pH of TE in the ITP mode, and the second stage of analysis was continued in the zone electrophoresis (ZE) mode.

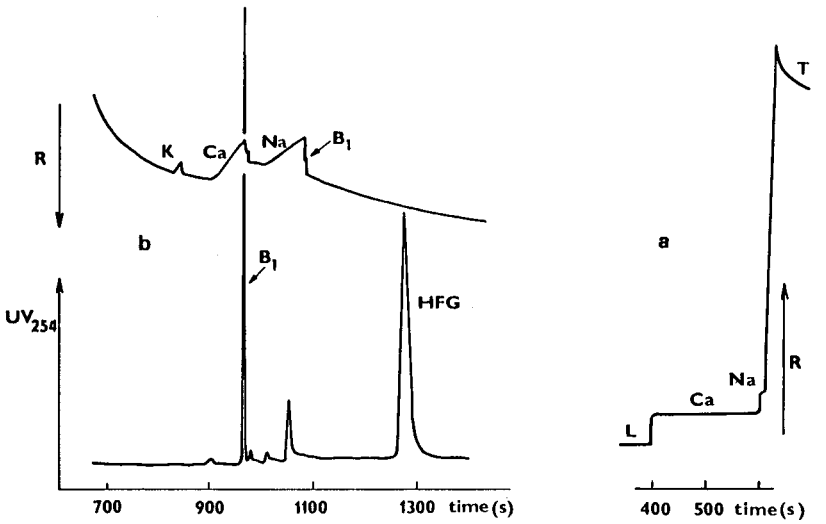

Fig. 5. ITP–ZE of the extract of feedstuffs supplement. A 24.6-μl volume of ten times diluted extract of 1.8 g of biofactor supplement per 100 ml water was analysed in electrolyte system II. (a) Pre-separation run; (b) analytical run. R = Resistance.

A critical point was found to be the timing of the column switching. Three seconds before the sample portion of interest reaches the bifurcation point was found to be optimum. When the time was shorter, a part of the analyte could be lost by migration towards the auxiliary electrode. When a larger portion of the isotachophoretic zones migrates to the analytical capillary, they remain in isotachophoretic migration for a time, and a shorter path is available for ZE separation. Obviously, a universal conductivity detector situated before the bifurcation point is of key importance here.

For the analysis of HFG by the ITP–CZE combination in the electrolyte system II the calibration was evaluated in ZE mode with UV_{254} detection. Linear dependence was found when peak area was plotted *versus* amount of HFG in the range 7.5–480 μg/l (10^{-8}–10^{-6} *M*), and the equation of the calibration line was $y\,(mm^2) = -1.5 + 51.75\,x$ (pmol) with correlation coefficient $r = 0.9999$. Linearity of the plot confirms the

reliability of the procedure. The amount of electricity necessary for the zone to pass the detector was found to be very reproducible, differing by less than 1% for individual runs, which is in good agreement with similar observations [11]. The same holds for the crude extracts of feedstuffs. The results of analyses of HFG in various kinds of feedstuff supplements are given in Table II.

TABLE II

AMOUNTS OF HALOFUGINONE EXTRACTED FROM FEEDSTUFFS AND ANALYSED USING THE ITP–ZE TECHNIQUE

A 24.6-μl volume of the 10–50 times diluted extract was injected and analysed in electrolyte system II.

Sample	Halofuginone content (mg/kg)	Relative standard deviation (n = 3) (%)
Ia	104.9	0.33
Ib	97.5	0.95
Ic	102.0	1.16
II	19.4	2.56

Finally, we discuss certain phenomena that may occur with the ITP–ZE combination and which may be exemplified here on zones of B_1 and HFG.

In general, three types of combination of electrolytes can be used depending on the background electrolyte applied in the second stage. Either leading electrolyte (LE) or TE or some other electrolyte (XE) can serve as background electrolyte (BGE): TE–LE–LE, TE–LE–TE, TE–LE–XE. The combination TE–LE–TE is the simplest as it needs no manipulation with electrolytes during analysis. From the point of electromigration, in all the above cases there exists a possibility of the existence of a transient, local ITP migration during the second stage (ZE) of the analysis [13,14]. Let us examine our cases, namely, the TE–LE–TE scheme. When some compounds are present in the sample having mobility higher than that of the co-ion of the BGE used in the ZE stage of the analysis, they may influence the ZE migration by forming transient local regions. Compounds migrating at the rear boundaries of these high-mobility zones migrate isotachophoretically and show very sharp peaks. Here, this is the case with vitamin B_1 (see Fig. 5), which is present in the extract of feedstuffs. In such a case a very high number of theoretical plates can be adjudged to be in ITP zones migrating apparently in a ZE mode. To give an example we can calculate the maximum plate number (N_{max}) using the relation [15]:

$$N = 0.82\,\bar{u}\,\frac{l}{r}\sqrt[3]{\frac{\lambda}{D^2\,\delta\,\chi\,\bar{u}}}$$

where $\bar{u}$ is the effective mobility, l is the length of the capillary, r is the radius of the capillary, λ is the thermal conductivity of BGE, D is the diffusion coefficient of the substance, δ is the temperature coefficient of the mobility and χ is the specific

conductivity of BGE. This relation includes diffusion and Joule heat as the only sources of zone broadening and does not include any other dispersion processes, *e.g.* injection of the sample. Therefore, using this equation we can calculate the theoretical limit of separation efficiency which is not accessible in practice. For HFG the experimentally found [10] N (11 700) is lower than N_{max} (126 000) confirming ZE migration, while for vitamin B_1 N (264 000) is higher than N_{max} (259 000) and therefore B_1 cannot migrate in the ZE mode.

As can be seen in Fig. 5, conductivity detection reveals the range of local ITP zones. The zone of vitamin B_1 in this system can be found by analysing a higher amount of this compound. The slower migration of HFG (compared to vitamin B_1, the effective mobility of which was found $42.4 \cdot 10^{-9}$ m^2 V^{-1} s^{-1} at pH 4.0) is not influenced, which can also be recognized from the diffuse shape of the zone.

CONCLUSION

The combination of CITP–CZE in column-switching mode is a very promising method for trace analysis of substances in the presence of other micro- and macrocomponents. Even with a commercial apparatus designed for column-switching ITP and equipped with an analytical capillary I.D. about ten times wider than those commonly used in CZE nowadays high sensitivity (10^{-8} M) and reproducibility (R.S.D. 1%) of analyses can be easily reached. The pre-condition for accurate results is the positioning of the detector in the isotachophoretic step that enables exact sampling for the ZE step and having a universal detector in addition to the UV detector in the ZE step to reveal transient isotachophoretic zones in ZE and to achieve high sensitivity of detection.

REFERENCES

1 *Stenorol*, Division Agro-Vétérinaire, Roussel-Uclaf, Paris.
2 A. C. Bratton and E. K. Marshall, Jr., *Biol. Chem.*, 128 (1939) 537.
3 N. T. Crosby and E. Q. Laws, *Analyst*, 89 (1964) 319.
4 J. Pellizarni, *J. Chromatogr.*, 98 (1974) 323.
5 W. Korol, S. Matyka and T. Harenza, *Med. Weter.*, 39 (1983) 303.
6 K. Frgalová, J. Valová and A. Hera, *Biol. Chem. Vet.*, 24 (1988) 407.
7 F. M. Everaerts, J. L. Beckers and Th. P. E. M. Verheggen, *Isotachophoresis. Theory, Instrumentation and Applications*, Elsevier, Amsterdam, 1976.
8 Z. Deyl (Editor), *Electrophoresis. A Survey of Techniques and Applications. Part A: Techniques*, Elsevier, Amsterdam, 1979.
9 P. Boček, M. Deml, P. Gebauer and V. Dolník, in B. J. Radola (Editor), *Analytical Isotachophoresis*, VCH Verlagsgesellschaft, Weinheim, 1988.
10 F. Foret and P. Boček, in A. Chrambach (Editor), *Advances in Electrophoresis*, Vol. 3, VCH Verlagsgesellschaft, Weinheim, 1989, pp. 272–347.
11 D. Kaniansky and J. Marák, *J. Chromatogr.*, 498 (1990) 191.
12 F. Foret, V. Šustáček and P. Boček, *J. Microcolumn Sep.*, 2 (1990) 299.
13 J. L. Beckers and F. M. Everaerts, *J. Chromatogr.*, 508 (1990) 3.
14 J. L. Beckers and F. M. Everaerts, *J. Chromatogr.*, 508 (1990) 19.
15 F. Foret, M. Deml and P. Boček, *J. Chromatogr.*, 452 (1982) 601.

Journal of Chromatography, 545 (1991) 315–329
Elsevier Science Publishers B.V., Amsterdam

CHROM. 23 160

Recycling and screen-segmented column isotachophoresis, two free-fluid approaches for fractionation of proteins

JITKA CASLAVSKA, PETR GEBAUER[a], ALEX ODERMATT and WOLFGANG THORMANN*
Department of Clinical Pharmacology, University of Berne, Murtenstrasse 35, CH-3010 Berne (Switzerland)

ABSTRACT

Recycling and screen-segmented column isotachophoresis (ITP), two approaches for the milligrams to grams preparative-scale purification of proteins, are discussed and compared. Recycling ITP was performed in a recycling free-flow focusing apparatus. In this process, fluid flows rapidly through a narrow channel and the effluent from each channel is reinjected into the electrophoresis chamber through the corresponding input port. The residence time in the cell is of the order of 1 s per single pass, which does not allow complete separation, so recycling is essential to attain the steady state. Immobilization of the advancing zone structure is obtained via a controlled counterflow. Thirty fractions of about 4 ml each are obtained. Column ITP was executed in a Rotofor apparatus and in a similar column operated vertically and without rotation. These instruments feature a screen-segmented annular separation space with twenty subcompartments of about 2 ml each. With both approaches, the collected fractions were analysed separately for conductivity, pH and UV absorbance. Selected fractions were characterized by analytical electrophoretic methods. Examples presented include the cationic and anionic ITP behaviour of model proteins, including bovine serum albumin, ovalbumin and ribonuclease A, and the ITP removal of the major impurities from a commercial ovalbumin sample. These examples revealed that the screen-segmented column is suitable for ITP protein purification and operates optimally in a horizontal rotating mode and without internal cooling. The recycling experiments showed that counterflow improves separation and the steady-state patterns are dependent on the fluid layer thickness in the separation cell but, with a given gap, essentially independent of applied current and recycling pump rate.

INTRODUCTION

Isotachophoresis (ITP) is both an attractive purification method which has never been fully characterized [1] and a promising analytical tool for low- and high-molecular-mass components [2]. We are attempting to establish the most suitable free fluid approach for ITP of proteins on the gram scale. So far we have accumulated experience in recycling [3,4] and continuous fow ITP [4] and constructed a mathematical model for the prediction of the ITP behaviour of proteins [5,6].

[a] Permanent address: Institute of Analytical Chemistry, Czechoslovak Academy of Sciences, CS-611 42 Brno, Czechoslovakia.

0021-9673/91/$03.50

Key factors in the design of preparative free-fluid ITP instruments are convective fluid stabilization, temperature control and sample fractionation and detection. Many designs have been discussed (for an overview, see refs. 3 and 7), with recycling and continuous flow ITP currently being the most promising approaches. Monofilament plastic screens placed in the current path were found to be effective for fluid stabilization in recycling [8], rotating [9,10] and vertical column [10] isoelectric focusing. No report was found describing the use of screen segmentation for preparative free-fluid ITP of proteins. Therefore, we decided to explore the potential of using the screen-segmented Rotofor apparatus [9] in various operational modes, including horizontal and vertical chamber arrangements. The ITP fractionation of various model proteins and the purification of ovalbumin in a cationic ITP configuration are described. Data from the Rotofor column were compared with those obtained by performing ITP in a recycling free-flow focusing (RF3) apparatus which was modified for recycling ITP (RITP) via incorporation of an optical boundary sensor in one of the recycling loops and a continuously operating counterflow of leader. The impact of the fluid layer thickness of the RITP separation cell on protein zone formation and fractionation is also discussed. A careful characterization and comparison of the two preparative free-fluid ITP approaches is the topic of this paper.

EXPERIMENTAL

Vertical column isotachophoresis

For ITP experiments in a vertical column, a screen-segmented column identical with that in the commercial Rotofor cell (Bio-Rad Labs., Richmond, CA, U.S.A.) (see below) was used. This cell features an annular chamber with a cooling finger in the centre, polyester screen segmentation and a total column volume of about 52 ml. The separation chamber and electrode vessels were separated by dialysis membranes made from Spectrapor tubing (Spectrum Medical Industries, Los Angeles, CA, U.S.A.). In order to prevent the penetration of electrode reaction products into the column, electrode chambers were modified for flow-through operation and electrode buffers were recirculated from 1-l volume vessels by a peristaltic pump (Vario-Perpex; Werner Meyer, Lucerne, Switzerland) at a flow-rate of 35 ml/min. Before the experiment, the whole separation column (all twenty segments) was filled with the leading electrolyte. Leader from the first segment (whose one wall is formed by the membrane) was removed and the segment was filled with the terminator. Then the electrolyte of the second segment was replaced with the sample dissolved in 2 ml of the leading electrolyte. Immediately thereafter the column was closed, brought to an upright position and the current was applied.

After a run, power was typically disconnected and recycling of the buffers was ceased, prior to collection of fractions using the Rotofor fraction collection box. With this approach the formation of ITP protein zones was studied in both downward and upward migration directions. For the latter configuration, on-line fractionation by continuous protein elution towards the column top was also investigated. For that process, leading electrolyte was pumped (0.6 ml/min) through the second to last segment using a syringe pump (Model 355; Sage Instruments, Cambridge, MA, U.S.A.) equipped with a 60-ml syringe and the effluent was monitored with a Uvicord detector (Model 2158; LKB, Bromma, Sweden) and a high-performance liquid chromatographic flow cell.

Horizontal column isotachophoresis

ITP experiments in the rotating screen-segmented column were performed in the commercial Rotofor apparatus. To increase the rotational speed from about 1 to 4.5 rpm, its motor was replaced with a Model AB 3006-005 (Hurst; Princeton, IN, U.S.A.). Further, the ion-exchange membranes used for isoelectric focusing were replaced with dialysis membranes (see above). The disturbing effects of electrode reaction products were eliminated by filling the electrode chambers with ten times more concentrated electrolytes than used in the separation compartment (in cationic runs, both electrode chambers were filled with 0.1 *M* acetic acid). The application of the sample was performed in the same way as described for the vertical column. Otherwise the experiments were executed according to the manufacturer's specifications for isoelectric focusing.

Recycling isotachophoresis

A prototype of a commercial, recycling free-flow focusing apparatus (Model RF3, Protein Technologies, Tucson, AZ, U.S.A.; distributor, Rainin Instrument, Woburn, MA, U.S.A.) was used for all experiments. This instrument was modified for ITP as described previously [3]. The RF3 instrument is equipped with a built-in power supply for operation at constant voltage, current or power (1500 V, 400 mA, 200 W). Its processing compartment features the separation cell, two electrolyte reservoirs, a multi-channel peristaltic pump, a heat-exchange unit, a 30-channel pulse damper/bubble trap and a 30-tube fraction collector. The total processing volume is about 130 ml. Throughout this work, separation cells of 20 cm length and 4 cm width (made from thick slabs of acrylic) having fluid layer thicknesses of 0.75, 0.5 and 0.25 mm and providing 30 fractions each were used. The outlet temperature was monitored by a sensor located in the tubing bundle between the separation cell and heat-exchange reservoir. Cooling of the system was achieved by attaching an external thermostatic circulator (2219 Multi Temp II; LKB) to the heat-exchange reservoir. The temperature of the cooling fluid (20% ethylene glycol in water) was -2 to 5°C. Typically the fluid temperature within the cell increased to about 15 and 20°C with a recycling pump rate of 30 and 15%, respectively.

For operation in the ITP mode, the electrolyte chambers were separated from the separation channel by dialysis membranes which, for better stability, were backed up by two layers of chromatographic paper (3MM CHR; Whatman, Maidstone, UK). Electrode buffer reservoirs of 250 ml (RF3 standard is 60 ml) were used and filled with buffers of 10-fold higher concentration than employed within the separation cell. The sample was injected in channel 2, which is near the terminator electrolyte chamber, and the vent was moved to channel 14. The advancing protein boundary was detected by a Model 2138 Uvicord S detector (Pharmacia–LKB, Uppsala, Sweden) with a 277-nm filter. The detector was inserted into the recycling loop of channel 26 (near the leading electrolyte chamber). The detected signal was registered as a function of time on a strip-chart recorder (Series 1200; W + W Scientific Instruments, Basle, Switzerland). The counterflow inlet and outlet were placed in channels 30 and 1, respectively. The counterflow was generated using a low-pulse peristaltic pump (Minipuls 3; Gilson Medical Electronics, Middleton, WI, U.S.A.) together with a laboratory-made pulse damper and bubble trap, and was regulated manually.

All the experiments were performed in a batch mode of operation according to

the manufacturer's instructions. The separation cell was filled with the leading electrolyte. The multi-channel peristaltic pump was set to a pumping rate of 15–30% and the recycling of the electrolytes was started. The sample, dissolved in a maximum of 10 ml of the leading electrolyte and filtered through a 0.45-μm membrane syringe filter, was slowly and carefully injected into the electrolyte stream inside the separation cell. After sample injection, power was applied at a constant current of 34–50 mA. In experiments without counterflow, collection of the 30 fractions occurred immediately after the front protein boundary was recorded via an increase in absorbance (277 nm) within channel 26. In all other experiments, on the occurrence of the absorbance change the counterflow was activated and manually adjusted so as to maintain a constant absorbance level. The ITP zone structure was thereby immobilized. Typically the counterflow pumping rate did not exceed 1.5 ml/min for the anionic and 3.0 ml/min for the cationic systems.

Analysis of collected fractions

For pH measurements a Model 720 pH meter and a Ross Model 8103 SC pH electrode (both from Orion, Cambridge, MA, U.S.A.) were used. The conductivity was measured with a Model 101 conductivity meter (Orion) equipped with a Model PW 9510/65 cell (Philips, Eindhoven, Netherlands). The absorbance was measured at 280 nm in a Lambda 15 UV–VIS spectrophotometer (Perkin-Elmer, Überlingen, Germany). In some instances the fractions containing the protein zones had to be diluted 10-fold and for presentation of the data the absorbance values were multiplied by ten. Selected fractions were also analysed by capillary ITP using a Tachophor 2127 analyser (LKB). This instrument was equipped with a 28 cm × 0.5 mm I.D. PTFE capillary, and a conductivity and UV detector (277-nm filter) at the column end. The same electrolyte systems as used for preparative ITP were employed. The measurements were performed at a constant current of 150 μA.

The staining of bovine serum albumin was performed by adding 5 μl of bromophenol blue solution (7.5% in 0.1 *M* sodium hydroxide) to each 75 mg of protein. The bovine serum albumin plateau concentration was calculated from a measured standard solution containing also bromophenol blue.

Chemicals

All chemicals were of research-grade purity. Bromophenol blue, ribonuclease A, γ-amino-*n*-butyric acid, 2-amino-2-methyl-1,3-propanediol (ammediol) and β-alanine were obtained from Sigma (St. Louis, MO, U.S.A.), albumin from chicken egg (crystallized five times, 11840/D8) from Serva (Heidelberg, Germany), bovine serum albumin from Fluka (Buchs, Switzerland) and potassium acetate, formic acid and acetic acid from Merck (Darmstadt, Germany).

RESULTS AND DISCUSSION

Test of performance

In order to compare the performances of the various instrumental approaches, *i.e.*, their ability to run under ITP conditions and to provide ITP zones, all experiments reported in this section were made with the same anionic model system, an ITP configuration which was recently described theoretically and validated by capillary

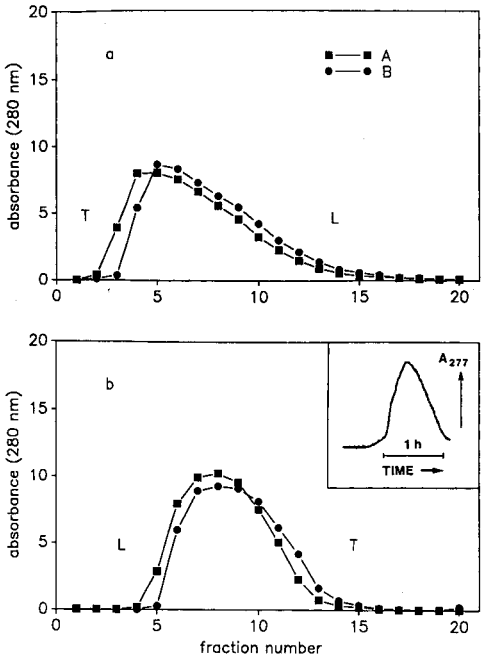

Fig. 1. Formation of a BSA zone (220 mg of protein) in vertical column ITP with downward [(a) constant 8 mA for 60 min] and upward [(b) 8 mA for 100 min] migration. Graphs A and B represent the harvested protein distributions without and with internal cooling, respectively. L and T refer to the positions of leading and terminating zones, respectively. The voltages at collection time were 400 and 900 V, respectively. The plotted absorbance values represent measurements for 10-fold diluted fractions which were multiplied by ten. The graph depicted in the inset in (b) represents the detected BSA zone (75 mg) after elution in a run with upward migration at a constant 10 mA and internal cooling. The peak maximum was detected after 230 min (absorbance range was 2.0).

ITP [6]. It consists of 0.01 *M* formic acid and ammediol (pH_L = 9.0) as the leader, 0.01 *M* β-alanine and ammediol (pH_T = 9.5) as the terminator and bovine serum albumin (BSA) stained with bromophenol blue as the sample.

In the vertical column two running modes were tested, *viz.*, migrating the ITP system upwards (against gravity) and downwards, both either with or without cooling by circulating tap water (15°C) through the cooling finger of the column. Fig. 1 shows results in the form of BSA absorbance profiles, as determined by measuring the UV absorbance of the collected fractions. In all four experiments the upper BSA boundary was sharper than the lower transition. As was observed visually, the disturbance at the lower zone boundary is caused mainly by sedimentation of drops of the dense protein zone into the lower buffer [leader in (a), terminator in (b)]. Obviously, in upwards migration the disturbing effect is counteracted by electromigration which proceeds in the opposite direction, the BSA zone thus being continuously restored. In downwards migration there is no such effect and therefore the resulting BSA profile is much broader (Fig. 1a). The monitored BSA absorbance profile after continuous elution from the top is depicted as the inset in Fig. 1b. There is a good correlation between zone shape, but the elution process is slow and dilutes the sample.

Another important but less disturbing effect is thermal convection of the liquid within each segment. Joule heating of the electrolytes leads to the formation of temperature gradients. With cooling by circulating water through the cooling finger, the most pronounced temperature gradient is formed towards the wall of this finger, forcing the contents of each segment to circulate so that the liquid flows downwards at the cooling finger wall (at the inner wall of the annular column). Without internal cooling, the driving temperature gradient is formed towards the outer column wall. In this instance the circulation of the liquid in the segments is both reversed and decreased. These fluid flow patterns were observed visually by having small amounts of dyed BSA within the leader/terminator boundary. Operation without internal cooling produces less thermal convection, which results in slightly narrower BSA concentration profiles (Fig. 1b). Based on the above observations, it can be concluded that the best result was obtained by migrating the system upwards and operating it without cooling.

Having a horizontal arrangement of the annular and screen-segmented column without rotation around the separation axis, gravity was found to cause protein slumping (data not shown) in a similar way to that previously observed for isoelectric focusing [10]. Fig. 2 shows the results of running the same anionic ITP system in the horizontal rotating arrangement. Experiments showed that an increased rotation

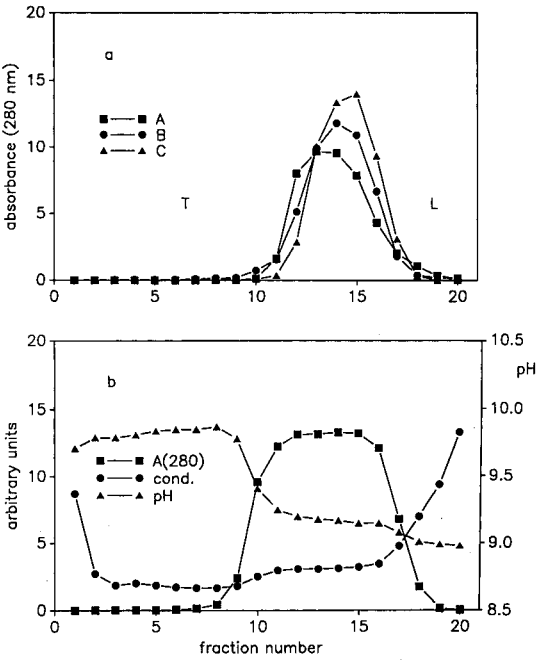

Fig. 2. Formation of a BSA zone in horizontal column ITP (Rotofor) with (a) 230 mg and (b) 480 mg of protein. The graphs in (a) were obtained under the following conditions: (A) 1 rpm, with internal cooling; (B) 4.5 rpm, with cooling; (C) 4.5 rpm, without cooling. The run depicted in (b) was executed at 4.5 rpm without cooling. A constant current of 15 mA during 50 min of electrophoresis time was applied in all instances. The units for the conductivity are 0.01 S/m. The plotted absorbance values represent measurements for 10-fold diluted fractions which were multiplied by ten.

speed (from 1 rpm as provided with the commercial Rotofor to 4.5 rpm) improved the formation of a BSA ITP zone (*cf.*, graphs A and B in Fig. 2a); therefore, all further experiments were performed under these conditions. Comparison of graphs B and C also shows that some improvement was reached when operating without internal cooling. As the last experiment (rotating horizontal mode, 4.5 rpm, without cooling) gave the best result for the screen-segmented column, an additional experiment was made with a larger amount of BSA. With 480 mg of BSA a good ITP zone profile with reasonably sharp boundaries and a well developed concentration plateau corresponding to a steady-state BSA concentration of 20 mg/ml was obtained

A large number of recycling ITP experiments showed that BSA establishes ITP zones under a relatively wide range of experimental conditions and that they compare well with computer-simulated data [3,4]. Fig. 3a shows a typical profile obtained by operating at a constant current of 50 mA and with a fluid layer gap of 0.75 mm. The relatively short path length in the separation cell brought up the question of whether the sample zone can reach a steady state within the time of the experiment. Fig. 3b shows the result with application of a counterflow otherwise executed with the same conditions as used for Fig. 3a. The two experiments appear to be at the steady state when judged by the zone shape. However, careful inspection of the two protein profiles reveals that the counterflow caused an additional sharpening, resulting in a narrower zone with an increased BSA plateau concentration [26 instead of 22 mg/ml (Fig. 3a)]. Fig. 3c illustrates that with variation of electric current and/or recycling rate, small changes in zone profiles were obtained. The plateau BSA concentrations varied from 26 mg/ml (current 50 mA, flow-rate 30%, profile A and Fig. 3b) to 28 mg/ml at 34 mA and a 30% pump rate (profile B) and 30 mg/ml at 34 mA and a 15% pump rate (profile C).

Test of separation power

The second part of the investigations was aimed at establishing whether the instrumental arrangements are suitable for running multi-zone ITP systems involving proteins. For all the experiments presented here, a cationic model system was selected consisting of 0.01 *M* potassium acetate and acetic acid ($pH_L = 4.75$) as the leader and 0.01 *M* acetic acid as the terminator. Ovalbumin (OVA) and ribonuclease A (RNA) were used as the model protein pair. Preliminary investigations by analytical ITP showed that these proteins are separated well in the given electrolyte system and that γ-aminobutyric acid (GABA) can be successfully used as a spacer.

Fig. 4 shows the results obtained in the screen-segmented column (all without cooling). Small amounts of both proteins were sampled together with a large amount of spacer; this amount was selected so that the adjusted spacer zone filled about seven column segments. Fig. 4a and b show a comparison of two runs in the vertical column with downwards and upwards migration, respectively. It is seen that, in contrast to the anionic system, downwards migration provides much better results. Fig. 4c shows the profiles obtained in the rotating horizontal mode (4.5 rpm); here the result is comparable to that in Fig. 4a. Cooling was found to slightly deteriorate the separation. It can be concluded for this type of column that RNA and OVA are concentrated at the front and rear boundaries of the well developed spacer zone, respectively (as is indicated by both the UV absorption and pH profiles). Although there is no baseline resolution, the two proteins are well separated. This was also confirmed by capillary

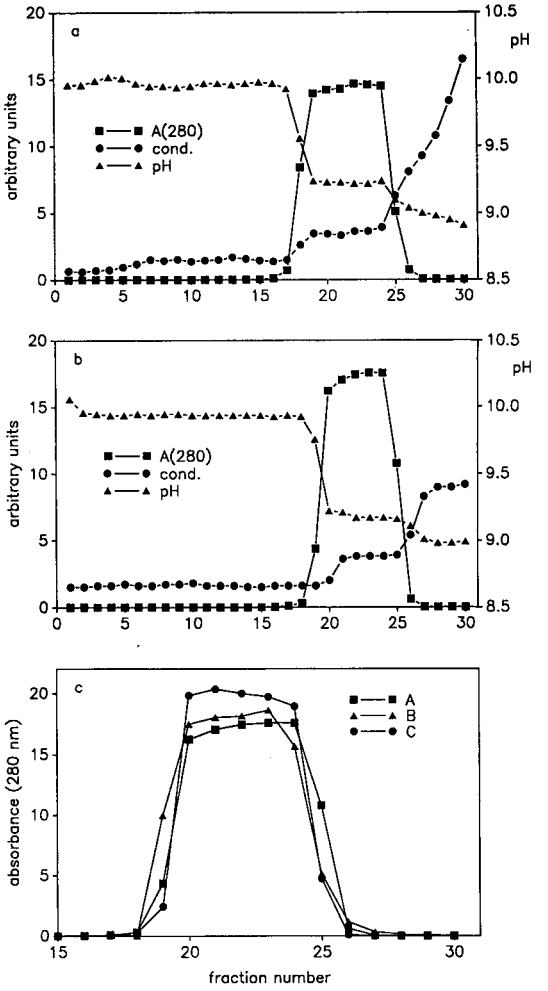

Fig. 3. Recycling ITP data for 750 mg of BSA run without a counterflow [(a) 53 min run time] and with 56 min of counterflow [(b) 105 min run time]. The current was a constant 50 mA and the pump rate was 30% in both instances. The total voltages at the collection time were (a) 1062 V and (b) 804 V. In the latter instance the voltage dropped from 1016 to 804 V during the counterflow period. The processing charges were (a) 159 C and (b) 315 C. (c) Counterflow data with a constant (A) 50 mA, (B) 34 mA and (C) 34 mA together with a recycling pump rate of 30, 30 and 15%, respectively. The total processing time intervals (counterflow periods) were 105 (56), 135 (64) and 122 (49) min, respectively. The final (values at time of counterflow activation) voltages were 804 (1016), 445 (503) and 394 (383) V and the total processing charges were 315, 275 and 249 C, respectively. In all instances a cell with a 0.75-mm gap was employed. The scales are the same as in Fig. 2b.

ITP analyses of the collected fractions (Fig. 5). In both experiments the major RNA fractions were essentially free from OVA whereas the major OVA fractions were found to have a residual RNA content. This was much more pronounced in the upwards migration experiment (Fig. 5b). The result of fractionation via continuous elution after

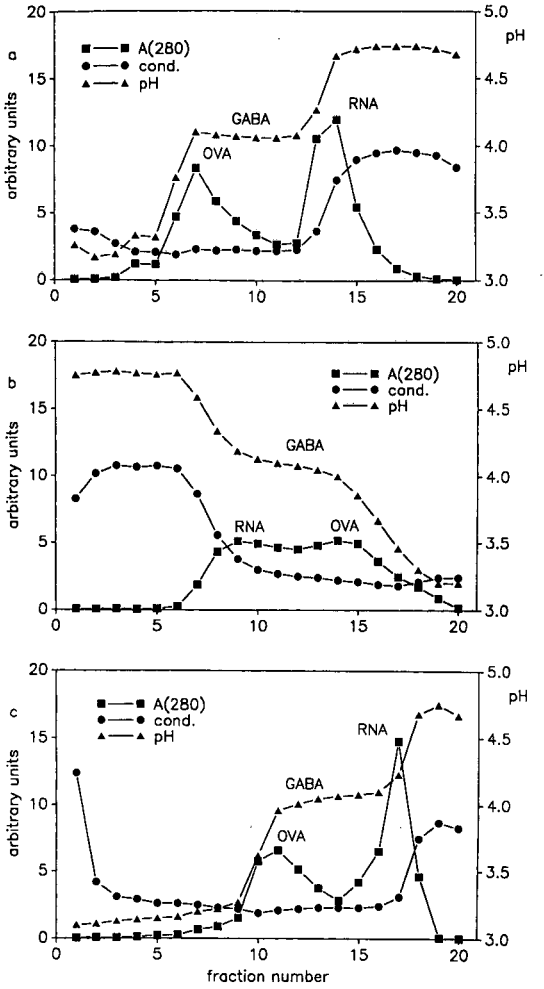

Fig. 4. Column ITP of RNA and OVA with GABA as spacer in (a) a vertical arrangement with downward migration, (b) a vertical set-up with upward migration and (c) in the Rotofor at 4.5 rpm. All experiments were performed without internal cooling. The sampled amounts and electrical conditions were as follows: (a) 12.6 mg OVA, 12.5 mg GABA, 13.1 mg RNA, 5 mA for 150 min, 170 V final; (b) 9.4 mg OVA, 11.7 mg GABA, 10.2 mg RNA, 5 mA for 150 min, 160 V final; (c) 12.9 mg OVA, 9.4 mg GABA, 11.0 mg RNA, 15 mA for 60 min, 390 V final. The units for the conductivity are 0.01 S/m. Absorbance values from undiluted samples were multiplied by ten.

upward migration is depicted in Fig. 6. This approach was found to substantially elongate a run (with the advantage of having an increased separation capacity), but with the disadvantages of sample dilution and partial remixing in the elution chamber. Fig. 7 shows the result of a similar run in the recycling apparatus with counterflow. Here a much longer spacer zone could be generated and the separation of the two proteins is almost complete. For this example, the peak concentration of OVA was

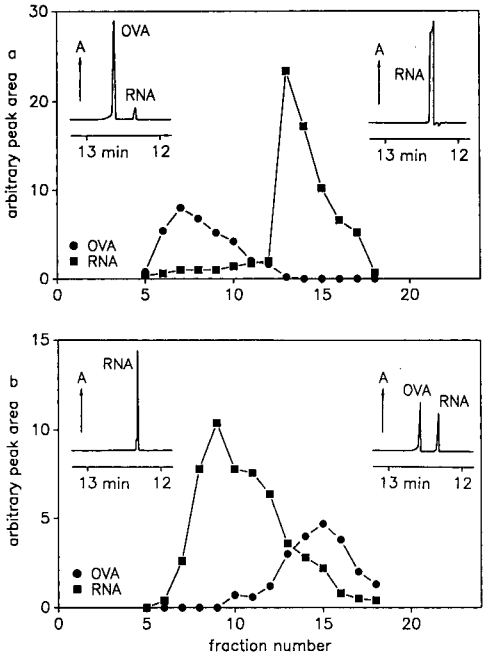

Fig. 5. Capillary ITP analysis data for the separation depicted in (a) Fig. 4a and (b) Fig. 4b. For each fraction and protein the peak area of the appropriate UV signals was plotted. The insets depict the Tachophor UV (277 nm) responses of fractions corresponding to the absorbance maxima [(a) fractions 7 and 14; (b) fractions 9 and 14]. Volumes of 2 μl of undiluted fractions were injected and analysed with a constant 150 μA.

found to be 11 mg/ml and the apparent (see below) RNA content was determined as 9.7 mg/ml. The RNA plateau concentration was 12.6 mg/ml (data not shown).

We could show by analytical ITP (data not shown) that the RNA fractions from

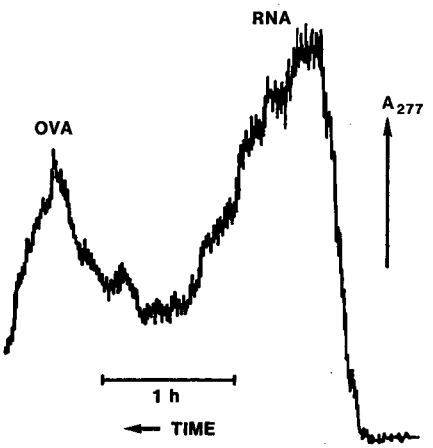

Fig. 6. Elution data (absorbance range 0.1) of an experiment with 6 mg of RNA, 51 mg of GABA and 5.5 mg of OVA. The current was 12 mA for the first 65 min and 10 mA during sample elution. The RNA and OVA peaks were detected after 95 and 115 min, respectively.

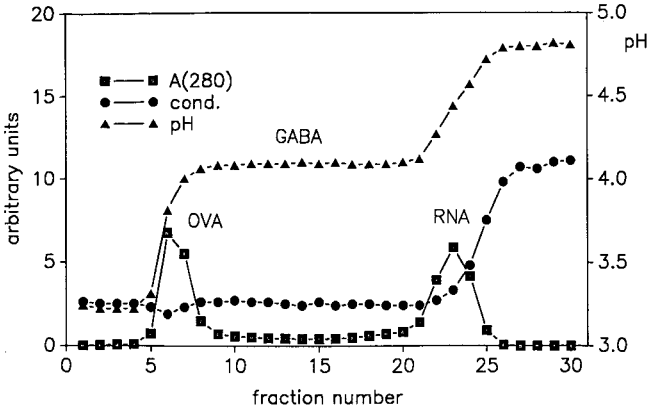

Fig. 7. Recycling ITP of 105 mg of RNA, 42 mg of GABA and 125 mg of OVA. The current and the pump rate were 50 mA and 30%, respectively. Counterflow, activated after 53 min (460 V), was applied for 47 min (511 V final). The charge applied was 300 C. Conductivity and absorbance scales are identical with those given in Fig. 2b.

the above-described experiments also contained some major impurities from the commercial ovalbumin sample used. We therefore adopted the problem of purification of ovalbumin by removal of two of its major impurities, lysozyme and conalbumin, to give the second model example in this part of the study. Fig. 8a depicts the result obtained with the rotating segmented column (operated without cooling at 4.5 rpm). Similar data were obtained in the recycling apparatus. As shown in Fig. 8b and c, operation with a counterflow (Fig. 8c) provides better results than operation without a counterflow (Fig. 8b). The OVA peak concentration (fraction 16, Fig. 8c) was found to be 25 mg/ml. The effectiveness of the recycling ITP purification procedure is indicated by capillary ITP analyses of individual fractions. Fig. 9a and b show the original ovalbumin sample analysed without and with GABA as spacer, respectively, illustrating a relatively high content of impurities migrating in front of the GABA zone (predominantly lysozyme and conalbumin, as stated by the supplier). Fig. 9c shows the analysis of a fraction containing mainly OVA and some residual impurities. In Fig. 9d the analysis of a fraction with maximum impurity concentration is shown

The present model system was further employed to investigate the impact of other parameters. Of great interest was the question of how the separation performance is affected by the thickness of the liquid layer in the RITP separation cell. Fig. 10 depicts a comparison of the absorbance profiles from OVA purification having cells with thickness 0.75 (as in all previous runs), 0.50 and 0.25 mm. No significant influence of the cell gap was observed when operating without a counterflow (Fig. 10a). The application of a counterflow, however, was found markedly to dilute and broaden the OVA zone with decreasing cell thickness (Fig. 10b). With no counterflow separation was incomplete and comparable in all three instances, whereas with a counterflow the resolution was found to increase with decreasing gap size. Variation of the electric current and the recycling pump rate did not affect the separation in a given cell assembly, as is shown in Fig. 10c (data for a 0.25-mm cell). These results demonstrate that identical zones (*i.e.*, steady state) are obtained with

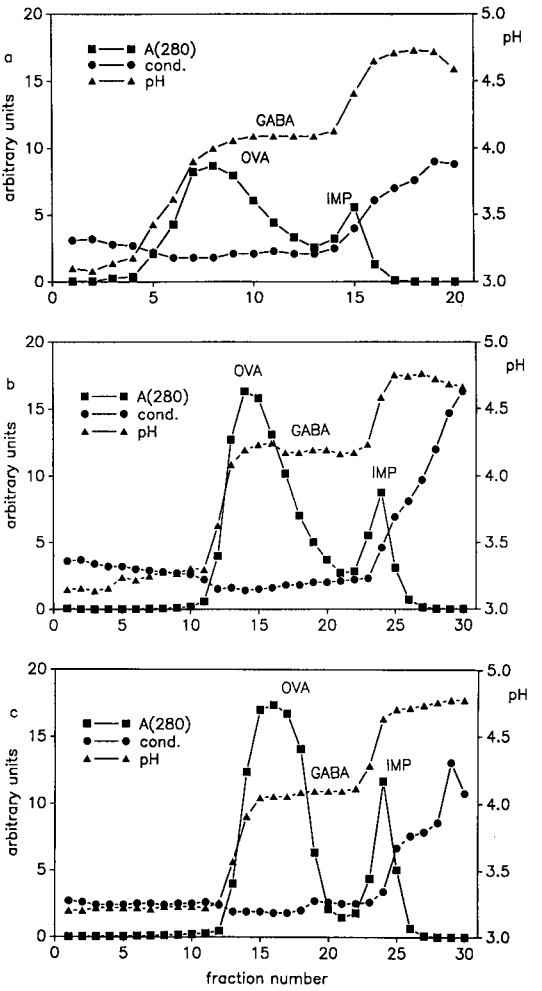

Fig. 8. (a) ITP of 310 mg of OVA and 9.1 mg of GABA in the Rotofor (no cooling) at 4.5 rpm. A constant 15 mA was applied for 60 min (final voltage 430 V). Recycling ITP data for 710 mg of OVA and 14 mg of GABA (b) without counterflow (60 min run time) and (c) after 52 min of counterflow (112 min run time). In both instances the current and the recycling pump rate were a constant 50 mA and 30%, respectively. The total voltages at the collection time were 510 and 463 V (450 V at counterflow activation), respectively. The processing charges were 180 and 346 C, respectively. Scales are identical with those in Fig. 2b.

a relatively wide range of parameters; 300 C were apparently sufficient to reach steady state. This is considered to provide confirmation that the three runs depicted in Fig. 10b are at the steady state. The internal volumes of the three cells (6, 4 and 2 ml) are small compared with the total volume of the recycling channels (*ca.* 120 ml) and are therefore not considered to be responsible for the change in the zone patterns. It is shown in this work that counterflow, at a given gap size, influences the steady-state distribution. Further tests are needed to elucidate the impact of counterflow on zone formation at various gap sizes.

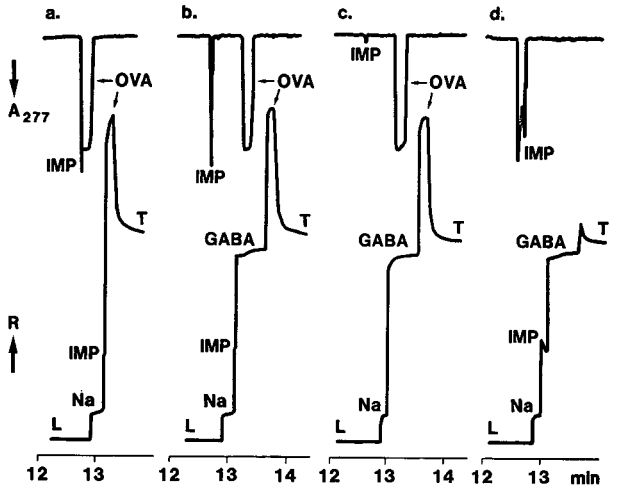

Fig. 9. Capillary ITP analyses of (a) commercial OVA, (b) OVA with GABA and (c, d) two fractions of a typical OVA/GABA recycling ITP run which were spiked with GABA. Samples of 1 μl of a 24 mg/ml OVA solution (a, b) or of undiluted fractions (c, d) were injected. For runs b–d 0.5 μl of a 4.2 mg/ml solution of GABA was co-administered. The lower and upper graphs depict the conductivity (expressed as increase in resistance, R) and UV absorbance at 277 nm, respectively. A constant current of 150 μA was applied. IMP: impurity.

CONCLUSIONS

ITP of proteins in screen-segmented columns, reported here for the first time, is an attractive approach for the fractionation of proteins in the milligrams to grams range. These investigations revealed that (i) in all operational modes ITP zone formation was slightly better without internal cooling (*cf.*, Figs. 1 and 2); (ii) having a vertical column downward migration provided better ITP zones in one instance (Fig. 4a and b) whereas upward migration was better for another (Fig. 1a and b); (iii) collection of all twenty fractions at once gave better results than fractionation via continuous elution at one column end, for which the experiments became very long and fractions were diluted with leader and partially mixed (Figs. 4 and 6); and (iv) having a horizontal column rotate around its separation axis was found to be essential and rotation at 4.5 rpm was shown to be preferred to 1 rpm (Fig. 2). For all systems investigated, the horizontal arrangement with 4.5 rpm and without internal cooling provided the best results.

The recycling ITP data demonstrated that (i) a counterflow was required for the purification of proteins (Figs. 8a and b, and 10a and b); (ii) a counterflow changed the steady-state protein profile (Fig. 3); and (iii) steady-state profiles were dependent on the gap size but not markedly influenced by the applied current or recycling pump rate (Fig. 10). The last fact provides an explanation for the previously reported difference between the plateau BSA concentrations found for recycling and continuous flow ITP [4]. This effect, however, cannot be explained with the current mathematical ITP models. The impact of gap size on the steady-state distribution is another phenomenon that remains to be explained from a theoretical point of view.

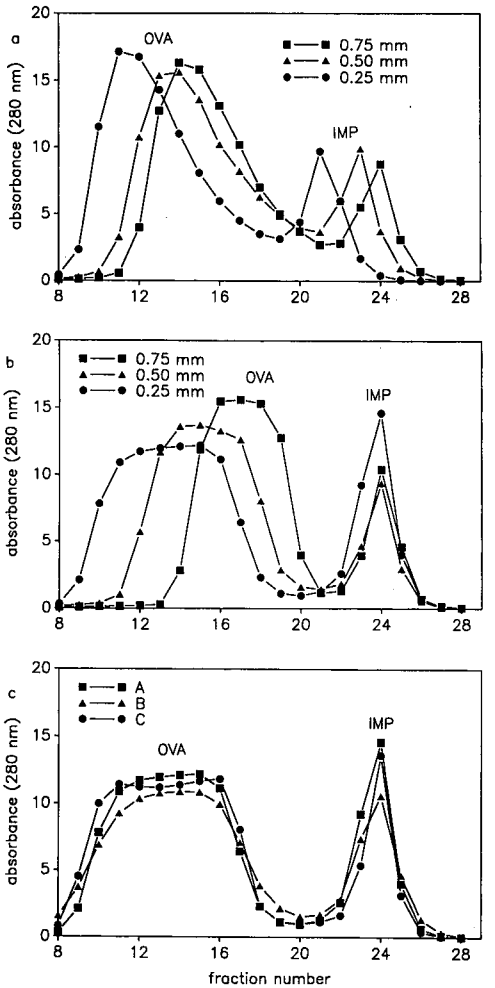

Fig. 10. Recycling ITP absorbance data of 710 mg of OVA and 14 mg of GABA (a) without and (b) with counterflow as functions of the gap size. The pumping rate was 30% in all instances. Without counterflow the total charges were 180 C (conditions: 50 mA, 60 min, 510 V final), 159 C (34 mA, 78 min, 623 V) and 159 C (34 mA, 78 min, 1095 V) for the 0.75-, 0.5- and 0.25-mm cells, respectively. With counterflow the charges were 346 C (conditions: 50 mA, 463/450 V final/at counterflow activation), 380 C (50 mA, 798/730 V) and 534 C (50 mA, 1561/1604 V), respectively. The durations of counterflow were 52, 60 and 120 min, respectively. (c) Recycling ITP absorbance data for 720 mg of OVA and 14 mg of GABA with counterflow in the 0.25-mm gap cell. The applied charges were (A) 534, (B) 308 and (C) 316 C, the constant currents were 50 mA (conditions: 1560/1604 V final/at activation of counterflow), 34 mA (1052/1091 V) and 34 mA (1050/1092 V), the recycling pump rates were 30, 30 and 15%, counterflow was activated after 58, 84 and 85 min and collection occurred after 178, 151 and 155 min, respectively.

Comparison of column ITP and recycling ITP data revealed that a better resolution was obtained with the latter approach (*cf.*, Figs. 4 and 7, Fig. 8). For example, in recycling ITP the load capacity was not completely exhausted in the experiments depicted in Fig. 8b and c. Therefore, the resolution could be enhanced by

employing larger amounts of spacer. In column ITP the protein zone pattern occupied almost the whole column length (Fig. 8a). Recycling ITP runs were executed at *ca.* 330 A/m^2 (cell with 0.75 mm gap; 25–50 W) compared with *ca.* 65 A/m^2 (5–10 W) in the column experiments. The throughputs investigated were all of the order of several hundred milligrams of protein per hour. Although not yet thoroughly investigated, scale-up of recycling ITP should be simpler than for column ITP.

Commercially available OVA contains major impurities which, in a cationic ITP configuration, were found to migrate in front of this protein. Using GABA as a spacer, OVA could be purified in both types of instruments. Analysis by capillary ITP revealed that the major OVA fractions were essentially free from the impurities (Fig. 9). This example constitutes an interesting model system for evaluation of the recycling ITP operational modes and we are therefore planning to study further the removal and purification of these impurities by recycling ITP.

ACKNOWLEDGEMENTS

The generous loan of the Tachophor 2127 and Uvicord 2158 instruments by LKB is gratefully acknowledged. The authors thank the Liver Foundation, Berne, for the purchase of the Rotofor, T. Long for providing the counterflow pulse damper and Ciba-Geigy for the ovalbumin sample. P.G. thanks his employer for granting study leave. This work was supported by the Swiss National Science Foundation.

REFERENCES

1 C. J. Holloway and R. V. Batterby, *Methods Enzymol.*, 104 (1984) 281, and references cited therein.
2 P. Boček, M. Deml, P. Gebauer and V. Dolník, *Analytical Isotachophoresis*, VCH, Weinheim, 1988.
3 J. E. Sloan, W. Thormann, G. E. Twitty and M. Bier, *J. Chromatogr.*, 457 (1988) 137.
4 W. Thormann, M. A. Firestone, J. E. Sloan, T. D. Long and R. A. Mosher, *Electrophoresis*, 11 (1990) 298.
5 R. A. Mosher, D. Dewey, W. Thormann, D. A. Saville and M. Bier, *Anal. Chem.*, 61 (1989) 362.
6 W. Thormann and R. A. Mosher, *Electrophoresis*, 11 (1990) 292.
7 W. Thormann and R. A. Mosher, in C. Schafer-Nielsen (Editor), *Electrophoresis '88*, VCH, Weinheim, 1988, p. 121.
8 M. Bier, N. B. Egen, T. T. Allgyer, G. E. Twitty and R. A. Mosher, in E. Gross and J. Meienhofer (Editors), *Peptides: Structure and Biological Function*, Pierce, Rockford, IL, 1979, p. 35.
9 N. B. Egen, W. Thormann, G. E. Twitty and M. Bier, in H. Hirai (Editor), *Electrophoresis '83*, Walter de Gruyter, Berlin, 1984, p. 547.
10 N. B. Egen, G. E. Twitty, W. Thormann and M. Bier, *Sep. Sci. Technol.*, 22 (1987) 1383.

Journal of Chromatography, 545 (1991) 331–336
Elsevier Science Publishers B.V., Amsterdam

CHROM. 23 169

Step change of co-ion, a new option in capillary zone electrophoresis

J. SUDOR, J. POSPÍCHAL, M. DEML and P. BOČEK*
Institute of Analytical Chemistry, Czechoslovak Academy of Sciences, Veveří 97, 611 42 Brno (Czechoslovakia)

ABSTRACT

A new variant of a dynamic step of the operational ionic matrix in capillary zone electrophoresis has been developed. The method extends the range of pK values of substances that can be analysed in one run and opens up a new means of optimization of the separation in comparison with classical zone electrophoretic mode where the composition of the background electrolyte–ionic matrix is maintained constant. The method is based on carrying out the separation at one pH for a certain period of time and, at another pH for another period. The change in the pH of the operational ionic matrix during the separation run is achieved by a fast-moving step of the co-ion. The method enables one to shorten the analysis time and is easy to use on commercial equipment. The analytical potential of the method is demonstrated by the separation of a six-component model mixture of phenol derivatives with 5 units difference in pK values.

INTRODUCTION

Electrophoretic separations of complex mixtures often do not yield a complete separation of all substances and/or the analysis time is too long if the separation run is carried out at a constant composition of the separation matrix (background electrolyte). Such cases can be expected especially when mixtures of substances covering a broad range of pK values are to be analysed.

Recently, a new option has been developed [1] for coping with this problem. The proposed method enables one to separate a sample in an on-line arrangement at two different pHs, which increases the separation power and provides more possibilities for optimization of the separation time. The basis of the technique is the generation of a dynamic change of the background electrolyte which proceeds fast along the separation capillary and introduces new operational conditions (pH).

These changes can be classified according to the direction of the migration and the shape of the concentration profile. In principle, with respect to the electromigration of solutes, there are two possibilities for dynamic changes, namely dynamic changes in the composition of the co-ion and/or the counter-ion. With respect to the shape of the dynamic change used, it has been shown that three principal types can be distinghuised, namely step, pulse and gradient.

In recent papers, the utilization of a pH step [2] and pulse [3,4] has been report-

0021-9673/91/$03.50

ed, with H^+ serving as the counter-ion. Further, the use of a dynamic pH gradient has been investigated in which H^+ served as the co-ion [5,6]. The common feature in these studies was direct control of the H^+ flow from the anodic chamber, which is easy as long as a reasonable pH range is used, *i.e.*, an acidic medium. There is, of course, a problem in controlling the H^+ flow at a concentration level of 10^{-7} ml/l, when a pH range from 7–11 should be used.

The objective of this paper is to show that the problem of dynamic buffering of pH in neutral and alkaline media may be easily solved by employing a dynamic step of the buffering anionic system. The technique proposed is exemplified by the separation of 2,5-dinitrophenol, 4-nitrophenol, 3-nitrophenol, 3-chlorophenol, 4-chlorophenol and phenol, were the analysis was started at pH 7 and finished at pH 11, and the appropriate dynamic change in pH was created by a moving boundary of carbonate → oxalate.

EXPERIMENTAL

A laboratory-assembled system was used in all electrophoretic experiments. The fused-silica capillary (VŠCHT, Prague, Czechoslovakia) was 58 cm × 85 μm I.D. Its inner surface was coated with linear polyacrylamide according to Hjertén [7].

A Jasco Model 875 UV detector was used (Japan, Spectroscopic, Tokyo, Japan), modified by replacing the original flow cuvette with a capillary holder. The detection cell was situated 42 cm from the injection end of the capillary (cathode side). The full-scale range was 0.02 absorbance units. The wavelength selected was 232 nm.

A laboratory-made high-voltage power supply was used and is described elsewhere [8]. The driving current was 40 μA at 12 kV across the whole capillary.

A Servogor (Goerz, Vienna, Austria) model 2S linear recorder was used. The sample was injected by a siphoning system: the sample contained a $3 \cdot 10^{-4}$ *M* solution of each solute and the sampling time was 5 s. The amount sampled was 10^{-13} mol at a 70-mm difference between levels of buffer and sample.

To prevent changes in the pH in the cathodic electrolyte chamber owing to electrolysis, it was filled with buffer. For pH 7.2, 8.3 and 9.5 N-(2-hydroxyethyl) morpholine, tris(hydroxymethyl)aminomethane and 2-amino-2-methyl-1,3-propanediol, respectively, were used.

All chemicals were of analytical reagent grade and were obtained from Lachema (Brno, Czechoslovakia), except 4-nitrophenol (Merck, Darmstadt, Germany), 3-nitrophenol (Loba, Vienna, Austria) and N-(2-hydroxyethyl)morpholine, tris(hydroxymethyl)aminomethane and 2-amino-2-methyl-1,3-propanediol (Serva, Heidelberg, Germany).

The procedure for producing the dynamic step of the co-ion (anion) was simple, as shown in Fig. 1. The injection end of the capillary together with a platinum wire serving as a cathode are dipped into the primary electrolyte chamber and subsequently into the modifying electrolyte chamber.

RESULTS AND DISCUSSION

For work at high pH, especially if the pH is changed during the run, it is very important either to eliminate electroosmosis or to keep the electroosmotic flow in the

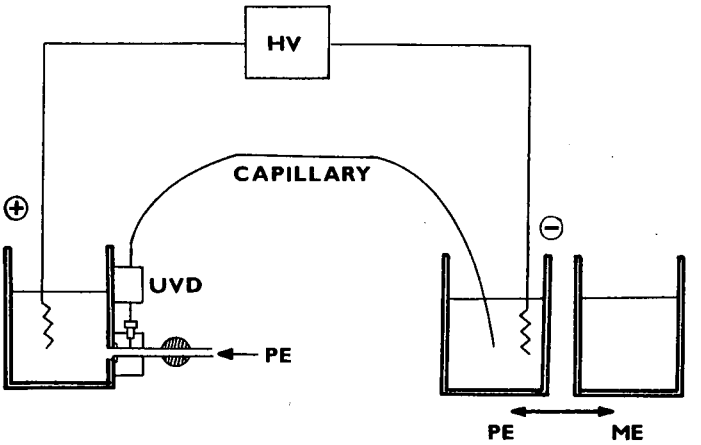

Fig. 1. Scheme of the electrophoretic equipment with modification of the ionic matrix. HV = High-voltage power supply; UVD = ultraviolet detector; PE and ME = primary and modifying electrolyte, respectively.

broad pH range as constant as possible, in order to ensure reproducibility of measurement. For this reason the inner surface of the capillary was coated with a layer of linear polyacrylamide and the electroosmotic properties of the coated capillary were tested by using picric acid, servingt as a mobility standard. By measuring the migration velocity of picric acid, the value $u(\mathrm{eo}) \leqslant 4 \cdot 10^{-9}$ m^2 V^{-1} s^{-1} for cathodic electroosmosis was found. This value was checked regularly and was stable during all experiments (about 1 month).

Nitro and chloro derivatives of phenol were selected as model species and are listed in Table I. Obviously, these species have very close ionic mobilities and they cover a broad range of pK values (5.2 – 10).

The separation of a model mixture of the above species at various constant pH values of the primary electrolyte are shown in Fig. 2. Fig. 2a shows the separation of pH 7.2 At this pH only the most acidic compounds, 2,5-dinitrophenol and 4-nitrophenol, can be analysed, as the other substances do not have sufficient mobility to reach the detector in an acceptable time. Analysis at pH 8.3 is shown in Fig. 2b. At this pH the species with increasing pK values up to 9.38 (4-chlorophenol) reach the

TABLE I

MOBILITIES AND DISSOCIATION CONSTANTS [9] FOR A MODEL MIXTURE

Substance	Mobility (10^{-9} m^2 V^{-1} s^{-1})	pK
2,5-Dinitrophenol	31.3	5.216
4-Nitrophenol	33.4	7.149
3-Nitrophenol	33.4	8.399
3-Chlorophenol	33.4	9.023
4-Chlorophenol	33.4	9.378
Phenol	34.4	9.998

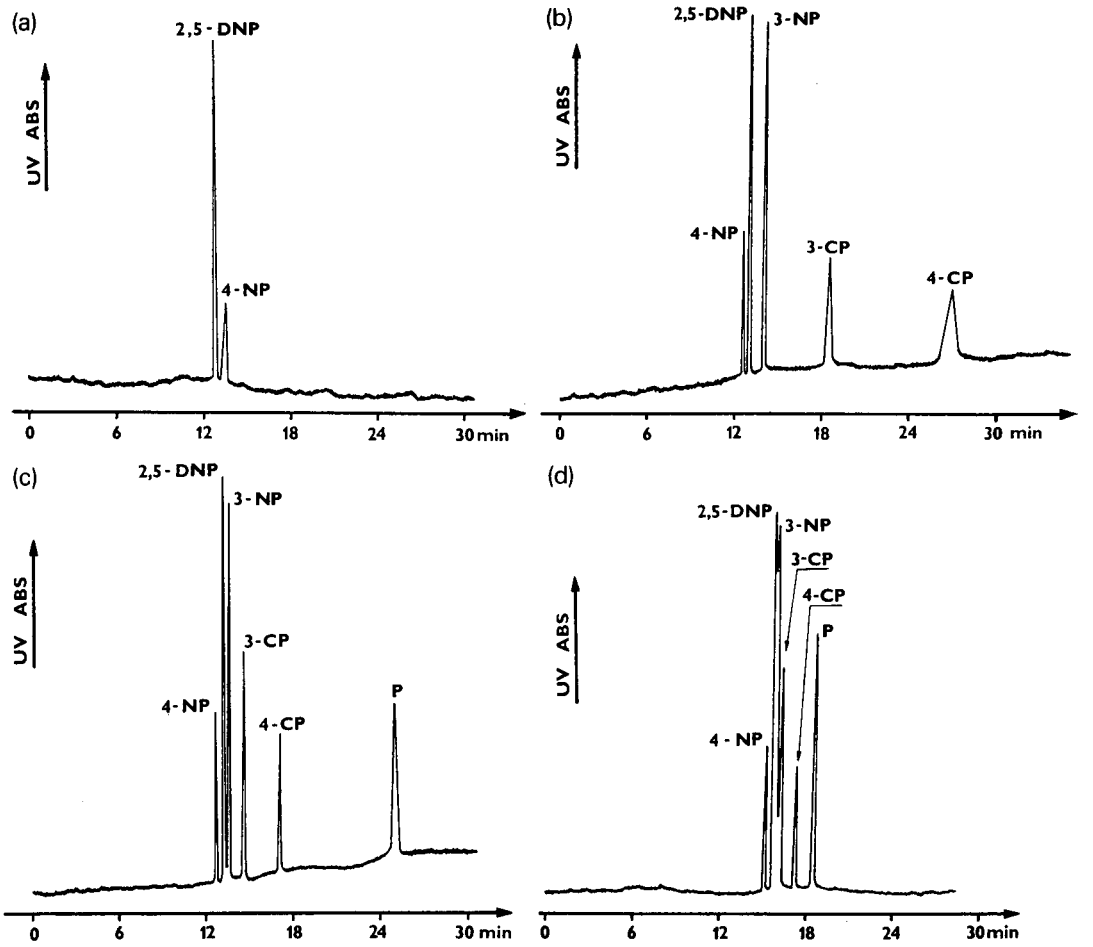

Fig. 2. Capillary zone electrophoresis of the model mixture in the primary electrolyte (0.01 *M* lithium oxalate) at constant pH: (a) 7.2; (b) 8.3; (c) 9.5; (d) 10.5. DNP = 2,5-dinitrophenol; 4-NP = 4-nitrophenol; 3-NP = 3-nitrophenol; 3-CP = 3-chlorophenol; 4-CP = 4-chlorophenol; P = phenol.

detector in less than 30 min. By increasing the pH to 9.4 and 10.5 (Fig. 2c and d), it is possible to analyse all the substances up to pK = 10 (phenol), but the 2,5-dinitrophenol–3-nitrophenol pair gives a mixed zone. The time required for a run is 25 and 19 min, respectively.

Obviously, one constant pH value during a run does not result in an acceptable analysis, and a dynamic step of pH may be used advantageously here.

The principle of the proposed method is depicted in Fig. 3, where the calculated trajectories (time *vs.* position in the capillary) of the separated substances are plotted. As can be seen in the lower part, all substances are easily separated in the primary ionic matrix, but the mobilities of 3-nitrophenol, 3-chlorophenol, 4-chlorophenol and phenol are too low to reach the detector in a reasonable time.

By replacing oxalate with carbonate, a modifying step is created, which in-

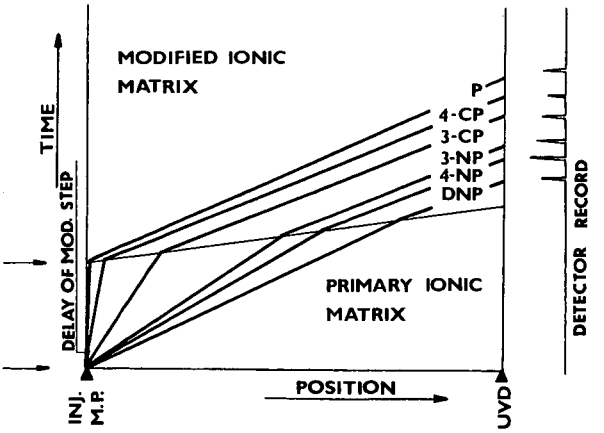

Fig. 3. Principle of the method. Trajectories of the sample components in the $x-t$ plane. INJ, injection; UVD, ultraviolet detection; M.P., starting-modification point. On the right the corresponding detection record is shown for abbreviations, see Fig. 2.

creases the pH along the column to 11. Hence, a new modified ionic matrix is created along the migration path. The dynamic step of carbonate → oxalate, *i.e.*, of modified → primary matrix, is faster than for any of the actual solutes and it passes them. When the solutes are in the modified matrix they are fully ionized and migrate with high velocities to the detector. Obviously, the separation can be affected by setting up pH values of the primary and modified matrix–electrolyte (in Fig. 3 we are changing the slopes of the trajectories), or we can change the time delay of the modifying step.

Experiments in which the dynamic step was utilized are shown in Fig. 4. In Fig.

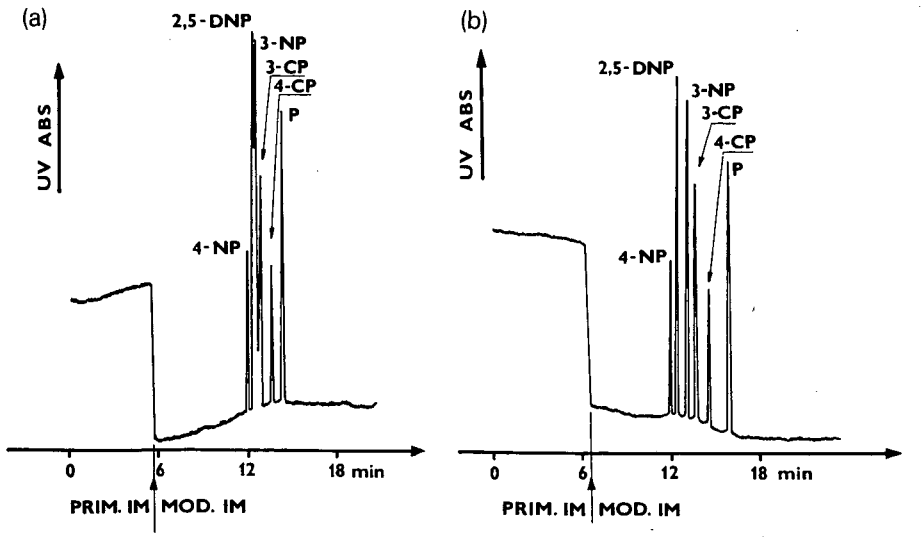

Fig. 4. Capillary zone electrophoresis of the model mixture in the primary electrolyte of pH 7.2 using an ionic matrix step. Time delay of the step: (a) 0 s; (b) 20 s.

4a, the time delay of the step was 0 s, and analysis was performed in less than 13 min. The starting and final pH values were 7.2 and 11, respectively. Here, 2,4-dinitrophenol, 3-nitrophenol and 3-chlorophenol form the mixed zone. It is clear that the residence time of these substances in the primary matrix (pH 7.2) was too short. By introducing a time delay of 20 s, *i.e.*, by increasing the time of separation and residence time in the primary electrolyte, complete separation was achieved in 16 min (Fig. 4b). An additional increase in the time delay then leads only to an increased time of separation.

Finally, we conclude that a dynamic step of the co-ion provides a new means of increasing the separation power and optimizing the separation. The advantage of this method is that it requires a very simple mechanical experimental arrangement and may be easily used in commercial equipment.

REFERENCES

1 J. Sudor, Z. Stránsky, J. Pospíchal, M. Deml and P. Boček, *Electrophoresis*, 10 (1989) 802.
2 F. Foret, S. Fanali and P. Boček, *J. Chromatogr.*, 516 (1990) 219.
3 M. Deml, J. Pospíchal and P. Boček, in *Proceedings of the 2nd National Conference on Isotachophoresis, Spišská Nová Ves, Czechoslovakia*, April 4–6, 1989, p. 46.
4 P. Boček, M. Deml and J. Pospíchal, *J. Chromatogr.*, 500 (1990) 673.
5 P. Boček, M. Deml, J. Pospíchal and J. Sudor, *J. Chromatogr.*, 470 (1989) 309.
6 V. Šustáček, F. Foret and P. Boček, *J. Chromatogr.*, 480 (1989) 274.
7 S. Hjertén, *J. Chromatogr.*, 347 (1985) 191.
8 M. Deml, P. Boček and J. Janák, *J. Chromatogr.*, 109 (1975) 49.
9 T. Hirokawa, M. Nishino, N. Aoki, Y. Kiso, Y. Sawamoto, T. Yagi and J. Akiyama, *J. Chromatogr.*, 271 (1983) D1.

Journal of Chromatography, 545 (1991) 337–342
Elsevier Science Publishers B.V., Amsterdam

CHROM. 23 151

Data acquisition and digital filtering in analytical isotachophoresis

J. C. REIJENGA

Laboratory of Instrumental Analysis, Eindhoven University of Technology, P.O. Box 513, 5600 MB Eindhoven (The Netherlands)

ABSTRACT

Voltage-to-frequency conversion (VFC) or 12-bit integrating analog-to-digital conversion with data bunching/averaging during 50 ms is suggested as the optimum data acquisition technique in isotachophoresis. Computer simulation of digital filtering of the conductivity and UV signal in analytical isotachophoresis in the time domain with Savitzky–Golay filtering, commonly used in chromatography, leads to unwanted oscillations at the stepwise change of the signal at the zone-to-zone boundary. If it is really necessary to remove noise prior to further signal evaluation, a rectangular moving average filter is preferred. In that case, a signal restoration algorithm should be applied to the filtered signal.

INTRODUCTION

The conductivity and UV detector signals in analytical isotachophoresis are characterized by a number of zones or plateaux of constant amplitude, separated by a more or less stepwise increase or decrease in time [1,2]. Disturbances can be of electronic, chemical or physical in nature, the origin of which is beyond the scope of this paper. It suffices to know that these disturbances can lead to either drift during detection of a zone, a distortion of the stepwise change or noise superimposed on the signal.

Plotting the signal on a potentiometric recorder is usually no problem, because of the time constant of the instrument (*ca.* 0.3 s). Obviously, this time constant should not be so high as to disturb the stepwise changes of the signal. When computerized data acquisition is applied, analog-to-digital conversion (ADC) sampling frequencies in the range 10–50 Hz are mostly used [3–6]. If present, stochastic or periodic disturbances below this frequency range are also sampled. In this instance, a digital filter is applied. In recent publications on computerized data evaluation in isotachophoresis [5,7] application of a time-domain filter according to the procedure of Savitzky and Golay [8] was described. In their original paper, Savitzky and Golay indicated that, for noise reduction in signals with Gaussian peaks, their filter performs better than exponential, triangular and (rectangular) moving average filters.

In isotachophoresis, the main criterion for the choice of filter type is that the

0021-9673/91/$03.50

stepwise change is not affected. This paper will show, through computer simulation of digital filtering, that of the time-domain filters mentioned the Savitzky–Golay type is less suitable. Whenever filtering is really necessary, a (rectangular) moving average (MA) type of filter is preferred.

EXPERIMENTAL

Data acquisition

The isotachophoretic signal contains both qualitative and quantitative information. In data acquisition, the associated parameters are resolution and sampling frequency, respectively. The reproducibility of the signal amplitude in present-day detectors (conductivity, potential gradient, UV absorption) does not require a resolution greater than 12 bits.

Capillary isotachophoresis is usually carried out at current densities that represent a compromise between speed of analysis and zone boundary disturbance due to convection and diffusion [9]. The resulting zone boundary profile gives rise to a zone transition of *ca.* 1 s. In order to describe this zone transition, and thus determine accurately the location of the inflection point, sampling frequencies higher than 20 Hz are unnecessary. Otherwise, additional information (fluctuations), not originating from isotachophoretic phenomena, are also sampled. Moderate speed ADCs employ either of two principles of operation: successive approximation or integration. In the former instance, averaging times are typically 50 ms [10]. These devices are thus overspecified by a factor 1000 at a sampling frequency of 20 Hz. In addition, fluctuations in the range 20–20 000 Hz can lead to aliasing. For data acquisition in chromatography, therefore, voltage-to-frequency convertors (VFCs) or integrating ADCs are preferred. Most chromatographic data acquisition stations are equipped with such devices, which combine integrating capacity with high resolution [11]. The former characteristics makes them especially useful for isotachophoresis.

Simulation of digital filtering

Computer simulation of digital filtering was performed with CLEOPATRA [12], modified and adapted [13] for use in a practical course for second-year students of the Chemical Engineering Faculty at our University. One of the modules of the program performs time-domain filter functions on signals generated by the program, or on data files. The latter can consist of real data measured by another program, with the important restriction that they consist of 256 data points only. For simulation and demonstration purposes, however, this poses no problems.

Simulation of isotachophoretic signals

In order to generate isotachophoretic signals, a computer program (ITPSIMUL) was written in Quickbasic (Microsoft, Redmond, WA, U.S.A.). A 256-point isotachopherogram could be generated, choosing the number of zones and their respective height and length. The stepwise signal increase from zone to zone is usually disturbed by a zone boundary profile due to convection and diffusion [1,9]. As an approximation, an eleven-point Gaussian-shaped disturbance was assumed and thus convoluted with the generated isotachopherogram. Finally, white noise could be added to the signal. The generation of such an isotachopherogram is illustrated in Fig. 1.

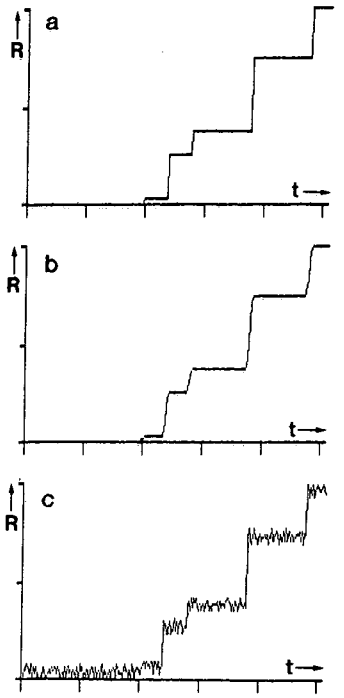

Fig. 1. Isotachopherogram, generated by the program ITPSIMUL, (a) consisting of a number of zones with infinitely sharp boundaries (b), after convolution with a Gaussian disturbance and (c) after addition of 5% white noise. R = Resistance; t = time.

The signals were stored in sequential files, compatible with the modified CLEOPATRA format.

RESULTS AND DISCUSSION

Noise reduction

A noisy baseline was generated and filtered with both a Savitzky–Golay (S–G) and a (rectangular) moving average (MA) digital filter with a filter width ranging between 5 and 21 points. The results are shown in Fig. 2. The MA-type filter is always more effective in noise reduction, although the net gain is only 30% at higher filter widths. However, one should realize that the results indicate that thirteen-point MA filter performs better than a 21-point S–G filter.

If using a conventional algorithm, an additional advantage of an MA filter is that the algorithm executes faster, because of the equal weighting factors. An n-point S–G filter requires $(n-1)/2$ multiplications and $(3n-3)/2$ additions per data point, an MA filter 1 and n, respectively. Faster algorithms for these filters have also been developed [14].

Signal distortion

As mentioned above, the simulated isotachopherograms were convoluted with

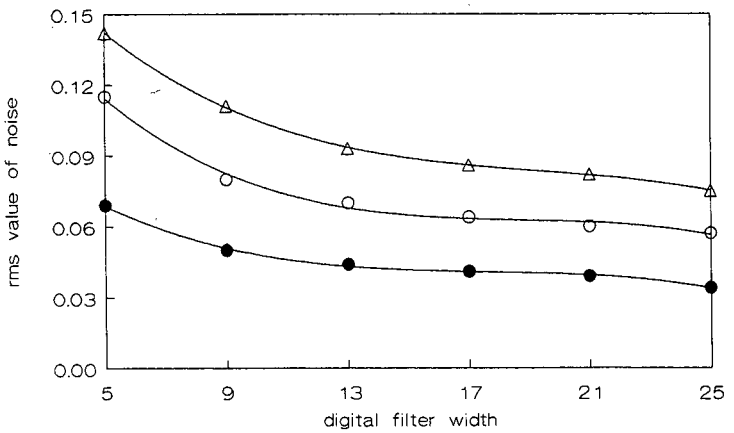

Fig. 2. Root-mean-square (rms) value of the noise on a straight baseline after applying a digital filter with different width. (○) Savitzky–Golay, (●) rectangular moving average and (△) exponential filter. The rms value of the noise in the original signal was 0.161.

an eleven-point Gaussian disturbance. In practice, a zone transition time of 1 s corresponds to a relatively sharp boundary, and is usually encountered only in optimized cationic separations. Thus, with a sampling frequency of 10–20 Hz an excellent description of the signal during the zone transition is obtained. There is obviously no

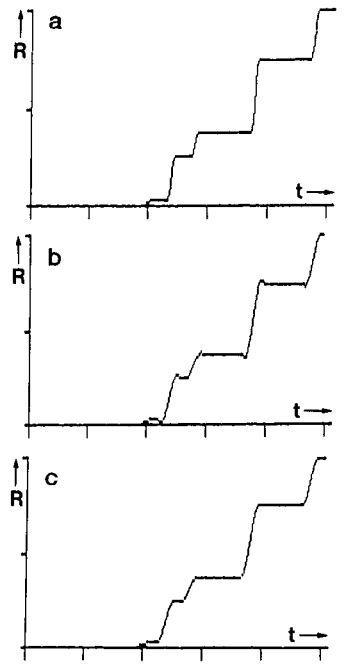

Fig. 3. Simulated isotachopherogram (a) filtered with (b) a seventeen-point cubic S–G filter (c) a nine-point MA filter. These filters effect comparable degrees of noise reduction.

signal distortion if the width of the MA filter is smaller than the number of data points during the zone transition.

For very noisy signals, *e.g.*, from a UV detector at 206 nm [15], combined with sharp zone boundaries, a filter with a larger width may be necessary. In that event, signal distortion can take place. Fig. 3, illustrates the effect of both an S–G and an MA filter. Noise has been omitted in order to show the difference between the two filters. It is seen that the S–G filter introduces an oscillation, which gives two or more additional inflections points. This has severe consequences for the algorithm that determines the number and length of the zones in the filtered signal. An MA filter of comparable performance in terms of noise reduction does not introduce these oscillations, but instead causes a minor uncertainty in the exact location of the inflection point.

Signal restoration

To overcome the effects of possible distortion, a restoration algorithm was developed and applied to the filtered signal. The idea is to replace a filtered data point

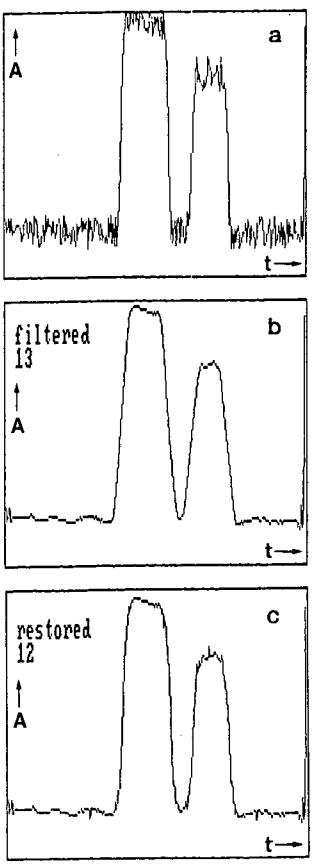

Fig. 4. Effect of the restoration algorithm on a filtered noisy signal. (a) Original signal filtered with (b) a thirteen-point MA filter and (c) restored. A = Absorbance.

with the average of the filtered and the original data point, if the filtered signal deviates substantially from the original. To this end, the standard deviation of the difference between the filtered and the original baseline is determined first. A threshold value of twelve times this standard deviation is taken. The effect is illustrated in Fig. 4, a simulated very noisy UV signal. It can be seen that the restoration algorithm improves the zone boundary sharpness of the filtered signal at the cost of a slightly higher noise level. The execution time of this restoration algorithm is small compared with that of the MA filter. It is therefore advised to include this restoration algorithm in the smoothing routine.

CONCLUSIONS

Data acquisition using a VFC or integrating ADC with a 50-ms averaging time is recommended. Only for noisy signals should a rectangular moving average filter with a minimum width be used. In that event, a signal restoration algorithm should be applied to the filtered signal.

REFERENCES

1 F. M. Everaerts, J. L. Beckers and Th. P. E. M. Verheggen, *Isotachophoresis–Theory, Instrumentation and Applications* (*Journal of Chromatography Library*, vol. 6), Elsevier, Amsterdam, 1976.
2 P. Bocek, M. Deml, P. Gebauer and V. Dolnik, *Analytical Isotachophoresis*, VCH, Weinheim, 1988.
3 J. C. Reijenga, W. van Iersel, G. V. A. Aben, Th. P. E. M. Verheggen and F. M. Everaerts, *J. Chromatogr.*, 292 (1984) 217.
4 J. C. Reijenga, Th. P. E. M. Verheggen and F. M. Everaerts, *J. Chromatogr.*, 267 (1983) 75.
5 B. J. Wanders, Graduation Report, University of Technology, Eindhoven, 1988.
6 F. S. Stover, K. L. Deppermann and W. A. Grote, *J. Chromatogr.*, 269 (1983) 198.
7 B. J. Wanders, A. A. G. Lemmens, M. M. Gladdines and F. M. Everaerts, *J. Chromatogr.*, 470 (1989) 79.
8 A. Savitzky and M. J. E. Golay, *Anal. Chem.*, 36 (1964) 1627.
9 J. C. Reijenga, Th. P. E. M. Verheggen and F. M. Everaerts, *J. Chromatogr.*, 328 (1985) 353.
10 *Data Acquisition Handbook*, Analog Devices, Norwood, MA, 1982.
11 Product Data Book, Burr Brown, Tucson, AZ, 1982.
12 G. Kateman, P. F. A. van der Wiel, T. H. A. M. Janse and B. G. M. Vandeginste, *CLEOPATRA (Chemometrics Library: an Extendable Set of Programs as an Aid in Teaching, Research and Application)*, Elsevier Scientific Software, Amsterdam.
13 J. H. M. Wijtvliet, Internal Reports, Computer Department, University of Technology, Eindhoven, 1987, 1988.
14 I. E. Bush, *Anal. Chem.*, 55 (1983) 2353.
15 Th. P. E. M. Verheggen, F. M. Everaerts and J. C. Reijenga, *J. Chromatogr.*, 320 (1985) 99.

Journal of Chromatography, 545 (1991) 343–347
Elsevier Science Publishers B.V., Amsterdam

CHROM. 23 176

Two-dimensional electrophoresis: agarose gel isotachophoresis followed by sodium dodecyl sulphate–polyacrylamide electrophoresis

FERNANDO ACEVEDO* and ZERE GOITOM
Department of Dermatology, Karolinska Hospital, Karolinska Institute, S-104 01 Stockholm (Sweden)

ABSTRACT

High resolution of proteins by gel isotachophoresis (ITP) has been achieved in previous work, and two-dimensional electrophoresis was applied in order to obtain further information on the proteins separated by ITP in agarose gels. Gradient or discontinuous buffer acrylamide gels in the presence of sodium dodecyl sulphate (SDS) and β-mercapthoethanol were used for the second electrophoresis. After two-dimensional ITP–SDS polyacrylamide gel electrophoresis (PAGE), several components were observed on the plates after either silver or Coomassie Brilliant Blue staining. The enhanced technique with SDS-PAGE revealed further heterogeneity among C3-complement proteins, with at least eight α- and eight β-chains of C3-complement. Two albumins spots were also observed after staining. The proposed technique provides a powerful addition to earlier methods for the separation of proteins.

INTRODUCTION

The most striking results with two-dimensional (2D) electrophoresis were obtained by O'Farrell [1] by combining isoelectric focusing (IEF) and sodium dodecyl sulphate–polyacrylamide gel electrophoresis (SDS-PAGE). However, the use of IEF is limited by precipitation or aggregation phenomena because the solubility of most proteins is lowest at their isoelectric points. In addition, the behaviour of some proteins *e.g.* serum albumin, which spread over a wide pH zone on focusing, limits the application of IEF for the separation of blood plasma proteins. To overcome these problems, ITP has been applied. The relative migration of plasma proteins in ITP is similar to that obtained in electrophoresis, and the resolution of the proteins achieved by ITP is comparable that given by IEF but the drawbacks mentioned are avoided [2].

The application of 2D ITP–SDS-PAGE followed by Coomassie Brilliant Blue (CBB) staining, silver staining and sequential immunostaining for the analysis of plasma proteins is described in this paper.

EXPERIMENTAL

Human plasma samples were supplied by the blood centre at the Karolinska Hospital. Agarose, ampholines, electrode strips and paper sample applicators were

0021-9673/91/$03.50

obtained from Pharmacia LKB Biotechnology (Bromma, Sweden), servalytes from Serva Feinbiochemica (Heidelberg, Germany), nitrocellulose membrane Immobilon from Millipore (Bedford, MA, U.S.A.), rabbit immunoglobulins (Igs) and horseradish peroxidase-conjugated swine antibodies against rabbit Igs from Dakopatts (Copenhagen, Denmark). All chemicals were of analytical-reagent grade.

Isotachophoresis in agarose gels

The procedure was basically as decribed earlier previously [1]. Isotachophoresis was run in flat-bed agarose gels (12 × 24 cm, 1 mm thick). The plasma proteins were electrophoresed towards the anode in 1% agarose IEF. Appropriate combinations of ampholytes and servalytes were used as spacers [3].

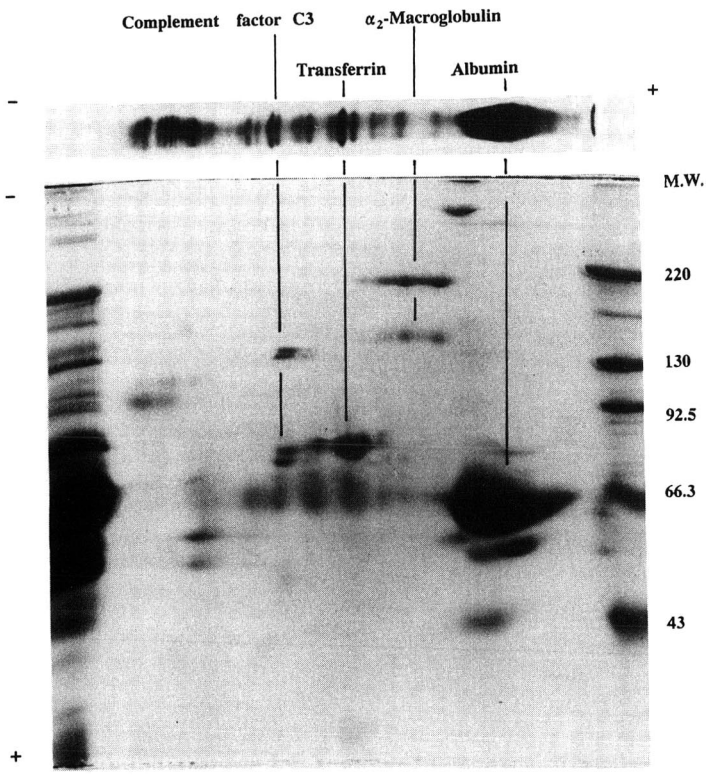

Fig. 1. 2D ITP–SDS-PAGE of human blood plasma proteins stained with CBB. First dimension (ITP) (top): leading ion, 40 m*M* glutamic acid; counter ion, 40 m*M* histidine; spacers, included in the gel, 1.2 ml of Servalytes 5–6; terminating ion; β-alanine; anode, 20 ml of 40 m*M* glutamic acid–250 m*M* histidine; cathode, 10 ml of 1 *M* β-alanine–250 m*M* histidine; power, 5W. Second dimension (discontinuous SDS-PAGE): separation gel, $T_{8.7}C_2$, in 400 m*M* Tris–HCl (pH 9.18); stacking gel, $T_{3,2}C_{6,25}$, in 125 m*M* Tris–HCl (pH 6.8); electrode buffer, 170 m*M* glycine–50 m*M* Tris. Left lane, human blood plasma sample; right lane, molecular weight standards. M.W. = molecular weights (kilodalton).

2D-Isotachophoresis–polyacrylamide gel electrophoresis

Strips 1.0 cm wide from the agarose gel plate were covered with buffer containing SDS and β-mercaptoethanol for 5 min. Thereafter, the strips were placed on the top of discontinuous 8.7% acrylamide gels [4] or 6–20% acrylamide gradient gels and run overnight. The proteins were revealed by CBB staining silver staining [5] or immunodetection [6,7].

Immunodetection

The transfer of the proteins to nitrocellulose (NC) was done by capillarity. Immunological detection was performed using peroxidase-labelled antibodies and staining with 4-chloro-1-napthol [7]. The NC filters were dried and photographed. If desired, the NC filters were used for the sequential immunological detection of other proteins.

RESULTS AND DISCUSSION

The relative positions of the non-denatured proteins in the ITP gels after the first dimension are determined by their electrophoretic mobilities, *i.e.*, α-, β- of γ-proteins. After denaturation with SDS and reduction with 2-mercaptoethanol, the sub-

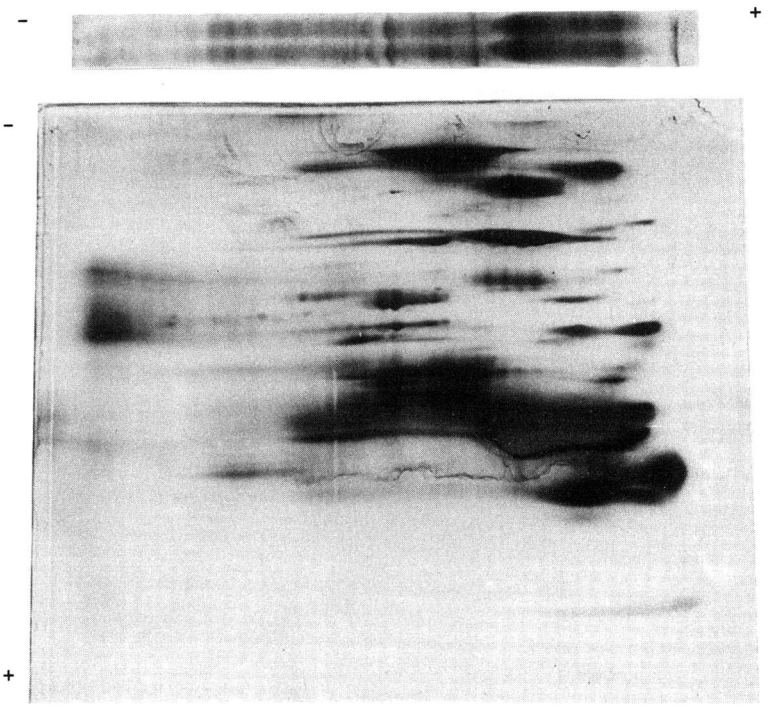

Fig. 2. Silver staining [5] in 2D ITP–SDS-PAGE of human blood plasma proteins. First dimension (ITP) (top): as in Fig. 1 except that the spacers were 0.8 ml of Ampholines 5–7 and 0.8 ml of Servalytes 5–6. Second dimension (gradient gel SDS-PAGE): gradient, T_6C_2 to $T_{20}C_2$ in 340 m*M* glycine–100 m*M* Tris buffer.

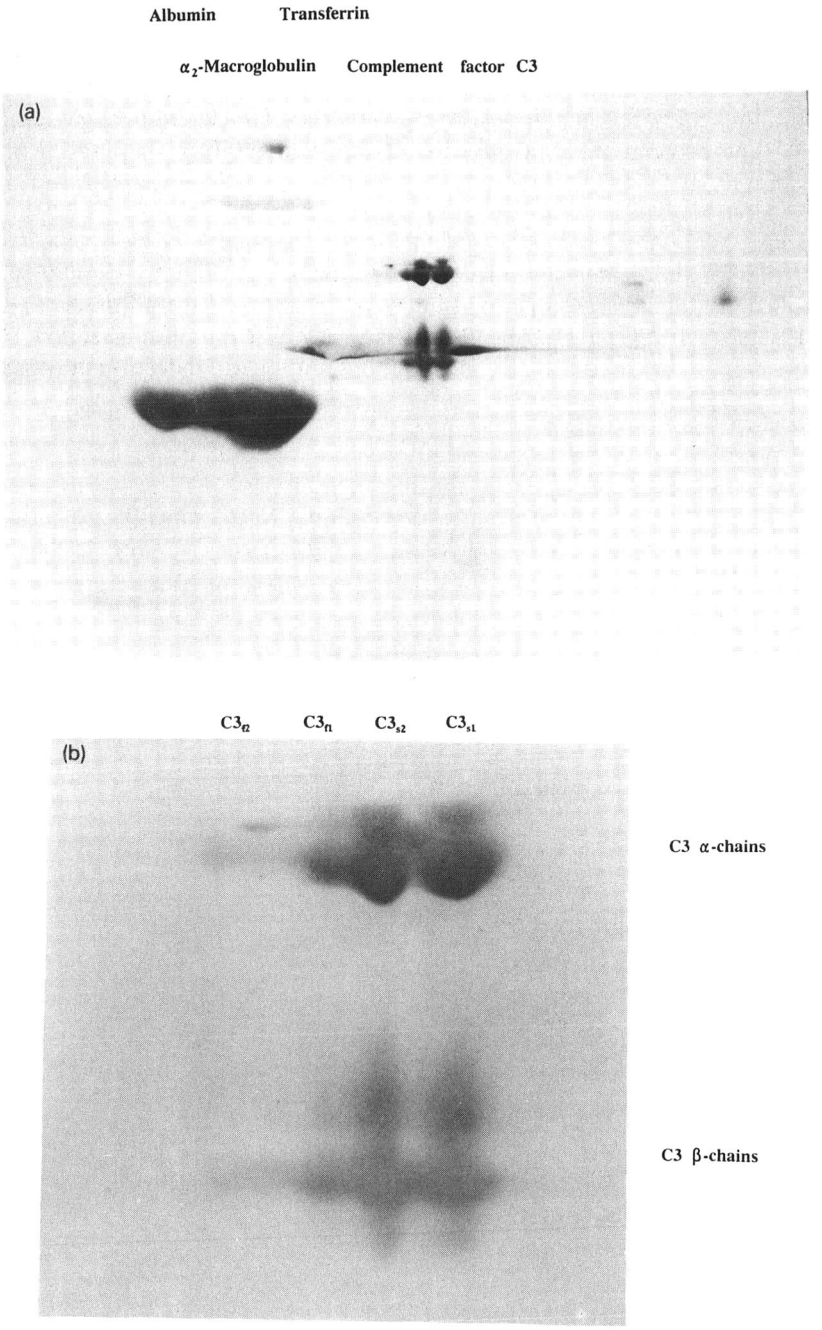

Fig. 3. Immunodetection of some human blood plasma components after 2D ITP–SDS-PAGE. (a) The stained proteins were albumin, α_2-macroglobulin, transferrin and C3-complement. (b) The α- and β-chains of C3-complement observed after 2D ITP–SDS-PAGE followed by immunostaining with antihuman $C3_c$.

units can be separated in acrylamide gels and revealed either with CBB, as in Fig. 1, with silver staining, as in Fig. 2 or by immunodetection, as in Fig. 3. After immunostaining with anti-human C3-complement at least eight α- and eight β-chains can be recognized (Fig. 3b). This heterogeneity has not been reported previously. At least two albumin spots can also be distinguished after immunostaining. These and other heterogeneities could also be observed after non-specific staining with CBB or silver.

The distribution of the proteins in the 2D ITP–SDS-PAGE differs from that obtained by 2D IEF–SDS-PAGE. Most of the stained compounds in the former show molecular weights over 40 kilodalton, whereas after 2D IEF–SDS-PAGE a high content of small proteins is observed [8]. This is due to the presence of denaturing agents required during the IEF separation of plasma proteins. The separation of human plasma proteins by 2D cellulose acetate–SDS-PAGE [9] produces a pattern resembling that obtained by 2D ITP–SDS-PAGE. However, the better resolution achieved by ITP permits the distinction of variants of several proteins.

The concentration step of the stacking zone in discontinuous buffer systems for SDS-PAGE, as in Fig. 1, causes a flattening of the sharp bands from the agarose migrating into the acrylamide gel with loss of resolution. Therefore, polyacrylamide gradient gels, as in Fig. 2, are more suitable for the second dimension in the technique presented here.

ACKNOWLEDGEMENTS

This work was supported by grants from the Swedish Medical Research Council (12-5665), the Karolinska Institute, the Swedish Medical Association, the Swedish Psoriasis Association and the Magnus Bergvall, Finsen and Edvard Wellander Foundations.

REFERENCES

1 P. H. O'Farrel, *J. Biol. Chem.*, 250 (1975) 4007.
2 F. Acevedo, in C. Schafer-Nielsen (Editor), *Electrophoresis '88*, VCH, Weinheim, 1988, p. 112.
3 F. Acevedo, *J. Chromatogr.*, 470 (1989) 407.
4 U. K. Laemmli, *Nature (London)*, 227 (1970) 680.
5 J. H. Morrissey, *Anal. Biochem.*, 117 (1981) 307.
6 H. Towbin, T. Staehelin and J. Gordon, *Proc. Natl. Acad. Sci. U.S.A.*, 76 (1979) 4350.
7 A. T. Andrews, *Electrophoresis–Theory, Techniques, and Biochemical and Clinical Applications*, Oxford Science, Oxford, 1986, p. 67.
8 R. P. Tracy, R. M. Currie and D. S. Young, *Clin. Chem.*, 28 (1982) 890.
9 A. Lapin, H. Regele, H. Kopsa, M. Rohac and F. Gabl, in C. Schafer-Nielsen (Editor), *Electrophoresis '88*, VCH, Weinheim, 1988, p. 106.

Journal of Chromatography, 545 (1991) 349–358
Elsevier Science Publishers B.V., Amsterdam

CHROM. 23 143

Isoelectric focusing field-flow fractionation

II. Experimental study of focusing of methyl red in the trapezoidal cross-section channel

JOSEF CHMELÍK

Institute of Analytical Chemistry, Czechoslovak Academy of Sciences, Veveří 97, 611 42 Brno (Czechoslovakia)

ABSTRACT

Isoelectric focusing field-flow fractionation is a technique for the separation of ampholytes using in addition to the electric field and pH gradient the flow of the carrier ampholyte solution through the fractionation channel as the third active separating factor. Flow action permits a decrease in the channel dimension in the direction of the electric field and thereby also a decrease in the absolute values of the voltage while keeping a high field strength, which results in lower Joule heat production and a shorter time required for focusing. Focusing of methyl red in the trapezoidal cross-section channel was investigated as a function of the applied voltage and flow-rate of the carrier ampholyte solution. On the basis of the results obtained, it is obvious that methyl red is readily focused under suitable conditions inside the channel. Focusing is more efficient at higher electric field strengths and lower flow-rates of carrier ampholyte solution.

INTRODUCTION

Isoelectric focusing (IEF) is an electrophoretic technique that gives a very high resolution of amphoteric compounds [1]. The separation is carried out in a pH gradient which is established between two electrodes. In this technique, amphoteric compounds migrate until they align themselves at their isoelectric positions, where these compounds possess no net overall charge and therefore they concentrate at these points as migration ceases. IEF is an equilibrium technique in which diffusion works in the opposite direction to the driving forces, concentrating amphoteric compounds around the equilibrium position. As soon as dynamic equilibrium between the concentrating and dispersive processes has been established, focused zones of amphoteric compounds are formed.

In addition to the electric field and pH gradient used in IEF, isoelectric focusing field-flow fractionation (IEF_4) employs a third active separation-affecting factor, *viz.*, the flow of the liquid through the separation channel with the direction of the flow perpendicular to that of the electric field [2]. The shape of the flow velocity profile formed is influenced by the geometry of the fractionation channel [3]. Amphoteric

0021-9673/91/$03.50

solutes are transported via isoelectric focusing to the equilibrium positions and narrow focused solute zones with nearly Gaussian concentration distribution are formed. Provided that different solutes exhibit different isoelectric points, they are focused in different positions across the fractionation channel where the local values of pH are the same as the isoelectric points of the solutes. The velocity profile formed in the liquid flow causes the migration of focused zones along the channel at different velocities, so that the solutes are longitudinally separated.

The flow acting as the separation factor makes it possible to reduce the channel dimension in the direction of the electric field, which enables absolute voltage values to be decreased with the maintenance of a high field strength. This results in a decrease in the Joule heat production and the time required for focusing. Further, the laminar flow of the carrier liquid stabilizes the pH gradient against convection and the elution character of the technique enables liquid chromatographic detectors to be used for the detection of solute zones.

The technique was applied in practice by Chmelík *et al.* [4] in the trapezoidal cross-section channel and by Thormann *et al.* [5] in the rectangular cross-section channel. The latter group named this technique electrical hyperlayer field-flow fractionation.

The generation of pH gradient in the IEF_4 channel was studied in previous work [6]. It was found that the pH gradient generation was sufficiently fast and reproducible for IEF_4. The present work was aimed at investigating focusing of a low-molecular-weight amphoteric dye (methyl red) in the trapezoidal cross-section channel and at studying the influences of some experimental parameters on the methyl red zone width. A number of theoretical and experimental studies characterizing the focusing of amphoteric compounds in different techniques has been published (for a review, see ref. 7). However, this work is the first experimental investigation of focusing of a low-molecular-weight amphoteric compound in the IEF_4 channel.

THEORETICAL

Svensson [1,8] and Vesterberg and Svensson [9] derived an equation to express the zone width of a focused amphoteric compound:

$$\sigma_\Phi = \sqrt{\frac{-D}{E(\mathrm{d}u/\mathrm{dpH})\,(\mathrm{dpH}/\mathrm{d}x)}} \tag{1}$$

where σ_Φ is the standard deviation of the zone width in the direction of the applied electric field, D is the diffusion coefficient of an amphoteric compound, E is the electric field strength around the isoelectric point of an amphoteric compound, $\mathrm{d}u/\mathrm{dpH}$ is the mobility slope of an amphoteric compound at its isoelectric point and $\mathrm{dpH}/\mathrm{d}x$ is the pH gradient at the zone location.

From eqn. 1 it follows that the smaller is the compound to be separated (having a higher value of D) the larger is the zone width. The zone width is inversely proportional to the square root of the electric field strength. By increasing the field strength the zone width and also the duration of focusing are reduced. The zone width is also inversely proportional to the pH gradient and the mobility slope. Whereas the diffusion coefficient and the mobility slope are internal properties of the amphoteric

compound, the electric field strength and pH gradient can be created in such a way as to make the separation of amphoteric compounds as effective as possible.

Another important parameter is the time of focusing. Focusing consists of two phases, a relatively rapid separation phase and a slower stabilizing phase. During the former phase the amphoteric compounds migrate to their isoelectric positions, generating pure zones of individual components. During the latter, much slower, phase the ampholytes are assuming their final steady-state profiles [7]. For long focusing times the zone width approaches its steady-state value.

The efficiency of the field-flow separation system is characterized by the height equivalent to a theoretical plate, H. Directions of the applied field and carrier liquid flow and the system of coordinates of trapezoidal cross-section channel are shown schematically in Fig. 1. For focusing field-flow fractionation in the trapezoidal cross-section channel we derived [2,3,10] the equation

$$H = \frac{U_{av}}{D} \frac{24m^4\sigma_\Phi^4 \tan^2\alpha}{3 + \tan^2\alpha} + \frac{W^2(\Phi_{max})\bar{U}(\Phi_{max})}{105D} \tag{2}$$

where U_{av} is the average linear velocity of the carrier liquid flow at the considered coordinate ψ, m is a dimensionless parameter of the order of 2, α is the angle included by the adjacent longer walls of the channel, $W(\Phi_{max})$ is the width of the channel in the position of the zone maximum Φ_{max} and $\bar{U}(\Phi_{max})$ is the linear velocity of the carrier liquid averaged at a given position Φ_{max} over the whole ψ range (interval).

From the well known equation

$$H = \sigma_\tau^2/L \tag{3}$$

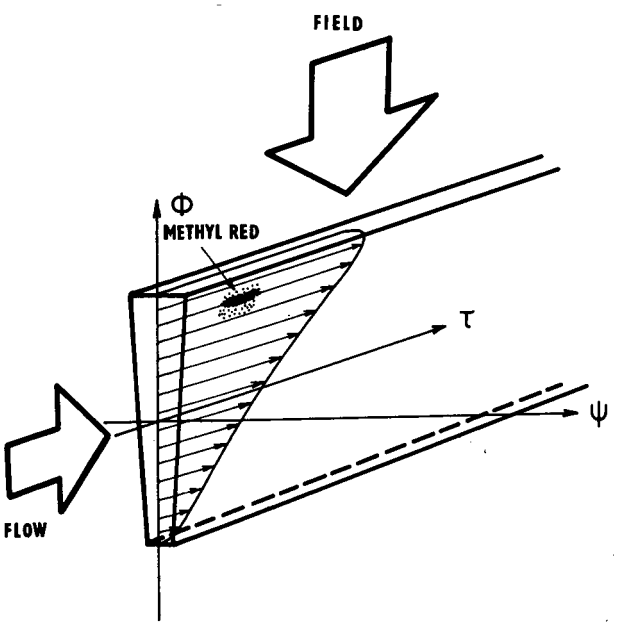

Fig. 1. Schematic representation and coordinate system of the trapezoidal cross-section channel.

the standard deviation of the zone of an amphoteric compound in the direction of the carrier liquid flow, σ_τ, can be expressed by the equation

$$\sigma_\tau = \sqrt{\frac{L}{D}\left[\frac{24U_{av}m^4\sigma_\Phi^4\tan^2\alpha}{3+\tan^2\alpha} + \frac{W^2(\Phi_{max})\bar{U}(\Phi_{max})}{105}\right]} \tag{4}$$

where L is the length of the channel.

EXPERIMENTAL

The scheme of the experimental arrangement is shown in Fig. 2. An M 122 doser (Mikrotechna, Prague, Czechoslovakia) with two injection syringes was used to pump solutions of electrode electrolytes, *i.e.*, solutions of 0.2 *M* acetic acid (pump A) and 0.2 *M* sodium hydroxide (pump B) into the electrode reservoirs. The flow-rates were 500 μl/min in both instances. An LD 2 linear feeder (Development Workshops of Czechoslovak Academy of Sciences, Prague, Czechoslovakia) was used to pump 1% ampholyte solution (Servalyt 4-9T; Serva, Heidelberg, Germany) into the channel in the flow-rate range 124–380 μl/min. Another LD 2 device with the same ampholyte solution was used to pump the sample, 0.02 *M* methyl red (Chemapol, Prague, Czechoslovakia) in ampholyte solution, into the channel with the aid of a six-port valve with a 30-μl sample loop through an injection capillary situated at a distance of 20 mm from the channel inlet where the carrier ampholyte solution is pumped. The results of focusing were recorded by an HP 1040 A diode-array detector in the range 400–600 nm. A stabilized power supply unit (Aritma, Prague, Czechoslovakia) was used in the range up to 60 V and the maximum current was 80 μA.

The fractionation channel was composed of three parts of Perspex clamped together with screws. The main part of the channel was a block comprising the slit of trapezoidal cross-section. The block was assembled by joining the two symmetrical parts into which side walls of the channel were milled. The block was provided with three capillaries, at the inlet and outlet of the channel and at the sample injection port. The upper and lower parts of the channel were identical and served for fixing wire

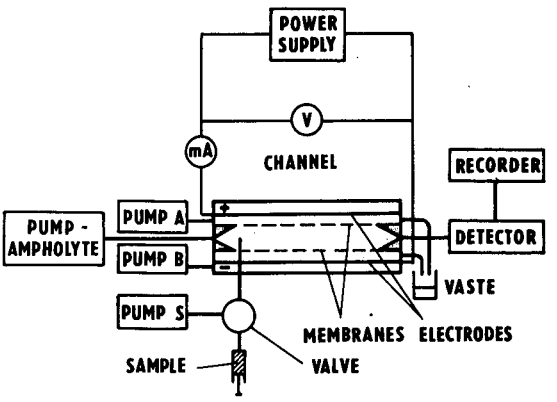

Fig. 2. Block diagram of the experimental arrangement.

platinum electrodes and comprising electrode reservoirs. They were situated on the opposite sides of the channel and were separated from its internal space with PGCL ultrafiltration membranes (Millipore, Bedford, MA, U.S.A.) with a nominal molecular weight cut-off 10 000. A diagram of the channel is shown in Fig. 3. The dimensions of the trapezoidal cross-section channel were length 250 nm, height 5 mm and widths of opposite walls of the trapezoid 0.45 and 0.95 mm.

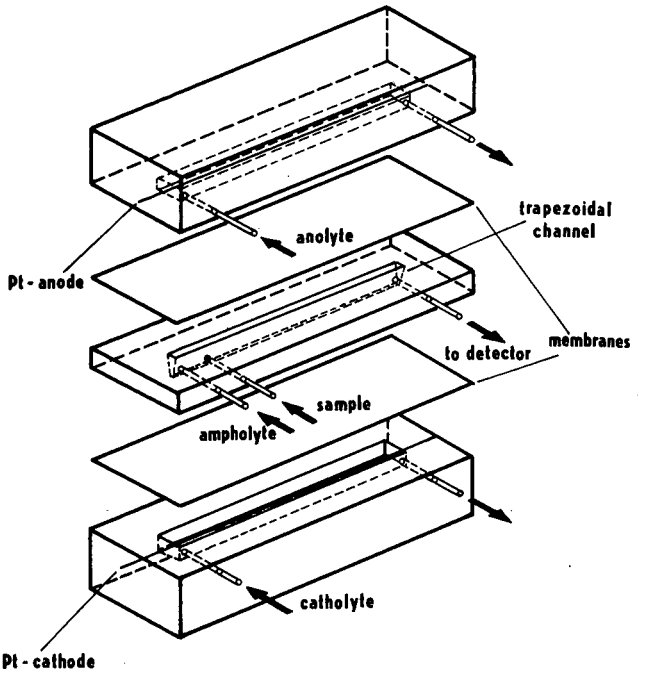

Fig. 3. Schematic representation of the channel for IEF_4.

Although measurements were performed at different flow-rates, the samples of methyl red were injected into the channel in the same way. The starting flow-rate of ampholyte solution at the inlet of the channel was 124 μl/min (pump-ampholyte in Fig. 2). The flow-rate of ampholyte solution at the sample injection port was 80 μl/min (pump S in Fig. 2) for 1 min. After this period the pump was stopped and the flow-rate of pump-ampholyte was changed to the required value. This procedure was used to ensure the same shape of the injected methyl red zone.

Suitable concentrations of ampholyte, sample and electrode solutions were chosen on the basis of previous measurements [6].

RESULTS AND DISCUSSION

From the theoretical considerations mentioned above, it follows that the standard deviation of a solute zone at the outlet of the channel, σ_τ, is approximately

proportional to the second power of the standard deviation of the solute zone in the direction of the applied electric field, σ_Φ, and σ_Φ is inversely proportional to the square root of the electric field strength. This means that σ_t is inversely proportional to the electric field strength, *i.e.*, the higher the electric field strength used, the smaller is the width of the solute zone at the outlet of the channel. The width of the solute zone in the direction of the electric field is exponentially (with a negative sign) proportional to the focusing time and approaches its steady-state (minimum) value for long focusing times, and the same holds for the width of the solute zone at the outlet of the channel. For these reasons its dependences on the flow-rate of the carrier ampholyte solution and the applied electric field were investigated. A change of the methyl red colour from yellow to red occurs in the pH range between the neutral medium of the ampholyte solution (pH 6.2) and its isoelectric point (p*I* 3.9). This change aids both visual investigation and spectrophotometric detection of the processes in the channel. For this reason the fractograms were recorded at four different wavelengths, 400, 450, 500 and 550 nm. The fractograms at 400 nm presumably show the yellow neutral form of methyl red and the fractograms at 550 nm presumably correspond to the red acidic (isoelectric) form.

Orientations of pH gradient and electric field lead in these experiments to focusing of acidic solutes in wider section of the channel where solutes elute at higher velocities. Location of the methyl red zone inside the trapezoidal cross-section channel is shown schematically in Fig. 1. From visual investigation it is obvious that only a small part of the channel is required for transferring methyl red from the site of injection to the position corresponding to its isoelectric point.

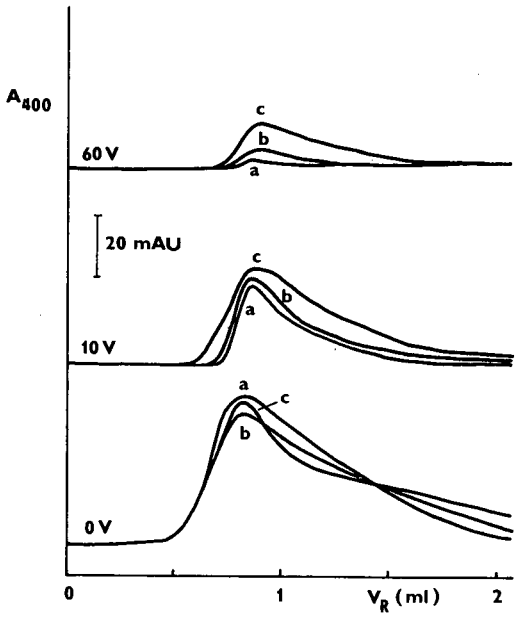

Fig. 4. Dependence of the width of the methyl red zone on the flow-rate of the carrier ampholyte solution at three voltages (0, 10 and 60 V). Flow-rates: (a) 124; (b) 190; (c) 380 μl/min. Fractograms were recorded at 400 nm. V_R = Retention volume.

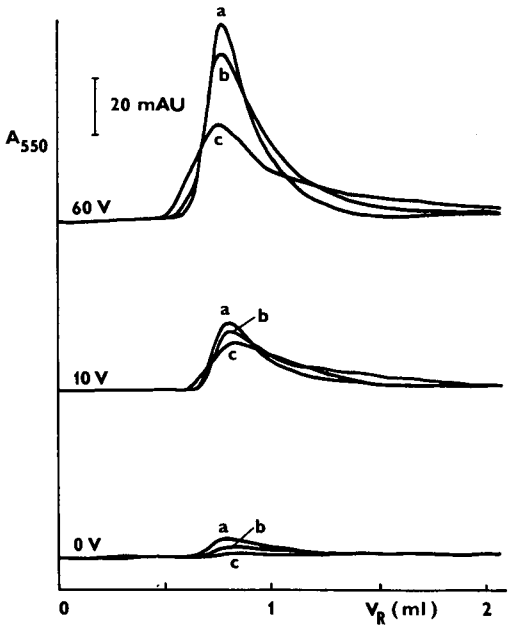

Fig. 5. As Fig. 4, with fractograms recorded at 550 nm.

The results of spectrophotometric detection show the increase in the content of the red form with increasing focusing time and electric field strength. The fractograms describing the dependence of the width of the methyl red zone on the flow-rate of the carrier ampholyte solution at three voltage values (0, 10 and 60 V) are shown in Figs. 4 (at 400 nm) and 5 (at 550 nm). It is apparent that with a decreasing flow-rate, *i.e.*, with increasing focusing time, zones become sharper and the extent of the change of the yellow neutral form of methyl red to its red isoelectric form is greater. Results of the investigation of the dependence of the methyl red zone width on the applied electric field at a flow-rate of 124 μl/min are shown in Figs. 6–9 for four wavelengths. The results at 400 nm (Fig. 6) show the decrease in the content of the neutral yellow form with increasing applied electric field. Because both methyl red forms absorb light at 450 and 500 nm (the spectra of yellow and red forms of methyl red in ampholyte solutions were published in a previous paper [6]), the observed changes in fractogram shapes provide information both on sharpening of zones and on the change in the content of yellow and red forms (Figs. 7 and 8). The increase of the red form and the decrease of the yellow form can be seen from the reversed ratios of peak heights at 450 and 500 nm at low and high voltages, respectively. The methyl red samples are found to be eluted as much sharper zones with increasing electric field strength, indicating the formation of much narrower zones in the direction of the electric field. The fractograms at 550 nm (Fig. 9) show the increase in concentration of the red isoelectric form with increasing electric field strength.

On the basis of the results obtained so far, it is apparent that methyl red (a low-molecular-weight amphoteric dye) is readily focused under suitable conditions

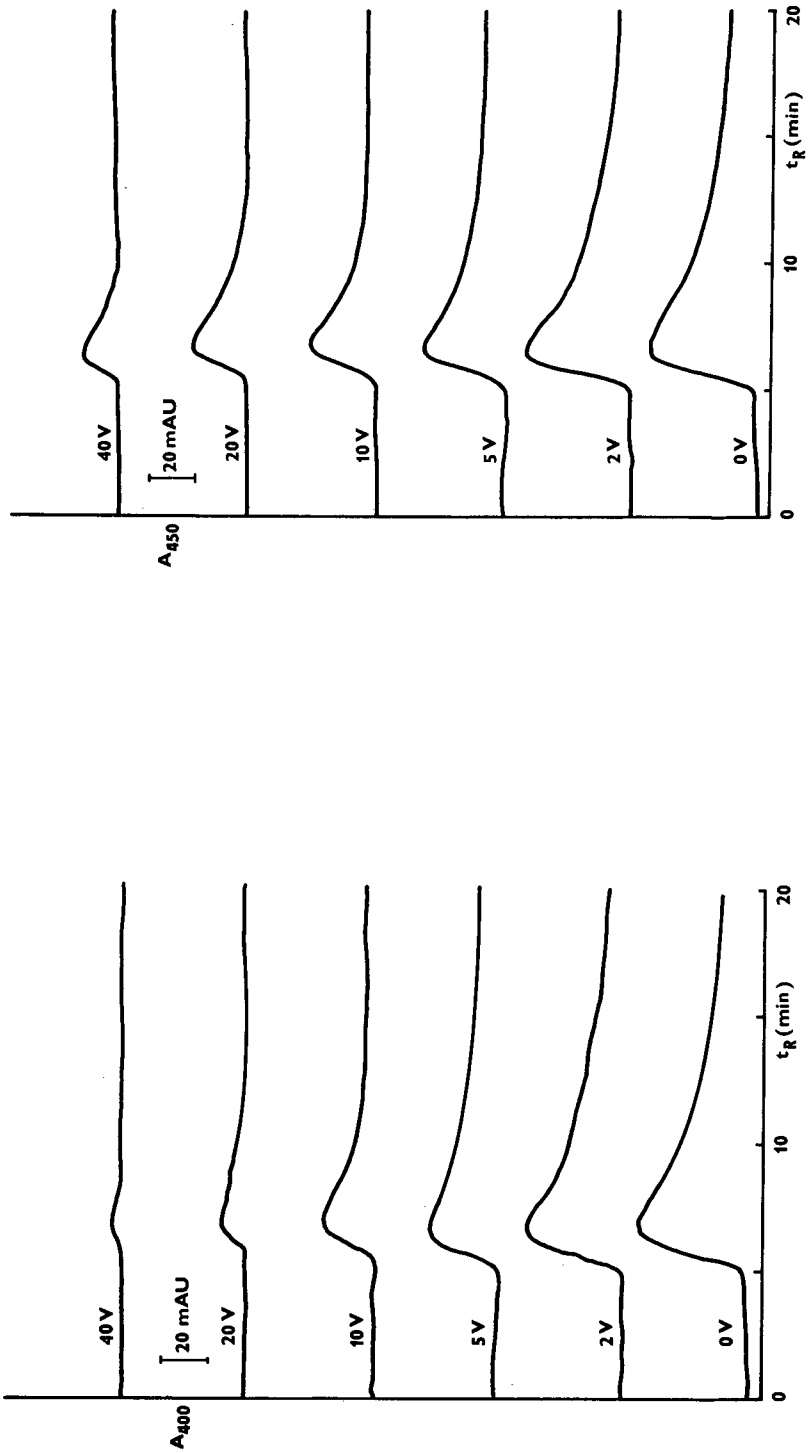

Fig. 6. Dependence of the width of the methyl red zone on the applied electric field at a flow-rate of 124 μl/min. Fractograms were recorded at 400 nm. t_R = Retention time.

Fig. 7. As Fig. 6, with fractograms recorded at 450 nm.

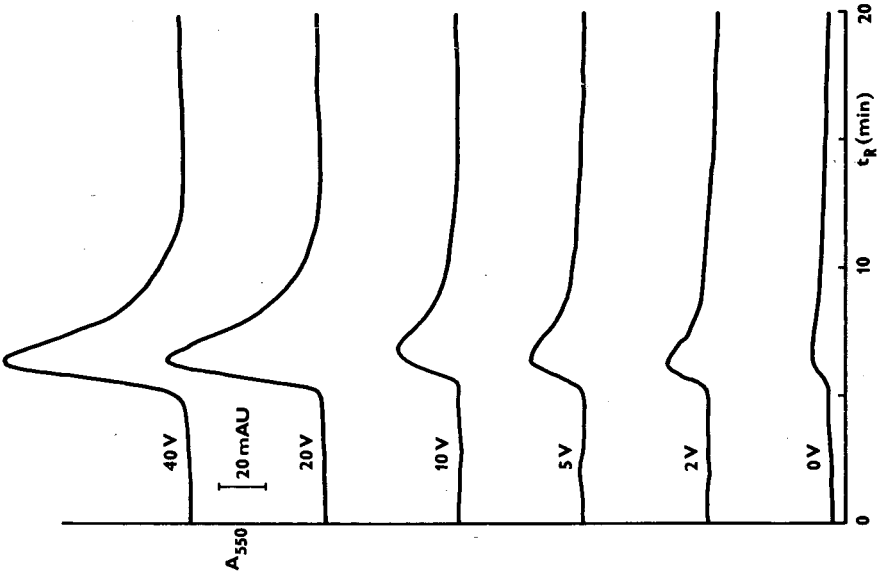

Fig. 8. As Fig. 6, with fractograms recorded at 500 nm.

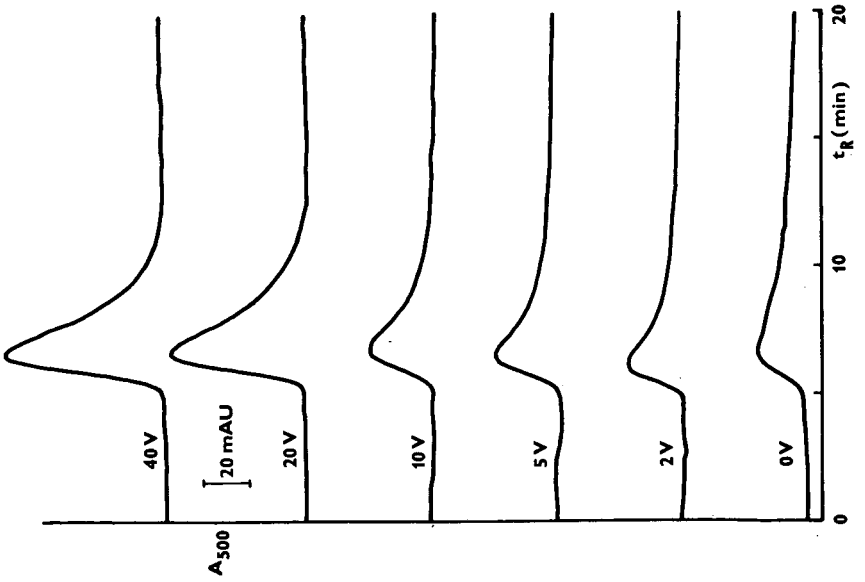

Fig. 9. As Fig. 6, with fractograms recorded at 550 nm.

inside the trapezoidal cross-section IEF_4 channel. Focusing is more efficient at higher electric field strengths and at lower flow-rates of carrier ampholyte solutions. Further research is aimed at the investigation of focusing and separation of high-molecular-weight compounds.

ACKNOWLEDGEMENT

The author is indebted to Dr. L. J. Zeman (Millipore, Bedford, MA, U.S.A.) for providing PGCL ultrafiltration membranes.

REFERENCES

1 G. Svensson, *Acta Chem. Scand.*, 15 (1961) 325.
2 J. Chmelík and J. Janča, *National Meeting of the Czechoslovak Chemical Society, Proceedings, Section 1.7*, Czechoslovak Chemical Society, Bánská Štiavnica, 1984, p. 38.
3 J. Janča and J. Chmelík, *Anal. Chem.*, 56 (1984) 2481.
4 J. Chmelík, M. Deml and J. Janča, *Anal. Chem.*, 61 (1989) 912.
5 W. Thormann, M. A. Firestone, M. L. Dietz, T. Cecconie and R. A. Mosher, *J. Chromatogr.*, 461 (1989) 95.
6 J. Chmelík, *J. Chromatogr.*, 539 (1991) 111.
7 W. Thormann and R. A. Mosher, in A. Chrambach, M. J. Dunn and B. J. Radola (Editors), *Advances in Electrophoresis*, Vol. 2, VCH, Weinheim, 1988, p. 47.
8 H. Svensson, *Acta Chem. Scand.*, 16 (1962) 456.
9 O. Vesterberg and H. Svensson, *Acta Chem. Scand.*, 20 (1966) 820.
10 J. Janča, J. Chmelík, V. Jahnová, N. Nováková and E. Urbánková, *J. Appl. Polym. Sci., Appl. Polym. Symp.*, 45 (1990) 39.

Journal of Chromatography, 545 (1991) 359–368
Elsevier Science Publishers B.V., Amsterdam

CHROM. 23 175

Effect of urea addition in micellar electrokinetic chromatography

SHIGERU TERABE*

Department of Material Science, Faculty of Science, Himeji Institute of Technology, Harima Science Park City, Kamigori, Hyogo 678-12 (Japan)

YASUSHI ISHIHAMA

Department of Industrial Chemistry, Faculty of Engineering, Kyoto University, Sakyo-ku, Kyoto 606 (Japan)

HIROYUKI NISHI and TSUKASA FUKUYAMA

Analytical Chemistry Research Laboratory, Tanabe Seiyaku Co., Ltd., 16–89, Kashima 3-Chome, Yodogawa-ku, Osaka 532 (Japan)

and

KOJI OTSUKA

Department of Industrial Chemistry, Osaka Prefectural College of Technology, Saiwai-cho, Neyagawa, Osaka 572 (Japan)

ABSTRACT

The addition of urea to a micellar solution was developed for the separation of hydrophobic compounds by micellar electrokinetic chromatography (MEKC). The logarithm of the capacity factor (k') decreased linearly with increasing concentration of urea. The use of a high concentration of urea allowed the MEKC separation of hydrophobic compounds, which were mostly included in the micelle and could not be resolved by conventional MEKC. The addition of urea also expanded the migration-time window and hence enhanced the resolution. The effect of urea is discussed from the standpoint of the contribution of urea to a diminished water structure around a hydrophobic solute. Two succesful examples of the application of the technique are given for the MEKC separation of a complex mixture and hydrophobic compounds.

INTRODUCTION

Micellar electrokinetic chromatography (MEKC) [1–3], which is also known as micellar electrokinetic capillary chromatography (MECC) [4], is the most popular among various electrokinetic chromatographic (EKC) techniques [5]. The separation principle of EKC is the same as that of chromatography, although the two phases between which the solute is partitioned do not always exist as distinctly separated phases in EKC but mostly constitute a homogeneous solution. The phase which corresponds to the stationary phase in conventional chromatography has to be subject to electrophoresis to migrate with a different velocity from the surrounding medium, which corresponds to the mobile phase.

0021-9673/91/$03.50

An ionic micellar solution, which is easily prepared by dissolving an ionic surfactant in a buffer solution at a concentration higher than the critical micelle concentration (CMC), is employed in MEKC, which has been proved to be useful for the separation of a wide range of compounds including both charged and uncharged molecules [6–8]. Under neutral or alkaline conditions, the electroosmotic flow is stronger than the electrophoretic migration of the ionic micelle, while electroosmosis and electrophoresis oppose their migration directions, and a solute that is totally excluded from the micelle migrates with the fastest velocity equal to the electroosmotic velocity and the micelle migrates with the slowest velocity equal to the difference between the electroosmotic and electrophoretic velocities. The migration velocity and hence the migration time of the solute depend on the distribution of the solute between the micelle and the aqueous phase.

The capacity factor, k', which is the ratio of total moles of the solute in the micelle to the total moles of the solute in the aqueous phase, is calculated from migration time data by the equation [2].

$$k' = \frac{t_R - t_0}{(1 - t_R/t_{mc})t_0} \tag{1}$$

where t_R, t_0 and t_{mc} are the migration time of the sample solute, that of the solute entirely excluded from the micelle and that of the micelle, respectively. The migration time of the micelle is generally measured with a tracer of the micelle, which totally combines with the micelle. Sudan III [1], Sudan IV [9] and timepidium bromide [10] have been conveniently employed as tracers of the sodium dodecyl sulphate (SDS) micelle; in particular, timepidium bromide is suitable in terms of chemical purity [9]. Methanol usually serves as a tracer of the electrosmotic flow, because it is poorly incorporated into the micelle [12] and successfully detected by a UV detector owing to the refractive index change.

The capacity factor is also expressed as [2]

$$k' = K(V_{mc}/V_{aq}) \tag{2}$$

where K is the distribution coefficient and V_{mc} and V_{aq} are the volumes of the micellar and the aqueous phase, respectively. The distribution coefficient is determined by the characteristics of both the micellar and the aqueous phase. For a pertinent micelle, k' will be dependent on the solubility of the solute in the aqueous phase.

In MEKC, the optimum value of the capacity factor is *ca.* 2 for the maximum resolution [2] and a k' range of 0.5–10 is recommended under conventional conditions. However, k' values often exceed 10 for hydrophobic compounds because they tend to be included in the micelle with high partition ratios and the resolution of such compounds is therefore not successful with simple micellar solutions such as SDS, which are widely used in MEKC.

For the separation of hydrophobic compounds by MEKC, three techniques have been developed: (1) the addition of an organic modifier to the micellar solution [11,12]; (2) the use of bile salt micelles [13,14]; and (3) the addition of cyclodextrin (CD) to the micellar solution [15]. The last method, named cyclodextrin-modified MEKC

(CD/MEKC), is promising especially for the separation of isomeric hydrophobic compounds [15] and for chiral separations [16].

In this paper, we describe the addition of urea to micellar solutions for the separation of hydrophobic compounds. Although urea is not often employed in high-performance liquid chromatography (HPLC), it has been proved to be a useful additive for aqueous phase modification in MEKC. Urea is a well known protein-denaturing agent and the solubilities of some hydrocarbons [17], amino acids [18] and related compounds [19] in high-concentration urea solutions have been examined to clarify the denaturing mechanism. The effect of urea on micelle formation has also been investigated [20,21] in terms of the contribution of the water structure to micelle formation.

EXPERIMENTAL

Apparatus

Capillary electrophoresis (CE) systems used in three different laboratories (Kyoto University, Tanabe Seiyaku and Osaka Prefectural College) were essentially the same as the system described previously [1,2,22]. Fused silica tubing of *ca.* 50 μm I.D. (Polymicro Technologies, Phoenix, AZ, U.S.A. and Scientific Glass Engineering, Ringwood, Victoria, Australia) was used as separation capillaries without any inside coatings. The CE instruments consisted of regulated high-voltage d.c. power supplies (HepLL-30P0.08, HepLL-30N0.08 and HJLL-25-PO; Matsusada Precision Devices, Kusatsu, Shiga, Japan), variable-wavelength UV detectors for HPLC (Uvidec 100-III and 100-V, Jasco, Tokyo, Japan; and SPD-6A, Shimadzu, Kyoto, Japan), the cell holders of which were made from plastic or aluminium blocks with 0.7 mm × 50 μm stainless-steel apertures to accommodate the 50 μm I.D. fused-silica capillaries for on-column detection, and Chromatopac C-R3A and C-R6A data processors (Shimadzu). The detectors were operated at 210 or 220 nm. Sample solutions were introduced manually into the capillaries by the siphoning method, as described previously [1]. The capillaries were left at ambient temperature without any temperature control in the case of the laboratory-made instruments. A commercial CE system, P/ACE 2000 (Beckman, Palo Alto, CA, U.S.A.), with a 57 cm × 52 μm I.D. fused-silica capillary was also used for the temperature-controlled experiments.

Reagents

SDS and urea of protein-research grade purchased from Nacalai Tesque (Kyoto, Japan) were used as received. Urea of analytical-reagent grade was obtained from Katayama Kagaku (Osaka, Japan). Chemicals employed as test solutes were of analytical-reagent grade or equivalent and used as received. Six corticosteroids used as test samples were purchased from Sigma (St. Louis, MO, U.S.A.). All buffer solutions were prepared from analytical-reagent grade reagents and water purified with a Milli-Q or Milli-RO system (Millipore Japan, Tokyo, Japan).

Surfactant solutions were prepared by dissolving SDS and urea in 50 m*M* phosphate–100 m*M* borate buffer (pH 7.0), 20 m*M* phosphate–20 m*M* borate buffer (pH 9.0) or 50 m*M* borate buffer (pH 9.0) and passed through membrane filters of 0.45 μm pore size (Gelman Science Japan, Tokyo, Japan). Test solutes were dissolved in 20% aqueous or pure methanol at concentrations of 0.2–1 mg ml^{-1} to give adequate peak heights.

Solubility measurement

The solubilities of corticosteroids in urea solutions were determined by HPLC. About 5 mg of a sample were added to 1 ml of each solution (20 m*M* phosphate–20 m*M* borate buffer, pH 9.0) containing a different amount of urea in a test-tube. The test-tube was then sonicated for 30 min with an ultrasonic cleaner. The solution was passed through the membrane filter of 0.45 μm pore size and 20 μl of each filtrate were injected into the HPLC system (Shimadzu LC-5A), which was equipped with a Rheodyne Model 7125 loop injector, a Shimadzu SPD-2A UV detector (operated at 220 nm) and a Shimadzu CTO-2A column oven (40°C). The peak areas were measured with a Shimadzu Chromatopac C-R5A. The solubility of each sample was calculated from the peak area observed for the standard solution and that for the sample solution. The column employed was an Inertsil ODS-2 (5 μm) (150 mm × 4.6 mm I.D.) purchased from Gaskuro Kogyo (Tokyo, Japan). The retention times of fluocinolone acetonide, hydrocortisone acetate and fluocinonide were 3.3, 3.8 and 6.4 min, respectively, using a mobile phase of acetonitrile–water (50:50) at a flow-rate of 1.0 ml min^{-1}.

RESULTS AND DISCUSSION

Fig. 1 shows the dependence of ln k' of test samples on the concentration of urea in MEKC with 50 m*M* SDS solutions. All the ln k' values decreased linearly with increase in the concentration of urea. Similar dependences of ln k' on the concentration of urea were observed for aromatic compounds (Fig. 2), corticosteroids and alkyl *p*-hydroxybenzoates. These linear relationships mean that the free energy of transfer from the aqueous phase to the micelle decreased linearly with increase in urea concentration, provided urea did not cause a substantial alteration of CMC. The linear dependence of ln k' on the percentage of an organic modifier in the mobile phase has been well documented in reversed-phase HPLC [23].

It has been reported that the free energies of transfer of hydrocarbons from water to 7 *M* urea are negative and that the transfer process is spontaneous owing to

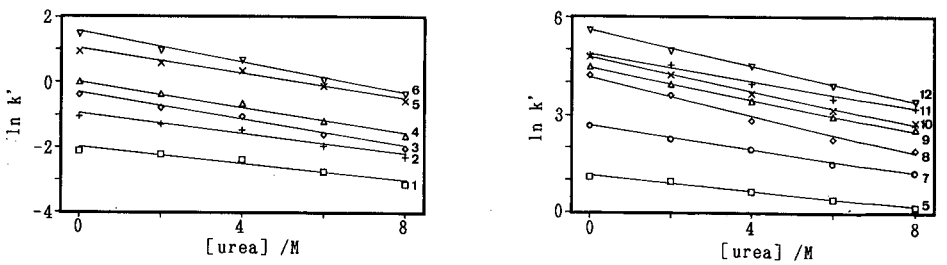

Fig. 1. Dependence of ln k' on the concentration of urea. 1 = Resorcinol; 2 = phenol; 3 = *p*-nitroaniline; 4 = nitrobenzene; 5 = toluene; 6 = 2-naphthol. Capillary, 70 cm × 52 μm I.D. (50 cm to the detector); separation solution, 50 m*M* SDS in 100 m*M* borate–50 m*M* phosphate buffer; applied voltage, 20 kV.

Fig. 2. Dependence of ln k' on the concentration of urea. 5 = Toluene; 7 = naphthalene; 8 = 9-fluorenone; 9 = fluorene; 10 = xanthene; 11 = dibenzyl; 12 = phenanthrene; 13 = stilbene; 14 = fluoranthene. Capillary, 65 cm × 50 μm I.D. (50 cm to the detector); separation solution, 50 m*M* SDS in 20 m*M* borate–20 m*M* phosphate buffer (pH 9.0); applied voltage, 20 kV.

a large positive entropy change, sufficient to override an opposing enthalpy change [17]. This effect is explained in terms of a diminished water structure (so-called "iceberg") around the hydrocarbon by the addition of urea to the aqueous solution [18,21].

We measured the thermodynamic quantities of micellar solubilization for the test solutes given in Fig. 1 and for *p*-alkylphenols in 50 m*M* SDS dissolved in 50 m*M* phosphate–100 m*M* borate buffer [24] and found that although the free energy and enthalpy changes were negative for all the solutes, the entropy changes were positive for *p*-alkylphenols and became more positive with increasing alkyl chain length. Micellar solubilization is a transfer process in a homogeneous solution and different from the above-mentioned system in this regard. However, the two processes are the same from the standpoint of the transfer of the solute from water to the other phase. The positive entropy change found in micellar solubilization can also be interpreted by the major contribution of the water structure around the alkyl group to the transfer process from the aqueous phase to the micelle.

From the above discussion, the effect of the urea addition to micellar solutions is straightforward for *p*-alkylphenols. Urea will increase the solubility of the alkylphenols in the aqueous phase by diminishing the water structure around the alkyl group as described above. Urea will concurrently prevent the alkylpheols from transferring to the micelle from the aqueous phase, by reducing the positive entropy of the transfer from water to the micelle. In fact, we observed in a preliminary experiment that entropy changes of the transfer process from 6 *M* urea to the SDS micelle (50 m*M* SDS at pH 7.0) were substantially reduced close to zero or even to small negative values for *p*-alkylphenols [24].

The above discussion is successfully applicable to the alkylphenols, but for the other solutes the effect of urea is more complicated, judging from the observed thermodynamic quantities of micellar solubilization. It is not easy to find a simple explanation for the observed effect of urea. However, it is obvious that urea increases the solubility of most solutes in water [17–19] and consequently that the distribution coefficient to the micelle is significantly reduced. We confirmed the solubility enhancement by urea for some steroidal compounds as shown in Fig. 3. The solubility of these compounds in 8 *M* urea increased 12–20 times as much as that in the absence of urea. A detailed discussion of the thermodynamic effect on MEKC will be presented elsewhere after obtaining more refined data.

In addition to the free energy changes of the transfer process, we have to take into account the effect of urea on micelle formation [20,21], because the SDS concentration was kept constant in this study. Schick [21] measured the CMC of SDS at different concentrations of urea up to 6 *M* and reported that the CMC of SDS in 6 *M* urea at 25°C increased 1.67 times higher than that in water. The increase in CMC indicates that micelle concentrations for 50 m*M* SDS will decrease from 43 m*M* in water (given in monomer concentration) to 38 m*M* in 6 *M* urea at 25°C [21]. Eqn. 2 suggests that low micelle concentrations produce small k' value, that is, 38 m*M* SDS micelle gives 12% lower k' values than 43 m*M* micelle for every solute. The observed k' at 6 *M* urea were reduced to 40–70% of those in the absence of urea and therefore, the contribution of the change in CMC to the reduced k' values should be less significant than that of the solubility change discussed above.

The migration time of the SDS micelle, t_{mc} , increased with increasing

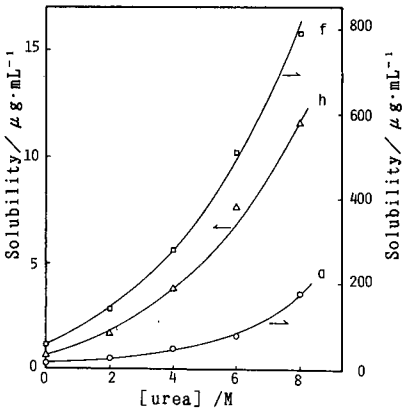

Fig. 3. Solubility of three corticosteroids as a function of the concentration of urea in a phosphate–borate buffer (pH 9.0): (a) Hydrocortisone; (f) fluocinolone acetonide; (h) fluocinonide.

concentration of urea, whereas the electroosmotic velocity did not alter significantly, as indicated in Table I. The ratio t_0/t_{mc} was reduced considerably and hence the migration-time window between t_0 and t_{mc} was considerably expanded. A wide migration-time window is favourable for high resolution, although it requires a long analysis time [2,25]. Similar tendencies of t_0/t_{mc} were also found under three different conditions, as shown in Fig. 4. The differences in the t_0/t_{mc} values among the three were mainly ascribed to the difference in electroosmotic velocities.

The data in Table I suggest that the electrophoretic mobility of the SDS micelle increased with increase in the concentration of urea. We can suggest two possibilities to explain the enhanced electrophoretic mobility: either diminished hydration around the micelle on the addition of urea or an increase in the effective charge on the micelle. At present, we have no preference for either explanation.

Fig. 5 shows the dependence of current on the concentration of urea at a constant applied voltage at a constant temperature. The current decreased linearly with an increase in urea concentration. With 8 *M* urea, which consisted of 43% urea

TABLE I

MIGRATION TIMES OF THE AQUEOUS PHASE AND THE MICELLE AT DIFFERENT UREA CONCENTRATIONS

Conditions in Fig. 1.

Migration time	Urea concentration (*M*)				
	0	2.0	4.0	6.0	8.0
t_0 (min)	3.92	3.92	4.65	5.46	6.38
t_{mc} (min)	14.57	16.10	22.76	30.11	36.45
t_0/t_{mc}	0.269	0.243	0.204	0.181	0.175

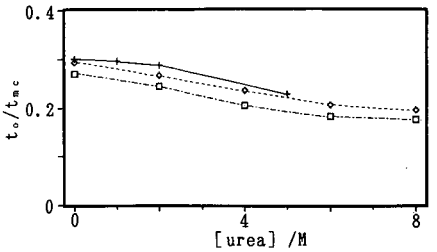

Fig. 4. Dependence of t_0/t_{mc} on the concentration of urea. Conditions: □ = as in Fig. 1; ◇ = as in Fig. 2; + = capillary, 65 cm × 50 μm I.D. (50 cm to the detector). Separation solution, 20 m*M* SDS in 50 m*M* borate buffer (pH 9.0); applied voltage, 15 kV.

and 57% buffer [26], the current decreased to about 50% of that observed in the absence of urea, as shown in Fig. 5. As the current depends not only on the concentration of electrolytes but also on the viscosity of the solution, the results in Fig. 5 seem reasonable, because a high concentration of urea does not seriously increase the viscosity of the solution; *e.g.*, the viscosity of 8 *M* urea in water is 1.66 times higher than that of water at 25°C [26]. In addition, the mobilities of ions will also be affected by a high concentration of urea.

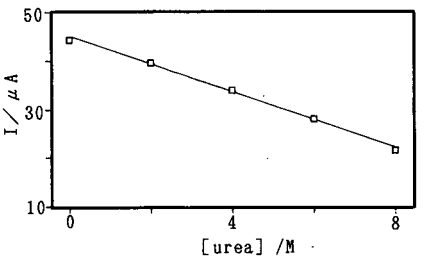

Fig. 5. Dependence of current on the concentration of urea. Capillary, 57 cm × 52 μm I.D. (50 cm to the detector); temperature, 20°C. Other conditions as in Fig. 1.

Two examples which successfully take advantage of the addition of urea in MEKC separation are presented in this paper in contrast to the separation in the absence of urea. Fig. 6 shows the separation of 23 phenylthiohydantoin (PTH)-amino acids using SDS solution with and without urea. We previously reported the separation of 22 PTH-amino acids by MEKC using SDS and dodecyltrimethylammonium bromide (DTAB) solutions [6]. Although the separation was successful in that study, some pairs of PTH-amino acids were not completely resolved from each other under single conditions. In Fig. 6a, where urea was not added, five pairs of PTH-amino acids were poorly or not resolved. The use of 100 m*M* SDS solution containing 4.3 *M* urea allowed a complete separation of 23 PTH-amino acids in one run, as shown in Fig. 6b. The optimum concentration of urea was critical in this

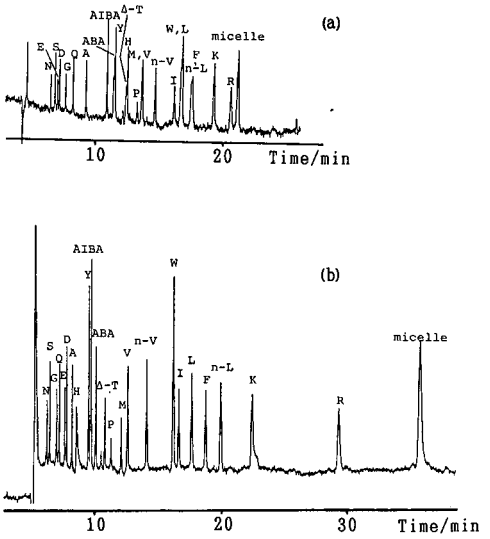

Fig. 6. Electrokinetic chromatogram of a mixture of 23 PTH-amino acids. The peaks are identified with one-letter abbreviations for the amino acids; AIBA = 2-aminoisobutyric acid; ABA = 2-aminobutyric acid; ΔT = PTH-dehydrothreonine. The micelle is traced with timepidium bromide. (a) Conditions as in Fig. 1, except for capillary length (50 cm, 30 cm to the detector) and applied voltage (10.5 kV); (b) separation solution, 100 m*M* SDS and 4.3 *M* urea in the same buffer as in (a); other conditions as in (a).

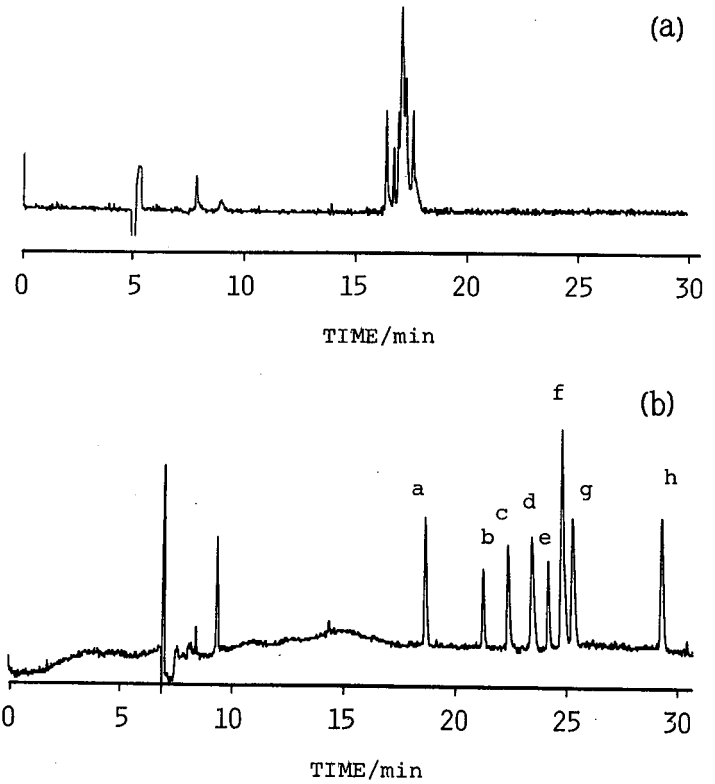

Fig. 7. Separation of eight corticosteroids: (b) hydrocortisone acetate; (c) betamethasone; (d) cortisone acetate; (e) triamcinolone acetonide; (g) dexamethasone acetate; (a, f and h) see Fig. 3. (a) Conditions are as in Fig. 2; (b) separation solution, same SDS solution as in (a) but containing 6 *M* urea; other conditions as in (a).

experiment, that is, the total selectivity was very sensitive to the concentration of urea for the complex mixture of such closely related compounds. PTH-threonine was not added in Fig. 6, because it gave a seriously tailed peak at a migration time close to PTH-serine (S). The pH of the separation solution was kept constant at 7.0 throughout the experiment, but optimization of pH will permit the complete separation of these PTH-amino acids in a shorter time.

Fig. 7 shows another successful application of the addition of urea to the MEKC separation of eight corticosteroids. As these solutes are poorly soluble in water, as mentioned above, they tend to be mostly incorporated into the micelle. Therefore, they were detected at migration times close to t_{mc} and their capacity factors were higher than 10, although no tracer of the micelle was added in Fig. 7. The use of 6 *M* urea dramatically improved the resolution, as shown in Fig. 7b. In this example, the concentration of urea was not critical and it was easy to obtain a complete separation.

CONCLUSIONS

Although the effect of urea on micellar solubilization is not completely understood, the addition of urea to micellar solutions causes considerable decreases in the capacity factors for most solutes in MEKC. The technique is especially useful for the separation of hydrophobic compounds from the standpoint of the extended applicability of MEKC. The expanded migration-time window generated by the addition of urea is also convenient for high resolution.

ACKNOWLEDGEMENTS

S.T. is grateful to Yokogawa Electric, Shimadzu and Hitachi for research funds and also to Beckman Instruments Japan for the loan of the instrument. S.T. and H.N. are grateful to Professor T. Nakagawa for helpful discussions. H.N. and T.F. are grateful to Dr. M. Matsuo and Dr. T. Kakimoto for their encouragement. K.O. thanks Mr. T. Nagata and Mr. T. Nakagawa for technical assistance and also acknowledges a Grant-in-Aid for Scientific Research (02750564) from the Ministry of Education, Science and Culture, Japan.

REFERENCES

1 S. Terabe, K. Otsuka, K. Ichikawa, A. Tsuchiya and T. Ando, *Anal. Chem.*, 56 (1984) 111–113.
2 S. Terabe, K. Otsuka and T. Ando, *Anal. Chem.*, 57 (1985) 834–841.
3 S. Terabe, K. Otsuka and T. Ando, *Anal. Chem.*, 61 (1989) 251–260.
4 D. E. Burton, M. J. Sepaniak and M. P. Maskarinec, *J. Chromatogr. Sci.*, 24 (1986) 347–351.
5 S. Terabe, *Trends Anal. Chem.*, 8 (1989) 129–134.
6 K. Otsuka, S. Terabe and T. Ando, *J. Chromatogr.*, 332 (1985) 219–226.
7 K. Otsuka, S. Terabe and T. Ando, *J. Chromatogr.*, 348 (1985) 39–47.
8 H. Nishi and S. Terabe, *Electrophoresis*, 22 (1990) 691–701.
9 S. Terabe, O. Shibata and T. Isemura, *J. High Resolut. Chromatogr.*, 14 (1991) 52–55.
10 H. Nishi, N. Tsumagari and S. Terabe, *Anal. Chem.*, 61 (1989) 2434–2439.
11 K. Otsuka, S. Terabe and T. Ando, *Nippon Kagaku Kaishi*, (1986) 950–955.
12 A. T. Balchunas and M. J. Sepaniak, *Anal. Chem.*, 59 (1987) 1466–1570.
13 S. Terabe, M. Shibata and Y. Miyashita, *J. Chromatogr.*, 480 (1989) 403–411.
14 H. Nishi, T. Fukuyama, M. Matsuo and S. Terabe, *J. Chromatogr.*, 513 (1990) 279–295.
15 S. Terabe, Y. Miyashita, O. Shibata, E. R. Barnhart, L. R. Alexander, D. G. Patterson, B. L. Karger, K. Hosoya and N. Tanaka, *J. Chromatogr.*, 516 (1990) 23–31.

16 H. Nishi, T. Fukuyama and S. Terabe, *J. Chromatogr.*, 553 (1991) in press.
17 D. W. Wetlaufer, S. K. Malik, L. Stoller and R. L. Coffin, *J. Am. Chem. Soc.*, 86 (1964) 508–514.
18 Y. Nozaki and C. Tanford, *J. Biol. Chem.*, 238 (1963) 4074–4081.
19 D. R. Robinson and W. P. Jencks, *J. Am. Chem. Soc.*, 87 (1965) 2462–2473.
20 P. Mukerjee and A. Ray, *J. Phys. Chem.*, 67 (1963) 190–192.
21 M. J. Schick, *J. Phys. Chem.*, 68 (1964) 3585–3592.
22 H. Nishi, N. Tsumagari, T. Kakimoto and S. Terabe, *J. Chromatogr.*, 465 (1989) 331–343.
23 W. R. Melander and C. Horváth, in C. Horváth (Editor), *High-Performance Liquid Chromatography: Advances and Perspectives*, Vol. 2, Academic Press, New York, 1980, pp. 113–319.
24 S. Terabe and T. Katsura and Y. Ishihama, unpublished data.
25 S. Terabe, H. Utsumi, K. Otsuka, T. Ando, T. Inomata, S. Kuze and Y. Hanaoka, *J. High Resolut. Chromatogr. Chromatogr. Commun.*, 9 (1986) 666-670.
26 R. C. Weast (Editor), *CRC Handbook of Chemistry and Physics*, CRC Press, Boca Raton, FL, 66th ed., 1985, p. D-266.

Journal of Chromatography, 545 (1991) 369–374
Elsevier Science Publishers B.V., Amsterdam

CHROM. 23 161

Review

Analytical isotachophoresis in biological monitoring of exposure to industrial chemicals

JAN SOLLENBERG
Division of Analytical Chemistry, National Institute of Occupational Health, S-171 84 Solna (Sweden)

ABSTRACT

Isotachophoretic methods for the determination of compounds of interest in biological monitoring are reviewed. The analytes are charged biotransformation products such as acids or amines. Comparisons are made between isotachophoretic methods and other techniques regarding sensitivity, need for preseparation or derivatization and similar technical aspects.

CONTENTS

1. INTRODUCTION

Biological monitoring of exposure to industrial chemicals requires evaluation of the uptake (internal exposure or internal dose) of such chemicals in the body by analysis of biological samples from the exposed subject. Mostly urine, blood and expired air are used for the direct measurement of the chemical or a biotransformation product. Indirect measurement of biochemical or physiological changes that occur in response to the exposure are also included. Many compounds are biotransformed to more water-soluble and ionized products and for the analysis of these, isotachophoresis (ITP) can be an attractive technique.

This paper reviews ITP methods used for analysis of compounds of interest in biological monitoring.

0021-9673/91/$03.50

TABLE 1

ELECTROLYTE SYSTEMS USED IN THE CITED ISOTACHOPHORETIC METHODS

Exposure = the industrial chemical to which the subject is exposed; analyte = the product to be analysed in biological monitoring; specimen = biological specimen for analysis. Abbreviations: HA = hippuric acid; MHA = methylhippuric acid; MA = mandelic acid; PGA = phenylglyoxylic acid; HPMC = hydroxypropylmethylcellulose; TCA = trichloroacetic acid.

Exposure	Analyte	Specimen	Leading electrolyte	Terminating electrolyte	Ref.
Anionic systems					
Toluene, xylene, styrene	HA, MHA, MA, PGA	Urine	5 m*M* HCl–20 m*M* β-alanine; pH 3.75; 0.4% HPMC	5 m*M* caproic acid	1
Ethylbenzene	MA, PGA	Urine	5 m*M* TCA + β-alanine to pH 3.35; 0.4% HPMC	5 m*M* caproic acid	5
Halothane	Trifluoroacetic acid	Urine, blood	10 m*M* HCl + β-alanine to pH 3.6–3.9; 1% Triton X-100	10 m*M* caproic acid	13
Methanol	Formate	Blood, plasma	5 m*M* HCl; 0.1% Triton X-100 or 0.4% HPMC	10 m*M* acetic acid	16
Vinyl chloride	Thiodiacetic acid	Urine	10 m*M* HCl + β-alanine to pH 3.4 for preseparation capillary and to pH 4.3 for analytical capillary; 0.2% HPMC	10 m*M* acetic acid	18
Ethylene glycol	Glycolic, glyoxylic oxalic and formic acids	Blood, plasma	3 m*M* HCl–2 m*M* NaCl, pH 2.5; 0.2–0.4% HPMC	10 m*M* acetic acid	19
Cationic systems					
–	Creatinine	Urine	10 m*M* potassiumacetate + acetic acid to pH 5.3; 0.2% HPMC	5 m*M* HCl	10
Triethanolamine	Triethanolamine	Urine	5 m*M* ethanolamine + acetic acid to pH 5.3; 0.4% HPMC	4 m*M* histidine + acetic acid to pH 5.3	9

2. STYRENE, ETHYLBENZENE, TOLUENE, XYLENE

In 1977, Sollenberg and Baldesten [1] published a method for the determination of mandelic, phenylglyoxylic, hippuric and methylhippuric acids in urine. These acids are biotransformation products of styrene (the first two acids), toluene and xylene, respectively, and their excretion in urine is used for biological monitoring of the corresponding solvents. When the investigation started, spectrophotometric and thin-layer chromatographic methods were used for routine determination of these acids. Existing gas chromatographic (GC) methods [2,3] were laborious and required derivatization of the acids with diazomethane or a silyl reagent before analysis. With the described ITP method these acids could be determined in the same run with no pretreatment other than extraction from the urine sample with diethyl ether. Table 1 gives the compositions of the electrolytes used. In a contemporary paper the first high-performance liquid chromatographic (HPLC) method for the determination of hippuric and methylhippuric acids in urine was described [4].

In connection with studies on the biotransformation of ethylbenzene in the rat, an HPLC procedure was developed for the analysis of the products; 59 rat urine samples were analysed for mandelic and phenylglyoxylic acids, which are the main products, and these samples were also analysed simultaneously by the ITP method (with minor modifications, Table 1) [5]. There was no significant difference between the results obtained by the two methods. However, the limit of determination was 0.01 mmol/l for both mandelic and phenylglyoxylic acids by HPLC whereas it was 0.04 and 0.02 mmol/l, respectively, by ITP.

Another comparison between the ITP method and an HPLC method was made when methylhippuric acid was determined in human urine [6]. The two methods gave essentially identical data for urine samples with added methylhippuric acid. However, the limit of determination was 0.2 mmol/l for both methods. In this study the pH of the leading electrolyte was 4.15.

The cited ITP method was used for routine work but also for some investigations, *e.g.*, on xylene exposure [7] and on relationships between occupational styrene exposure and excretion of mandelic and phenylglyoxylic acids in urine [8]. From these relationships conceivable biological exposure limits were calculated. Such values can be expressed as the concentration of the excreted product in the urine sample divided by the concentration of creatinine in the same sample. This is usually done to adjust for variations in urine flow as a substitute for excretion rate when the time between voidings and the urine volume is not known. The excretion of creatinine is assumed to be constant. Mostly, creatinine in urine samples is determined spectrophotometrically in automated analysers.

However, in connection with this study, ten samples were analysed for creatinine by ITP [9] using an electrolyte system as described by Mikkers and Everaerts [10] (Table 1). The analysis is very simple and no pretreatment of the urine sample was applied before injection into the ITP instrument. The urine samples were simultaneously analysed using a Merckotest-Creatinin kit and the results were compared by linear regression analysis. The equation was $y = 0.39 + 0.96x$; $r = 0.998$, where y is the ITP result and x the Merckotest result. The concentration range of creatinine was 6–20 mmol/l.

Another slight modification of the ITP method was used for the determination

of hippuric acid in urine in a study on toluene exposure [11]. The extraction of the urine samples step was omitted and only a 10-fold dilution with water was made before analysis. The results were compared with those obtained for the same urine samples made using an HPLC method and were found to be in accordance. It was found that a metabolite of salicylic acid, salicyluric acid (*o*-hydroxyhippuric acid), interfered with hippuric acid in the ITP analysis. By changing the pH of the leading electrolyte from 3.75 tot 3.15, separation was achieved but the time of analysis was prolonged.

Zschiesche *et al.* [12] compared thin-layer chromatographic (TLC), HPLC, GC, spectrophotometric and ITP [1] methods for the determination of mandelic, phenylglyoxylic and hippuric acids in urine. Phthalic acid was used as an internal standard in the ITP analyses. When hippuric acid was determined, the correlations between ITP and HPLC and between ITP and GC were similar. However, GC had the lowest detection limit (0.2 μmol/l) followed by HPLC and then ITP (50 μmol/l). In contrast to the HPLC and ITP methods, the GC procedure required derivatization of the hippuric acid with diazomethane.

3. HALOTHANE

The main biotransformation product of the anaesthetic halothane (2-bromo-2-chloro-1,1,1-trifluoroethane) that is excreted in urine is trifluoroacetic acid. Morio *et al.* [13] described the ITP determination of trifluoroacetic acid in urine and blood from patients who had had halothane anaesthesia. They claimed that this ITP method is advantageous compared with paper chromatographic, TLC, ion-exchange chromatographic, GC and HPLC methods for the determination of trifluoroacetic acid in urine. No preparation of the samples is required, the sample volume is small and the analysis time is short. Down to 2 nmol can be measured in a volume between 5 and 200 μl. The daily urinary excretion of trifluoroacetic acid from seven patients who had had halothane anaesthesia was measured for 14 days. The highest elimination rate was on the second day and it has ceased by the thirteenth day. However, the dose of halothane was not measured.

After occupational exposure to 5 ppm of halothane for a working week, it has been estimated that the concentration of trifluoroacetic acid in the urine at the end of the week will be about 50 μmol/l [14]. Consequently, the sensitivity of the ITP method is sufficient also for biological monitoring of halothane exposure of operating personnel.

The electrolyte system used was hydrochloric acid–β-alanine in the leading electrolyte and caproic acid in the terminating electrolyte (Table 1). In another paper [15] the composition of electrolytes for the optimum separation of trifluoroacetic acid from urinary acids is discussed. Experimentally determined conditions were assessed by computer simulation and it was shown that separation was achieved in the pH range 3.5–3.7.

4. METHANOL

Øvrebø *et al.* [16] developed a method for the determination of formic acid in plasma from methanol-poisoned patients. No pretreatment of the sample was neces-

sary, as opposed to other methods described for this type of analysis. However, this method was not used for occupational exposure measurements but for cases of acute poisoning where the concentration of formate is certainly higher. A plasma sample of 1–5 μl was used for the analysis and down to 0.2 mmol/l could be measured. The ITP instrument was equipped with a single capillary of 0.5 mm I.D. In plasma from ten poisoned patients the formate concentration ranged from 0.4 to 17.1 mmol/l.

In persons not exposed to methanol the concentration of formate in the blood ranged from 0 to 0.4 mmol/l and in a group of workers exposed to about 100 ppm of methanol the mean concentration of formic acid in the blood increased from 0.07 to 0.17 mmol/l [17]. The described ITP method is therefore not sensitive enough for measurements of occupational exposure without modifications. Hydrochloric acid was used as the leading and acetic acid as the terminating electrolytes (Table 1).

5. VINYL CHLORIDE

Thiodiacetic acid is a metabolite of vinyl chloride. Krivánková *et al.* [18] developed a sensitive ITP method for the determination of this acid in urine from vinyl chloride-exposed persons. No pretreatment of the urine was necessary, but an ITP instrument equipped with a column-coupling system was required. The leading electrolytes in the preseparation column and in the analytical capillary were of the same composition but had different pH values 3.4 and 4.3, respectively (Table 1).

Urine samples were collected from persons exposed to vinyl chloride in PVC production. In these samples the thiodiacetic acid concentration varied between 0.075 and 0.15 mmol/l, compared with a range of 0.025–0.067 mmol/l in urine from non-exposed persons. No measurements of the vinyl chloride exposure were reported, but the increase in the concentration of thiodiacetic acid in urine from exposed persons was obvious. By using the column-coupling technique the method was sensitive and the detection limit was $6 \cdot 10^{-6}$ mol/l.

6. ETHYLENE GLYCOL

Ethylene glycol is biotransformed into several products, including glycolic, glyoxylic, oxalic and formic acids. The determination of these acids by ITP has been described by Øvrebø *et al.* [19], who developed a method for their determination in blood from ethylene glycol-poisoned humans. The leading ion was chloride at pH 2.5 and the terminator was acetate (Table 1). Preparation of plasma by using oxalate, citrate or EDTA should be avoided as they interfere in the separation of the analytes. Furthermore, oxalic acid is one of the biotransformation products. Heparin was recommended for plasma preparation. In a plasma sample from an ethylene glycol-intoxicated patient glycolic acid was found whereas the other biotransformation products were below the detection limit of 0.2 mmol/l.

7. TRIETHANOLAMINE

Occupational exposure to triethanolamine can occur by inhalation of aerosols (the vapour pressure of the amine is very low). Sollenberg [9] developed an ITP method for the determination of triethanolamine in urine from workers exposed to

synthetic cutting fluids. Such fluids contain triethanolamine as an anti-corrosive agent. Triethanolamine taken up in the body is excreted to a large extent untransformed in the urine. A urine sample was applied to a cation-exchange column which was eluted with dilute ammonia solution, thus eluting only a fraction of the cationic content of the sample. The eluate was analysed by ITP using an instrument equipped with a column-coupling system. By using ethanolamine as the leading ion having a mobility slightly higher than that of triethanolamine and histidine as the terminator with a slightly lower mobilitiy, the analyte could be conveniently separated (Table 1). The detection limit was $2 \cdot 10^{-6}$ mol/l. Preliminary results indicated that triethanolamine can be found in urine from persons exposed to aerosols from synthetic cutting fluids. The method can therefore be useful for biological monitoring of exposure to triethanolamine.

REFERENCES

1 J. Sollenberg and A. Baldesten, *J. Chromatogr.*, 132 (1977) 469.
2 J.-P. Buchet, R. Lauwerys and H. Roels, *Arch. Mal. Prof. Med. Trav. Secur. Soc.*, 35 (1974) 511.
3 K. Engström and J. Rantanen, *Int. Arch. Arbeitsmed.*, 33 (1974) 163.
4 M. Ogata, R. Sugihara and S. Kira, *Int. Arch. Occup. Environ. Health*, 39 (1977) 199.
5 J. Sollenberg, A. W. Smallwood and L. K. Lowry, *J. Chromatogr.*, 343 (1985) 175.
6 J. Sollenberg, F. C. Phipps, B. Stringer and L. K. Lowry, *J. Chromatogr.*, 343 (1985) 419.
7 L. K. Lowry, T. W. Thoburn, F. C. Phipps, B. J. Gunter and J. Sollenberg, in M. H. Ho and H. K. Dillon (Editors), *Biological Monitoring of Exposure to Chemicals. Organic Compounds*, Wiley, New York, 1987, p. 143.
8 J. Sollenberg, R. Bjurström, K. Wrangskog and O. Vesterberg, *Int. Arch. Occup. Environ. Health*, 60 (1988) 365.
9 J. Sollenberg, unpublished results.
10 F. Mikkers and F. Everaerts, in F. M. Everaerts (Editor), *Analytical Isotachophoresis*, Elsevier, Amsterdam, 1981, p. 1.
11 R. Andersson, A. Carlsson, M. Byfält Nordqvist and J. Sollenberg, *Int. Arch. Occup. Environ. Health*, 53 (1983) 101.
12 W. Zschiesche, K. Gossler, K. H. Schaller, G.Triebig, D. Weltle and J. Angerer, *Berufskrankheiten in der keramischen und Glas-Industrie, Heft 28*, Berufsgenossenschaft der keramischen und Glas-Industrie, Würzburg, 1978–79.
13 M. Morio, K. Fujii, R. Takiyama, F. Chikasue, H. Kikuchi and L. Ribaric, *Anesthesiology*, 53 (1980) 56.
14 E. Dallmeier and D. Henschler, *Dtsch. Med. Wochenschr.*, 106 (1981) 324.
15 T. Hirokawa, H. Takemi, Y. Kiso, R. Takiyama, M. Morio, K. Fujii and H. Kikuchi, *J. Chromatogr.*, 305 (1984) 429.
16 S. Øvrebø, D. Jacobsen and O. M. Sejersted, in C. J. Holloway (Editor), *Analytical and Preparative Isotachophoresis*, Walter de Gruyter, Berlin, 1984, p. 261.
17 K. Baumann and J. Angerer, *Int. Arch. Occup. Environ. Health*, 42 (1979) 241.
18 L. Krivánková, E. Samcová and P. Boček, *Electrophoresis*, 5 (1984) 226.
19 S. Øvrebø, D. Jacobsen and O. M. Sejersted, *J. Chromatogr.*, 416 (1987) 111.

Journal of Chromatography, 545 (1991) 375–378
Elsevier Science Publishers B.V., Amsterdam

CHROM. 23 219

Capillary isotachophoretic determination of cysteinyl leukotrienes

DIMITRIOS TSIKAS* and JOACHIM FAULER
Department of Clinical Pharmacology, Hannover Medical School, Konstanty-Gutschow-Strasse 8, W-3000 Hannover 61 (Germany)
GORIG BRUNNER
Department of Gastroenterology and Hepatology, Hannover Medical School, Hannover (Germany)
and
JÜRGEN C. FRÖLICH
Department of Clinical Pharmacology, Hannover Medical School, Konstanty-Gutschow-Strasse 8, W-3000 Hannover 61 (Germany)

ABSTRACT

The cysteinyl leukotrienes (LTs) C_4, D_4 and E_4 are among the most potent lipid mediators of anaphylaxis and inflammation. A capillary isotachophoretic method is described for the determination of these cysteinyl LTs. The method is based on anionic separation and detection using UV (254 nm) and conductivity detectors. The total analysis time is of the order of 30 min. The limit of detection of the method was determined to be 0.5 nmol of LTE_4. Despite of similar chemical structures, all three cysteinyl LTs can be determined simultaneously.

INTRODUCTION

Cysteinyl leukotrienes (LTs) C_4, D_4 and E_4 (Fig. 1) are arachidonic acid metabolites formed via the 5-lipoxygenase pathway [1]. These endogenous substances are among the most potent lipid mediators of anaphylaxis and inflammation [1,2]. LTE_4 is the main cysteinyl LT metabolite in human urine [3]. Determination of LTE_4 can be accomplished by bioassay [4], radioimmunoassay [5,6], high-performance liquid chromatography (HPLC) with UV detection [5,7] and gas chromatography–mass spectrometry [8]. Recently Holloway and Battersby [9] and our group [10] have shown that capillary isotachophoresis is a useful method for the determination of glutathione (GSH) derivatives of aromatic and aliphatic electrophiles. As cysteinyl LTs are GSH derivatives of the epoxide LTA_4, we investigated whether capillary isotachophoresis (ITP) is applicable to their determination. This paper describes the capillary isotachophoretic determination of LTC_4, LTD_4 and LTE_4. The method is based on anionic separation and detection using UV and conductivity detectors.

0021-9673/91/$03.50

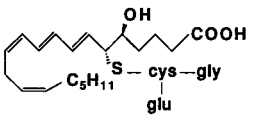

LTC_4

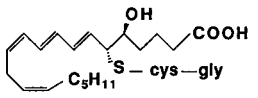

LTD_4

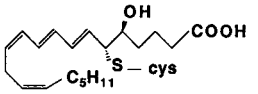

LTE_4

Fig. 1. Structures of the investigated cysteinyl leukotrienes LTC_4, LTD_4 and LTE_4.

EXPERIMENTAL

Isotachophoresis of LTC_4, LTD_4 and LTE_4 was performed on an LKB (Bromma, Sweden) Model 2127 Tachophor fitted with a polytetrafluoroethylene capillary (23 cm × 0.5 mm I.D.). Anionic analyses were performed with a leading electrolyte consisting of 5 m*M* hydrochloric acid, adjusted to pH 7.0 by the addition of Tris, and 0.25% (w/w) hydroxypropylmethylcellulose (HPMC) to reduce electroendosmosis. The terminating electrolyte consisted of 10 m*M* phenol, adjusted to pH 10.0 by the addition of freshly prepared and filtered barium hydroxide solution. All analyses were carried out at room temperature. The zones were detected by UV (254 nm) and conductivity detectors. The isotachopherograms were recorded with an LKB 2120 line recorder at a chart speed of 0.5 mm/s. Analyses were carried out at a constant current of 25 μA. The terminator passed the detectors at a potential of about 10 kV. Injections were made with a 10-μl Hamilton syringe. The total analysis time was of the order of 30 min. The zones were measured by both UV and conductivity signals.

Cysteinyl leukotrienes were obtained from Paesel (Frankfurt, Germany) and used as received or purified by reversed-phase HPLC. Hydrochloric acid, barium hydroxide and phenol were purchased from Merck (Darmstadt, Germany), HPMC from Ega-Chemie (Steinheim, Germany) and Tris from Baker (Deventer, Netherlands).

RESULTS AND DISCUSSION

Fig. 2 shows an isotachopherogram from the analysis of a mixture of LTC_4, LTD_4 and LTE_4. All three cysteinyl LTs appear as UV-absorbing zones and can be completely separated by this ITP method. Specific zone lengths and reciprocal reference unit (RRU) values were determined by separate injection of each cysteinyl LT. The specific zone lengths for LTE_4, LTD_4 and LTC_4, obtained from the slopes of their calibration graphs, were determined to be 5.804, 6.12 and 6.35 s/nmol,

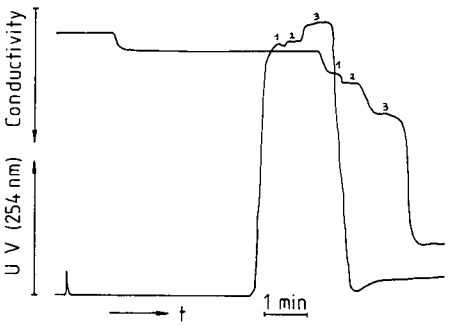

Fig. 2. Isotachopherogram for the separation of a mixture of (1) LTC_4 and (2) LTD_4, 4 nmol each, and (3) LTE_4, 10 nmol. For ITP conditions, see text.

respectively, which are lower than those of the GSH conjugates of aromatic electrophiles [10]. The RRU values of LTE_4, LTD_4 and LTC_4 estimated relative to the terminating ion from the relative step heights of the conductivity signal were determined to be (mean ± S.D.) 2.689 ± 0.085 ($n = 5$), 4.375 ± 0.112 ($n = 4$) and 5.185 ± 0.075 ($n = 4$), respectively. The corresponding RRU values of aromatic GSH conjugates are of the same order. The calibration graph for LTE_4 obtained by injection of 0.5–10 μl of a standard methanolic stock solution of LTE_4 was linear in the range 1–20 nmol and can be described by the regression equation $y = 4.489 + 5.804x$; $r^2 = 0.988$.

The sensitivity of the method is sufficient for the accurate detection of 0.5 nmol (220 ng) of LTE_4. This relatively high detection limit does not allow the application of this ITP technique to the determination of LTE_4 in human urine. However, the method could be useful for studying the formation and metabolism of cysteinyl LTs. Further, the on-line combination of ITP with mass spectrometry has recently been demonstrated for the first time by Udseth *et al.* [11], and has been shown to be suitable to the determination of analytes in the lower nanomolar range. ITP–mass spectrometry could allow more sensitive analysis and the determination of LTE_4 and other cysteinyl LTs in urine and other biological fluids using heavy stable isotope-labelled internal standards.

Because the method is applicable to cysteinyl LTs with closely similar structures, it could be an alternative technique for the analysis of all cysteinyl LTs, such as N-acetyl-LTE_4, the major cysteinyl LT metabolite in the urine of rat, and its metabolites of ω- and β-oxidation.

ACKNOWLEDGEMENT

The authors thank Miss A. Hofrichter for excellent technical assistance.

REFERENCES

1 B. Samuelsson, *Science (Washington, D.C.)*, 220 (1983) 568.
2 R. A. Lewis and K. F. Austen, *J. Clin. Invest.*, 73 (1984) 889.
3 S. Hammarström, L. Örning, K. Bernström, B. Gustafsson, E. Norin and L. Kaijser, *Adv. Prostaglandin Thromboxane Leukotriene Res.*, 15 (1985) 185.

4 G. Hansson, S.-E. Dahlén and E. Granström, in F. Berti, G. Folco and G. P. Velo (Editor), *Leukotrienes and Prostacyclin*, Plenum Press, New York, 1983, p. 65.
5 S. Hammarström, *Annu. Rev. Biochem.*, 52 (1983) 355.
6 L. Levine, R. Morgan, R. A. Lewis, K. F. Austen, D. A. Clark, A. Marfat and E. J. Corey, *Proc. Natl. Acad. Sci. USA*, 78 (1981) 7692.
7 D. C. Henke, S. Kouzan and T. E. Eling, *Anal. Biochem.*, 140 (1984) 87.
8 M. Balazy and R. C. Murphy, *Anal. Chem.*, 58 (1986) 1098.
9 C. J. Holloway and R. V. Battersby, *Electrophoresis*, 7 (1986) 304.
10 D. Tsikas and G. Brunner, *J. Chromatogr.*, 470 (1989) 191.
11 H. R. Udseth, J. A. Loo and R. D. Smith, *Anal. Chem.*, 61 (1989) 228.

Journal of Chromatography, 545 (1991) 379–389
Elsevier Science Publishers B.V., Amsterdam

CHROM. 23 159

Capillary electrophoresis of peptides

Analysis of adrenocorticotropic hormone-related fragments

TOM A. A. M. VAN DE GOOR*

Laboratory of Instrumental Analysis, Eindhoven University of Technology, P.O. Box 513, 5600 MB Eindhoven (The Netherlands)

PETER S. L. JANSSEN, JAN W. VAN NISPEN and MARIO J. M. VAN ZEELAND

Organon International BV, Scientific Development Group, P.O. Box 20, 5340 BH Oss (The Netherlands)

and

FRANS M. EVERAERTS

Laboratory of Instrumental Analysis, Eindhoven University of Technology, P.O. Box 513, 5600 MB Eindhoven (The Netherlands)

ABSTRACT

Capillary electrophoresis can be used succesfully to analyse small peptides to give additional information to that obtained using high-performance liquid chromatography (HPLC). The separation of a modified adrenocorticotropic hormone (4–9) fragment (Org 2766) and several of its fragments was investigated using capillary zone electrophoresis. Prediction of migration in aqueous systems using pK_a-related data and the migration behaviour using sodium dodecyl sulphate in the buffer are discussed, as is the choice of buffer systems. The electrophoretic patterns are compared with the HPLC separation.

INTRODUCTION

Adrenocorticotropic hormone (ACTH) has long been known for its stimulation of the adrenal cortex to produce and release steroid hormones. In addition to extra-adrenal activities, *e.g.*, lipolytic and melanotropic effects, ACTH also influences behaviour in animals and man [1]. In recent years several studies have shown that ACTH and related peptides stimulate the recovery of sensorimotor function after nerve damage [2]. Org. 2766, a modified ACTH-(4–9) fragment (I), also active in this respect, was found to prevent neuropathies induced by cystostatic drugs in both animals and man [3].

Part of the development work of a compound involves finding conditions to separate the parent compound from its fragments, either synthetic products or metabolites. High-performance liquid chromatography (HPLC) is an established technique for the separation of peptides. Capillary electrophoresis is a rapidly expanding separation method in which automation common in chromatography is combined

0021-9673/91/$03.50

with the separation power of electrophoresis [4,5]. Capillary zone electrophoresis (CZE) has been shown to be an additional technique to HPLC in the analysis of small peptides [6–11]. Small differences in peptide charge and size can lead to separation with a different selectivity as compared with HPLC

In the development of an adequate separation of I from five of its possible fragments, we investigated the use of CZE in aqueous systems and tried to predict the optimum separation using a simple program for the prediction of peptide charge and mobility. The performance in several buffers was also investigated.

To obtain a better resolution for compounds with an overall charge of zero, sodium dodecyl suplhate (SDS) can be added to the buffer at a concentration above its critical micelle concentration (CMC). This leads to the formation of an extra micellar phase in the system. Because these micelles are charged and migrate with a different velocity than the electroosmotic flow (EOF), separations are based on the difference in affinity for the micellar phase. This technique, known as micellar electrokinetic capillary chromatography (MECC) [12], can lead to a different selectivity. The influence of the SDS concentration on the separation was investigated.

For reasons of comparison we also examined the separation of the peptides by HPLC.

EXPERIMENTAL

Instrumentation

CE experiments were performed on a P/ACE System 2000 capillary electrophoresis instrument (Beckman, Palo Alto, CA, U.S.A.) using UV detection at 200 and 214 nm. The capillary used was a 57 cm (50 cm to the detector) × 75 μm I.D. untreated fused-silica tube from Poly Micro Technology (Phoenix, AZ, U.S.A.), mounted in the Beckman capillary cartridge. After installation, the capillary was treated for 45 min with 0.1 *M* KOH and subsequently rinsed for 45 min with water. Data were collected using the P/ACE System 2000 software and analysed with CAESAR capillary electrophoresis software, which was developed in our laboratory.

HPLC experiments were carried out on an HP 1090 M liquid chromatograph (Hewlett-Packard, Palo Alto, CA, U.S.A.) provided with a ternary solvent-delivery system, an autoinjector, an autosampler and a diode-array detector. The apparatus was equipped with a computer workstation and printer/plotter facilities. As supporting material a reversed-phase octadecylsilica column (Supelcosil LC-18 DB, 5-μm particles, 250 × 4.6 mm I.D.) (Supelco, Bellefonte, PA, U.S.A.) was used. A guard column (20 × 4.6 mm I.D.) filled with the same material preceded the analytical column.

Materials

Fig. 1 shows the amino acid composition of the hexapeptide I and its fragments which were synthesized by the peptide chemistry group of Organon. Part of the sequence of ACTH is also shown.

All other chemicals used were of analytical-reagent grade and obtained from Merck (Darmstadt, Germany), except for SDS, which was of electrophoresis grade from Polysciences (Warrington, PA, U.S.A.). All buffers and samples were prepared using ultrapurified water (Milli-Q system; Waters–Millipore, Bedford, MA, U.S.A.) with a resistance of better than 10 MΩ/cm.

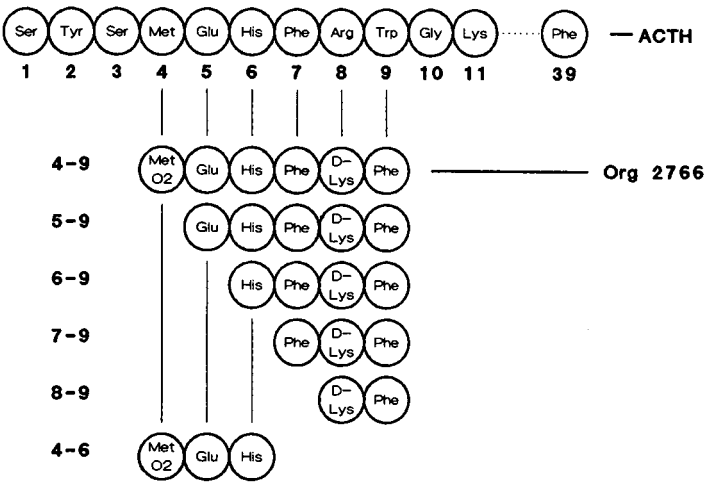

Fig. 1. Primary structure of I (Org 2766) and several of its fragments.

Methods

CE analyses were performed in the following way. Prior to each analysis the capillary was washed successively for 2 min with 0.1 *M* KOH, 2 min with water and 2 min with the buffer system, to obtain reproducible conditions in the separation system. Samples were dissolved in water unless stated otherwise and were analysed immediately. Injection was performed using pressure and the injection volume was in the range 5–25 nl (a 1-s pressure injection represented about 5 nl). The temperature was preset to 25°C and kept constant during the analyses. All analyses were performed using a potential difference of 25 kV.

The choice of electrolyte systems is a critical issue in CZE. To illustrate the effect of some essential parameters, characteristics of the aqueous buffers used are given in Table I.

Buffers used in MECC separations were prepared by mixing appropriate amounts of the aqueous buffer of pH 8.3 with the same buffer containing 100 m*M* SDS.

TABLE I

OPERATIONAL BUFFER SYSTEMS

No.	pH	Concentration[a]	Conductivity (mS/cm)	EOF · 10^{-5} (cm^2/V s)	UV absorbance (AU at 214 nm)
1	2.2	25 m*M* phosphate + KOH	4.03	<3.2	0.000
2	3.8	20 m*M* formate + alanine	0.95	16.4	0.002
3	4.4	20 m*M* ε-aminocaproate + acetic acid	0.84	29.7	0.007
4	6.2	20 m*M* histidine + MES	0.39	52.8	0.059
5	7.5	40 m*M* imidazole + MOPS	0.73	57.6	0.057
6	8.3	100 m*M* borate + KOH	1.90	67.9	0.000

[a] MES = 2-(N-morpholino)ethanesulphonic acid; MOPS = 3-(N-morpholino)propanesulphonic acid.

TABLE II

GRADIENTS APPLIED IN HPLC

Gradient No.	Time (min)	Elution profile[a]			Temperature (°C)
		A (%)	B (%)	C (%)	
1	0	20	65	15	35
	60	20	55	25	
2	0	20	65	15	35
	30	20	55	25	
3	0	20	62	18	45
	20	20	54	26	

[a] A, 0.5 *M* NaH_2PO_4 and H_3PO_4 to pH 2.1; B, water; C, acetonitrile–water (60:40).

For the HPLC separation a phosphate buffer–acetonitrile gradient system [13] was applied: solvent A, 0.5 *M* NaH_2PO_4 and H_3PO_4 to pH 2.1; solvent B, water; and solvent C, acetonitrile–water (60:40). Three different linear gradient runs were applied (Table II). All separations were performed at a flow-rate of 1.0 ml/min. Prior to use the mobile phases were filtered and degassed with helium. Peptide samples were dissolved in the initial mobile phase and 100 μl of this solution, corresponding to 10–15 μg of each peptide, were injected. Detection was at 210 nm. The retention times and peak areas were recorded.

Calculations of the titration curves and mobility for the several peptide fragments were performed using CAS, peptide mobility software, also developed in our laboratory.

RESULTS AND DISCUSSION

Using the animo acid composition of the peptide it is possible to calculate an imaginary titration curve for this compound using the pK_a values of the various amino acids [14]. The charge of the peptides under various pH conditions can then be easily calculated. In Fig. 2 the charge *versus* pH curves are given for the different peptide fragments calculated. For $MetO_2$ the same pK_a values are used as for methionine.

Charge is, of course, one of the main parameters that determine the electrophoretic migration behaviour of peptides in an aqueous buffer system. Several workers have tried to propose a model including other parameters, *e.g.*, molecular weight or number of animo acids for accurate determination of the migration characteristics.

By plotting charge divided by the two-thirds power of the molecular weight against pH, an estimate for the relative electrophoretic mobility can be obtained [9] and these data are given in Fig. 3. Measurement of the real effective mobilities under different pH conditions and comparison of the data with the calculated mobilities are necessary in order to validate this model.

Fig. 4 shows the electropherograms of I and its fragments using the six different buffer systems. A baseline separation in less than 12 min is shown in Fig. 4A. The peak performance is poor, because the buffer has a high conductivity, resulting in

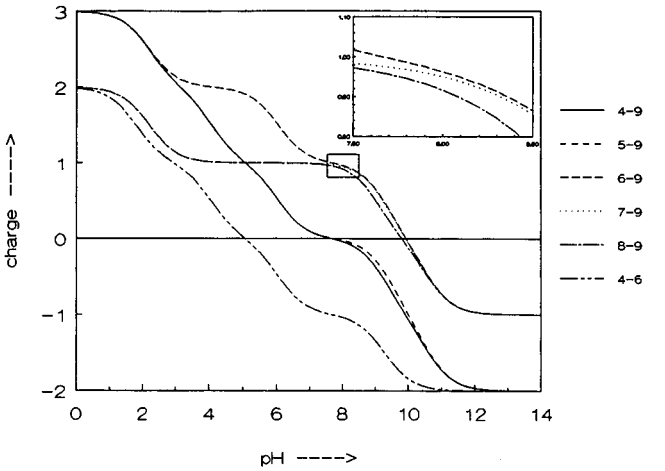

Fig. 2. Calculated titration curves for I and fragments. The inset shows the minor differences around pH 8.

extensive Joule heating. This was also clear from the changes in migration time, which were high. It should be emphasized that the solutes are migrating as positive ions.

In Fig. 4B and C the separations show very good peak shapes. Plate numbers of 200.000–300.000 were measured for all peaks. That minor changes in pH can cause a different migration order is clear from the position of peak 4. Clearly all compounds migrate as positive ions, which indicates that hydrostatic effects on the negatively charged capillary surface play only a minor role. The negative dips in the electropherograms mark the osmotic flow.

Fig. 4D and E shows the influence of highly UV-absorbing buffers. A clear negative peak marks the osmotic flow and the peak heights are considerably smaller. The detection limits in these systems are therefore higher than in the other systems.

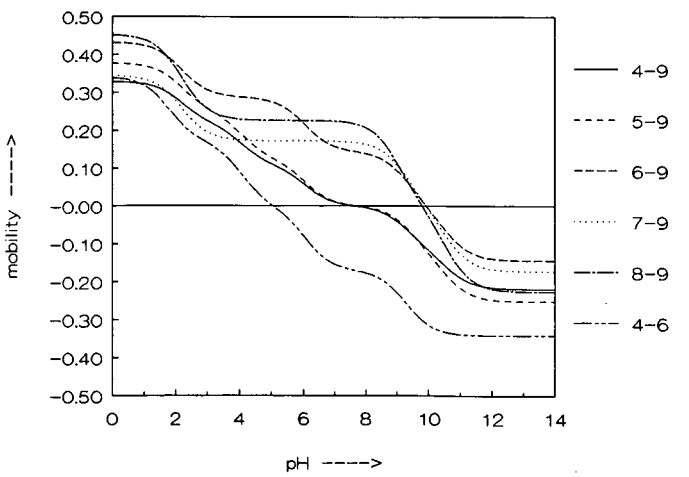

Fig. 3. Calculated relative mobilities ($\cdot 10^{-1}$) for I and fragments.

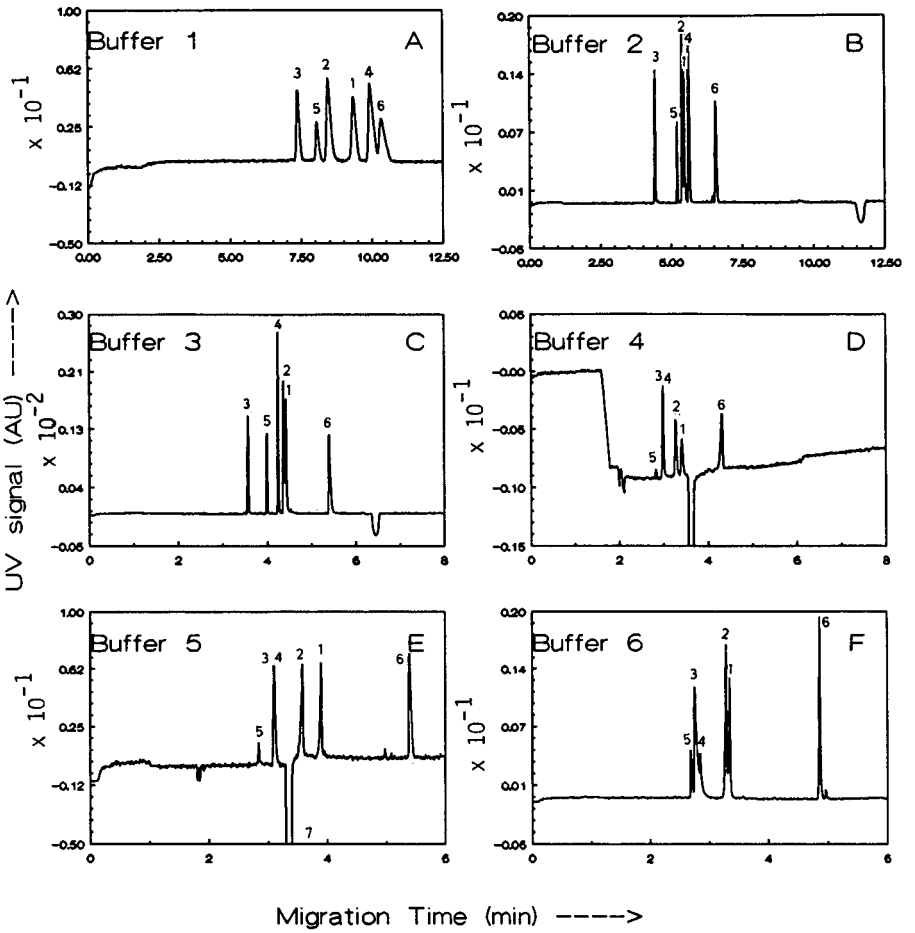

Fig. 4. Electropherograms of I and fragments separated using buffers 1–6. UV detection at 214 nm. Fragments: (1) 4–9; (2) 5–9; (3) 6–9; (4) 7–9; (5) 8–9; (6) 4–6.

Note that at this moderate pH, part of the compounds is positively and part negatively charged. Both electropherograms show a triplet of small negative dips, which was present in every analysis. Considering the migration time it can be that we are dealing with small metal ions, detected through exclusion of the positive UV-absorbing buffer ions.

When we compare the observed migration order of the compounds in the different systems with the calculated migration order presented in Fig. 3, we can conclude that the migration order can be predicted exactly. A group of three peaks as in Fig. 4F is also found in the predicted migration behaviour. However a correction factor should be used to obtain the same absolute values. When we plot $1.1391 \times$ (calculated mobility $\times 10^{-2}$) $- 0.7252$ against (measured mobility $\times 10^{-8}$) we obtain Fig. 5. A good correlation with a regression coefficient of 0.94 was found, although six different buffer systems were used. Comparing data obtained within one system we

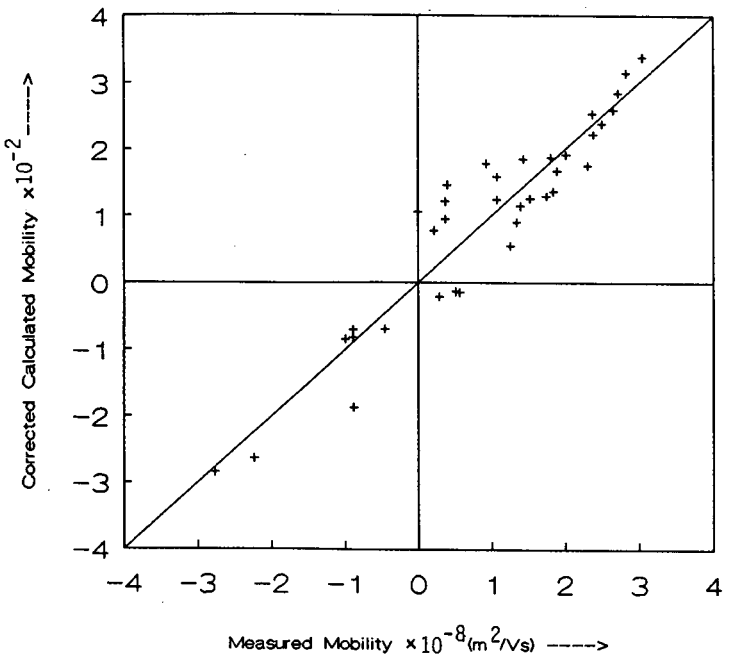

Fig. 5. Comparison of calculated and measured mobilities.

find an even better correlation with a regression coefficient of 0.98 for high pH to 0.99 for the low and middle pH region.

In order to use CE for the purity control of synthetic peptides, optimization of the separation of the compound from its fragments or impurities has to be performed. To determine possible impurities also, calibration graphs have to be constructed and detection limits have to be established.

In Fig. 6 the calibration graph for I using buffer systems 1 and 6 is given. The

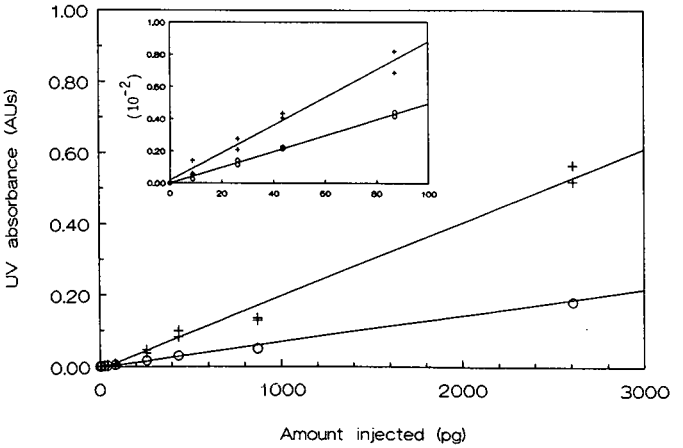

Fig. 6. Calibration graphs for I using buffers (+) 1 and (o) 6. The inset shows the lower region of the curve.

amount of sample used was in the range 8–2610 pg and all measurements were performed in duplicate. A good correlation was found between the amount injected and the UV absorbance, with regression coefficients of 0.995 and 0.999, respectively. The samples were dissolved in water and therefore a non-uniform electric field gradient was present after the injection. Dissolving the sample in the operating buffer improves the linearity of the calibration graph. Detection limits were *ca.* 5 pg injected in both instances. As mentioned earlier, buffer 1 shows poorer reproducibility.

Fig. 7 shows the electropherogram for I in buffer system 6. No significant impurities can be observed. It should be borne in mind, however, that fragments 4–9 and 5–9 elute very closely in this system. A large surplus of 4–9 as compared with 5–9 can easily mask the presence of the latter. However, checking in system 1, where these two components do not elute very closely, did not show any extra peak.

Addition of SDS to the buffer system can influence the selectivity. In Fig. 8 three electropherograms are shown of I and fragments in buffer 6 with different amounts of SDS added. Mainly compounds which are overall zero charged at the pH of buffer 6 are strongly influenced by addition of SDS. Charged compounds (*e.g.*, fragment 4–6), are hardly influenced, especially when one takes into account the decrease in the EOF. Therefore, compounds which are difficult to separate or which migrate very closely can be separated if they have different affinities for the micellar phase. Fragments 4–9 and 5–9 show an improved resolution when the amounts of SDS added is increased. On the other hand, fragments 6–9 and 7–9 continue to migrate with almost similar velocity. Fig. 9 shows the complete behaviour in the region 0–90 m*M* SDS. Plate numbers decrease, however, at high concentrations of SDS because it contributes to the conductivity of the electrophoresis buffer. When we compare the conductivity of buffer 6 (32 μA at 25 kV) with the same buffer containing 90 m*M* SDS (123 μA at 25 kV), we can observe a clearly increased production of Joule heat and a decrease in plate number.

Using HPLC, in the initially performed 60-min run (gradient 1, Table II) all six peptides were completely separated and showed a relatively wide difference in reten-

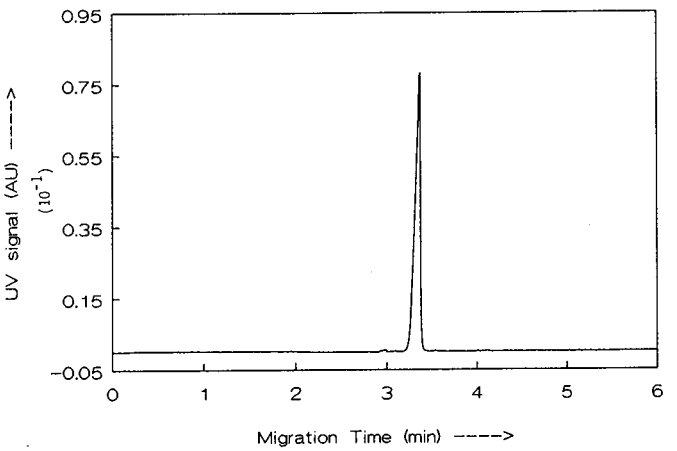

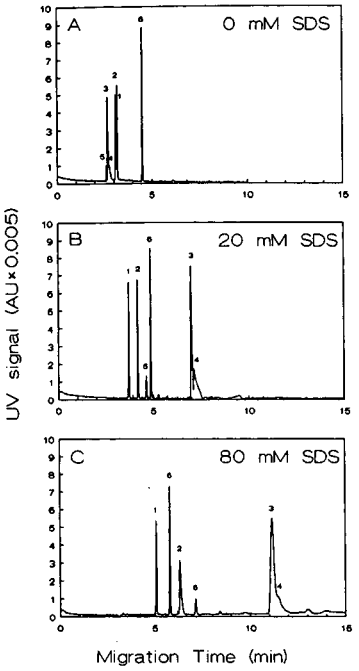

Fig. 8. Electropherograms of I and fragments separated using buffer 6 with 0, 20 and 80 m*M* SDS added.

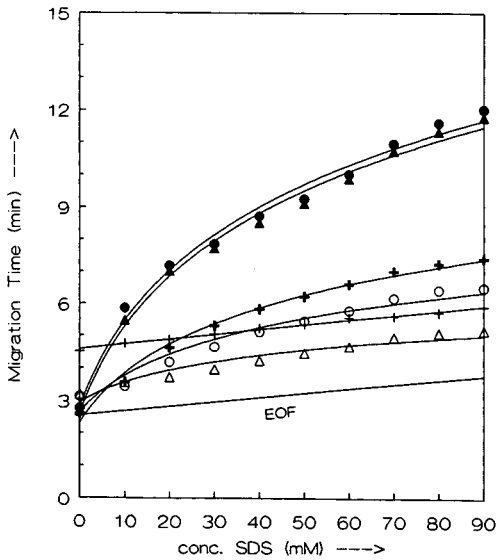

Fig. 9. Influence of addition of SDS to buffer 6 on the separation of I and fragments. (△) 4–9; (○) 5–9; (▲) 6–9; (●) 7–9; (+) 8–9; (+) 4–6.

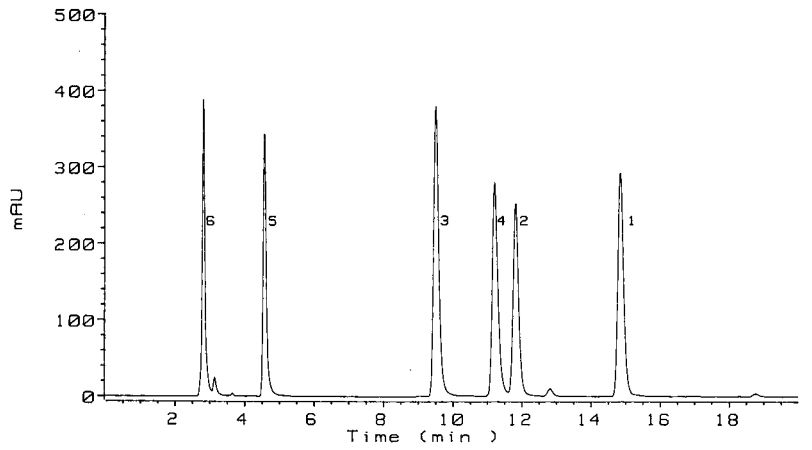

Fig. 10. HPLC elution pattern of I and fragments. (1) 4–9; (2) 5–9; (3) 6–9; (4) 7–9; (5) 8–9; (6) 4–6.

tion times. We therefore tried to perform a faster elution by applying a run with the same solvent composition but over a 30-min period (gradient 2) Again a good separation of the six compounds was obtained. Finally, we further speeded up the separation to 20 min by raising the temperature to 45°C and slightly adapting the solvent composition (gradient 3). Even in this short run a complete separation of the peptides was obtained, as illustrated in Fig. 10. In all three gradients the actual elution order of the peptides was in accordance with the predicted elution order based on the peptide hydrophobicity calculation of Meek and Rosetti [15] for phosphate–acetonitrile gradients. Only the pair 7–9/5–9 eluted in the reverse order.

As expected, no correlation was found between the CZE analysis in the aqueous buffer systems and HPLC. Using two-phase systems in both MECC and HPLC, leads to the question of whether these two methods can give comparable results. In reversed-phase HPLC we have a moving polar mobile phase and an apolar stationary phase, whereas in MECC the 'stationary phase' is also apolar but migrating. However, no similar migration orders were found between the HPLC and MECC.

CONCLUSION

Small peptides are suitable for analysis by capillary electrophoretic methods. The mobility of these compounds can often be predicted fairly well using the pK_a values of the separate amino acids, especially when the investigated peptides are closely related. One should keep in mind, however, that pK_a values of amino acids in peptides can be influenced by neighbouring groups. Both the elution orders and measured migration times, however, were close to the predicted values, although a correction factor had to be used.

Choice of buffer systems can therefore be made based on calculations, although some parameters have to be taken into account. The buffer components should preferably have a high buffering capacity in the given pH region and have a low conduc-

tivity. In this respect, fairly high-concentration buffers can be used without problems of Joule heating. A small UV absorbance of the buffer is recommended because it makes the determination of the EOF possible without addition of a marker. This EOF dip can be used to check the reproducibility of the system and can be used as an internal standard for correction of migration times.

To identify fragments in purity control of peptides, the migration behaviour of standards should be known. If not, one should use several systems to minimize possible overlapping of compounds. For fairly apolar species the addition of SDS can cause extra selectivity which can be used to improve critical separations.

The different separation mechanism in CE, both CZE (based on charge/mass ratio) and MECC (based on the affinity for the micellar phase), and HPLC (mainly based on hydrophobicity), will result in complementary information. Therefore, both techniques are valuable in peptide analysis.

REFERENCES

1 D. de Wied and J. Jolles, *Physiol. Rev.*, 62 (1982) 976–1059.
2 W. H. Gispen, P. de Koning, R. R. F. Kuiters, C. E. E. M. van der Zee and J. Verhaagen, *Prog. Brain Res.*, 72 (1987) 319–325.
3 R. Gerritsen van der Hoop, C. J. Vecht, M. E. L. van der Burg, A. Elderson, W. Boogerd, J. J. Heimans, E. P. Vries, J. C. van Houwelingen, F. G. I. Jennekens, W. H. Gispen and J. P. Neijt, *N. Engl. J. Med.*, 322 (1990) 89–94.
4 F. E. P. Mikkers, F. M. Everaerts and Th. P. E. M. Verheggen, *J. Chromatogr.*, 169 (1979) 11–20.
5 J. W. Jorgenson and K. D. Lukacs, *Anal. Chem.*, 53 (1981) 1298–1302.
6 R. M. McCormick, *Anal. Chem.*, 60 (1988) 2322–2328.
7 H. Ludi, E. Gassmann, H. Grossenberger and W. Marki, *Anal. Chim. Acta*, 213 (1988) 215–219.
8 P. D. Grossman, K. J. Wilson, G. Petrie and H. H. Lauer, *Anal. Biochem.*, 173 (1988) 265–270.
9 J. Frenz, S. L. Wu and W. S. Hancock, *J. Chromatogr.*, 480 (1989) 379–391.
10 R. G. Nielsen, R. M. Riggin and E. C. Rickard, *J. Chromatogr.*, 480 (1989) 393–401.
11 P. D. Grossmann, J. C. Colburn, H. H. Lauer, R. G. Nielsen, R. M. Nielsen, R. M. Riggin, G. S. Sittampalam and E. C. Rickard, *Anal. Chem.*, 61 (1989) 1186–1194.
12 S. Terabe, K. Otsuka, K. Ichikawa, A. Tsuchiya and T. Ando, *Anal. Chem.*, 56 (1984) 113–116.
13 P. S. L. Janssen, J. W. van Nispen, M. J. M. van Zeeland and P. A. T. A. Melgers, *J. Chromatogr.*, 470 (1989) 171–183.
14 R. M. C. Dawson, D. C. Elliot and K. M. Jones, *Data for Biochemical Research*, Oxford University Press, Oxford, 1974.
15 J. L. Meek and Z. L. Rosetti, *J. Chromatogr.*, 211 (1981) 15–28.

Journal of Chromatography, 545 (1991) 391–396
Elsevier Science Publishers B.V., Amsterdam

CHROM. 23 178

Use of discrete spacers for the separation of proteins by gel isotachophoresis

FERNANDO ACEVEDO
Department of Dermatology, Karolinska Hospital, Karolinska Institute, S-104 01 Stockholm (Sweden)

ABSTRACT

Discrete amphoteric spacers can generate a linear pH gradient concomitant with a conductivity gradient on isotachophoresis. The design of the system requires a mixture of discrete spacers calculated to generate an electrophoretic mobility–pH or charge–pH relationship as linear as possible and a mixture of counter ions calculated to provide a buffer capacity proportional to the charge of the mixture of spacers over the expected pH gradient. The separation of human blood plasma proteins in agarose gels is used as an example. The spacers were amphoteric ions: amino acids, amino acid derivatives and sulphonic compounds. The results obtained using mixtures of discrete spacers resemble those obtained using commercially available ampholyte mixture as judged from the separation of the C3-complement proteins. The major advantage of the use of discrete spacers in ITP lies in the possibility of designing separation systems for specific proteins.

INTRODUCTION

Commercially available ampholyte mixtures have been successfully used for the separation of proteins by isotachophoresis (ITP) in agarose gels [1]. However, these mixtures are not defined in terms of the individual components. The object of this study was to investigate the requirements of the ITP system in order to obtain optimum protein separations in agarose gels by the use of discrete spacers.

The principle used for the design of isotachophoretic systems for the separation of proteins using commercially available ampholyte mixtures is that a pH gradient concomitant with a conductivity gradient should be generated. The approach is based on the following considerations: (1) On isoelectric focusing (IEF), proteins are separated in a pH gradient, generated by ampholytes and stabilized between the anode and the cathode; on ITP, proteins are separated in an electrophoretic mobility or conductivity gradient, generated by spacers and stabilized between the leading ion and the terminating ion; (2) graphical representation of the conductivity *versus* the distance in IEF will show small rises and falls in conductivity centred around a horizontal line in a wavy pattern. The hills of increased conductivity originate from the charges of the different ampholytes used to generate the pH gradient. The corresponding graph for ITP would then be like a staircase starting from the low conductivity of the terminating ion and rising to the high conductivity of the leading ion. The

0021-9673/91/$03.50

individual steps would represent the conductivity of the different spacer ions. The difference between these two curves is the increase in charge of the ampholytes in the latter. Therefore, to obtain a pH gradient concomitant with a conductivity gradient, one should have counter ions that can supply the charge to the ampholytes in a pH gradient [1]. In this way, proteins can be focused by ITP not only at their isoelectric points but also at almost any point on their titration curves. The advantage of this lies in the fact that the solubility of most proteins is lowest at their isoelectric points and some native proteins are not stable. This has been illustrated for plasma proteins [2] and particularly for C3-complement proteins in a recent study [3]. In ITP the slope of the pH gradient generated can also be regulated to increase the resolution as in IEF.

EXPERIMENTAL

Human plasma samples were supplied by the blood centre at the Karolinska Hospital. Agarose, electrode strips and paper sample applicators were obtained from Pharmacia (Uppsala, Sweden), nitrocellulose membrane Immobilon from Millipore (Bedford, MA, U.S.A.), rabbit immunoglobulins (Igs) and horsedish peroxidase-conjugated swine antibodies against rabbit Igs from Dakopatts (Copenhagen, Denmark), Gelbond from FMC Bioproducts (Rockland, ME, U.S.A.), swine serum from Flow Labs. (Uxbridge, Middlesex, U.K.) and dry defatted milk from Semper (Stockholm, Sweden). All chemicals were of analytical-reagent grade.

Isotachophoretic system

The procedure was basically as described previously [1]. Isotachophoresis was run in flat-bed gels. The plasma proteins were electrophoresed towards the anode in 1% agarose IEF, 12% sorbitol gels, on a flat-bed electrophoresis apparatus (Pharmacia FBE3000). The electrode solutions were absorbed in the electrode strips, placed on the edges of the gel. The gels were prerun at 5–10 W until the isotachophoretic front reached 1.0–1.5 cm from the cathode. Then the samples, 20 μl of 20% plasma in 100 m*M* Tris–HCl (pH 8.0), were applied on paper sample applicators, placed behind the front. Electrophoresis was carried out at 5–20 W (300–1200 V) until the front reached the anode. The leading ion, the counter-ions and the mixture of spacers were included in the gel mixture. The terminating ion (10 ml) was included in the cathode. The anode solution (20 ml) contained the counter-ions ten times more concentrated than in the gel and adjusted to pH 6 with sulphuric acid. The gels were stained with Coomassie Brilliant Blue or immunostained. In the latter instance, the proteins from the agarose gel were transferred to a nitrocellulose filter (NCF) by overlaying the gel with a stack consisting of a wet NCF, a sheet of wet blotting paper, eight layers of dry blotting paper (Munktell, Stora, Sweden), a glass plate and, on the top, a 5-kg weight, for 20 min at room temperature. The immunological detection of proteins on NCF was performed essentially according to Towbin *et al.* [4], except that 5% dry defatted milk in 0.9% NaCl–10 m*M* Tris–HCl buffer (pH 7.4) (TBS) was used instead of bovine serum albumin. The Igs were diluted 1:1000 in 5% dry defatted milk–10% swine serum in TBS. The peroxidase-labelled antibodies were stained with 4-chloro-1-naphtol [5].

Spacers

The spacers were amphoteric ions such as amino acids, amino acid derivatives and sulphonic compounds as listed in Table I. The pK_a and pK_b values were determined by titration at 20°C. The criteria for the selection of the amphoteric ions were based on the pK_b value of the basic group and the commcercial availability. The concentration of the spacers in the mixture was calculated to generate a charge–pH or a mobility–pH relationship as linear as possible (a constant slope) in the pH interval between the two extreme pK_b values. For the mobility values the factor charge $\times$ (molecular weight)$^{-\frac{1}{2}}$ was used in the calculations, according to the approximation of Jokl [6].

TABLE I

CHARACTERISTICS OF SPACERS

Ion[a]	M.W.	$pK_{a,20°C}$	$pK_{b,20°C}$	Mixture[b]	Mixture[c]
MES[d]	195.2	1.3	6.1	23.21	21.81
ACES[d]	182.2	1.3	6.75	0.83	5.8
BES[d]	213.3	1.35	7.1	3.36	3.62
MOPS[d]	209.3	1.4	7.2	4.19	3.1
TES[d]	229.3	1.3	7.45	2.99	2.2
DIPSO[d]	243	1.3	7.5	2.61	2.07
HEPES[d]	238.3	3.05	7.5	2.61	2.07
TAPSO[d]	259.3	1.3	7.58	1.96	1.93
HEPPSO[d]	268.3	3.5	7.9	0.92	1.87
EPPS[d]	252.3	3.75	7.9	0.92	1.87
POPSO[d]	362.4	3.9	7.9	0.92	1.87
Tricine	179.2	2.15	8.05	1.07	2.1
GLYGLY	132.1	3.15	8.2	1.58	2.59
Bicine	163.2	1.95	8.25	1.97	2.74
TAPS[d]	243.3	1.3	8.4	3.4	3.44
Asparagine	150.1	2.25	8.85	7.95	4.4
Serine	105.1	2.21	9.15	4.03	3.99
Glutamine	146.2	2.35	9.15	4.03	3.99
Glycine	75.05	2.34	9.6	2.84	3.62
Alanine	89.1	2.35	9.87	5.55	3.06
β-Alanine	89.1	3.55	10.29	6.2	2.07
GABA	103.1	4.03	10.56	4.48	3.44
EACA	131.2	4.37	10.8	12.39	16.37

[a] Abbreviations: MES = 2-(N-morpholino)ethanesulphonic acid; ACES = N-(2-acetamido)-2-aminoethanesulphonic acid; BES = N,N-bis(2-hydroxyethyl)-2-aminoethanesulphonic acid; MOPS = 3-(N-morpholino)propanesulphonic acid; TES = N-tris(hydroxymethyl)methyl-2-aminoethanesulphonic acid; DIPSO = 3-[N,N-bis(2-hydroxyethyl)amino]-2-hydroxypropanesulphonic acid; HEPES = 4-(2-hydroxyethyl)-1-piperazineethanesulphonic acid; TAPSO = 3-[N-tris(hydroxymethyl)methylamino]-2-hydroxypropanesulphonic acid; HEPPSO = N-(2-hydroxyethyl)piperazine-N′-(2-hydroxypropanesulphonic acid); EPPS = N-(2-hydroxyethyl)piperazine-N′-(3-propanesulphonic acid); POPSO = piperazine-N,N′-bis(2-hydroxypropanesulphonic acid); GLYGLY = glycylglycine; TAPS = N-tris(hydroxymethyl)methyl-3-aminopropanesulphonic acid; GABA = γ-aminobutyric acid; EACA = ε-aminocaproic acid.

[b] Mixture 1 in mol%, calculated to generate a linear charge–pH relationship.

[c] Mixture 2 in mol%, calculated to generate a linear mobility–pH relationship [6].

[d] Good buffers [7].

Calculations

The proportions of the ions in the mixture were calculated by an iterative procedure with an accuracy of 0.01 pH unit over the pH interval of interest. The optimum result would be a constant slope for the charge–pH or mobility–pH graph. At the start of the calculations equal concentrations were allotted to all components in the mixture. In order to adjust the graph to a first-order linear relationship between charge and pH, the concentration of each particular ion was varied. The given value was multiplied by a factor proportional to the difference between the value for the slope of the calculated graph at the pK_b of the ion and the median of the slope for the overall graph. The process was repeated several times, until the individual additons to the generated slope for each spacer did not vary by more than 1%. The compositions of the mixtures of spacers obtained after such calculations are given in Table I (last two columns).

A mixture of bases as counter ions was chosen and calculated in a similar manner to the spacer ions. The concentration of the leading ion (glutamic acid) was just above that of the first spacer used and the total concentration of counter ions was about 50% of the total concentration of the leading ion and the spacers in order to obtain a pH value near the pK_b of the spacers. The terminating ion, absorbed in the cathode, was 200 m*M* lysine.

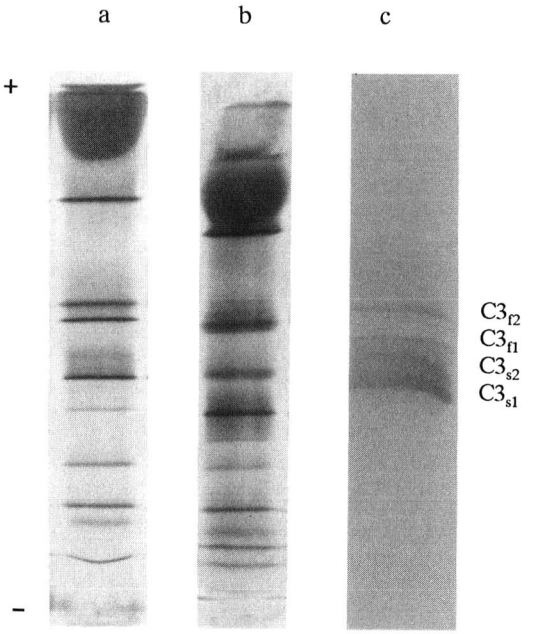

Fig. 1. Agarose gel ITP of human blood plasma proteins. The size of the gels was 12 × 12 × 0.1 cm. (a) The mixture of spacers was calculated to generate a linear charge–pH relationship (Table I, column 5, mixture 1). Leading ion, 40 m*M* glutamic acid; terminating ion, lysine; spacers, 250 m*M* of mixture 1; counter ions, 100 m*M* bistris, 34 m*M* tris and 17 m*M* 2-aminoethanol. Coomassie Brilliant Blue staining. (b) The mixture of spacers was calculated to generate a linear mobility–pH relationship (Table I, column 6, Mixture 2). All other ions as in (a). (c) Immunoblot stained with antibodies against $C3_c$-complement factor after ITP of human blood plasma in a gel similar to that illustrated in (a).

Pieces of 0.5 cm (along the electrophoresis path) × 2 cm (wide) were cut and left overnight in 1 ml of water for pH and conductivity measurements.

RESULTS

Two different calculations for the composition of the mixture of spacers were made, one to obtain a linear charge–pH relationship and the other to obtain a linear mobility–pH relationship. Fig. 1 illustrates the results after agarose gel isotachophoresis of human blood plasma proteins using mixtures of discrete spacers calculated as described above. No major difference was observed between the two gels. Lane c shows the result after immunodetection of C3 components in a gel identical with that illustrated in lane a. Four different bands were stained, in agreement with earlier reported results using ampholyte mixtures as spacers [3].

The conductivity and pH measurements in gels identical with those illustrated in Fig. 1, except for a longer electrophoretic path, are shown in Fig. 2. An almost linear pH gradient concomitant with a conductivity gradient was obtained in both instances.

DISCUSSION

The best results for the separation of plasma proteins by ITP using discrete spacers were obtained when the mixture of spacers was such that it could generate a pH–charge relationship as linear as possible and the counter ions were such that they could provide a buffer capacity corresponding to the charge of the mixture of spacers over the expected pH interval.

The pH gradient generated in ITP by using mixtures of spacers calculated upon mobility did not differ from the gradient generated by using mixtures of spacers calculated upon charge (Fig. 2). One reason for this is the small differences in molec-

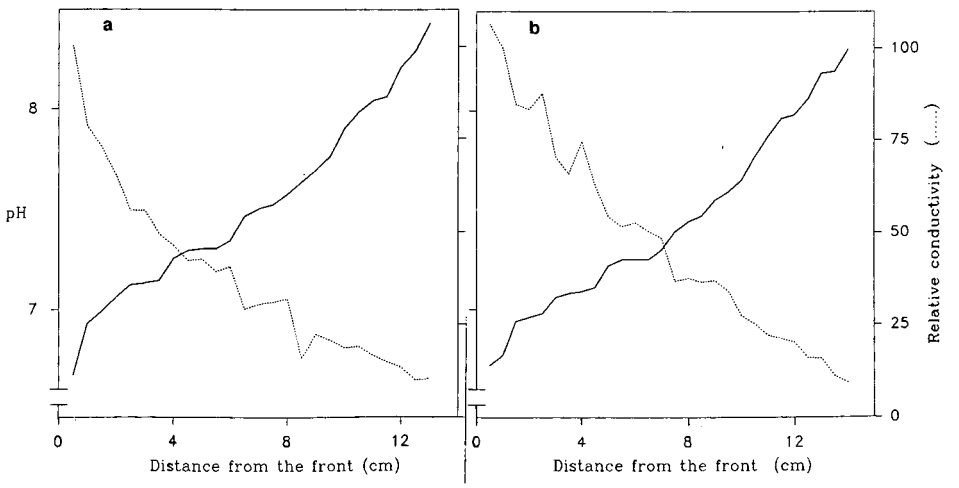

Fig. 2. pH and relative conductivity for gels identical with those illustrated in Fig. 1a and b, respectively, except that the size of the gels was 24 × 12 × 0.1 cm and ITP was run along the length.

ular weight among the spacers used. However, the conductivity gradient generated in ITP in the former instance was close to a straight line.

The short electrophoretic path required to obtain a pH gradient concomitant with a conductivity gradient is one of the major advantages of the present system. This is particularly useful for preparative purposes where the size of the equipment is usually a limiting factor. In a single lane (Fig. 1), as much as 10 μl of plasma per millilitre of gel were separated. In addition, isotachophoretic systems with narrower pH intervals, designed for the separation of specific proteins, or using a particular set of discrete spacers, may be calculated using the general principles described here.

CONCLUSIONS

The selection of appropriate mixtures of discrete spacers and counter ions determines the quality of the separation of proteins by gel ITP. The main requirements for the use of discrete spacers in isotachophoresis for the separation of proteins are a pH–charge relationship as linear as possible for the mixtures of spacers, the counter ions should provide a buffer capacity paralleling the charge of the mixture of spacers and the proportions between the spacers and the counter ions should be close to 2.

ACKNOWLEDGEMENTS

This work was supported by grants from the Swedish Medical Research Council (12-5665), the Karolinska Institute, the Swedish Medical Association, the Swedish Psoriasis Association and the Magnus Bergvall, Finsen and Edvard Wellander Foundations.

REFERENCES

1 F. Acevedo, *J. Chromatogr.*, 470 (1989) 407.
2 F. Acevedo, in C. Schafer-Nielsen (Editor), *Electrophoresis '88*, VCH, Weinheim, 1988, p. 112.
3 F. Acevedo and H. Hammar, *Br. J. Dermatol.*, 121 (1989) 329.
4 H. Towbin, T. Staehelin and J. Gordon, *Proc. Natl. Acad. Sci. U.S.A.*, 76 (1979) 4350.
5 A. T. Andrews, *Electrophoresis —Theory, Techniques, and Biochemical and Clinical Applications*, Oxford Science, Oxford, 1986, p. 67.
6 V. Jokl, *J. Chromatogr.*, 13 (1964) 451.
7 W. J. Fergusson and N. E. Good, *Anal. Biochem.*, 104 (1980) 300.

Journal of Chromatography, 545 (1991) 397–402
Elsevier Science Publishers B.V., Amsterdam

CHROM. 23 177

Effect of sodium dodecyl sulphate in protein samples on separation with free capillary zone electrophoresis

ERNST KENNDLER* and KARIN SCHMIDT-BEIWL
Institute for Analytical Chemistry, University of Vienna, Währingerstrasse 38, A-1090 Vienna (Austria)

ABSTRACT

The addition of sodium dodecyl sulphate (SDS) to samples of proteins (conalbumin and ovalbumin), but not to the carrier electrolyte (borate, 0.1 mol/l, pH 10) leads to a total loss in resolution of the analytes in free capillary zone electrophoresis, even at SDS concentrations of 0.1% (w/w). Simultaneously, a sharpening effect on the single peak obtained from the two proteins is observed, simulating favourable dispersion properties of the separation system (apparent plate number of 1 500 000). No such effects are found if SDS is added to the carrier electrolyte. It is demonstrated that the effects observed are not caused by binding of SDS onto the proteins but seem to be generated by conductivity gradients present in the system.

INTRODUCTION

Capillary zone electrophoresis (CZE), carried out either in open or in gel-filled capillaries, is a high-performance separation method with special interest for the separation of proteins and oligonucleotides. While gel-filled capillaries can be applied in a similar fashion to sodium dodecyl sulphate–polyacrylamide gel electrophoresis (SDS-PAGE) for the separation of proteins according to their molecular weight, in free zone electrophoresis the migration of the analytes depends on their effective mobilities.

In electrophoresis the matrix components as well as the analytes may determine the electrical properties of the sample zone, namely its conductivity. Ionic matrix components in high concentrations especially affect and even dominate these properties to such an extent that the electrophoretic behaviour of the analytes in the sample differs significantly from that derived from standard solutions.

SDS is often present as a matrix component in protein samples either to increase the protein solubility, or when the samples are isolated from gels after SDS-PAGE on microscale. Although in these cases SDS is often regarded as not interfering with subsequent electrophoretic separation using classical methods (zone electrophoresis or isoelectric focusing), no investigations have yet been carried out with respect to potential interferences in free CZE. Therefore, the influence of SDS present in protein samples on the zone electrophoretic patterns of the analytes was investigated.

0021-9673/91/$03.50

EXPERIMENTAL

Chemicals

Proteins applied were ovalbumin (recristallized five times; Serva, Heidelberg, Germany) and conalbumin (research grade; Serva). All other chemicals used were of reagent grade (E. Merck, Darmstadt, Germany). Water was redistilled twice from a quartz apparatus.

The carrier buffer was boric acid–sodium borate (0.1 mol/l), pH 10.

The concentration of the proteins (dissolved in the borate buffer) was 1 mg/ml.

The different SDS concentrations in the buffers and in the samples are given in weight percentages.

Apparatus

Zone electrophoresis was carried out with a P/ACE System 2000 instrument (Beckman, Palo Alto, CA, U.S.A.), equipped with a fused-silica capillary (50 cm distance to the detector, 75 μm I.D.). The field strength was 350 V/cm and the electric current was 120 μA. The time of the hydrodynamic injection was 1 s, carried out pneumatically. Two washing steps were programmed: in the first step, rinsing with sodium hydroxide (0.1 mol/l) was carried out for 3 min; in the second step, the capillary was flushed with working buffer for the same time.

A UV detector was used at 214 nm, positioned at the cathode side of the capillary.

Data were recorded and processed with a computerized system (System Gold, Beckman).

RESULTS AND DISCUSSION

In Fig. 1 the capillary zone electropherograms of conalbumin and ovalbumin, selected as analytes, are shown. In all cases the carrier buffer was borate in aqueous solution, which did not contain SDS. When the two proteins were dissolved in SDS-free buffer, the electropherogram indicated by 0% in Fig. 1 was obtained. It can be seen that the two proteins are well resolved and exhibit migration times of 5.5 and 6.8 min, respectively, under the given conditions (obtained by anionic separation and an electro-osmotic flow of the bulk liquid directed towards the cathode).

The ovalbumin peak is relatively broad. This is not caused by low efficiency of the separation system but by the (well known) inhomogeneity of the protein due to the various subunits ovalbumine consists of, which lead to several bands in PAGE also (see, *e.g.*, refs. 1–4).

The addition of SDS to the sample solution (but not to the carrier electrolyte) leads, however, to a significant change in the electropherogram: the two protein peaks are detected with a smaller difference in their migration times, even at an SDS concentration of only 0.05% (w/w). Further, both proteins are found in a single and extremely sharp peak at SDS concentrations in the sample of 0.1% and higher. It can be seen that this loss in resolution is caused by the fact that the selectivity of the separation (given by the relative difference of the migration times) is drastically decreased, although the apparent efficiency of the separation system (given by the peak widths) is enhanced. The apparent theoretical plate number of the peak with 0.5%

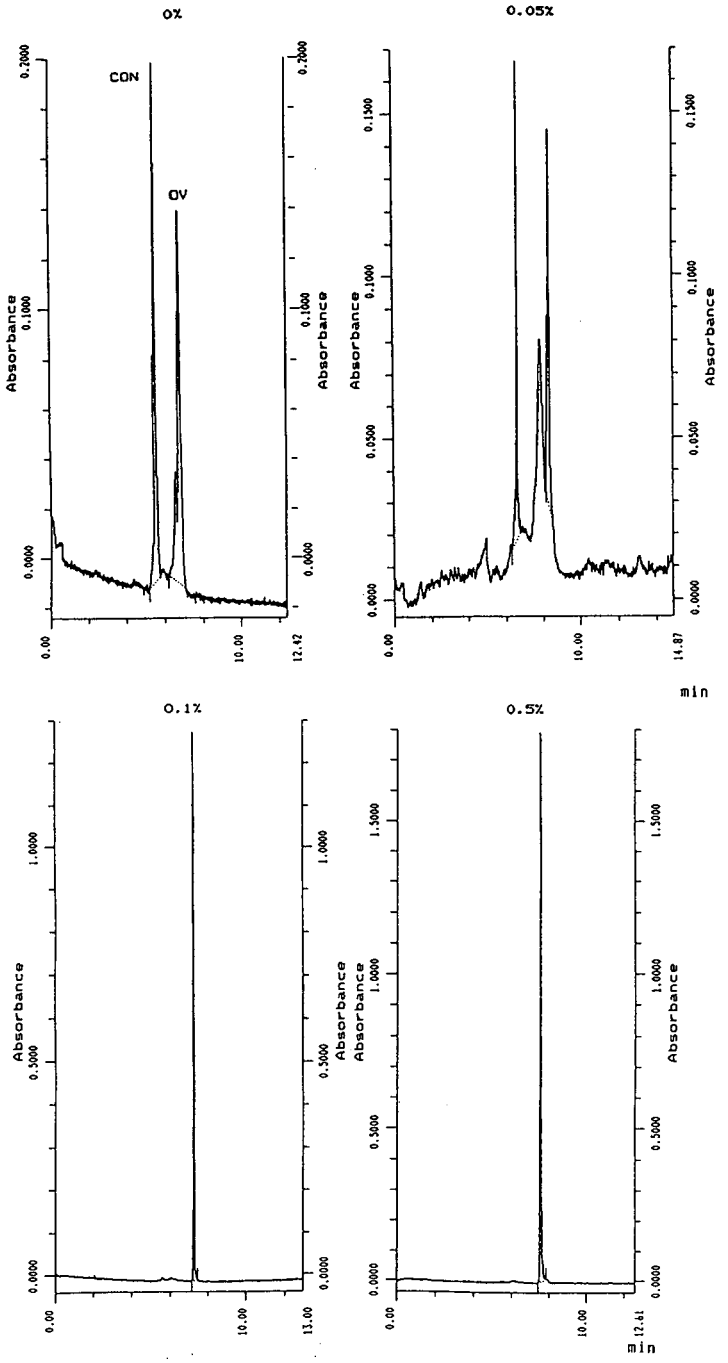

Fig. 1. Capillary zone electropherograms of conalbumin and ovalbumin at different concentrations of SDS added to the sample solution. Peaks: CON = conalbumin; OV = ovalbumin. The separations were carried out in aqueous borate buffer (0.1 mol/l) at pH 10 which did not contain SDS. The proteins were dissolved in buffer at a concentration of 1 mg/ml. The samples contained different concentrations of SDS (weight percents), indicated in the electropherograms by 0% (no SDS added), 0.05%, 0.1% and 0.5%. Instrumental conditions: fused-silica capillary (50 cm distance to the detector, 75 μm I.D.); field strength, 350 V/cm; electric current, 120 μA. Detection, UV at 214 nm.

SDS in the sample is about 1 500 000. The plate number, N, is calculated as for gradient-free chromatography or zone electrophoresis from the migration time t_M and the standard deviation σ_t of the peak (given in time units), by the expression $N = (t_M/\sigma_t)^2$.

The electropherogram shown in Fig. 1 obtained with a concentration of SDS of, *e.g.*, 0.5% in the sample would lead to a misinterpretation of the result: the sample seems to consist of a single, pure protein on the one hand, which is not the case; on the other hand, a very high plate number is indicated for the separation system.

This high (apparent) plate number and reduction in selectivity are not observed when the sample and the carrier electrolyte contain the same amount of SDS, as shown in Fig. 2. It can be seen that (besides an increase in the migration times) the pattern of the peaks is nearly identical to that obtained from an SDS-free system (Fig. 1, 0%). Both proteins are separated and the ovalbumin peak is also relatively broad. From this electropherogram it can be concluded that the decrease in selectivity when SDS is

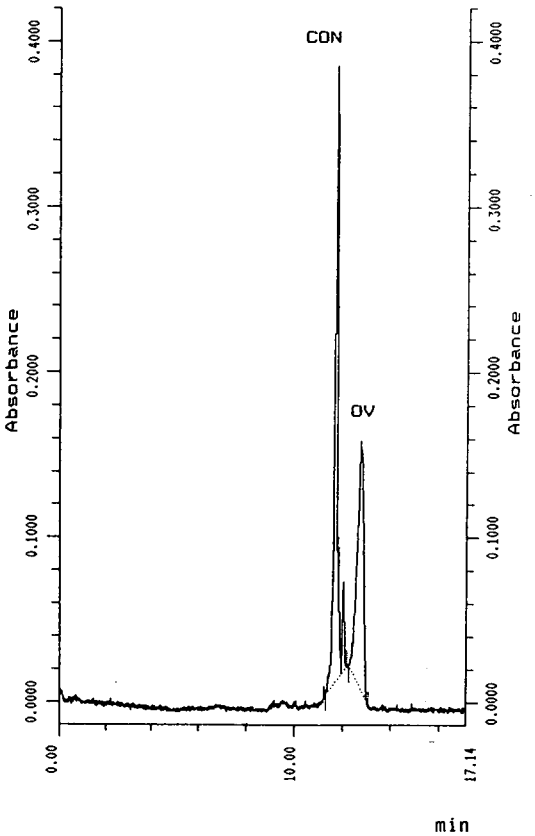

Fig. 2. Capillary zone electropherogram of conalbumin and ovalbumin obtained with a buffering carrier electrolyte containing the same SDS concentration as the sample. Peaks: CON = conalbumin; OV = ovalbumin. Both the sample and the carrier electrolyte had an SDS concentration of 0.5%. Buffer: borate (0.1 mol/l) pH 10. The analytes were dissolved in the buffer at a concentration of 1 mg/ml. Instrumental conditions were as in Fig. 1.

added to the sample is not caused by binding of SDS to the proteins, an effect which is used in SDS-PAGE and which is applied to eliminate mobility differences in order to separate proteins with respect to their molecular weight [5–8]. This binding is a reversible process and would therefore take place in a system totally filled with SDS rather than in one where SDS is present only in the sample and not in the carrier electrolyte.

It must be noted that the binding process in SDS-PAGE is supported by treating the protein–SDS mixture at elevated temperatures, as described in the literature [9]. In fact, this elimination of the mobility differences can also be observed in the electropherograms shown in Fig. 3, where SDS was added to the protein solutions and the mixture was kept at 100°C for 10 min prior to electrophoresis. It can be seen that even at an SDS concentration of 0.05% in the sample (a mass ratio of only 0.25 with respect to the proteins when it is known that SDS usually binds to most proteins with

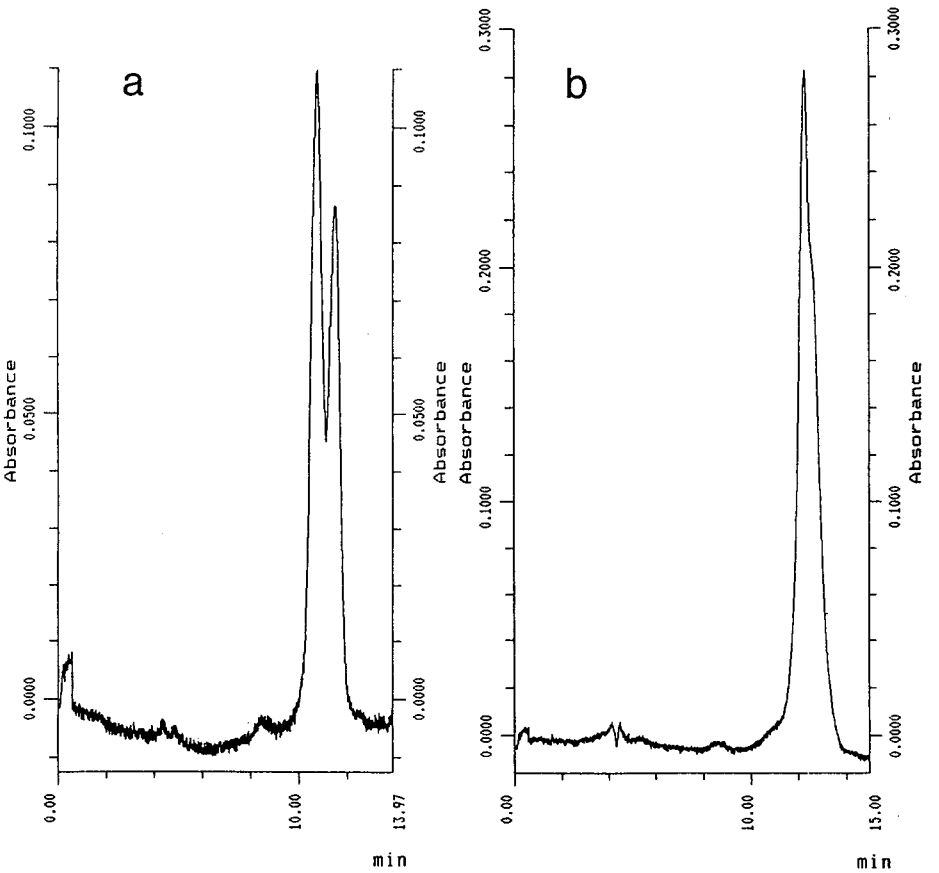

Fig. 3. Capillary zone electropherograms of conalbumin and ovalbumin in samples containing SDS, treated at elevated temperature prior to electrophoresis. The proteins were dissolved in borate buffer, and SDS was added at concentrations of 0.05% (a) and 0.5% (b), respectively. The mixtures were kept at 100°C for 10 min prior to injection. The separations were carried out at pH 10 with borate buffer (0.1 mol/l) containing SDS at the same concentration as the samples. Instrumental conditions were as in Fig. 1.

mass ratios between 0.9 and 1.4 [10]) the pattern of the electropherogram changes when compared with Fig. 2. Both peaks exhibit a similar migration time, which indicates that the mobility differences are increasingly eliminated due to the binding of SDS. This effect increases at an SDS concentration of 0.5% (2,5-fold with respect to the proteins), where both analytes are almost forming a single peak due to their virtually identical mobilities. This peak is much broader than that obtained under conditions where SDS was added in the same amount to the sample, but where no heat treatment was carried out, and where SDS was not added to the carrier electrolyte (Fig. 1, 0.5%).

From these results it can be concluded that the cause of the peak sharpening effect cannot lie in the binding processes between SDS and the proteins. It seems that the sharpening is originated by mobility gradients caused by SDS in the sample. In this case the additive acts in a similar fashion to the terminating ion in isotachophoresis, which is also termed displacement electrophoresis because of its analogy to displacement chromatography, where such sharpening effects are applied, *e.g.*, for the enrichment of trace analytes.

The assumption that the sharpening effect is caused by mobility gradients between the sample and the carrier electrolyte on the one hand, and between the analytes and SDS in the sample on the other hand, is supported also by the fact that peak sharpening is not observed when SDS gradients are not formed between sample and carrier electrolyte (Fig. 2).

As such effects, which depend on the mobilities of the analytes, of the additives (like SDS) and of the carrier electrolytes, are difficult to predict in real samples, electropherograms must be critically evaluated in practise to avoid misinterpretations. An unusual high plate number especially must be confirmed as it can be simulated by gradients present in the system.

ACKNOWLEDGEMENTS

The authors acknowledge a grant from E. Merck (Darmstadt, Germany), and appreciate the help of Beckman Instruments in providing an apparatus for capillary zone electrophoresis.

REFERENCES

1 F. Chang, W. D. Powrie and O. Fennema, *J. Food Sci.*, 35 (1970) 774.
2 R. D. Galyean and O. J. Cotterin, *J. Food Sci.*, 44 (1979) 1344.
3 K. Watanabe, T. Matsuda and R. Nakamura, *J. Food Sci.*, 50 (1985) 507.
4 S. A. Woodward and O. J. Cotterin, *J. Food Sci.*, 51 (1986) 333.
5 A. L. Shapiro, *Biochem. Biophys. Res. Commum.*, 28 (1967) 815.
6 K. Weber and M. Osborn, *J. Biol. Chem.*, 244 (1969) 4406.
7 D. M. Neville, *J. Biol. Chem.*, 246 (1971) 6328.
8 G. A. Banker and C. Cotman, *J. Biol. Chem.*, 247 (1972) 5856.
9 A. H. Gordon, *Electrophoresis of Proteins in Polyacrylamide and Starch Gels*, North-Holland/American Elsevier, Amsterdam, New York, 1975.
10 R. Pitt-Rivers and F. S. Impiombato, *Biochem. J.*, 109 (1968) 825.

Journal of Chromatography, 545 (1991) 403–406
Elsevier Science Publishers B.V., Amsterdam

CHROM. 23 174

Determination of p*I* by measuring the current in the mobilization step of high-performance capillary isoelectric focusing

Analysis of transferrin forms

FERENC KILÁR
Central Research Laboratory, University of Pécs, Medical School, Szigeti út 12, H-7643 Pécs (Hungary)

ABSTRACT

In high-performance isoelectric focusing in capillaries, the focusing pattern of a sample is obtained during the mobilization step. A current parameter can be assigned to each peak in this pattern. Keeping the experimental conditions unchanged, these current parameters characterize the positions of the respective substances in the pH gradient and therefore they can be used for the determination of the isoelectric points of the substances.

INTRODUCTION

In high-performance capillary isoelectric focusing, the focused pattern of the sample is detected in an electrophoretic (mobilization) step [1–3]. Mobilization of the pH gradient formed in the focusing step is achieved by applying an anion or a cation in the catholyte or anolyte, respectively, and then the focused substances and ampholytes pass the detection site in an electrophoretic process [2,3].

The flux of the mobilizing ions from the electrolytes into the capillary tube during the mobilization is governed by the relationships.

$$N'_{X^{n}+} = I' \cdot (u'_{X^{n}+}) \cdot (n'_{X^{n}+})/\kappa' \text{ (for the cations)}$$
$$N'_{X^{n}-} = I' \cdot (u'_{X^{n}-}) \cdot (n'_{X^{n}-})/\kappa' \text{ (for the anions)}$$

where κ' is the conductivity in the anolyte or catholyte used for the mobilization, n' is the number of ions (X^{n-} or X^{n+}) in the catholyte or anolyte, respectively, u' is the mobility of the ions and I' is the current in the tube (primed symbols refer to the mobilization step) [2]. The electrophoretic migration of the mobilizing ions into the tube results in an increase in the current.

0021-9673/91/$03.50

In this paper, experimental data are presented that show that measuring the current can be used for the evaluation of capillary isoelectric focusing experiments.

EXPERIMENTAL

Iron-free and iron-containing transferrin samples were used in high-performance isoelectric focusing experiments as has been described [3,4]. The current was recorded either with a two-channel recorder or manually. All experiments were repeated 2–5 times to control the reproducibility.

RESULTS AND DISCUSSION

Electropherograms of a typical capillary isoelectric focusing experiment and the change in the current are shown in Fig. 1, which demonstrates that the transferrin

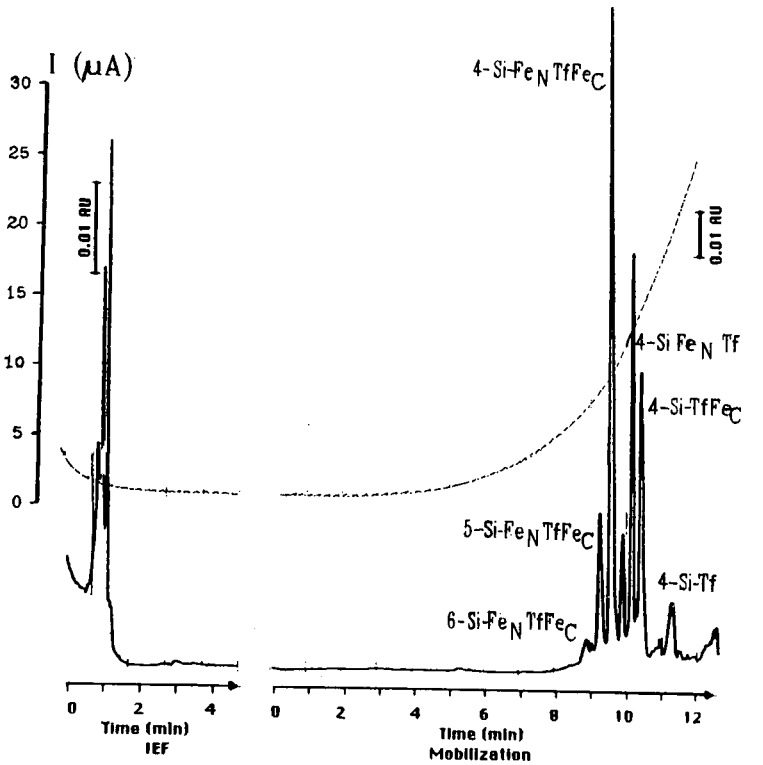

Fig. 1. High-performance capillary isoelectric focusing experiment of a transferrin sample. Si = sialo; Tf = transferrin; Fe_NTf and $TfFe_C$ = monoferric transferrin forms containing iron at the N- or C-terminal lobe, respectively; $Fe_N TfFe_C$ = diferric transferrin. The current (dotted line) decreases in the focusing step as a result of the immobilization of all the substances in the pH gradient. After a certain time the current reaches a 'plateau value', which shows the formation of the steady state in the capillary. On replacing the electrolyte at one end of the capillary the current increases, indicating the electrophoretic migration of the mobilizing ion into the tube. Experimental conditions: tube length, 185 mm; detection point, 155 mm; tube diameter, 0.1 mm; voltage, 5000 V; protein concentration, 1 mg/ml; ampholyte, 2% BioLyte 5/7; anolyte 20 m*M* H_3PO_4 (focusing)–20 m*M* NaOH (mobilization); catholyte, 20 m*M* NaOH; the protein was dissolved in distilled, deionized water.

TABLE I

CURRENT AND p*I* VALUES CHARACTERIZING TRANSFERRIN FORMS

Transferrin forms[a]	Current[b]	p*I*[c]
6-Si-Fe_NTfFe_C	8.7±0.2	5.25
5-Si-Fe_NTfFe_C	9.5±0.2	5.35
4-Si-Fe_NTfFe_C	10.5±0.2	5.45
4-Si-Fe_NTf	14.0±0.4	5.75
4-Si-TfFe_C	15.5±0.4	5.85
4-Si-Tf	21.0±0.5	6.10

[a] Si = sialo; Tf = transferrin; Fe_NTfFe_C = diferric transferrin; Fe_NTf and TfFe_C = monoferric transferrins containing iron at the N and C terminal binding site, respectively.

[b] The current values were obtained in experiments described in ref. 3. Experimental conditions: tube length, 185 mm; detection point, 155 mm; tube diameter, 0.1 mm; voltage, 5000 V; protein concentration, 1 mg/ml; ampholyte, 2% BioLyte 5/7; sample dissolved in distilled, deionized water; anolyte, 20 m*M* H_3PO_4 (focusing)–20 m*M* NaOH (mobilization); catholyte, 20 m*M* NaOH.

[c] Data extracted from Fig. 2 in ref. 5.

forms can be characterized with a current parameter. If the experimental conditions (*i.e.*, the length and diameter of the tube, the compositions of the sample and the electrolytes and the applied voltage) were kept constant the change in current was the same in separate runs. A summary of the measured current values and the p*I* values obtained from the literature [5] characterizing transferrin forms are given in Table I (note that the two monoferric transferrin forms are mixed up in Fig. 2 in ref. 5). Fig. 2 shows a p*I*–current curve obtained using the data in Table I.

Why is this curve important? The determination of the p*I* of focused substances is one of the purposes of performing isoelectrofocusing experiments. Generally, internal standards and their 'retention time' values (*i.e.*, the time parameter of the peaks in the electropherograms) are used to construct a calibration graph in the evaluation. Using the curve in Fig. 2, however, the p*I* values can be calculated without having internal standards in each run, *i.e.*, the current values characterizing peaks in the electropherograms can be used for the calculation of their p*I* values. According to the experimental errors in Table I, the p*I* values can be determined with an error of about 0.03 pH unit.

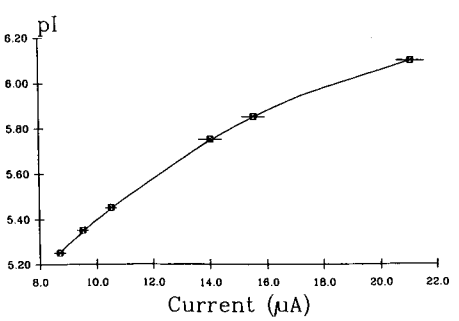

Fig. 2. Calibration graph for p*I* determination using the current as a parameter in high-performance isoelectric focusing experiments. Experimental conditions as in Fig. 1.

TABLE II

CALCULATED p*I* VALUES OF TRANSFERRIN FORMS

Isoform[a]	Molecular forms[a,b]			
	Tf	$TfFe_C$	Fe_NTf	Fe_NTfFe_C
2-Si	n.d.	6.01 ± 0.03	5.90 ± 0.03	5.75 ± 0.03
3-Si	n.d.	5.92 ± 0.03	5.85 ± 0.03	5.60 ± 0.03
4-Si	*6.10*	*5.85*	*5.75*	*5.45*
5-Si	6.03 ± 0.03	5.76 ± 0.03	5.60 ± 0.03	*5.35*
6-Si	5.92 ± 0.03	5.61 ± 0.03	5.46 ± 0.03	*5.25*

[a] Abbreviations as in Table I.

[b] The numbers in italics were obtained from ref. 5 and used for the calibration graph (Fig. 2). n.d. = Not determined.

Table II gives the isoelectric points of transferrin isoforms that overlap in the pH gradient and therefore cannot be analysed in one run. When experiments were repeated using different experimental conditions (longer, shorter or narrower capillaries, etc.), the p*I* values of these isoforms obtained were the same (but not the current parameters, of course).

Finally, an interesting observation is that the 'retention time' in the mobilization step is dependent on the duration of the focusing step (compare, *e.g.*, the positions of the iron-free 4-Si-transferrin component in the Figs. 1a, 1b and 5 in ref. 3). However this was not observed with the above-mentioned 'current' parameter. The explanation of this phenomenon is not known.

These experimental results may make it possible to perform theoretical calculations for capillary isoelectric focusing runs and thus to determine the isoelectric points of substances from measured current values without using any internal standards in the experiments.

REFERENCES

1 S. Hjertén and M.-D. Zhu, *J. Chromatogr.*, 346 (1985) 265.
2 S. Hjertén, J.-L. Liao and K. Yao, *J. Chromatogr.*, 387 (1987) 127.
3 F. Kilár and S. Hjertén, *Electrophoresis*, 10 (1989) 23.
4 F. Kilár and S. Hjertén, *J. Chromatogr.*, 480 (1989) 351.
5 G. de Jong and H. G. van Eijk, *Electrophoresis*, 9 (1988) 589.

Journal of Chromatography, 545 (1991) 407–412
Elsevier Science Publishers B.V., Amsterdam

CHROM. 23 171

Isotachophoretic determination of 2–5A phosphodiesterase

GERNOT BRUCHELT*
Children's Hospital, University of Tübingen, Rümelinstrasse 23, D-7400 Tübingen (Germany)
MANFRED BUEDENBENDER, KARL-HEINZ SCHMIDT and BETTINA JOPSKI
Department of Surgery, University of Tübingen, Tübingen (Germany)
and
JOERN TREUNER and DIETRICH NIETHAMMER
Children's Hospital, University of Tübingen, Rümelinstrasse 23, D-1400 Tübingen (Germany)

ABSTRACT

Together with 2–5A synthetase and ribonuclease L, 2–5A phosphodiesterase belongs to the 2–5A system, which plays an important role in the action of interferon. Analytical capillary isotachophoresis was used for the determination of 2–5A phosphodiesterease activity. Enzyme assay was optimized using snake venom phosphodiesterase as a source of 2–5A phosphodiesterase activity. The 2–5A trimer core was used as a substrate. Enzyme activity was determined in time- and concentration-dependent reactions. In addition, 2–5A phosphodiesterase activity was determined in lysates of mononuclear blood cells.

INTRODUCTION

The 2–5A system is one of the effector systems known to be involved in the action of interferons [1]. In the presence of double-stranded RNA, the interferon-induced enzyme 2–5A synthetase is activated and forms a number of 2–5 oligoadenylates from ATP (containing 2–14 adenosine residues). These oligoadenylates activate a ribonuclease (RNaseL), which splits viral or messenger RNA, thus preventing protein synthesis. A third enzyme, 2–5A phosphodiesterase (2–5A PDE), splits the 2–5 phosphodiester bonds of the oligoadenylates and returns RNaseL to its inactivated form. The formation of the dimeric form of 2–5 oligoadenylates in the 2–5A synthetase reaction and its degradation by 2–5A PDE is shown in Fig. 1 as an example. The physiological role of 2–5A PDE is to inhibit the diffusion of the 2–5 oligoadenylates from the place where they are formed. In this way, the action of activated RNaseL can be located near the partially double-stranded RNA, and, consequently, the single-stranded areas of this RNA (*e.g.* a viral RNA during the replication phase) are split preferentially [2].

Some assays for 2–5A PDE activity have been described in the literature, most of them using radiolabeled compounds [3–4]. Here, we present a novel and simple assay using analytical capillary isotachophoresis. The optimal assay conditions were

0021-9673/91/$03.50

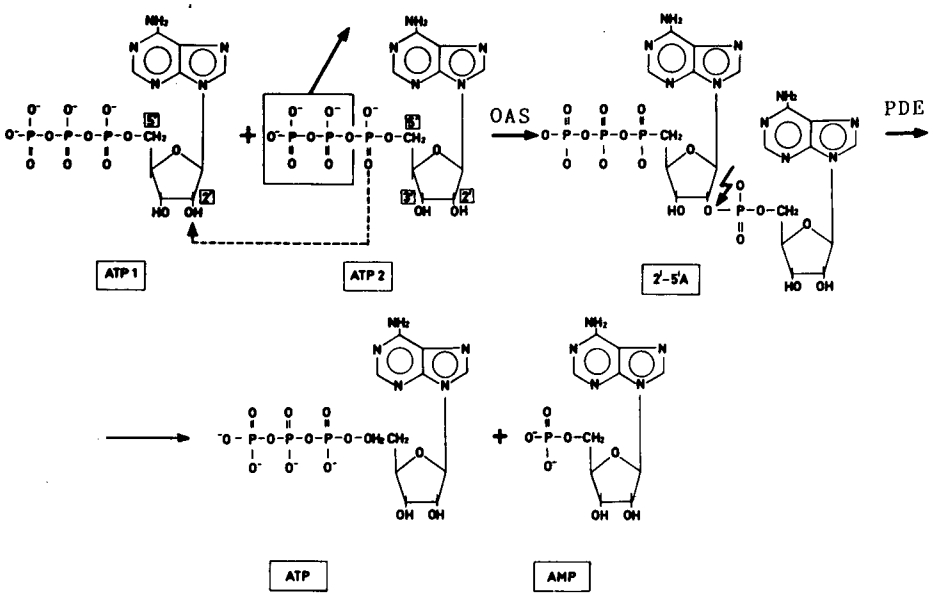

Fig. 1. Synthesis of 2–5 oligoadenylates (dimeric form) by 2–5A synthetase (2,5-oligoadenylate synthetase, OAS) and its degradation by 2–5A phosphodiesterase (PDE).

developed using the 2–5A trimer core (ApApA) as a substrate (the 2–5A cores have the same structure as the 2–5As, except they lack the initial triphosphate group in the 5′-position; 2–5A cores are not able to activate RNaseL but are degraded by 2–5A PDE to the same extent as the corresponding 2–5As [5].) The degradation of ApApA was followed using snake venom phosphodiesterase (SV-PDE), an enzyme known to have 2–5A PDE activity [6], and by lysates of mononuclear blood cells which contain 2–5A PDE activity.

EXPERIMENTAL

Isotachophoresis

The isotachophoretic analysis was performed on an LKB Tachophor 2127. Signals were registered by either UV absorbance at 254 nm or registration of the conductivity (*C*) signal. 0.01 *M* HCl–*β*-alanine plus 0.3% (w/v) methylcellulose 4000 (Fluka, Switzerland), pH 3.65, was used as leading electrolyte (LE) and 0.01 *M* caproic acid (Merck, Germany) as terminating electrolyte (TE). The current during signal detection was 75 μA. Analysis was carried out at 15°C in a 23 cm × 0.5 mm I.D. capillary. Chart speed during detection was 10 cm/min. Usually, 5-μl samples were injected onto the Tachophor.

2–5A Phosphodiesterase assay

A 10-μl volume of incubation buffer containing 2–5A trimer core [A2′p5′A2′p5′A (abbreviation ApApA), P. L. Biochemicals, U.S.A.] was incubated with 10 μl of 2–5A PDE-containing solution (lysates of mononuclear blood cells

(MNBCs) or SV–PDE (EC 3.1.4.1, Sigma, U.S.A.) in an eppendorf cup at 37°C. At the end of the incubation, the reaction mixture was heated for 2.5 min in a boiling water bath. The samples were centrifuged and the supernatants were frozen at −70°C until isotachophoresis was carried out.

Lysates of mononuclear blood cells

MNBCs were isolated using Lymphoprep (Nyegaard, Norway) from heparinized whole blood samples, washed twice and subsequently lysed using a buffer containing 0.5% Nonidet-P 40 (Sigma).

RESULTS

Isotachophoretic characterization of 2–5A cores

Fig. 2 shows the isotachophoretic pattern of the dimeric (ApA), trimeric (ApApA) and tetrameric (ApApApA) forms of 2–5A cores. Since the commercially available trimeric form is the cheapest, it was chosen as substrate for the 2–5A PDE reaction.

The calibration curve for ApApA, $y = 1.5 + 9.1x$ (x-axis: ApApA, 0–5 mmol/l; y-axis: zone length, 0–47.5 mm), showed strong linearity ($r^2 = 0.990$; S.D. = 2.733). No spontaneous degradation of ApApA occurred during a 2-h incubation period in the absence of 2–5A PDE activity (data not shown).

Degradation of ApApA in the presence of different amounts of SV-PDE

Fig. 3 shows the degradation of ApApA after 5 and 60 min incubation in the presence of different amounts of SV-PDE. Whereas 100% degradation occurred using 0.04 I.U./ml SV-PDE after 60 min, only a very small amount of ApApA was split using 0.0004 I.U./ml SV-PDE.

In order to follow the time course of ApApA degradation more exactly, the following experiments were carried out using 0.01 I.U./ml SV-PDE.

Time course of 2–5A core degradation using SV-PDE

In Fig. 4, the time course of the degradation of ApApA in the presence of 0.01 U/ml SV-PDE is presented. ApApA signals are indicated by arrows. Several reactions

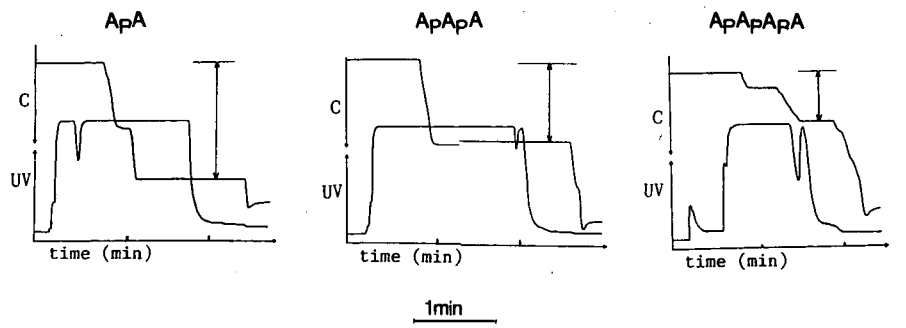

Fig. 2. Isotachopherograms of commercially available 2–5A cores, ApA (74%), ApApA (48%) and ApApApA (34%). Numbers in parenthesis are conductivity signals (C): LE–TE 100%.

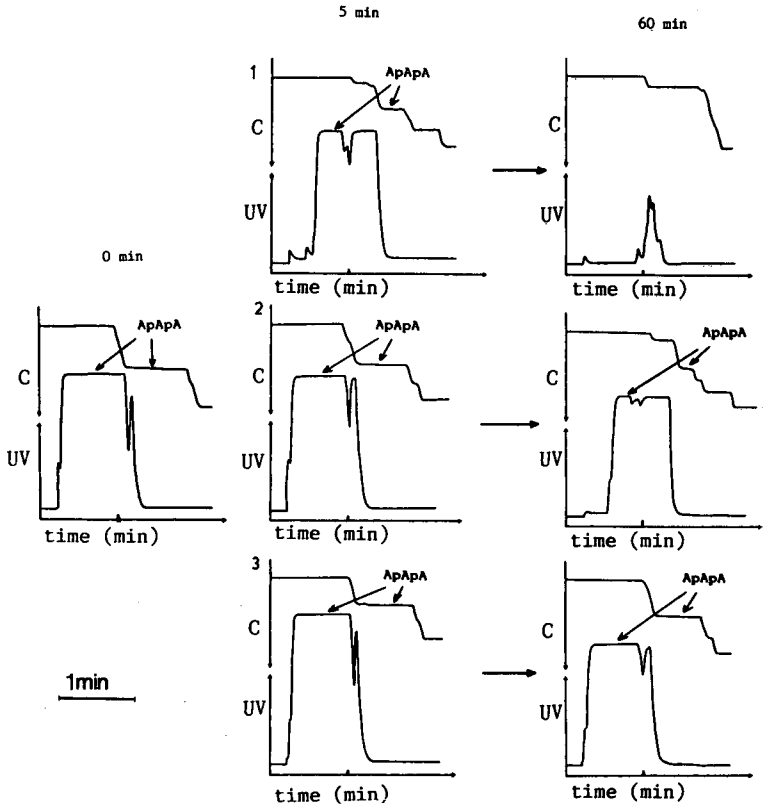

Fig. 3. Degradation of ApApA (3 mmol/l) after 5 and 60 min incubation at 37°C with 0.04 I.U/ml (1), 0.004 I.U./ml (2) and 0.0004 I.U./ml (3) SV-PDE.

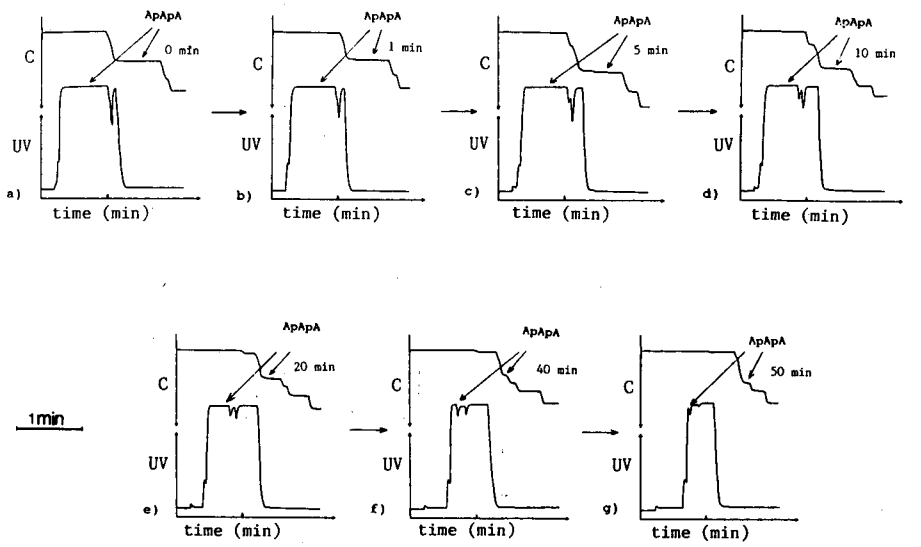

Fig. 4. Time course of ApApA degradation in the presence of 0.01 I.U./ml SV-PDE. Changes in ApApA signals during the incubation are indicated by arrows. Incubation mixture: 10 μl ApApA (3 mmol/l) plus 10 μl SV-PDE (0.01 I.U./ml).

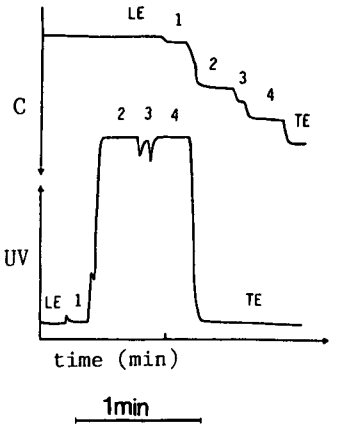

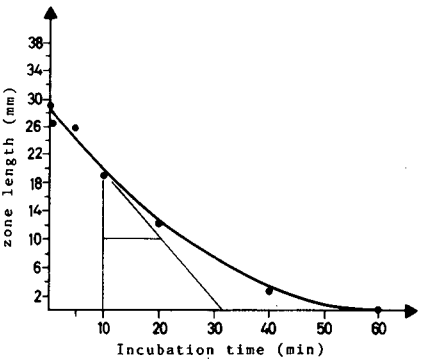

Fig. 5. Identification of products formed during the degradation of ApApA by SV-PDE by comparing the conductivity signals with pure substrates (1) Phosphate: 2–3% (pure substrate 0–5%); (2) ApApA; 54% (pure substrate: 51%); (3) AMP: 60% (pure substrate: 63%); (4) ApA: 76% (pure substrate: 74%).

Fig. 6. Time course of ApApA degradation: 10 μl ApApA (3 mmol/l) plus 10 μl SV-PDE (0.01 I.U./ml) were incubated for 60 min at 37°C.

occur in parallel during this process: SV-PDE activity splits ApApA into ApA and AMP; subsequently, ApA is split into AMP and adenosine, which cannot be detected in the isotachopherogram. In addition, SV-PDE activity leads to the degradation of AMP, forming inorganic phosphates, which are finally the only substances detectable in the isotachopherogram after complete ApApA degradation (see Fig. 3.1). In Fig. 5 the identification of the substances occurring during ApApA degradation is shown by comparing their conductivity signals with those of the corresponding pure substrates (data in parenthesis).

The time course of the degradation of 3 mmol/l ApApA (20 μl reaction volume) over a time period of 60 min using 0.01 U of SV-PDE is shown in Fig. 6. From these data a turnover rate of $0.98 \cdot 10^{-1}$ mmol/l ApApA per min at 37°C can be calculated.

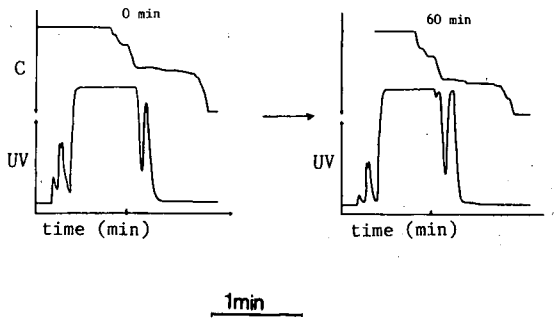

Fig. 7. Degradation of 10 μl ApApA (3 mmol/l) in the presence of 10-μl lysates of $5 \cdot 10^5$ MNBCs after 60 min incubation at 37°C.

2–5A PDE activity in MNBCs

Fig. 7 shows the degradation of ApApA by lysates of $5 \cdot 10^5$ MNBCs after 60 min incubation at 37°C. In the example given, 15.7% of ApApA was degraded. In order to examine the reproducibility of these determinations, two further runs were done with the same sample, yielding exactly the same results (15.7 ± 0% degradation; $n = 3$).

DISCUSSION

The present work shows that analytical capillary isotachophoresis is a very suitable method for the determination of 2–5A PDE activity. It is characterized by high accuracy, indicated by, for example, the high linear regression coefficient in the calibration curve, and by a precision great enough to allow the determination of enzyme activity after a 5–10% decrease of the ApApA concentration. The reliability of this method is remarkably high, as was demonstrated in Fig. 7. Although 2–5 oligoadenylates (ppppApA, pppApApA, pppApApApA, etc) are the natural substrates of this enzyme, ApApA is equally suitable as a substrate for the test. The only reason for its use is that it was the cheapest of all oligoadenylates commercially available.

In cellular systems, 2–5 oligoadenylates are rapidly degraded by 2–5 PDE activities [6], thus leading to reversibility and regional action of the interferon-induced 2–5A system. However, in some cases, *e.g.* in severe virus infection, it may be advantageous to prolong the activation of RNaseL. For this reason, some analogue of 2–5 oligoadenylates that mimic the interferon effects and which are degraded much more slowly by 2–5A PDE than the substrates naturally formed have been developed [7–9]. For testing the resistance of such 2–5 analogues to 2–5A PDE activity, the isotachophoretic 2–5A PDE assay may be a cheap and suitable alternative to radioactive methods.

REFERENCES

1 S. Pestka, J. A. Langer, K. C. Zoon and Ch. E. Samuel, *Ann. Rev. Biochem.*, 56 (1987) 727–777.
2 T. W. Nilsen and C. Baglioni, *Proc. Natl. Acad. Sci. U.S.A.*, 76 (1979) 2600–2604.
3 P. F. Torrence, J. Imai and M. I. Johnston, *Anal. Biochem.*, 129 (1983) 103–110.
4 A. Schmidt, A. Zilberstein, L. Shulman, P. Federman, H. Beressi and M. Revel, *FEBS Lett.*, 95 (1978) 257–264.
5 D. A. Eppstein, B. B. Schryver, Y. V. Marsh, M. A. Larsen and C. G. Kurahara, *J. Interferon Res.*, 3 (1983) 305–311.
6 A. Schmidt, Y. Chernajovsky, L. Shulman, P. Federman, H. Berissi and M. Revel, *Proc. Natl. Acad. Sci. U.S.A.*, 76 (1979) 4788–4792.
7 D. Alster, D. Brozda, Y. Kitade, A. Wong, R. Charubala, W. Pfleiderer and P. F. Torrence, *Biochem. Biophys. Res. Commun.*, 141 (1986) 555–561.
8 D. Eppstein, Y. V. Marsh, B. B. Schryver, M. A. Larsen, J. W. Barnett, J. P. H. Verheyden and E. J. Prisbe, *J. Biol. Chem.*, 257 (1982) 13390–13397.
9 Ch. Lee and R. J. Suhadolnik, *FEBS Lett.*, 157 (1983) 205–209.

Journal of Chromatography, 545 (1991) 413–419
Elsevier Science Publishers B.V., Amsterdam

CHROM. 23 153

Isotachophoresis of some synthetic colorants in foods

J. KAROVIČOVÁ, J. POLONSKÝ*, A. PRÍBELA and P. ŠIMKO
Faculty of Chemical Technology, Slovak Technical University, Radlinského 9, 812 37 Bratislava (Czechoslovakia)

ABSTRACT

An isotachophoresis study of fifteen food products coloured with synthetic colorants showed that this method is suitable for the determination of dyes in foodstuffs.

INTRODUCTION

Food additives are incorporated in food products to improve their sensory qualities [1,2]. The concentrations of these additives must be carefully controlled as they may have various harmful effects to human health. Studies on health-related aspects of the use of synthetic colorants have been reported [3–6]. At present, the following synthetic substances are approved in Czechoslovakia: tartrazine, Sunset Yellow FCF, cochineal red, Ponceau 6R, amaranth, erythrosine, indigotine, Patent Blue V and Brilliant Black BN [7]. All of these are acidic and water-soluble.

Acidic dyes can be isolated by amyl alcohol extraction followed by multiple aqueous extraction [8]; for solid samples ammoniacal methanol or ethanol solutions are used [9]. Other frequently used methods include adsorption on polyamides [8], kaolin, natural aluminosilicate, activated carbon [10] and Polyclar AT [11,12].

For thin-layer chromatography, various supports are used, *e.g.*, paper, starch, cellulose, alumina, magnesium oxide, silica gel, polyamides, ion-exchange resins, etc. Separations of synthetic dyes have been effected with various developing systems, from universal, *e.g.*, 2% sodium citrate in 5% ammonia, to specific, *e.g.* *n*-butanol–acetic acid–water (1:1:1) [13–15]. Dyes have been identified by spectral methods (UV and visible), from the characteristics of line spectra and by fluorescence. Methods have also been elaborated for the determination of binary dyestuff mixtures spectrophotometrically, using computer-aided numerical evaluation [16–18].

Some workers [19–21] have used high-performance liquid chromatography, including the use of diode-array detectors, to determine synthetic dyes. Barros *et al.* [22] used differential-pulse polarography.

The utilization of capillary isotachophoresis in the determination of food additives has been reported by Zuche and Gruending [23], who determined synthetic sweeteners, Klein and Stoya [24], acesulpham K, Kvasnička [25], aspartame, Kaiser

0021-9673/91/$03.50

and Hupf [26,27] and Nierle [28], conserving agents, and Hiroaka and Kunijiro [29,30], who attempted the separation of flavonoid pigments and anthocyanines.

EXPERIMENTAL

We used a CS ZKI 001 isotachophoretic analyser (Spišská Nová Ves, Czechoslovakia) with a conductivity detector and a TZ 4200 double-line recorder (Laboratorní přístroje, Prague, Czechoslovakia), and several electrolytic systems as shown in Table I. The samples were diluted with water according to their colour content and injected into the column using the four-way valve of the instrument. The duration of the analysis was 30–40 min, depending on the electrolytes used. The synthetic colorants were identified using standards. Samples of synthetic colorants were supplied by the producers. Their purity was not specially controlled and for quantitative evaluation we took the longest zone of a revelant colorant such as that of a pure colorant. Quantitative analysis was performed using the calibrating.

Certain food products (powdered puddings, syrups) could not be analysed by capillary isotachophoresis without prior separation of the synthetic colorants from them, using either extraction [methanol–ammonia solution (95:5)] from powdered samples (this method is not quantitative and standard additions must be used in the analysis), extraction into *n*-amyl alcohol (liquid samples) or adsorption on powdered or granulated polyamides (using 50 ml of sample with 2.5 ml of acetic acid and 25 g of granulated polyamides, the mixture being shaken for 20 min until loss of colour; subsequently, the adsorbed granulate was extracted three times with methanol ammonia solution, the extracts were combined, concentrated on a water-bath and adjusted to 10 ml before measurement).

RESULTS AND DISCUSSION

First, model solutions using standards prepared from synthetic colorants

TABLE I

COMPOSITIONS OF ELECTROLYTE SYSTEMS (ES) AND CONDITIONS OF SEPARATION

Parameter[a]	ES I	ES II	ES III	ES IV
Concentration of leading electrolyte (hydrochloric acid) (*M*)	10^{-2}	10^{-2}	10^{-2}	10^{-2}
Counter ion	β-Alanine	ε-ACA[b]	Histidine	Histidine
pH	3.5	4.5	6.0	6.0
Additive MHEC[c] (%)	0.1	0.1	0.1	0.1
Terminating electrolyte	Acetic acid	Caproic acid	Caproic acid	MES[d]
Concentration (*M*)	5.10^{-3}	5.10^{-3}	5.10^{-3}	5.10^{-3}, histidine 5.10^{-3}, pH 5–6

[a] Other conditions: driving current, 300 μA in the preseparation column, 50 μA in the analytical column.
[b] ε-Aminocaproic acid.
[c] Methylhydroxyethylcellulose.
[d] Morpholinoethanesulphonic acid.

TABLE II

CHARACTERISTIC CONSTANTS (r.s.h.) OF THE INDIVIDUAL STANDARDS OF SYNTHETIC COLORANTS IN ELECTROLYTIC SYSTEMS (ES) I–IV

Synthetic colorant	R.s.h.[a]			
	ES I	ES II	ES III	ES IV
Tartrazine	0.184	0.270	0.572	0.285
Sunset Yellow FCF	0.200	0.285	0.560	0.290
Cochineal red	0.196	0.272	0.565	0.283
Amaranth	0.191	0.266	0.554	0.262
Azorubine	0.268	0.309	0.756	0.423
Patent blue	0.320	0.434	0.825	0.464
Brilliant black	0.190	0.269	0.585	0.273
Indigotine	0.202	0.276	0.562	0.284

[a] R.s.h. = relative step height = $(h_i - h_L)/(h_T - h_L)$, where h_i = the line of the ith ion; h_L = the line of the leading electrolyte and h_T = the line of the terminating electrolyte.

(concentration 100 mg dm^{-3}) were used. This guarantees that the separation capacity of the column is not exceeded. Measurements were carried out in the preseparation column; this concentration precluded the possibility of the formation of a non-stationary zone [31]. Visual observation of the column was found to provide a suitable orientation for the evaluation of the separation of individual standards, assisting in the determination of the order of the dyes identified. By comparing the characteristic constants (r.s.h.) of the individual standards of synthetic colorants in the electrolyte systems I–IV as shown in Table II, it was found that only Patent blue and azorubine had sufficiently different r.s.h. values. For this reason, we investigated the possibility of the separation of the individual dyes into groups with two or three members in a mixture, aiming at a model mixture with the maximum number of dyes that could be separated in the individual electrolyte systems used. In combination with Indigotine we found that individual dyes were separated into independent zones but the detector failed to identity this owing to the minimal mobility differences between the individual component dyes. Also for this reason a selective visible spectrophotometric detector would be more suitable when analysing synthetic dyes. Our measurements demonstrated in electrolyte system I that up to four variously combined dyes could be separated as shown in Table III. This was better than the results obtained with

TABLE III

SEPARATED COMBINATIONS OF FOUR SYNTHETIC COLORANTS IN ELECTROLYTE SYSTEM I

No.	Synthetic colorants
1	Azorubine–Patent blue–Sunset Yellow FCF–tartrazine
2	Azorubine–Patent blue–Sunset Yellow FCF–cochineal red
3	Azorubine–Patent blue–Sunset Yellow FCF–brilliant black
4	Azorubine–Patent blue–Sunset Yellow FCF–amaranth
5	Azorubine blue–amaranth–indigotine
6	Indigotine–Patent blue–azorubine–brilliant black

electrolyte systems II–IV. In Table III, colorants are given according to the system and not according to their mobility.

The simplest and fastest method for the isolation of synthetic colorants from product mixtures is direct extraction using methanol–ammonic solution (95:5). This is only usable with solid samples as both methanol and ammonia mix well with water. The extracts thus obtained can be used directly for paper chromatography and capillary isotachophoresis. This method was used with powdered pudding samples.

When analysing liquid samples, water-immiscible extraction agents must be used, or the dyes can be adsorbed on a suitable adsorbent with reverse elution back into solution. In direct sampling of a liquid sample into the instrument, a record was needed from the analytical column; with sufficiently preconcentrated extracts, however, records from the isotachophoretic preseparation column were often adequate, resulting in a faster (15–20 min).

Extracts obtained by amyl alcohol extraction were suitable for paper chromatography but their further use for isotachophoretic analysis presented problems. In addition, in 10% hydrochloric acid one cannot analyse anything by isotachophoresis.

TABLE IV

RESULTS OF SAMPLE ANALYSES

No.	Sample	Composition of colour mix	Quantitative composition (mg kg^{-1})
1	Extra Tang (powdered beverage)	Tartrazine,	405 ± 36
		Sunset Yellow FCF	129 ± 17
2	Vita orange (powdered beverage)	Tartrazine	382 ± 22
3	Vita blackcurrant (powdered beverage)	Tartrazine	148 ± 19
4	Powdered pudding, "Golden ear" brand	Sunset Yellow FCF	64 ± 18
5	Powdered pudding, Orange flavour	Sunset Yellow FCF	197 ± 24
6	Raspberry drops (hard candy)	Azorubine	334 ± 43
7	Powdered pudding	Amaranth	79 ± 19
8	Powdered pudding, strawberry flavour	Amaranth, cochineal red	*ca.* 420 ± 16
9	Powdered pudding, raspberry flavour	Amaranth	269 ± 38
10	Powdered pudding, lemon flavour	Tartrazine	268 ± 25
11	Vita strawberry (powdered beverage)	Amaranth, cochineal red	*ca.* 350 ± 20
		Azorubine	195 ± 36
12	Amyl-vanilla (powdered pudding)	Tartrazine,	202 ± 32
		Sunset Yellow FCF	52 ± 13
13	Egg-shaped hard candy	Tartrazine	279 ± 43
14	Vita raspberry (powdered beverage)	Azorubine	583 ± 42
15	Orange lemonade	Sunset Yellow FCF	50 ± 8 (mg dm^{-3})

The method using adsorption on degreased wool fibre is time consuming; in addition, it was found experimentally that it also lacked quantitativeness.

Substantially better results were obtained when using granulated polyamide adsorption, with subsequent extraction into methanol–ammonia solution. The amount of dye adsorbed could be increased considerably by increasing the amount of adsorbing material.

Isolation of synthetic dyes from polyamide granues was carried out by extraction using 2% aqueous ammonia; ethanol–ammonia solution, (95:5), methanol–ammonia solution (95:5) or ethanol–ammonia solution (90:10), using various amounts and temperatures. None of the extraction mixtures offered complete isolation of the dye from the adsorbent. We decided to use methanol–ammonia solution (95:5) and determined the amount of dye remaining adsorbed, under standard conditions, per unit weight of the adsorbent. This amount was determined by isotachophoresis, based on the difference in the amount of dye before adsorption and after its reverse elution from the adsorbent. Laboratory temperatures were used throughout, with increasing amounts of the adsorbent. The amount of colorant not extracted from the polyamide granules was from 7.3 to 13.6%, depending on the colorant (tartrazine 7.3%, amaranth 13.6%).

The method described is suitable for model solutions of synthetic colorants as well as products samples containing only such colorants.

The results showed that electrolyte system I is suitable for analyses of food

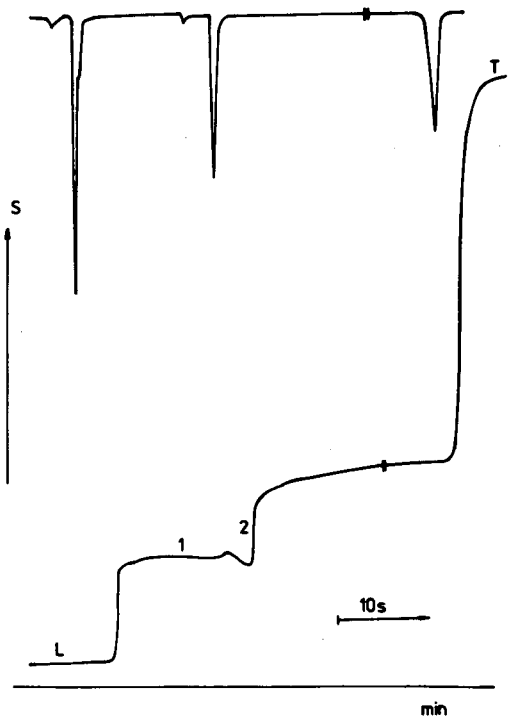

Fig. 1. Isotachopherogram of synthetic colorants in sample Extra Tang in electrolyte system I. S = Response of conductivity detector. 1 = Tartrazine; 2 = Sunset Yellow FCF; L = leading electrolyte; T = terminating electrolyte.

products for the determination of synthetic colorant contents, for which the qualitative composition of the samples is known in advance from paper chromatographic recordings [using *n*-butanol–acetone–water (1:1:1) as developing solvent]. The results were obtained by evaluating the isotachopherograms from the analytical column and by adjustment of the individual analytical times. Table IV shows some of the samples and mean values, obtained in those measurements, with the confidence interval of the mean shown at the 5% significance level ($\bar{x} \pm K_n R$), where $R = x_{max} - x_{min}$ and $K_n = 1.3$ [32]. Fig. 1 shows the record from the analysis of the sample Extra Tang.

Most of the samples analysed must be diluted with water at least 1:10 so that the amount of dye in the sample does not exceed the permitted limiting value of 100 mg kg^{-1}, with the exception of samples 6 and 13. Samples 8 and 11 also contained amaranth and cochineal red, but these have formed a mixed zone. However, as the difference in the b constants in the linear equations for amaranth is small [amaranth, $a = 0.237$; $b = 0.779$; $r = 0.9984$; cochineal red, $a = -0.589$; $b = 0.688$; $r = 0.9992$; a = section on y-axis (mm); b = gradient in mm/(mg dm^{-3})], a rough estimate of the dye contents in the mixture zone can be obtained by using the mean value, $b = 0.734$.

In conclusion, capillary isotachophoresis can be used in the determination of synthetic colorants in some food products. It is known that not all permitted colorants are simultaneously used for colouring products, but a maximum of six colorants are used in combination. The analysis of the products has shown that the artificial colourings used were mainly sunset yellow, tartrazine, azorubine, amaranth and cochineal red.

REFERENCES

1 J. Davídek, G. Janíček and J. Pokorný, *Chemie Potravin*, SNTL/Alfa, Prague, 1983, p. 629.
2 L. Rosíval and A. Szokolay, *Cudzorodé Látky v Poživatinách*, Osveta, Martin, 1983, p. 611.
3 Y. Riazuddin, A. R. Shakoori and Z. Nawaz, *Pak. J. Zool.*, 18 (1986) 317.
4 B. Bertram, *Dtsch. Apoth.-Ztg.*, 127 (1987) 499.
5 C. Melino and A. Pasquarella, *Clin. Ter.*, 117 (1986) 261.
6 R. Combes, *Arch. Toxicol.*, 59 (1986) 67.
7 A. Szokolay, *Posudzovanie Cudzorodých Látok v Poživatinách z Hl'adiska Racionálnej Výživy*, Slov. Spoločnosť pre Racionálnu Výživu, Bratislava, 1981, p. 210.
8 A. Príbela, *Analýza Cudzorodých Látok v Poživatinách*, Alfa, Bratislava, 1974, p. 290.
9 M. Y. Takahashi, H. Y. Yabiku and D. A. Marsiglia, *Rev. Inst. Adolfo Lutz*, 48 (1988) 7.
10 H. K. Park, *Han'guk Noghva Hakhoechi*, 30 (1987) 201.
11 J. Hernandez Mendez, B. Moreno Cordero and J. Peter Pavon, *J. Aliment.*, 22 (1985) 43.
12 J. Hernandez Mendez and B. Moreno Cordero, *J. Aliment.*, 22 (1985) 77.
13 K. Spears and J. Marshall, *J. Assoc. Publ. Anal.*, 25 (1987) 47.
14 Z. Yang and H. Gao, *Shipin Yu Fajido Gongye*, (1985) 9.
15 J. Maslonka, *Chromatographia*, 20 (1985) 99.
16 Y. Chen and Z. Zhuo, *Fenxi Huaxue*, 16 (1988) 9.
17 H. Sosaki and M. Tanaka, *Kaiho-Kagaku PC Kenkyukai*, 7 (1985) 92.
18 H. Sosaki, *Kaiho-Kagaku PV Kenkyukai*, 7 (1985) 141.
19 S. L. Reynolds, M. J. Scotter and R. Wood, *J. Assoc. Publ. Anal.*, 26 (1988) 7.
20 K. Korany and K. Gasztonyi, *Elemiszervizsgalati Kozl.*, 33 (1987) 108.
21 S. Ye, H. Han and Y. Chem, *Shipin Kexue*, 67 (1985) 48.
22 A. A. Barros, J. A. Rodrigues and J. Magalhaes, *Port. Electrochim. Acta*, 5 (1987) 317.
23 U. Zuche and H. Gruending, *Z. Lebensm.-Unters.-Forsch.*, 184 (1987) 503.
24 H. Klein and W. Stoya, *Ernährung*, 11 (1987) 322.
25 F. Kvasnička, *J. Chromatogr.*, 390 (1987) 237.
26 K. P. Kaiser and H. Hupf, *Dtsch. Lebensm. Rundschau*, 75 (1979) 300.
27 K. P. Kaiser and H. Hupf, *Dtsch. Lebensm.-Rundsch.*, 75 (1979) 346.

28 W. Nierle, *Getreide Mehl Brot*, 42 (1988) 138.
29 A. Hiroaka, Y. Kunijiro and H. Takashi, *Chem. Pharm. Bull.*, 35 (1987) 4317.
30 A. Hiroaka and Y. Kunijiro, *Chem. Pharm. Bull.*, 34 (1986) 2257.
31 P. Boček, M. Deml, P. Gebauer and V. Dolník, *Analytická Kapilárni Izotachoforéza*, Ústav Analytické Chemie ČSAV, Brno, 1986, p. 169.
32 K. Eckschlager, I. Horsák and Z. Kodejš, *SNTL*, Prague, 1980, p. 224.

Journal of Chromatography, 545 (1991) 421–425
Elsevier Science Publishers B.V., Amsterdam

CHROM. 23 162

Determination of disodium 3-amino-1-hydroxypropylidene-1,1-bisphosphonate pentahydrate

M. ZELLER*, R. KESSLER, H. J. MANZ and G. SZÉKELY
Ciba-Geigy Ltd., Central Analytical Department, 4002 Basle (Switzerland)

ABSTRACT

Capillary isotachophoresis was applied to the analysis of a new class of bisphosphonates. By using a commercial isotachophoretic system (Shimadzu IP-3A) with a fused-silica detection capillary in comparison with an LKB Tachophor equipped with a PTFE capillary a six-fold higher sensitivity is obtained. In addition, the time of analysis can be shortened. The developed system is applicable to the analysis of disodium 3-amino-1-hydroxypropylidene-1,1-bisphosphonate pentahydrate (Aredia), the main component of the drug formulation (dry substance for injection). Phosphite and phosphate, which are considered to be its trace level by-products, were determined simultaneously. The relative standard deviation for each compound was about 1%.

INTRODUCTION

Most applications dealing with the analysis of bisphosphonates or polyphosphonates [1–8] have been done by high-performance liquid chromatography [1], especially by ion chromatography [2–4], ion-pair chromatography and ion-exchange chromatography [5–7], and only a few by isotachophoresis (ITP) [8]. Capillary ITP is an electrophoretic method suitable for the separation of ionogenic organic and inorganic compounds which are soluble in water or water–organic and inorganic compounds which are soluble in water or water–organic solvent mixtures. For daily routine analysis of disodium 3-amino-1-hydroxypropylidene-1,1-bisphosphonate pentahydrate, $H_2NCH_2CH_2C(OH)(PO_3HNa)_2 \cdot 5H_2O$ (Aredia) (quality control and stability test), we use ITP.

Aredia is a new drug for the treatment of cancer. It has been shown that is is very effective in the treatment of tumour-induced hypercalcaemia because it inhibits

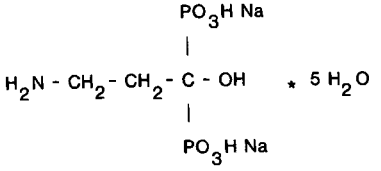

0021-9673/91/$03.50

bone resorption. In many cancer patients high blood levels of calcium occur owing to the effects of bone metastasis [9].

Hypercalcaemia can lead to disfunction of the gastrointestinal tract, of the kidneys and of the nervous system. In severe cases hypercalcaemia can even be fatal. The bisphosphonates are sympathetic chemical analogues of pyrophosphate, a natural inhibitor of crystal nucleation and bone mineralization.

Investigations have suggested that in some instances treatment with this bisphosphonate inhibits cancerous changes in the bone (metastases or secondary tumours). The drug is administered with slow intravenous infusions (between 1 and 4 h). To lower calcium levels in blood for several weeks, a single infusion is sufficient. However, the success of the therapy depends on the severity of the individual case [9,10].

Further clinical studies are necessary to determine the efficiency of Aredia in the treatment of bone metastasis without accompanying hypercalcaemia. Another very common site of metastasis is the skeleton. The disease spreads into the bone in about 60% of patients with cancer of the breast, prostate and lungs. There it causes progressive weakening and finally leads to the destruction of the bone tissue.

Therefore, it is necessary to have a highly reproducible, sensitive, accurate and simple method for the analysis of dosage forms for Aredia and potential by-products thereof.

EXPERIMENTAL

Chemicals and reagents

β-Alanine was purchased from Fluka (Buchs, Switzerland), hydroxypropylmethylcellulose (HPMC), used in the leading electrolyte system, from Prochem (Zürich, Switzerland) and Triton X-100 from Sigma (Heidelberg, Germany). All chemicals were of analytical-reagent grade and were used as received. Water was distilled twice in a quartz apparatus.

Instrumentation

Analytical capillary ITP was performed on two different instruments: an LKB 2127 Tachophor (Pharmacia, Bromma, Sweden) equipped with UV (254 nm) and conductivity detectors, using a PTFE capillary (43 cm × 0.5 mm I.D.), and an IP-3A semi-automatic ITP system from Shimadzu (Tokyo, Japan), using a PTFE separation capillary (16 cm × 0.7 mm I.D.) and a fused-silica detection capillary (17 cm × 0.2 mm I.D.).

Conditions

LKB Tachophor. The driving current was maintained for 16 min at 150 μA (starting voltage 3 kV) and then reduced to 50 μA for reasons of detection (end voltage 5 kV). The signals were recorded on an ITP-5A two-channel integrator (Shimadzu).

Shimadzu IP3-A. The current gradient applied was (1) 300 μA until 5.5 kV was reached, (2) 200 μA until 2261 μA min was reached, (3) 40 μA for about 4 min and (4) 15 μA for detection. The signals were recorded on an ITP-5A two-channel integrator (Shimadzu).

Electrolyte systems

LKB Tachophor. The leading electolyte was 25 ml of 0.1 *M* hydrochloric acid and 445.51 mg of β-alanine dissolved in 250 ml of 0.2% (w/v) nitrogen-saturated HPMC solution (pH 3.6) and the terminating electrolyte was 10 ml of 0.1 *M* sodium hydroxide and 20 ml of 0.1 *M* acetic acid diluted in water to 200 ml with 125 μl of Triton X-100 being added (pH 4.7).

Shimadzu IP3-A. The leading electrolyte was 50 ml of 0.1 *M* hydrochloric acid and 891.2 mg of β-alanine diluted in water to 500 ml with 500 μl of Triton X-100 being added (pH 3.6) and the terminating electrolyte was the same as for the LKB Tachophor.

Standard solution

Approximately 100.0 mg of Aredia working standard were accurately transferred into a 50-ml volumetric flask, 5 ml of phosphite solution (1 mg/ml HPO_3^{2-}) and 10 ml of phosphate solution (1 mg/ml PO_4^{3-}) were added and the mixture was diluted to volume with distilled water. A 6-μl volume of this solution containing *ca.* 9.1 μg of bisphosphonate, 0.6 μg of phosphite and 1.2 μg of phosphate was applied.

Sample solution

The contents of five vials of the drug formulation were dissolved in water and further water was added to give 100 ml.

RESULTS AND DISCUSSION

As shown in Fig. 1, we applied equal amounts to the two different detection

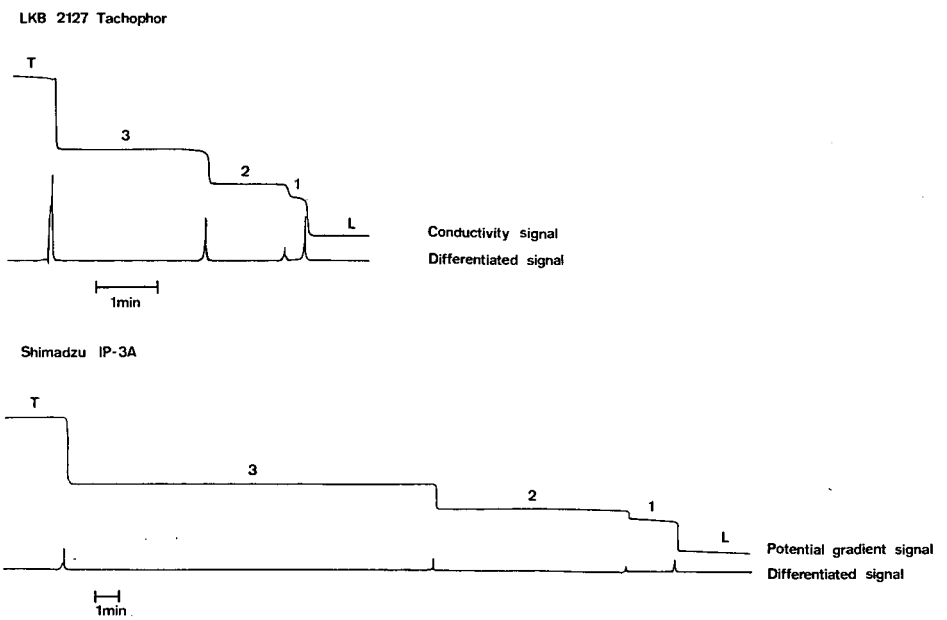

Fig. 1. Comparison of the LKB and Shimadzu systems. Equal amounts of standard solution (10 μl) were injected. (1) = 2 μg of phosphite; (2) = 0.5 μg of phosphate; (3) = 13 μg of bisphosphonate. L = leading ion (chloride); T = terminating ion (acetate).

TABLE I

ACCURACY OF THE ASSAY

Weight taken (mg)	Weight found from zone length (mg)	Recovery (%)
105.96	110.66	104.44
103.79	106.81	102.91
104.03	107.71	103.53
108.20	111.05	102.63
111.30	112.72	101.27
118.14	118.88	100.63
Mean		102.57
95% confidence limits		101.09–104.05

TABLE II

PRECISION (REPEATABILITY) OF THE ASSAY

Weight taken (mg)	Zone length relative to 30.0 mg (mm)
105.96	22.6
103.79	22.2
104.03	22.3
108.20	22.2
111.30	21.9
118.14	21.9
110.87	21.8
102.67	21.9
107.66	22.3
104.70	22.3
Mean	22.1
Standard deviation	0.25
Relative standard deviation	1.15%

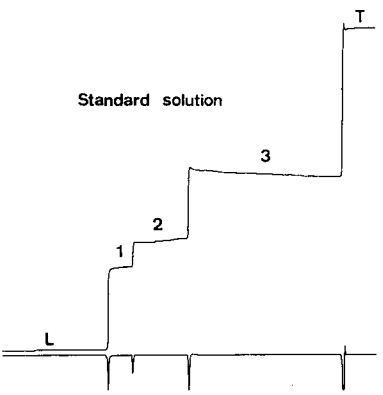

Fig. 2. Standard solution containing (1) 0.6 μg of phosphite, (2) 1.2 μg of phosphate, (3) 9.1 μg of bisphosphonate. L = leading ion (chloride); T = terminating ion (acetate); 6 μl of standard solution were injected; apparatus, LKB 2127 Tachophor with conductivity detector.

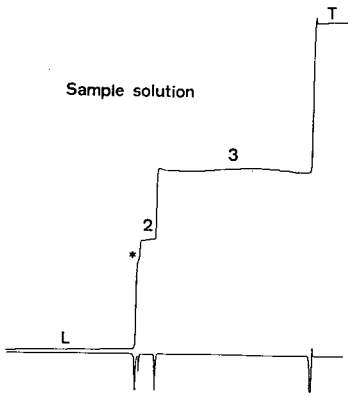

Fig. 3. Sample solution containing 150 mg of bisphosphonate per 100 ml. (* = Impurity from the electrolyte system; 2 = phosphate; 3 = bisphosphonate. L = leading ion (chloride); T = termination ion (acetate); 6 μl of sample solution were injected; apparatus, LKB 2127 Tachophor with conductivity detector.

capillaries. The increase in the zone length was derived from the ratio of the inside diameters of the two capillaries. With the fused-silica detection capillary, the zone lengths were six times longer. Obviously, the same volume needs a much longer capillary distance during detection because of the reduced diameter. Further, there is an increase in accuracy. ITP can be applied easily to this problem and it has the advantage of excellent accuracy and precision (see Tables I and II); further, UV-invisible components could be detected at trace levels.

By using the electrolyte systems mentioned above, routine analysis can be done in 35 min with good selectivity (Figs. 2 and 3). The total analysis time was *ca.* 10 min shorter by using the Shimadzu system than with the LKB system. One of the reasons is the semi-automatic rinsing and filling with the electroytes.

ACKNOWLEDGEMENTS

The authors are grateful to Mr. U. Emmenegger, Mr. R. Graff and Mr. F. Urrea for helpful cooperation.

REFERENCES

1 G. Flesch and S. A. Hauffe, *J. Chromatogr.*, 489 (1989) 446–451.
2 P. T. Daley-Yates, L. A. Gifford and C. R. Hoggarth, *J. Chromatogr.*, 420 (1989) 329–338.
3 Y. Baba, N. Yoza and S. Ohashi, *J. Chromatogr.*, 350 (1985) 119–125.
4 U. Forsman, M. Andersson and H. Törnros, *J. Chromatogr.*, 369 (1986) 151–157.
5 J. Weiss, *Tenside Surfact. Deterg.*, 23 (1986) 237–244.
6 H. Waldhoff and P. Sladek, *Fresenius' Z. Anal. Chem.*, 320 (1985) 163–168.
7 E. Vaeth, P. Sladek and K. Kenar, *Fresenius Z. Anal. Chem.*, 329 (1987) 584–589.
8 P. Glysen and G. Heynen, in A. Adam and C. Schots (Editors), *Biochemical Biological Applications of Isotachophoresis (Analytical Chemistry Symposium Series*, Vol. 5), Elsevier, Amsterdam, 1980, pp. 85–87.
9 H. P. Sleeboom and O. L. M. Bijvoet, *Tumour-Induced Hypercalceamia and its Treatment*, Ciba-Geigy, Basle, 1988.
10 *Medical and Pharmaceutical Information, Aredia disodium pamidronate*, Ciba-Geigy, Basle, 1989.

Journal of Chromatography, 545 (1991) 427–435
Elsevier Science Publishers B.V., Amsterdam

CHROM. 23 173

Determination of permethrine and tetramethrine by isotachophoretic analysis of hydrolytic products

VÁCLAV DOMBEK
Institute of Industrial Landscape Ecology, Czechoslovak Academy of Sciences, Chittussiho 10, 710 00 Ostrava 2 (Czechoslovakia)

ABSTRACT

A method for the isotachophoresis determination of the pyrethroid insecticides permethrine and tetramethrine in water is described. After extracting the insecticides from samples and evaporating the solvent, alkaline hydrolysis was carried out. The degradation products, *cis*- and *trans*-dichlorochrysanthemic acid, *cis*- and *trans*-chrysanthemic acid and phthalimide, were identified and determined by means of capillary isotachophoresis. The detection limit is 0.01 mg/l^{-1} for both insecticides with recoveries of 80–89% and 91–99% for permethrine and tetramethrine, respectively.

INTRODUCTION

Permethrine and tetramethrine are pyrethroid insecticides, for the determination of which various methods have been used.Recently voltammetric [1], bioassay [2] and spectrophotometric [3] techniques have been used. However, separation methods are the most important requirement. Some gas chromatographic (GC) determinations of permethrine and tetramethrine have been reported, using packed [4] and capillary columns [5], with flame ionization [6], electron-capture [7–9], Coulson electrolytic conductivity [10] and microwave plasma detection [11].

High-performance liquid chromatographic (HPLC) methods have been used in the normal- and reversed-phase modes with UV [12] and IR [13,14] detection. Columns with chiral packings are a promising approach [15].

Capillary isotachophoresis (ITP) has not previously been used for determining permethrine and tetramethrine insecticides. The direct isotachophoretic determination of non-ionic pesticides such as pyrethroids is not possible, but they can be determined after hydrolysis to ionic products.

This work is based on previous studies on the alkaline hydrolysis of alphamethrine [16] and the determination of alphamethrine and cypermethrine by ITP [17].

0021-9673/91/$03.50

EXPERIMENTAL

Chemicals

The solvents used were of Pestanal or analytical-reagent grade: pentane, light petroleum (Riedel-de Haën, Seelze, Germany), *tert.*-butyl alcohol (Reanal, Budapest, Hungary) (redistilled), diethyl ether and ethanol (Lachema, Brno, Czechoslovakia).

Chemically pure or analytical-reagent grade chemicals were used for ITP analyses: creatinine (Riedel-de Haën), morpholinoethanesulphonic acid (MES) (Serva, Heidelberg, Germany), and poly (vinyl alcohol) (PVA) Gohsenol GM-14L (M_r = 62 800). Hydrochloric acid was prepared by isothermal distillation and deionized water was prepared with a specific conductivity up to 1.5 μS cm^{-1} (mixed ion-exchange bed). Potassium phthalimide (Riedel-de Haën), anhydrous sodium sulphate (Lachema), argon (M 380) and a solution of Kolthoff-Vleeschhouwer buffer (pH 12, I = 0.193) were used.

Standards were chrysanthemic acid (*cis*, *trans*) and dichlorochrysanthemic acid (*cis*, *trans*), synthesized and provides by the Polish Academy of Sciences.

Model samples of water were prepared by addition of the formulations Reslin 25 EC (Wellcome Foundation, Berkhamsted, U.K.) [97.5 g l^{-1} of permethrine (75% *trans* and 25% *cis* isomers)] and Neopynamine NPB 13 EC (Sumitomo, Osaka, Japan) (13% of tetramethrine) to potable tap water to ensure a content of active compounds within the range 0.01–5.0 mgl^{-1}.

Apparatus

Isotachophoretic analyses were performed on a ZKI 001 ITP analyser (URVJT, Spišská Nová Ves, Czechoslovakia) in one- and two-capillary arrays. With the two-capillary system the current in the preseparation capillary (150 × 0.3 mm I.D.) was 30 μA. When using one capillary, the current was decreased from 100 to 30 μA to detection. The signal of the conductivity detector was recorded on a two-channel recorder at chart drive speeds of 1 and 2.5 mm s^{-1}. Sampling was performed with 10-, 25- and 50-μl microsyringes (Hamilton, Reno, NV, U.S.A.).

Isolation of insecticides from water

The isolation of permethrine and tetramethrine from water was tested by extraction with organic solvents (diethyl ether, pentane, light petroleum). The content of active compounds in the organic phase was determined by ITP after alkaline hydrolysis.

Double extraction with diethyl ether was used for the determination of permethrine. The water samples (volume 800 ml with addition of 80 g of sodium sulphate) were shaken with 40 ml and 15 ml of diethyl ether; for 10 min each. Double extraction with light petroleum was used for isolating tetramethrine. The water samples (volume 800 ml with addition of 20 g of sodium sulphate) were shaken with 20 ml and 15 ml of light petroleum, for 20 min each. The combined organic phases were evaporated on a water-bath with argon after transfer into glass ampoules.

All experiments were repeated three times. The blank was measured in the same way.

Alkaline hydrolysis

Alkaline hydrolysis of permethrine and tetramethrine was carried out in sealed glass ampoules (10 ml) in an argon atmosphere. Ethanol and *tert.*-butyl alcohol solutions of both insecticides (2.0 ml; $2 \cdot 10^{-3}$ mol l^{-1}) were added to 2.0 ml of buffer solution. After removal of air by argon, the ampoules were sealed and thermostated at 50, 65 and 80°C. After 24 h the ampoules were cooled and the contents were diluted to 25 ml with deionized water in a volumetric flask. A 10-μl volume of this sample was injected into the ITP analyser. The same procedure was applied without the argon atmosphere.

The hydrolysis of tetramethrine (2.0 ml of *tert.*-butyl alcohol solution) was carried out gradually with 1.0, 1.5, 2.0, 2.5, 3.0 and 4.0 ml of buffer solution to establish the influence of the alcohol:buffer volume ratio. The same procedure was carried out in an argon atmosphere with an ethanol solution of permethrine.

The time dependence of the recovery of hydrolytic products was studied by hydrolysis of 2 ml of tetramethrine in *tert.*-butyl alcohol ($2 \cdot 10^{-3}$ mol l^{-1}) with 1.5 ml of buffer solution in an air atmosphere. Time intervals were in the range 30 min–24 h. The same procedure was applied with permethrine (2 ml of $2 \cdot 10^{-3}$ mol l^{-1} solution in ethanol with 2.5 ml of buffer).

The hydrolysis of extracts of real samples was carried out as follows. For tetramethrine, after adding 0.65 ml of *tert.*-butyl alcohol and 0.5 ml of a buffer to the dry residue the ampoules were sealed and placed into the thermostat. After 6 h the cooled contents of the ampoules were transferred with deionized water into a 10 ml volumetric flask, diluted to volume and analysed by ITP. For permethrine, 0.5 ml of ethanol and 0.63 ml of buffer were added to the dry residue and, after air had been removed with argon, the ampoules were sealed and thermostated for 24 h at 50°C. The contents of the ampoules were transferred into 10-ml volumetric flask, diluted to volume and analysed by ITP.

All experiments were repeated three times.

ITP determination of decomposition products

The samples prepared by hydrolytic procedures were analysed by ITP in the following operational system: leading electrolyte (L) = HCl (10^{-2} mol l^{-1}) + creatinine + PVA (0.05%), pH_L = 4.80; terminating electrolyte (T) = MES ($5 \cdot 10^{-3}$ mol l^{-1}).

The single- and double-capillary systems were used for the analyses. The contents of chrysanthemic and dichlorochrysanthemic acids and phthalimide in the hydrolysates were determined by the linear calibration method.

Determination of permethrine and tetramethrine in water

For the determination of permethrine in water samples, a double extraction with diethyl ether and hydrolysis in ethanol solution (alcohol:buffer = 1:1.25) were used. For tetramethrine double extraction with light petroleum and hydrolysis in *tert.*-butyl alcohol solution (alcohol:buffer = 1:0.75) were used.

The water samples (ten different concentrations the range 0.01–5.0 mg l^{-1}) were extracted and, after evaporation of the solvent, the total solids were hydrolysed. Degradation compounds (dichlorochrysanthemic acid and phthalimide) were determined by ITP of the hydrolysates.

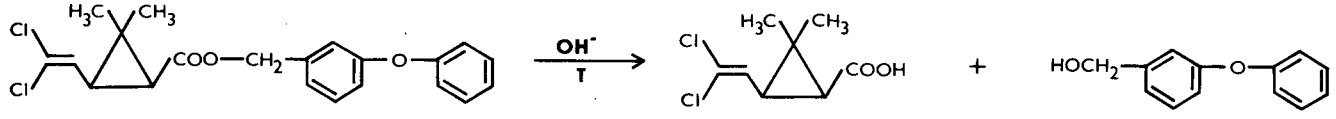

Permethrine

cis,trans-Dichlorochrysanthemic acid

(I)

Phenoxybenzyl alcohol

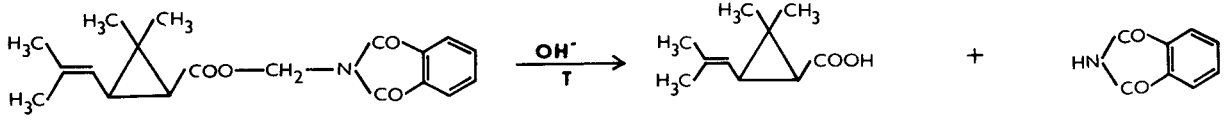

Tetramethrine

cis,trans-Chrysanthemic acid

(II)

Phthalimide

(III)

Fig. 1. Scheme of alkaline hydrolysis of permethrine and tetramethrine.

All experiments were repeated three times. The blank was measured in the same way.

RESULTS AND DISCUSSION

The reaction scheme of the alkaline hydrolysis of permethrine and tetramethrine is shown in Fig. 1. The degradation products, (I) dichlorochrysanthemic acid (from permethrine) and (II) chrysanthemic acid and (III) phthalimide (from tetramethrine), can be separated by ITP using one- and two-capillary arrays. Their ITP separation is shown in Fig. 2. The ITP determination of phenoxybenzyl alcohol is not possible as it does not migrate during the ITP separation.

The hydrolysis of permethrine in ethanol solution under an argon atmosphere gave the best recovery under the described conditions. With tetramethrine the best

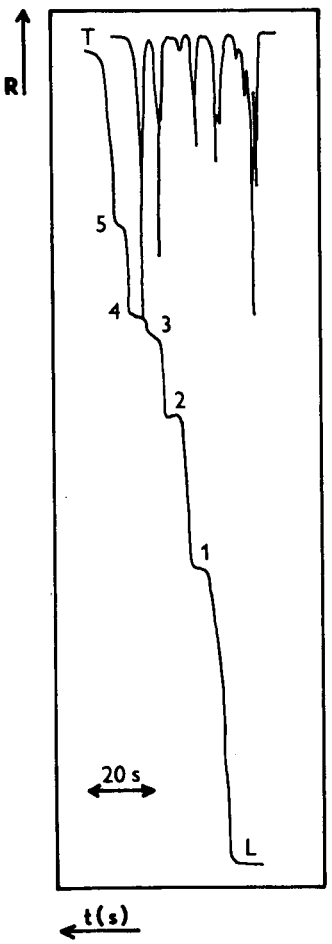

Fig. 2. Separation of degradation products. Injection of 40 μl of mixture ($1.5 \cdot 10^{-5}$ mol l^{-1}); one-capillary system; I = 30 μA. 1 = III; 2 = *trans*-I; 3 = *cis*-I; 4 = *trans*-II; 5 = *cis*-II. L = Cl^-; T = MES; t = time; R = resistance.

TABLE I

INFLUENCE OF TEMPERATURE ON THE RECOVERY OF HYDROLYSIS (AFTER 24 h)

Mean recoveries with standard deviations (n = 9).

Temperature (°C)	Dichlorochrysanthemic		Chrysanthemic		Phthalimide	
	Recovery (%)	S.D. (%)	Recovery (%)	S.D. (%)	Recovery (%)	S.D. (%)
50	92.0	2.32	57.2	1.82	90.6	2.21
65	92.5	2.28	57.8	1.91	90.9	2.25
80	92.9	2.31	57.9	1.78	91.2	2.19

results were attained *tert.*-butyl alcohol solution with an air atmosphere. Higher temperature of hydrolysis (65 and 80°C) did not significantly improve the recovery of hydrolysis (Table I). A temperature of 50°C was used in subsequent work.

The influence of alcohol:buffer volume ratio is important for the recovery of hydrolytic products (Table II). The best results were attained in solution with alcohol: buffer ratios of 1:1.25 for permethrine and 1:0.75 for tetramethrine.

The recovery of hydrolysis was calculated from the ITP-determined concentrations of compounds I (dichlorochrysanthemic acid), II (chrysanthemic acid) and III (phthalimide) in the hydrolysates. The time dependences were constructed as shown in Fig. 3.

Isolation of the insecticides from water by double extraction with diethyl ether (permethrine) or light petroleum (tetramethrine) gave the best results (Table III).

The ITP determination of permethrine and tetramethrine in water after extraction and hydrolysis yields reproducible and consistent results within a broad range of concentrations. The detection limits were of the order of 0.01 mg l^{-1} for both compounds. The method distinguished the *cis* and *trans* isomers of the insecticides. The recovery of the method is 80–89% for permethrine [relative standard deviation

TABLE II

INFLUENCE OF ALCOHOL:BUFFER VOLUME RATIO ON THE RECOVERY OF HYDROLYSIS (AFTER 24 h)

Mean recoveries with standard deviations (n = 9).

Alcohol:buffer volume ratio	Dichlorochrysanthemic		Chrysanthemic		Phthalimide	
	Recovery (%)	S.D. (%)	Recovery (%)	S.D. (%)	Recovery (%)	S.D. (%)
1:0.5	65.3	1.65	53.0	1.67	88.2	2.18
1:0.75	89.1	2.23	54.2	1.72	94.0	2.34
1:1	92.0	2.32	57.2	1.82	90.5	2.21
1:1.25	95.8	2.44	55.9	1.77	88.1	2.16
1:1.5	74.5	1.86	53.0	1.65	71.4	1.81
1:2	35.2	0.75	53.1	1.68	59.0	1.45

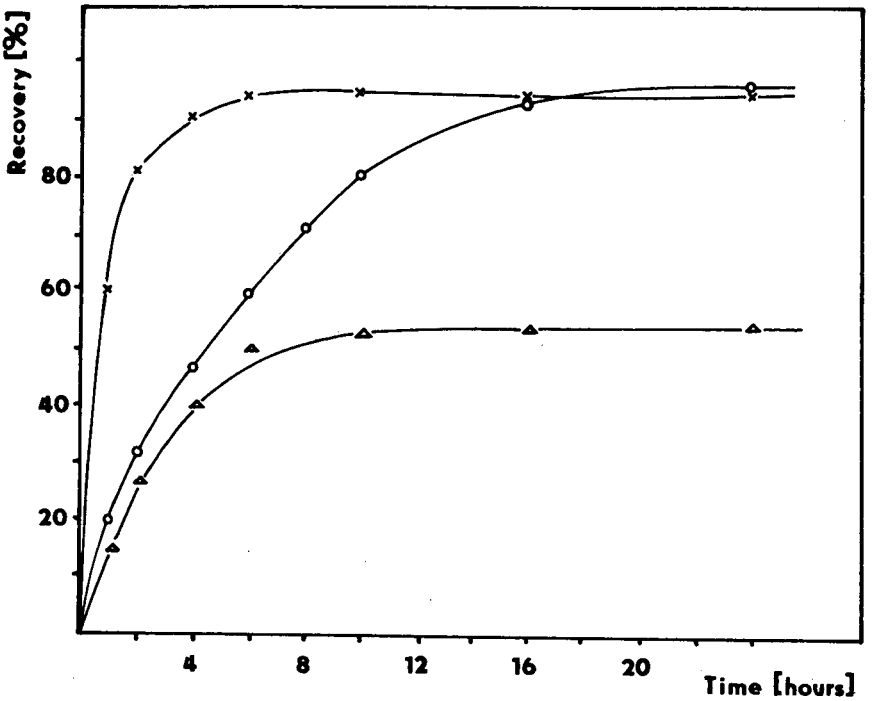

Fig. 3. Time dependences of recovery of hydrolysis (optimum conditions). △, Chrysanthemic acid (both isomers); ○, dichlorochrysanthemic acid (both isomers); X, phthalimide.

TABLE III

RECOVERY OF THE EXTRACTION OF PERMETHRINE AND TETRAMETHRINE FROM WATER (20 ml OF SOLVENT TO 400 ml OF WATER)

Mean recoveries with standard deviations (n = 9). Concentrations of insecticides present: 5.0 mg l^{-1}.

Solvent	Permethrine		Tetramethrine	
	Recovery (%)	S.D. (%)	Recovery (%)	S.D. (%)
Diethyl ether	88	1.31	44	1.68
Pentane	41	1.58	66	1.51
Light petroleum	44	1.21	98	2.03

TABLE IV

DETERMINATION OF PERMETHRINE AND TETRAMETHRINE IN WATER

Mean recoveries with standard deviations (n = 9).

Concentration of insecticides (mg l^{-1})	Permethrine		Tetramethrine	
	Recovery (%)	S.D. (%)	Recovery (%)	S.D. (%)
0.02	81.5	4.13	92.1	4.84
0.05	83.8	4.02	94.3	4.75
0.2	85.2	3.52	97.6	4.28
0.5	89.0	3.27	98.2	4.35
2.0	87.8	3.43	97.9	4.21

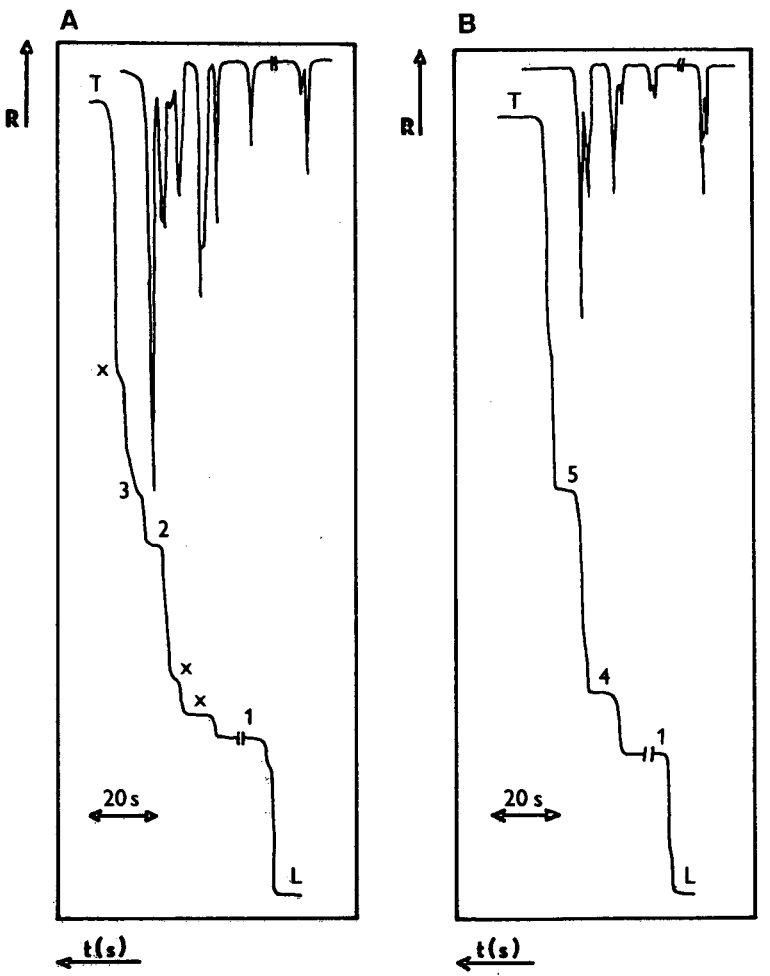

Fig. 4. Determination of (A) permethrine and (B) tetramethrine in water (0.2 mg l^{-1}). Injection of 20 μl of hydrolysate; one-capillary system; I = 30 μA. 1 = PO_4^{3-}; 2 = *trans*-I; 3 = *cis*-I; 4 = III; 5 = *trans*-II. L = Cl^-; T = MES, x = impurities; t = time; R = resistance.

(R.S.D.) = 4.15%] and 91–99% for tetramethrine (R.S.D. = 4.86%) in the range of concentrations of the insecticides in water of 0.01–5.0 mg l^{-1}.

Selected results of the ITP determination of permethrine and tetramethrine in water are summarized in Table IV. Typical isotachophoreograms are shown in Fig. 4. It is concluded that the proposed method is suitable for routine analyses in agriculture and ecology.

REFERENCES

1 P. Hernandez, J. Vicente and L. Hernandez, *Fresenius' Z. Anal. Chem.*, 334 (1989) 550.
2 L. H. Stanker, C. Bigbee, J. van Emon, E. Watkins, R. H. Jensen, Ch. Morris and M. Vanderlaan, *J. Agric. Food Chem.*, 37 (1989) 834.
3 J. M. Desmarchelier, *J. Stored Prod. Res.*, 12 (1976) 245.
4 N. Baba, A. Nagayasu and M. Ohno, *Agric. Biol. Chem.*, 34 (1970) 343.
5 A. Richard and G. Andermann, *J. Chromatogr. Sci.*, 22 (1984) 207.
6 R. A. Simonaitis and R.S. Cail, *Chromatographia*, 18 (1984) 556.
7 M. Chiba, *J. Environ. Sci. Health*, B13 (1978) 261.
8 A. E. S. M. Marei, L. O. Ruzo and J. E. Casida, *J. Agric. Food Chem.*, 30 (1982) 558.
9 W. Ebing, *Fresenius' Z. Anal. Chem.*, 327 (1987) 539.
10 G. H. Fujie and O. H. Fullmer, *J. Agric. Food Chem.*, 26 (1978) 395.
11 M. L. Bruce and J. A. Caruso, *Appl. Spectrosc.*, 39 (1985) 942.
12 D. Mourot, B. Delepine, J. Boisseau and G. Gayot, *J. Chromatogr.*, 168 (1979) 277.
13 E. Papadopoulou-Mourkidou, Y. Iwata and F. A. Gunter, *J. Agric. Food Chem.*, 29 (1981) 1105.
14 E. Papadopoulou-Mourkidou, Y. Iwata and F. A. Gunter, *J. Agric. Food Chem.*, 31 (1983) 629.
15 T. Doi, S. Sakane and M. Horiba, *J. Assoc. Off. Anal. Chem.*, 68 (1985) 911.
16 V. Dombek and Z. Stránský, *J. Chromatogr.*, 470 (1989) 235.
17 V. Dombek, *Thesis*, Palacký University, Olomouc, 1989.

Journal of Chromatography, 545 (1991) 437–444
Elsevier Science Publishers B.V., Amsterdam

CHROM. 23 190

Use of cyclodextrins in capillary zone electrophoresis

Resolution of terbutaline and propranolol enantiomers

SALVATORE FANALI
Istituto di Cromatografia del CNR, Area della Ricerca di Roma, C.P. 10, 00016 Monterotondo Scalo, Rome (Italy)

ABSTRACT

Terbutaline and propranolol were resolved using capillary zone electrophoresis. The effect of the type and the amount of cyclodextrins added to the background electrolyte on the migration time and the resolution of their enantiomers was studied. Good resolution of the racemic terbutaline was obtained using phosphate buffer at pH 2.5 containing either 5 m*M* heptakis(2,6-di-O-methyl)-*β*-cyclodextrin or 15 m*M* *β*-cyclodextrin. The background electrolyte, 50 m*M* phosphate buffer (pH = 2.5) – 4 *M* urea – 40 m*M* *β*-cyclodextrin in 30% (v/v) methanol, on the other hand, gave the best resolution of propranolol enantiomers.

INTRODUCTION

Cyclodextrins (CDs) are oligosaccharides containing several D-(+)-glucopyranose units with a shape similar to a truncated cone able to form inclusion complexes. CDs have been used successfully in analytical chemistry for improving the selectivity of the separation of positional and geometrical isomers and enantiomers [1–4].

Several techniques have employed CDs for the resolution of enantiomers, *e.g.*, thin-layer chromatography, gas chromatography, capillary isotachophoresis, high-performance liquid chromatography (HPLC), isoelectric focusing, electrokinetic chromatography and capillary zone electrophoresis [5–12]. As enantiomers possess the same chemical properties, they are difficult to separate from each other. Their resolution is generally performed by using a chiral environment that interacts with the analytes either strongly (indirect resolution) or weakly (direct resolution) [13]. Capillary zone electrophoresis (CZE) is a relatively new electrophoretic technique with a high resolving power and high sensitivity used for the separation of compounds with different mobilities [14].

In this work, CZE was used for the resolution of terbutaline by the direct resolution method. The chiral environment consisted of an aqueous background electrolyte (BGE) containing *β*-cyclodextrin or heptakis(2,6-di-O-methyl)-*β*-cyclodextrin. The effect of the shape and the amount of CD added to the background

0021-9673/91/$03.50

electrolyte on the migration time and the resolution of the two enantiomers of terbutaline was studied.

As the above electrolyte system could not resolve propranolol isomers, we searched for another system and found a BGE containing urea, β-cyclodextrin and methanol to be the best for this purpose.

EXPERIMENTAL

Chemicals

Sodium dihydrogenphosphate, phosphoric acid, ammonium acetate, acetic acid and methanol were purchased from Carlo Erba (Milan, Italy), (*S*)-(−)-propranolol hydrochloride, (*R*)-(+)-propranolol hydrochloride, DL-propranolol hydrochloride, terbutaline hemisulphate salt and β-cyclodextrin (β-CD) from Sigma (St. Louis, MO, USA) and α- and γ-cyclodextrin (α- and γ-CD), and urea from Fluka (Buchs, Switzerland). (+)-Terbutaline and (−)-terbutaline were separated by HPLC according to the published method [7], collected and spiked separately with racemic terbutaline for electrophoretic experiments. Heptakis(2,6-di-O-methyl)-β-cyclodextrin (di-OMe-β-CD) and heptakis(2,3,6-tri-O-methyl)-β-cyclodextrin (tri-OMe-β-CD) were obtained from Chinoin (Budapest, Hungary).

Apparatus

Electrophoretic experiments were carried out in an HPE 100 apparatus (Bio-Rad Labs., Richmond, CA, USA) equipped with an on-column UV detector operated at 206 nm. The regulated high-voltage power supply, able to deliver up to 12 kV, was used in either a constant-voltage or a constant-current mode.

A coated capillary tube cartridge (20 cm × 0.025 mm I.D.) (Bio-Rad Labs.) was used for the separations. Injection was done by electromigration by applying a constant voltage.

A Model 2210 line recorder (LKB, Bromma, Sweden) was used for recording the electropherograms.

Background electrolyte (BGE)

A stock solution of 0.1 *M* NaH_2PO_4 titrated with phosphoric acid to pH 2.5 was prepared and used for electrophoretic experiments in aqueous solution. The CDs were added separately to the stock solution.

A 50-ml volume of aqueous 0.1 *M* phosphate buffer prepared as described below was mixed with the appropriate amount of methanol and 4 *M* urea, and water was added to 100 ml, and the appropriate amount of CD was dissolved in the buffer–methanol solution.

RESULTS AND DISCUSSION

The enantiomeric resolution of racemic compounds can be performed by CZE using either an indirect or direct resolution method. In the direct method a chiral environment interacts with the two enantiomers and forms complexes with different stability constants. Complex formation will influence the effective mobilities of the analytes and thus permit their resolution.

Cyclodextrins have been used successfully in electrophoretic techniques in order to improve the selectivity of the separation of enantiomers. The mechanism is based on inclusion complexation between CDs and the analytes. The structure of the studied compounds has a very important role in the resolution. In fact, the chiral centre of its substituent must be at a favourable distance from the rim of CD in order to effect hydrogen bonding with the hydroxyl groups.

In this study we investigated the effect of α-, β- and γ-CD, 2,6-di-OMe-β-CD and 2,3,6-tri-OMe-β-CD on the migration time and resolution of two drugs, terbutaline and propranolol.

Terbutaline [2-*tert.*-butylamino-1-(3,5-dihydroxyphenyl)ethanol] is a sympathomimetic drug-selective β_2-receptor agonist used in the treatment of asthma and lung diseases. Propranolol [1-(isopropylamino)-3-(1-naphthyloxy)-2-propanol] is a β-blocker used in the treatment of angina pectoris [15,16]. The differences in the structures of the two compounds are shown in Fig. 1. It is clear that the chiral carbon of propranolol is at a longer distance from the aromatic group than that in terbutaline. Further, the substituents in the aromatic ring are different.

Different CDs were added to the aqueous BGE for the electrophoretic experiments in order to study the inclusion complexes with the analytes. Based on our previous experience with the resolution of sympathomimetic drugs by CZE, a BGE at a pH of 2.5 was selected [12]. At this pH both terbutaline and propranolol migrate as cations.

α-, β- and γ-CD, di-OMe-β-CD and tri-OMe-β-CD were used as complexing agents in the BGE. The resolution (R) of the enantiomers was calculated by using the equation

$$R = \frac{t(+) - t(-)}{w(+) + w(-)} \cdot 2 \qquad (1)$$

where t (s) is the migration time, w (s) the width of the peak at the baseline and (+) and (−) represent the dextro- and laevo-rotatory enantiomers, respectively.

The effect of the concentration of di-OMe-β-CD and β-CD on the migration

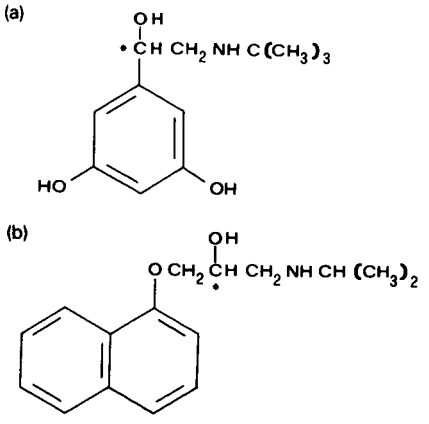

Fig. 1. Structures of (a) terbutaline and (b) propranolol.

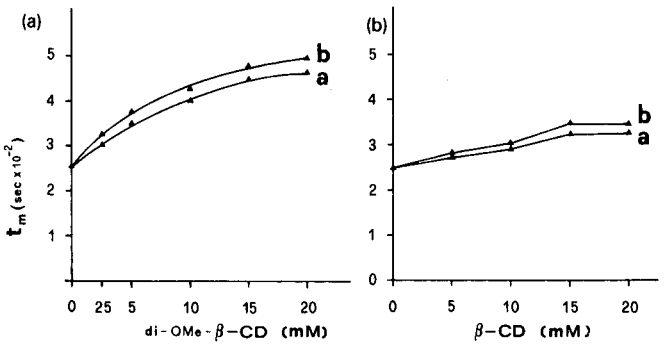

Fig. 2. Effect of the concentration of cyclodextrins added to the background electrolyte on the migration time of (+)- and (−)-terbutaline. (a) Di-OMe-β-CD; (b) β-CD. BGE: 0.1 *M* phosphate buffer (pH 2.5); sampling, electrokinetic, 8 kV, 10 s (10^{-5} *M* terbutaline); electrophoresis, 19 μA (constant), 9 kV.

time of the two enantiomers of terbutaline is illustrated in Fig. 2a and b, respectively. From these results it is clear that by using a higher amount of either di-OMe-β-CD or β-CD the migration time of the analyte compounds is increased, and this is more evident when derivatized CD (di-OMe-β-CD) is used as a chiral selector. This means that di-OMe-β-CD is a better complexing agent than β-CD. This can be explained by considering the structure of terbutaline and the CDs used. Terbutaline has two hydroxyl groups in the aromatic ring that influence the fitting in the cavity of the CD in order to form inclusion complexes. The two methyl groups for each glucose in di-OMe-β-CD influence the hydrophobicity of the CD [4].

In Fig. 3, the resolution of the terbutaline enantiomers is plotted against the concentration of β-CD and di-OMe-β-CD added to the aqueous BGE. In the two chiral environments used the resolution increases by adding a larger amount of CD and the maximum is obtained at 15 m*M* β-CD and 5 m*M* di-OMe-β-CD.

The electropherograms for the resolution of terbutaline into its enantiomers by using an aqueous BGE containing 5 m*M* di-OMe-β-CD ($R = 2.8$) and 15 m*M* β-CD ($R = 2$) are reported in Figs. 4 and 5, respectively. Both resolutions are very good and the differences consisted in a higher efficiency but lower resolution when β-CD was used. In all the separations performed by CZE, (+)-terbutaline moves towards the

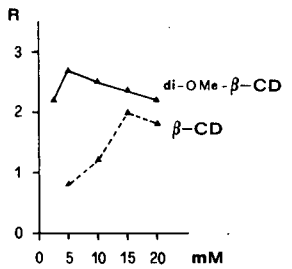

Fig. 3. Effect of the amount of cyclodextrins added to the BGE on the resolution (*R*) of terbutaline enantiomers.

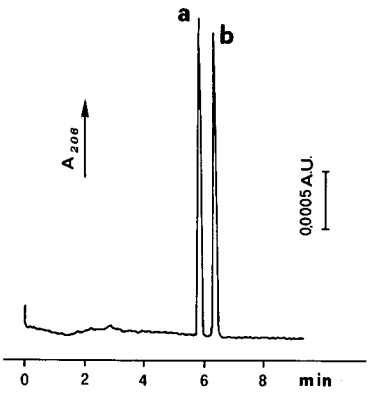

Fig. 4. Electropherogram of the enantiomeric resolution of terbutaline. BGE: 0.1 *M* NaH_2PO_4–H_3PO_4 (pH 2.5) containing 5 m*M* di-OMe-β-CD. Sampling and electrophoresis as in Fig. 2. (a) (−)-Terbutaline; (b) (+)-terbutaline.

cathode with a lower velocity than the (−)-isomer. This was verified by injecting separately the two enantiomers resolved by HPLC.

Experiments performed by adding different amounts of α- and γ-CD showed no resolution of the two enantiomers. The migration time of the racemic terbutaline was slightly changed. This can be explained by considering the shape of the cavity of the two CDs, which are too small and too large, respectively, for inclusion complex formation with terbutaline.

When using tri-OMe-β-CD a very poor resolution of racemic terbutaline was obtained on adding 80 m*M* of the modified cyclodextrin to the aqueous BGE. On

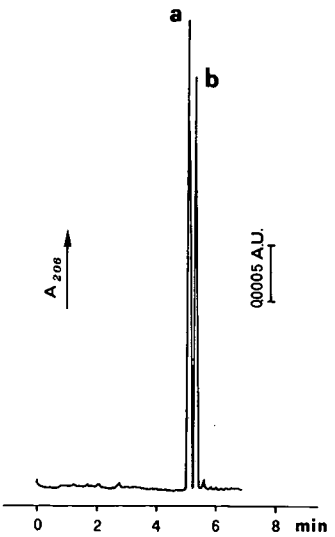

Fig. 5. Electropherogram of the separation of racemic terbutaline: (a) (−)-terbutaline; (b) (+)-terbutaline. BGE: 0.1 *M* phosphate buffer (pH 2.5) containing 15 m*M* β-CD. Sampling and electrophoresis as in Fig. 2.

increasing the amount of triOMe-β-CD the migration time changed (from 250 s at 0 m*M* to 277 s at 80 m*M*). This shows that the inclusion complex are probably formed but this modified CD gives a poor enantioselectivity effect. Of course, the enantioselectivity is improved when hydroxyl groups are on the rim of the CD and interact with the analytes by hydrogen bonding.

The same BGE used for the resolution of racemic terbutaline was tested for the separation of the enantiomers of propranolol. Different CDs (α-, β- and γ-CD, di-OMe-β-CD and tri-OMe-β-CD) were added separately to the aqueous BGE for the electrophoretic experiments and the migration time was measured. α-CD did not markedly influence the migration time of propranolol, consequently giving no resolution of the two enantiomers. The use of γ-CD, β-CD, di-OMe-β-CD and tri-OMe-β-CD affected the retardation of propranolol. In fact, its velocity diminished on increasing the amount of CD added to the BGE, showing an inclusion complexation of propranolol with these type of CDs. The results are reported in Fig. 6.

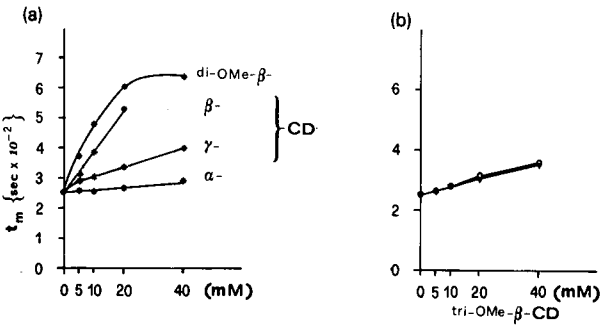

Fig. 6. Effect of the amount of cyclodextrins added to the BGE on the migration time of propranolol. BGE: 0.1 *M* phosphate buffer (pH 2.5) containing the appropriate amount of CD. Sampling: electrokinetic, 8 kV, 10 s (10^{-5} *M* racemic propranolol); electrophoresis as in Fig. 2. (a) α-, β-, γ-CD and di-OMe-β-CD; all curves racemic propranolol. (b) Tri-OMe-β-CD; (○) (*R*)-(+)-propranolol; (▼) (*S*)-(−)-propranolol.

Under the experimental conditions used (pH, ionic strength, chiral selector, solvent, etc.), no resolution was achieved for the two enantiomers of propranolol except when tri-OMe-β-CD was used. The best resolution of the two enantiomers was achieved by adding 40 m*M* of the CD derivative to the BGE ($R < 0.5$). Armstrong *et al.* [17] reported the resolution of propranolol enantiomers by HPLC using two 25-cm β-cyclodextrin columns in series. They also showed the structure of the inclusion complexes of the two enantiomers with β-CD. Thus, considering the success achieved by HPLC and the theoretical considerations about the inclusion complexes formed, we tried increasing the amount of the chiral selector in the aqueous BGE. As previously reported, aqueous solutions of urea are able to solubilize appreciable amount of β-CD and, further, urea does not bind CDs [18,19].

Experiments carried out by using 50 m*M* phosphate buffer (pH 2.5) containing 4 *M* urea and different amounts of β-CD ranging from 30 to 80 m*M* gave no resolution of racemic propranolol. We therefore tried a BGE with methanol as an organic modifier and containing 4 *M* urea and 40 m*M* β-CD. The methanol content in the BGE

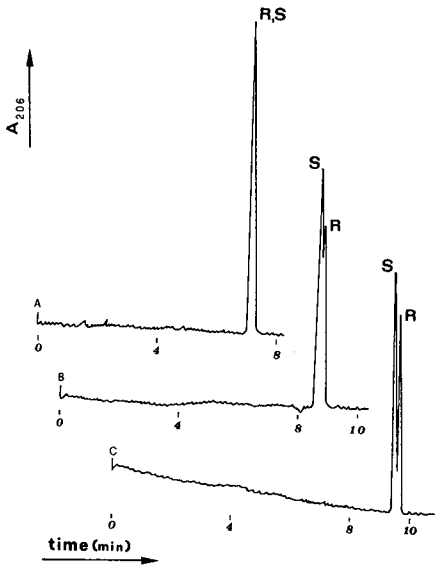

Fig. 7. Electropherograms of racemic propranolol separation. BGE: 50 m*M* phosphate buffer (pH 2.5) containing 4 *M* urea, 40 m*M* β-CD and increasing amounts of methanol (A, 0%; B, 10%; and C, 30%). Electrophoresis, 8 kV (constant), 4–6 μA; sampling, 4 kV, 5 s.

ranged from 0 to 40% (v/v). The electrophoretic resolution of (*S*)-(−)- and (*R*)-(+)-propranolol is reported in Fig. 7. It is evident that the resolution of racemic propranolol depends on the amount of organic modifier; the resolution was improved by increasing the methanol content, the best resolution being obtained when the BGE contained 30% of methanol. Although the mechanism of the separation is not clear, the most important effect is probably due to the change in the solvation of the included isomers. No further improvement in the resolution of the drug was obtained by increasing the amount of β-CD in this electrolyte system. The use of tri-OMe-β-CD in a phosphate–methanol buffer solution gave no resolution of racemic propranolol.

CONCLUSIONS

The results demonstrate that in CZE cyclodextrins are good enantioselective agents for the resolution of terbutaline. The resolution is obtained in less than 6 min. Terbutaline forms complexes with β-CD and di-OMe-β-CD and tri-OMe-β-CD, and the complexation increases with increase in the amount of the CDs added to the BGE.

The shape of the CD and the guest compound influence the resolution of the enantiomers. The use of urea and methanol influence the selectivity for the resolution of racemic propranolol. Propranolol was resolved into its enantiomers in a relatively short time (less than 10 min).

CZE can provide several advantages over other analytical techniques for enantiomeric resolution, *e.g.*, high resolution high efficiency and short analysis times. Further, in CZE expensive chiral compounds are not needed; in fact CDs are added to

the BGE at a relatively low concentration and only a few millilitres of the BGE are used in the electrophoretic experiments. On the other hand, the use of CZE for preparative purposes needs further work.

The use of a relatively short capillary (20 cm) and a small I.D. (0.025 mm) allow the broadening of the separated zones due either to diffusion and or Joule heating to be minimized. Further, the coating of the capillary eliminates the electroosmotic flow and thus improves the resolution [20].

The detection limit, *i.e.*, the minimum sample concentration that could be injected by the electrophoretic method to obtain a signal-to-noise ratio of 2:1, was found to be 1.10^{-7} *M* for terbutaline.

Analytical CZE can be used successfully for enantiomeric purity control of drugs (terbutaline and propranolol). Further, pharmacokinetic studies of terbutaline could be performed but the sensitivity should be improved, *e.g.*, by using an electrochemical detector, with CZE coupled with mass spectrometry.

ACKNOWLEDGEMENTS

The author thanks Mr. M. Cristalli for technical assistance and Dr. A. Nardi for the experimental work.

REFERENCES

1 E. Smolkova-Keulemansova, *J. Chromatogr.*, 251 (1982) 17.
2 J. Szejtli, *Cyclodextrins and Their Inclusion Complexes*, Akadémiai Kiadó, Budapest, 1982.
3 W. L. Hinze, *Sep. Purif. Methods*, 10 (1981) 159.
4 W. L. Hinze and D. W. Armstrong, *Anal. Lett.*, 13 (1980) 1093.
5 T. Koscielski, D. Sybilska, S. Belmiak and J. Jurczak, *Chromatographia*, 19 (1984) 292.
6 T. J. Ward and D. W. Armstrong, *J. Liq. Chromatogr.*, 9 (1986) 407.
7 A. Walhangen, L. E. Edholm, B. M. Kennedy and L. C. Xiao, *Chirality*, 1 (1989) 20.
8 J. Snopek, I. Jelinek and E. Smolkova-Keulemansova, *J. Chromatogr.*, 438 (1988) 211.
9 A. Guttman, A. Paulus, A. S. Cohen, N. Grinberg and B. L. Karger, *J. Chromatogr.*, 448 (1988) 41.
10 P. G. Righetti, C. Ettori, P. Chafey and J. P. Wahrmann, *Electrophoresis*, 11 (1990) 1.
11 S. Terabe, *Trends Anal. Chem.*, 8 (1989) 129.
12 S. Fanali, *J. Chromatogr.*, 474 (1989) 441.
13 S. Fanali and P. Bocek, *Electrophoresis*, 11 (1990) 757.
14 F. Foret and P. Bocek, in A. Chrambach, M. J. Dunn, B. J. Radola (Editors), *Advances in Electrophoresis*, VCH, Weinheim, 1989, p. 273.
15 L. Borgstrom, L. C. Xiao and A. Walhagen, *Chirality*, 1 (1989) 174.
16 I. R. Innes and M. Nickerson, in L. S. Goodman and A. G. Gilman (Editors), *The Pharmacological Basis of Therapeutics*, Macmillan, New York, 5th ed., 1975, pp. 547–552.
17 D. W. Armstrong, T. J. Ward, R. D. Armstrong and T. E. Beesley, *Science*, 232 (1986) 1132.
18 D. Y. Pharr, Z. S. Fu, T. K. Smith and W. L. Hinze, *Anal. Chem.*, 61 (1989) 275.
19 W. L. Hinze, D. Y. Pharr, Z. S. Fu and W. G. Burkert, *Anal. Chem.*, 61 (1989) 422.
20 J. W. Jorgenson and K. D. Lukacs, *Science*, 222 (1983) 266.

Journal of Chromatography, 545 (1991) 445–460
Elsevier Science Publishers B.V., Amsterdam

CHROM. 23 222

Analysis of barbiturates in human serum and urine by high-performance capillary electrophoresis–micellar electrokinetic capillary chromatography with on-column multi-wavelength detection

WOLFGANG THORMANN*, PETER MEIER, CLAUDIA MARCOLLI and FRANK BINDER
Department of Clinical Pharmacology, University of Berne, Murtenstrasse 35, CH-3010 Berne (Switzerland)

ABSTRACT

The analysis of barbiturates in human serum (or plasma) and urine by high-performance capillary electrophoresis–electrokinetic capillary chromatography with on-column fast-scanning multi-wavelength detection is discussed. The use of a buffer of *ca.* pH 8 and containing sodium dodecyl sulphate provides a medium suitable for fast and high-resolution separations of barbiturates. Seven barbiturates are characterized by their retention and absorption spectra between 195 and 320 nm. Comparison of these computer-stored data with those of unknown samples is shown to allow the identification of barbiturates in samples of patients undergoing pharmacotherapy and in toxicological urine and serum specimens. Three-dimensional electropherograms provide reliable information on the requirement and suitability of sample pretreatment procedures. With urine, extraction of barbiturates prior to analysis is necessary. With human serum several barbiturates, including phenobarbital, are shown to elute in an interference-free window in front of uric acid and the proteins, allowing these substances to be determined by direct sample injection. The need for multi-wavelength detection over a relatively wide wavelength range as a means of peak confirmation in electrokinetic capillary analyses is demonstrated and limitations of this technique for compounds with similar retention behaviour and absorption spectra are discussed.

INTRODUCTION

Screening and confirmation of drugs in body fluids, including barbiturates (Fig. 1) in serum (plasma) and urine, are important for the investigation of intoxication, for therapeutic drug monitoring and for pharmacokinetic and metabolic studies. Every laboratory involved with clinical toxicology should be prepared to analyse a biological specimen to determine (i) whether or not a barbiturate is present and (ii) its identity and in some instances also its concentration. Barbiturates have a low therapeutic index and are therefore prone to cause poisoning. Monitoring their concentrations in body fluids, especially in serum, is therefore essential to optimize pharmacotherapy [1]. As instrumental approaches for the analysis of barbiturates in body fluids, immunoassays [2–4] and many chromatographic methods [5–8] have been developed. Immunological techniques are very attractive because of their ease of performance, speed of analysis

0021-9673/91/$03.50

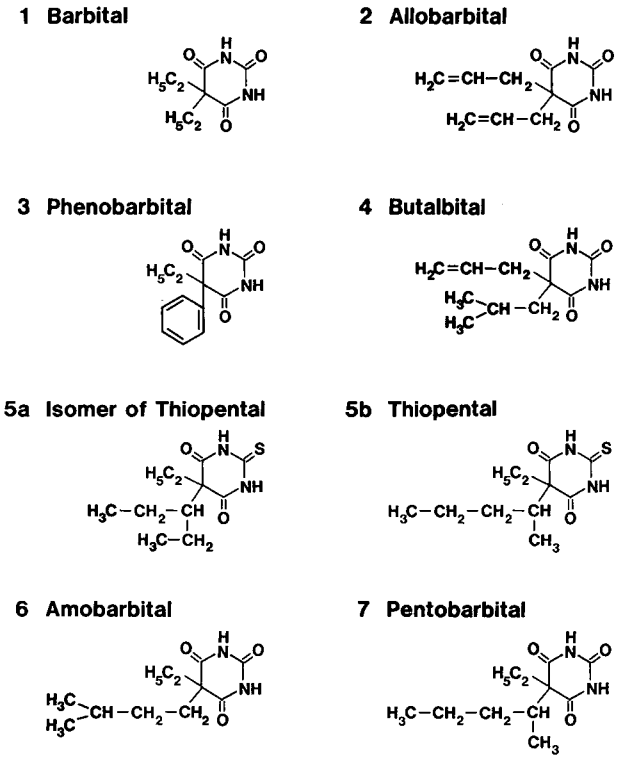

Fig. 1. Structures of the barbiturates investigated.

and sensitivity. However, with the exception of phenobarbital, these assays are not specific enough to monitor or identify a single compound. They simultaneously respond to different barbiturates at a characteristic specificity to each of them, providing their suitability to monitor the presence of barbiturates in a toxicological specimen. Chromatographic procedures have been applied for the determination of all common barbiturates. These methods separate and therefore provide data on multiple compounds in one run. They require, however, time-consuming sample pretreatments and are characterized by a low sample throughput.

Recently, high-performance capillary electrophoresis (HPCE) and micellar electrokinetic capillary chromatography (MECC, an interface between electrophoresis and chromatography) were found to be attractive approaches for the analysis of pharmaceuticals [9–15]. HPCE is a one-phase process with separation based on differences in electrophoretic mobilities. In MECC two distinct phases are used, an aqueous and a micellar phase or pseudo-stationary phase. These two phases are established by employing buffers containing surfactants [*e.g.*, sodium dodecyl sulphate (SDS)], which are added above their critical micellar concentration. Variation of the surfactant concentration has similar effects to changes in surface structure in HPLC (*e.g.*, change from C_8 to C_{18}). An MECC analysis is performed in equipment designed for HPCE, *i.e.*, in an open-tubular capillary of very small I.D. A high-voltage d.c.

electric field is applied along the column, thus causing both a movement of the entire liquid (the so-called electroosmotic flow) and migration of the charged micelles. Non-ionic solutes partition between the two phases and elute with zone velocities between those of the two phases. In this case separation is solely of chromatographic nature. For ionic solutes which are also differentially distributed between the two phases, separation is based on chromatography and electrophoresis. This was found to be the case with barbiturates having a buffer of *ca.* pH 8 and containing 50 m*M* SDS, hence the assay is referred to as an HPCE–MECC methodology.

Multi-wavelength detection, such as the use of a photodiode-array detector, is a powerful technique for solute monitoring in liquid chromatography [16] and has recently also been applied to HPCE [17,18]. It allows the collection of absorbance *vs.* time (*i.e.*, registration of a chromatogram or electropherogram), absorbance *vs.* wavelength (spectrum) and absorbance *vs.* time *vs.* wavelength data for a three-dimensional depiction of the data (Fig. 2), this permitting peak confirmation and peak

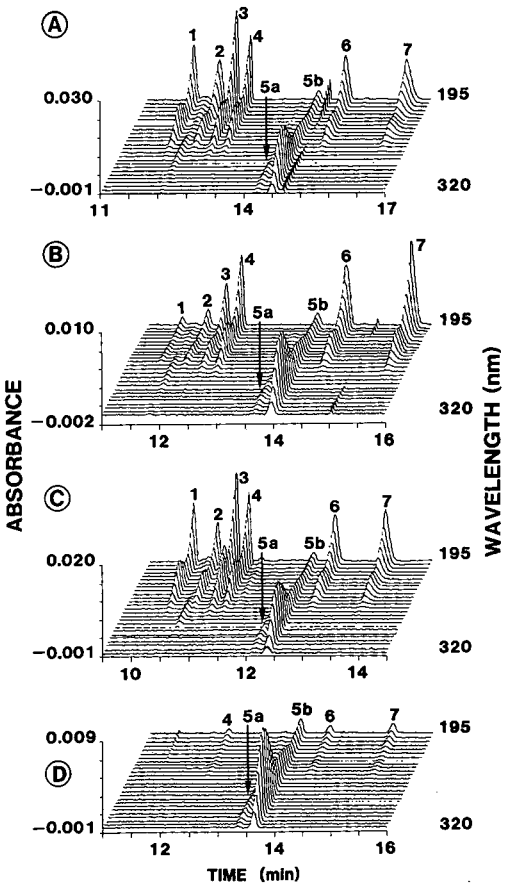

Fig. 2. Three-dimensional electropherograms of a model mixture of seven barbiturates in (A) buffer and (B) bovine plasma after Bond-Elut C_{18}, (C) chloroform and (D) pentane extraction. The applied voltage was a constant 20 kV in all instances and the currents were 60–63 μA. Barbiturates: 1 = barbital; 2 = allobarbital; 3 = phenobarbital; 4 = butalbital; 5a = isomer of thiopental; 5b = thiopental; 6 = amobarbital; 7 = pentobarbital. Sample concentrations and recoveries are summarized in Table I.

purity to be evaluated via comparison with absorption spectra. Using HPCE–MECC with a fast-scanning multi-wavelength detector [19], the objectives of the work described in this paper were (i) to investigate the suitability of direct sample introduction and different extraction procedures for barbiturates in human serum and urine, (ii) to measure barbiturates (parent drug and metabolites) in serum samples from patients undergoing barbiturate pharmacotherapy and (iii) to confirm the presence and determine the identity of barbiturates in urine specimens which were received in the departmental drug assay laboratory and were found to be barbiturate positive using immunoassays.

EXPERIMENTAL

Chemicals

The barbiturates, of European Pharmacopoeia quality, were purchased from Grogg Chemie (Stettlen, Switzerland), except thiopental, which was from Abbott Labs. (Cham, Switzerland). All other chemicals were of analytical-reagent or research grade. Bovine plasma was prepared by centrifugation of bovine blood (from the local slaughter house) and blank human serum was obtained by centrifugation of our own blood (500 *g* for 10 min).

Instrumentation and running conditions

Both laboratory-made and commercial HPCE instrumentation was used. The laboratory-made device featured a 75 μm I.D. fused-silica capillary of about 90 cm length (Product TSP/075/375, Polymicro Technologies, Phoenix, AZ, USA) together with a Model UVIS 206 PHD fast-scanning multi-wavelength detector with on-column capillary detector cell No. 9550-0155 (Linear Instruments, Reno, NV, USA) towards the capillary end. The effective separation distance was 70 cm. Two 50-ml plastic bottles served as electrode vessels and a VacTorr 150 vacuum pump (CGA/Precision Scientific, Chicago, IL, USA) was used to rinse the capillary with cleaning solution (0.1 *M* sodium hydroxide) and electrophoresis buffer. Current was applied at a constant voltage (20 kV) with an HCN 14-20000 power supply (FUG Elektronik, Rosenheim, Germany). The cathode was on the detector side. Sample application occurred manually via gravity through lifting the anodic capillary end, dipped into the sample vial, *ca.* 34 cm for a specified time interval (typically 5 s). Multi-wavelength data were read, evaluated and stored employing a Mandax AT 286 computer system and running the Model 206 detector software package version 2.0 (Linear Instruments) with windows 286 version 2.1 (Microsoft, Redmont, WA, USA). Conditioning for each experiment was effected by rinsing the capillary with 0.1 *M* sodium hydroxide solution for 3 min and with buffer for 5 min. Throughout this work the Model 206 detector was employed in the high-speed polychrome mode by scanning from 195 to 320 nm at 5-nm intervals (26 wavelengths). With these settings the sampling rate for each wavelength was 3.69 data points/s.

The commercial instrument was a Model 270A capillary electrophoresis system (Applied Biosystems, San Jose, CA, USA). This apparatus features automated capillary rinsing, sampling and execution of the electrophoretic run. For our experiments it was equipped with a 50-μm I.D. fused-silica capillary of effective separation length 44 cm. A Model D-2000 chromato-integrator (Merck–Hitachi,

Darmstadt, Germany) was used for recording the pherograms and for quantification by peak-area measurements. The integrator sampling period was set to one data point per 200 ms throughout this work. Before each run the capillary was rinsed with 0.1 *M* sodium hydroxide solution (1 min) and with buffer (2 min). Injection of sample occurred via vacuum suction for 2 s. In all experiments a constant voltage of 30 kV was applied and the temperature was set at 40°C. To obtain responses at different wavelengths, barbiturate samples were detected sequentially at 215 and 290 nm.

Absorption spectra were measured with a Lambda 15 UV–VIS spectrophotometer (Perkin-Elmer, Überlingen, Germany).

Electrophoresis buffers and standard solutions

For monitoring of barbiturates a buffer composed of 50 m*M* sodium dodecyl sulphate (SDS), 9 m*M* $Na_2B_4O_7$ and 15 m*M* NaH_2PO_4 (pH *ca.* 7.8) was employed.

Standard solutions of single barbiturates (100 μg/ml) were prepared in methanol whereas a standard model mixture composed of seven barbiturates (barbital, allobarbital, phenobarbital, butalbital, thiopental, amobarbital and pentobarbital; 500 μg/ml each) was dissolved in the electrophoresis SDS buffer. Spiking of blank and patients' samples occurred through addition of known aliquots of these standard solutions to the body fluids prior to sample extraction. For quantification of barbiturates in serum, aliquots of the methanolic standard solutions were added to a glass test-tube with a conical bottom, evaporated to dryness under a stream of nitrogen (40°C) and reconstituted with either bovine plasma, blank human serum or patients' serum.

Sample preparation for barbiturates in urine

Extraction of barbiturates from urine was achieved using Bond-Elut Certify cartridges and the Vac-Elut set-up (both from Analytichem International, Harbor City, CA, USA). With minor alterations, the manufacturer's instructions for chromatographic analyses were followed. The cartridges were conditioned immediately prior to use by passing sequentially 2 ml of methanol and an equal volume of 0.1 *M* phosphate buffer (pH 6) through the columns. The vacuum was turned off to prevent column drying. The columns were loaded by slowly drawing of a mixture of 5 ml of urine and 2 ml of 0.1 *M* phosphate buffer (pH 6). The columns were then rinsed with 1 ml of 0.1 *M* phosphate buffer–methanol (80:20), dried under full vacuum for 5 min, rinsed with 1 ml of 1 *M* acetic acid, again dried under full vacuum (10 min) and rinsed with 1 ml of hexane. Elution was effected with 4 ml of methylene chloride into a test-tube before evaporation to dryness under a gentle stream of nitrogen at 40°C. The residue was dissolved in 100–200 μl of running buffer.

Sample preparation for barbiturates in serum (plasma)

Bond Elut C_{18}. Extraction of barbiturates was achieved using Bond-Elut C_{18} cartridges and the Vac-Elut set-up. The cartridges were conditioned immediately prior to use by drawing first methanol then water (both twice) through each column. For these steps the columns were filled completely with the two solvents. The columns were loaded by application of 0.6 ml of a mixture of 0.75 ml of serum (plasma) and 0.15 ml of 0.1 *M* Na_2HPO_4 (pH *ca.* 8.5). After an incubation period of several minutes the solutions were slowly drawn, the columns were rinsed three times with water and dried

under full vacuum for about 1 min. Elution was effected first with 0.2 ml (after a short incubation period) and continued with 0.25 ml of methanol into a test-tube before evaporation to dryness under a gentle stream of nitrogen at 40°C. The residue was dissolved in 200 μl of running buffer.

Chloroform extraction. Liquid–liquid extraction with chloroform from acidified serum was executed after the method of Shiu and Nemoto [7]. A 0.2-ml volume of serum (plasma), 0.1 ml of 1 *M* hydrochloric acid and 2 ml of chloroform were placed in an 11-ml screw-capped Sovirel glass tube. After vigorous shaking for 15 min and centrifugation at 500 *g* for 10 min, the lower (organic) layer was transferred into a centrifuge glass tube with a short conical bottom and evaporated to dryness under a gentle stream of nitrogen at 40°C. The residue was reconstituted in 200 μl of electrophoresis running buffer and shaken for about 60 s.

Pentane extraction. Liquid–liquid extraction with pentane at pH 6.4 was also investigated for feasibility with the seven barbiturates. A 0.5-ml volume of serum (plasma), 1 ml of phosphate buffer (pH 6.4) and 5 ml of *n*-pentane were placed in an 11-ml screw-capped Sovirel test-tube. After vigorous shaking for 10 min and centrifugation at 1000 *g* for 10 min, the upper (organic) phase was transferred into a centrifuge glass tube with a conical bottom and evaporated to dryness under a gentle stream of nitrogen at 40°C. The residue was dissolved in 200 μl of running buffer and vortexed for 30 s.

Sample preparation for direct injection

Biological fluids were filtered using 0.2-μm Nalgene (25 mm diameter) disposable syringe filters (Nalge, Rochester, NY, USA) prior to sample injection.

Recovery

The recovery after sample pretreatment was determined by comparing electrophoretic peak areas after extraction with peak areas obtained by direct injection of equal amounts of the drugs in buffer.

RESULTS AND DISCUSSION

Analysis of barbiturates in human serum (plasma)

Multi-wavelength detection allows the monitoring of components that do not absorb at equal wavelengths in a single experiment. The three-dimensional electropherograms depicted in Fig. 2 represent the absorbance *vs.* retention times *vs.* wavelength relationships for a model mixture of seven barbiturates (see Fig. 1). Peak 5a represents an isomer of thiopental found in commercial thiopental, which was previously detected by HPLC [8]. Each component is characterized by its retention/migration behaviour with barbital being the fastest and pentobarbital the slowest of the investigated components. Barbiturates have pK_a values between 7.3 and 8.1 and are therefore all partially ionized at pH 7.8, hence they are migrating against the electroosmotic flow (same direction as SDS micelles). Partitioning between the buffer and the micelles is also occurring, as there is evidence that they elute in order of increasing pK_a values (*e.g.*, the pK_a values of phenobarbital, thiopental, amobarbital and pentobarbital are 7.4, 7.5, 7.9 and 8.1, respectively [20]). This correlates with the decrease in negative charge with increasing pK_a. The absorption spectrum of each

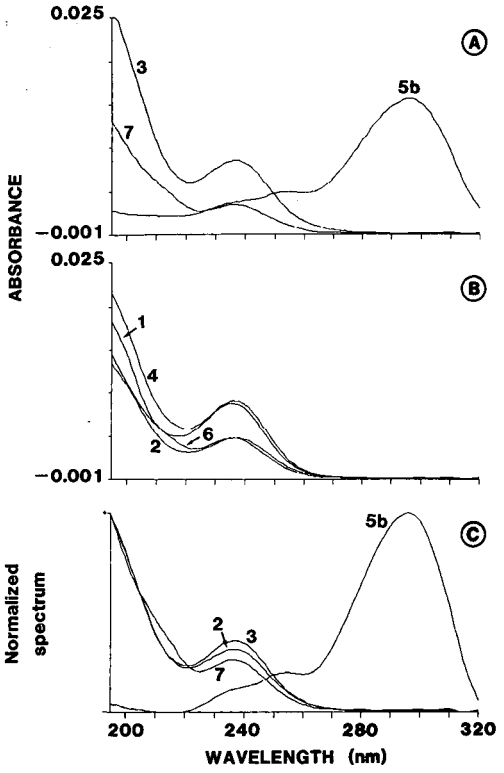

Fig. 3. (A, B) Absorption spectra and (C) normalized spectra obtained as time slices from data in Fig. 2A.

compound can be extracted from the gathered data points as so-called time slices (Fig. 3A and B). With the exception of thiopental, there is great similarity between these absorbance *vs.* wavelength relationships. The spectra were found to compare well with those measured on a regular spectrophotometer, with the exception that the absorbance with the Model 206 detector was higher at 195 nm. For the sake of comparison, normalized spectra, such as those shown for thiopental, pentobarbital, phenobarbital and allobarbital (Fig. 3 C), are employed.

For the monitoring of barbiturates in patients' samples, different extraction methods were investigated. In Fig. 2B–D three-dimensional pherograms of the seven barbiturates extracted from spiked bovine plasma using Bond-Elut C_{18} (B), chloroform (C) and pentane (D) pretreatment procedures are shown. The detected peaks could easily be identified by comparison of their spectra with those obtained from Fig. 2A and from their retention time (time of detection) relative to a known compound (*e.g.*, thiopental). Small peaks, such as that for butalbital after pentane extraction (peak 4 in Fig. 2D), were also verified by addition of a small amount of the drug to the reconstituted sample. It is clear from these results that (i) the early eluting barbiturates are poorly extracted by the Bond-Elut C_{18} procedure, (ii) all seven barbiturates are extracted well with acidified chloroform and (iii) the pentane extraction method is specific for thiopental. Recoveries, calculated from measured peak areas obtained with the automated apparatus (data not shown), are listed in Table I. It should be noted that

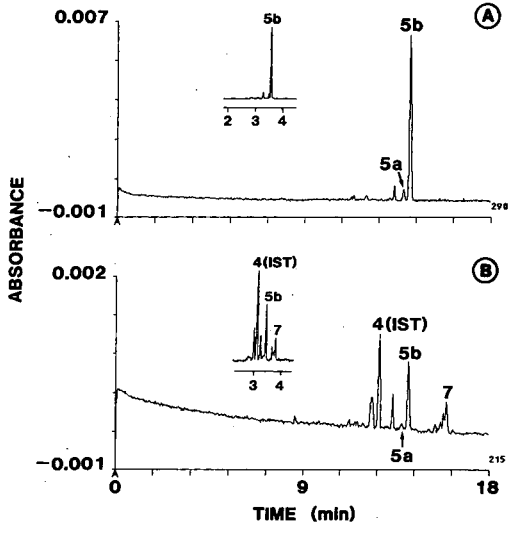

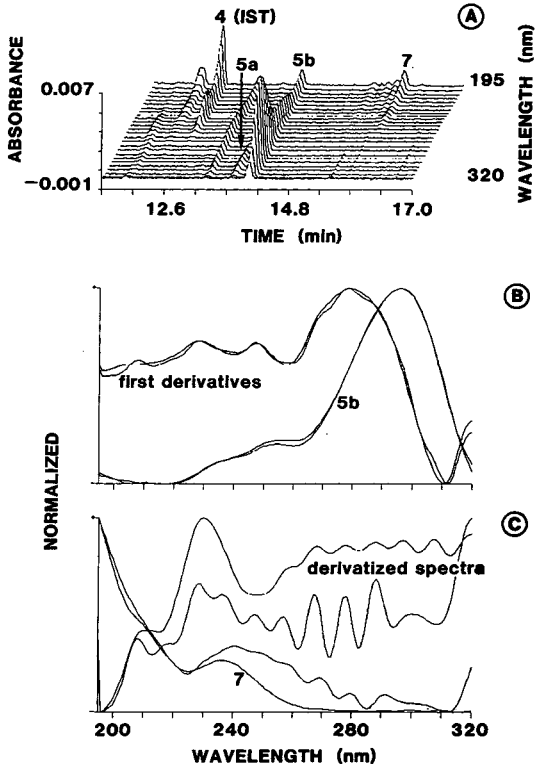

Fig. 4. Single-wavelength electropherograms (A, 290 nm; B, 215 nm) of a human serum sample after Bond-Elut C_{18} extraction. Conditions as in Fig. 2. The insets depict the corresponding pherograms obtained on the automated instrument with application of a constant 30 kV (70 μA) and having the plotting scale four-fold smaller for the 290-nm than the 215-nm data.

Fig. 5. (A) Three-dimensional data plot together with normalized time slices (spectra) of (B) thiopental and (C) pentobarbital of the serum sample in Fig. 4. Normalized and first derivatives are compared with those of the model compounds in Fig. 2.

TABLE I

RECOVERIES OF BARBITURATES

The values given represent percentage recovered, expressed in 5% increments. ND denotes that, under the described conditions, the component was not detectable with the ABI 270A. VL means that the component was detected as a very small peak which could not be reliably quantified. The investigated sample concentrations are listed under the matrix labels and calculated concentrations in case of 100% recovery (maximum concentrations after sample pretreatment) are given under the extraction procedures. The ratio of the two values provide a maximum concentration factor associated with an extraction procedure.

No.	Barbiturate	Matrix			
		Bovine plasma (33.3 μg/ml)	Bovine plasma (50 μg/ml)	Bovine plasma (62.5 μg/ml)	Human urine (10 μg/ml)
		Extraction			
		Bond-Elut C_{18} (82.5 μg/ml)[a]	Pentane (125 μg/ml)[a]	Chloroform (125 μg/ml)[a]	Bond-Elut Certify (250 μg/ml)[a]
1	Barbital	10	ND	60	VL
2	Allobarbital	20	ND	55	15
3	Phenobarbital	25	ND	75	65
4	Butalbital	65	VL	80	90
5b	Thiopental	85	45	80	75
6	Amobarbital	95	5	70	90
7	Pentobarbital	95	5	70	95

[a] Maximum concentration.

in all these investigations high barbiturate concentrations were employed. Concentrations in spiked bovine serum were between 33.3 and 62.5 μg/ml. Depending on the extraction procedure and assuming a 100% recovery, maximum barbiturate concentrations after sample pretreatment were therefore in the range 82.5–125 μg/ml (Table I). It was interesting to find that reconstituted samples after the extraction with chloroform had to be measured within 1–2 days, whereas the other samples appeared to be stable for more than 1 week when stored at 4°C.

On measuring blank human serum or blank bovine plasma, no peaks were found with all three extraction procedures when analysed in the range 195–320 nm (data not shown). However, investigation of serum samples from patients undergoing thiopental pharmacotherapy for several days or from toxicological specimens revealed bands that could be identified as one of the seven barbiturates. Using a serum sample from a patient under thiopental pharmacotherapy, spiked with butalbital (20 μg/ml) as internal standard and extracted with Bond-Elut C_{18}, single-wavelength data at 290 nm suggested the presence of thiopental (Fig. 4A). From the data obtained at 215 nm one could assume the presence of up to four or five barbiturates (Fig. 4B). Data obtained at two wavelengths are clearly insufficient for proper assignment of the peaks, but it is pleasing to note that the patterns obtained with the two instruments agree very well. By scanning from 195 to 320 nm while the zones were transported through the detector cell, the data depicted in Fig. 5A were obtained. Analysis of this run reveals that the time slice at 14.1 min, and also its first derivative, agree extremely well with those of

thiopental (Fig. 5B). The same is true for the internal standard, butalbital, at 12.7 min (data not shown). According to the retention, the peak at 15.95 min was assumed to be pentobarbital, a metabolite of thiopental. Graphical presentation of the time slice and its first derivative with standard data for pentobarbital does not prove the identity of the two compounds (Fig. 5C). The peak here is unfortunately too small for proper assignment by spectral comparison. The sample had to be spiked with pentobarbital and re-run for proper analysis. This example reveals that the signal should be larger than 0.001 absorbance for sample verification by spectral information obtained with the UVIS 206 detector. Linear regression of the detection times of butalbital, thiopental and pentobarbital from this run with the corresponding values from the experiment depicted in Fig. 2A revealed a correlation coefficient of 0.9999.

Preliminary attempts at the quantification of pentobarbital and thiopental in human plasma were performed by the internal standard method using butalbital (20 μg/ml, Figs. 4 and 5A) as reference compound, the Bond-Elut C_{18} extraction procedure and the automated instrument. Peak-area ratios were employed as the basis for data evaluation. Calibration graphs were constructed with spiked bovine plasma in the concentration range 1–60 μg/ml (eight data points). Pentobarbital was monitored at 215 nm whereas thiopental was measured at 215 and 290 nm. All three graphs showed good linearities with correlation coefficients of 0.994, 0.977 and 0.988,

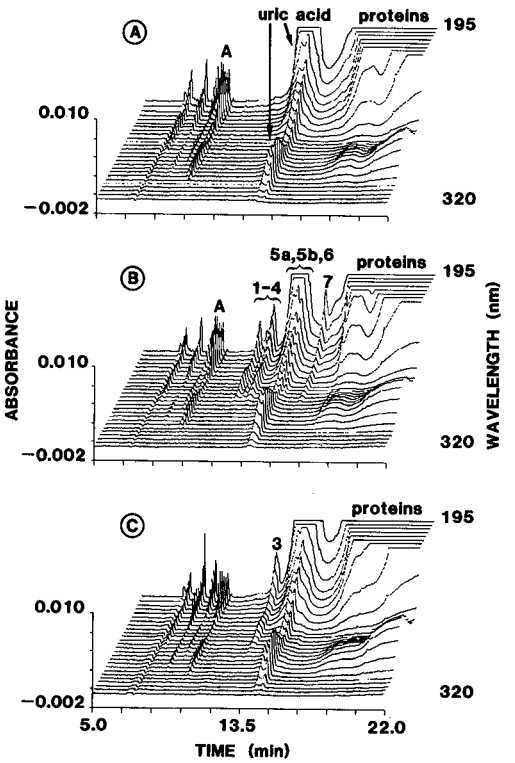

Fig. 6. Three-dimensional electropherograms obtained with direct injection of human serum having (A) blank serum, (B) blank serum spiked with barbiturates and (C) serum from a patient undergoing phenobarbital pharmacotherapy. A represents a group of three resolved peaks, the centre one being caffeine.

respectively, and passed through the origins. For the example presented in Figs. 4 and 5A the pentobarbital concentration was determined to be 4.9 μg/ml and the thiopental content was found to be 21.2 and 18.5 μg/ml for the calibrations at 215 and 290 nm, respectively, representing pharmacologically meaningful data [1–4].

The data presented in Fig. 6 were obtained with human serum samples which were only passed through a 0.2-μm syringe filter prior to sample injection. The data for the blank serum shown in Fig. 6A reveal that only components eluting between caffeine (here the peak at 9.54 min) and uric acid (the so-called analytical or separation window [14]) have a chance to be analysed with direct sample application, *i.e.*, without extraction. Analysis by an enzyme-multiplied immunoassay technique (EMIT) revealed a caffeine concentration of 4.43 μg/ml (22.8 μ*M*). Serum proteins are solubilized by the micelles and elute (as a very broad zone) after uric acid. The data depicted in Fig. 6B were obtained with the blank human serum which was spiked with the barbiturates in Fig. 1. The first four drugs were found to form their zones in front of uric acid, thiopental and amobarbital to coelute with uric acid and pentobarbital to be located in the "valley" between the broad uric acid band and the proteins. The suitability of direct sample introduction for drug monitoring is demonstrated with the example shown in Fig. 6C. A serum sample from a patient undergoing phenobarbital pharmacotherapy was injected, producing a clear phenobarbital zone within the analytical window. Its normalized spectrum was in good agreement with that given in Fig. 3 (data not shown). The serum concentration of phenobarbital was determined to be 20.4 μg/ml (88 μ*M*) using an EMIT. Hence HPCE–MECC permits the determination of serum phenobarbital at the pharmacologically interesting concentration level (the therapeutic range of this barbiturate is 10–30 μg/ml) and without elaborate sample pretreatment. It is interesting that bovine plasma does not exhibit a characteristic analytical window (data not shown).

Identification of barbiturates in human urine

Direct injection of urine provides very complex pherograms which precludes the determination of barbiturate concentrations at the μg/ml (μ*M*) level (see also ref. 10; three-dimensional data not shown). Fig. 7 depicts data obtained with a blank urine (A and B), illustrating that very few peaks are detected after extraction with Bond-Elut Certify at pH 6. One zone could be assigned to caffeine. The response of the seven investigated barbiturates after the extraction is depicted in Fig. 7C and calculated recoveries are listed in Table I. Similarly to the Bond-Elut C_{18} treatment, barbital and allobarbital are shown to be poorly extracted. Good recoveries were obtained for the other five barbiturates.

A urine specimen obtained from the emergency care unit was found to be markedly positive for benzodiazepines, cocaine, opiates and barbiturates using EMIT drug-screening procedures and for cannabinoids using a fluorescence polarization immunoassay. This very interesting, complex sample was pretreated with Bond-Elut Certify as described above and analysed with both instruments. Single-wavelength data for 290 and 215 nm obtained on the two instruments are depicted in Fig. 8A and B, respectively, and three-dimensional multi-wavelength data are presented in Fig. 9. Analysing this sample at one or two wavelengths is clearly insufficient for identification of the unknown peaks. Knowing the behaviour of barbiturates in that system, and looking at the data obtained at 290 nm, the presence of thiopental can be suspected.

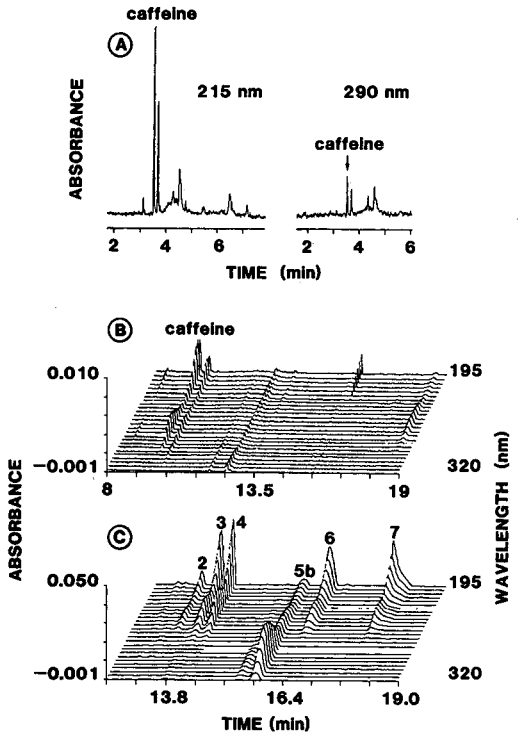

Fig. 7. Data for (A, B) blank urine and (C) blank urine spiked with seven barbiturates after Bond-Elut Certify extraction. Single-wavelength data (A) were obtained on the automated instrument with a constant 30 kV (70 μA). The three-dimensional data (B, C) were collected as described for Fig. 2. Barbiturate concentrations and recoveries are listed in Table I.

Spiking of the sample with this compound and re-running the experiment would indeed show an increase in the size of the larger peak in this pattern. This, however, would not provide complete proof but only confirmation that the presumption could be correct. Having data between 195 and 320 nm, as shown in Fig. 9A and B, and also reference spectra of barbiturates (Fig. 3) permitted a quick and reliable confirmation of the presence of thiopental and its metabolite, pentobarbital, in that sample. As is shown in Fig. 9C, there is excellent agreement between the time slices at 12.67 and 13.99 min with those for thiopental and pentobarbital, respectively.

Single- and multi-wavelength data obtained from a barbiturate-positive (benzodiazepine-negative) patient's sample (screening with EMIT; patient from the department's out-patient clinic) are presented in Figs. 10 and 11, respectively. Comparison with blank data reveals the appearance of one major peak which could be a barbiturate. Again, with detection at 215 and 290 nm (Fig. 10), identification is not possible. According to its spectrum and retention (Fig. 11A), one can conclude that it represents either allobarbital (Fig. 11B) or phenobarbital (Fig. 11C). However, the absorption spectra of these two compounds are very similar, which makes proper identification difficult. Also, the retention time intervals in our instrumental set-up

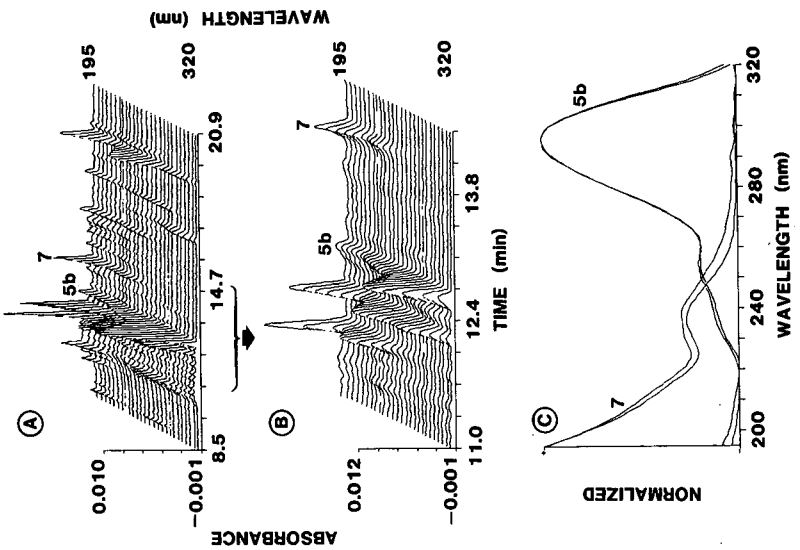

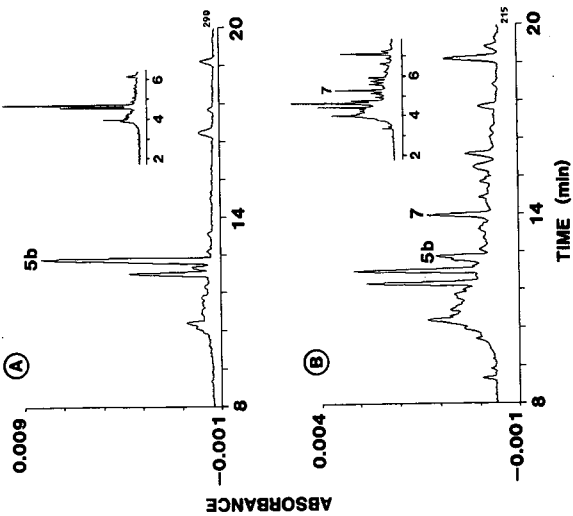

Fig. 8. Analysis of a Bond-Elut Certify pretreated toxicological urine specimen with detection at (A) 290 and (B) 215 nm. The insets depict the data obtained on the automated instrument. Conditions as in Fig. 7.

Fig. 9. (A) Three-dimensional data plot, (B) plot with expanded time and absorbance scales and (C) normalized spectra of thiopental and pentobarbital of the urine specimen in Fig. 8. There is excellent agreement between the normalized spectra of the two barbiturates from that experiment with those in Fig. 7C.

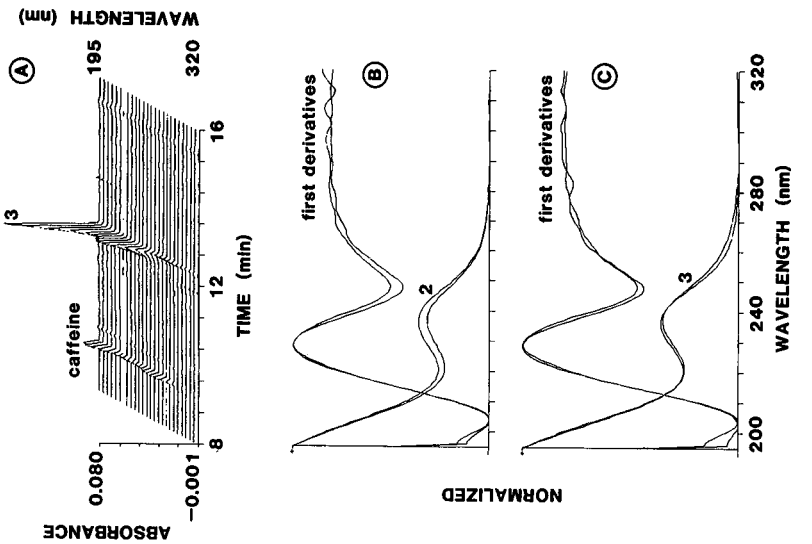

Fig. 11. (A) Three-dimensional electropherogram together with data analysis by normalized time slices for (B) allobarbital and (C) phenobarbital of the urine sample in Fig. 10.

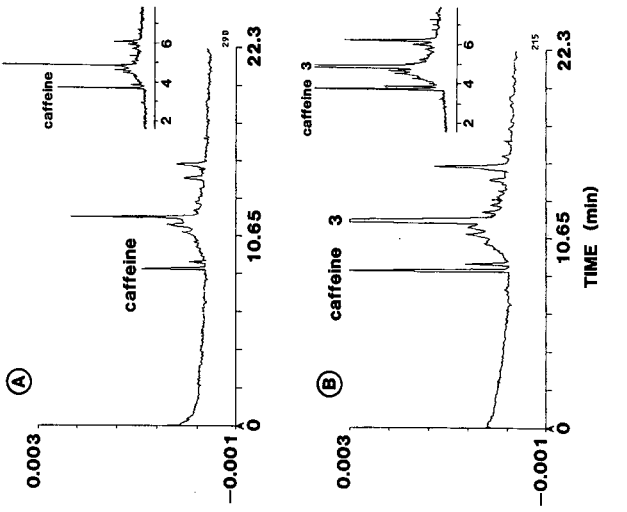

Fig. 10. Single-wavelength analysis of a Bond-Elut Certify pretreated urine sample containing one major peak with possible barbiturate identity. Conditions as in Fig. 8.

with manual sample introduction vary too much for this parameter to be used reliably for identification purposes. For complete confirmation this sample had to be spiked with phenobarbital. The example demonstrates that even with multi-wavelength monitoring zone assignment can be difficult when the retention behaviour and spectra are similar. This calls for the use of a combined technique, such as the on-line coupling of HPCE–MECC with mass spectrometry (MS). It is interesting to add that there is a small background interference at the location of phenobarbital in all pherograms in Figs. 7, 10 and 11.

CONCLUSIONS

These experiments have demonstrated the feasibility of monitoring barbiturates in human serum (plasma) and urine by HPCE/MECC with on-column multi-wavelength absorbance detection between 195 and 320 nm and using a phosphate–borate buffer of pH 7.8 containing 50 m*M* SDS. This approach is attractive for (i) drug and metabolite investigations, (ii) barbiturate identification in toxicological samples and (iii) efficient characterization of sample pretreatment schemes and the suitability of direct injection of urine and serum. The data indicate that some (including phenobarbital) but not all of the serum barbiturates investigated can be analysed without extraction. The preliminary quantitative results suggest the suitability of using HPCE–MECC as a therapeutic drug monitoring method for serum barbiturates. Extraction prior to analysis is necessary for urine barbiturates.

Characterization of sample zones by their retention behaviour and absorption spectra is a powerful approach for solute identification. In fact, having HPCE technology with multi-wavelength detection (as described here), its combination with MS [21,22] or HPLC [23] and together with the distinct advantages of electrokinetic capillary analyses (automation, small sample size, ease of buffer change and speed of analysis), HPCE–MECC may well become the most important analytical and confirmation method for drugs and metabolites in body fluids.

ACKNOWLEDGEMENTS

The authors acknowledge the valuable contributions of Dr. V. Purghart during the assembly phase of the laboratory-made instrument and Dr. P. Gebauer for performing the analyses with direct sample injection. The generous loan of the UVIS 206 detector by Linear Instruments, and of the HCN power supply by Mettler–Toledo (Greifensee, Switzerland) is gratefully acknowledged. This work was partly sponsored by the Research Foundation of the University of Berne and the Swiss National Science Foundation.

REFERENCES

1 R. F. Shaw, *Barbiturates (Abused Drugs Monograph Series)*, Abbott Laboratories, Diagnostics Division, Irving, TX, 1988; and references cited therein.
2 B. E. Pape, P. L. Cary, L. C. Clay and W. Godolphin, *Ther. Drug Monit.*, 5 (1983) 467.
3 A. T. Watson, J. E. Manno and B. R. Manno, *J. Anal. Toxicol.*, 7 (1983) 257.
4 D. L. Colbert, D. S. Smith, J. Landon and A. M. Sidki, *Clin. Chem.*, 30 (1984) 1765.
5 D. Berry, *J. Chromatogr.*, 86 (1973) 89.

6 C. Salvadori, R. Farinotti, Ph. Duvaldestin and A. Dauphin, *Ther. Drug Monit.*, 3 (1981) 171.
7 G. K. Shiu and E. M. Nemoto, *J. Chromatogr.*, 227 (1982) 207.
8 D. R. Stanski, P. G. Burch, S. Harapat and R. K. Richards, *J. Pharm. Sci.*, 72 (1983) 937.
9 M. C. Roach, P. Gozel and R. N. Zare, *J. Chromatogr.*, 426 (1988) 129.
10 Y. Tanaka and W. Thormann, *Electrophoresis*, 11 (1990) 760.
11 T. Nakagawa, Y. Oda, A. Shibukawa and H. Tanaka, *Chem. Pharm. Bull.*, 36 (1988) 1622.
12 T. Nakagawa, Y. Oda, A. Shibukawa, H. Fukuda and H. Tanaka, *Chem. Pharm. Bull.*, 37 (1989) 707.
13 H. Nishi, T. Fukuyama, M. Matsuo and S. Terabe, *J. Chromatogr.*, 513 (1990) 279.
14 H. Nishi, T. Fukuyama and M. Matsuo, *J. Chromatogr.*, 515 (1990) 245.
15 H. Nishi and S. Terabe, *Electrophoresis*, 11 (1990) 691.
16 M. Hayashida, M. Nihira, T. Watanabe and K. Jinno, *J. Chromatogr.*, 506 (1990) 133.
17 S. Kobayashi, T. Ueda and M. Kikumoto, *J. Chromatogr.*, 480 (1989) 179.
18 J. Vindevogel, P. Sandra and L. C. Verhagen, *J. High Resolut. Chromatogr.*, 13 (1990) 295.
19 K. Weinberger, *Am. Lab.*, December (1989) 12.
20 V. Dinnendahl and U. Fricke, *Arzneistoff-Profile*, Govi-Verlag, Frankfurt, 1987.
21 E. D. Lee, W. Mueck, J. D. Henion and T. R. Covey, *J. Chromatogr.*, 458 (1988) 313.
22 C. G. Edmonds, J. A. Loo, C. J. Barinaga, H. R. Udseth and R. D. Smith, *J. Chromatogr.*, 474 (1989) 21.
23 M. M. Bushey and J. W. Jorgenson, *Anal. Chem.*, 62 (1990) 978.

Journal of Chromatography, 545 (1991) 461–470
Elsevier Science Publishers B.V., Amsterdam

CHROM. 23 142

Characterization of humic substances by capillary isotachophoresis

PETR KOPÁČEK*

Laboratory of Analytical Chemistry, South Bohemian Biological Centre, Czechoslovak Academy of Sciences, Branišovská 31, CS-37005 České Budějovice (Czechoslovakia)

DUŠAN KANIANSKY

Institute of Chemistry, Komenský University, Mlynská Dolina CH-2, CS-84215 Bratislava (Czechoslovakia)

and

JOSEF HEJZLAR

Hydrobiological Institute, Czechoslovak Academy of Sciences, Na sádkách 7, CS-37005 České Budějovice (Czechoslovakia)

ABSTRACT

The use of capillary isotachophoresis (ITP) for the characterization of humic substances was studied. ITP separations of these complex mixtures were considerably improved on the addition of polyvinylpyrrolidone (PVP) to the leading electrolyte. It was preferred to work in the spike mode to improve the interpretability of the isotachopherograms obtained using a photometric detector (405 nm). Interaction of PVP with humic substances was found to differentiate humic and fulvic acids. ITP was useful also for characterizing differences in the molecular weights and hydrophobicities of humic substances fractionated by chromatography on Sephadex G-50 and on Phenyl-Sepharose CL-4B.

INTRODUCTION

Humic substances (HS) are complex mixtures of organic compounds formed in soil and water by chemical and biological degradation of plant and animal residues and by synthetic activities of microorganisms. From the physico-chemical point of view they are dark-coloured polymeric organic acids with high numbers of carboxylic and phenolic groups [1]. At present, separation methods fails to separate these complex mixtures into individual chemical. Nevertheless, their partial separations, based on well defined physical and/or chemical principles, are useful in understanding the nature and properties of HS.

The ionogenic nature of water-soluble HS enables electrophoretic separation methods to be employed for their characterization. Zone electrophoresis of HS in polyacrylamide gel [2,3], isoelectric focusing [4] and isotachophoresis (ITP) in polyacrylamide gel [5,6] are examples of the use of various electrophoretic methods for these purposes. Of these, the highest resolution has been reported for isoelectric

0021-9673/91/$03.50

focusing [6], and the resolving power of the ITP separation could be improved by adding ampholytic mixtures (continuous spacing constituents) to the samples [5,6].

In this work we studied potential of capillary ITP for characterizing HS and results concerning the optimization of the ITP working conditions are presented.

EXPERIMENTAL

Instrumentation

A CS isotachophoretic analyzer (VVZ PJT, Spišská Nová Ves, Czechoslovakia) was assembled with the column-coupling configuration of the separation unit [7,8] using modules provided by the manufacturer. The analytical column was equipped with a UVD 01 photometric detector (VVZ PJT).

The signals from the detectors were registered by a two-channel line recorder and that from the photometric detector (405 nm) was registered in parallel by an SP 4270 integrator (Spectra-Physics, Darmstadt, Germany).

The driving currents were 200 and 45 μA in the preseparation and analytical columns, respectively. Mixtures of discrete spacers (27 constituents) were chosen from the constituents suitable for this purpose [9]. The spacers were injected with the aid of a 30-μl sample loop and the sample was injected with a microsyringe (Hamilton, Bonaduz, Switzerland). The analysis was completed in *ca.* 28 min. For other experimental data, see Table I.

Chemicals for ITP experiments

Solutions of the leading and terminating electrolytes were prepared from chemicals of the highest available purity provided by Sigma (St. Louis, MO, U.S.A.), Fluka (Buchs, Switzerland) and Pierce (Rockford, IL, U.S.A.). Hydroxyethylcellulose (HEC) was used as an anticonvective additive in the leading electrolyte solutions. The preparation obtained (Serva, Heidelberg, Germany) was purified on a mixed-bed ion exchanger (Duolite MB; Duolite, France). Polyvinylpyrrolidone 360 000 (PVP) (Lachema, Brno, Czechoslovakia) was deionized in the same way as HEC.

Distilled water, further deionized on a mixed-bed ion exchanger (Duolite, MB), was used for the preparation of the solutions.

TABLE I

OPERATIONAL SYSTEMS

Solvent	Water
Leading anion	Cl^-
Concentration (m*M*)	10
Counter ion	β-Alanine
Additive to the leading electrolyte	0.1% (w/v) HEC
Co-additive to the leading electrolyte	0–2.5% (w/v) PVP[a]
pH of the leading electrolyte	3.50
Terminating anion	$(Caproate)^-$
Concentration (m*M*)	5

[a] For actual concentrations of PVP, see the legends to the figures and the text.

Humic substances and their preparations

HA-Fluka. Humic acid (HA) with molecular weight in the range 600–1000 dalton was obtained from Fluka (Cat. No. 53 680). A stock solution (0.2%, w/v) was prepared by dissolving the acid in a 10^{-3} mol/l aqueous solution of sodium hydroxide. The pH of the solution was adjusted to 5.0 on addition of morpholinoethanesulphonic acid (MES). Five-fold diluted stock solution was taken for ITP experiments.

HA-1, FA-1 and HyA-1. Humic, fulvic and hydrophilic acids were isolated from peatbog water sampled at Borkovické Blato, a bog area in South Bohemia. Humic (HA-1) and fulvic (FA-1) acids were obtained on an Amberlite XAD-8 (Serva) packed column by using the procedure described by Thurman and Malcolm [10]. In our modification of the procedure, dialysis in a Spectra/Por 6 tube (molecular weigth cut-off 1000; Spectrum, Los Angeles, CA, U.S.A.) was used instead of gel chromatography to remove low-molecular-weight compounds.

The effluent from the XAD-8 column was collected, its pH was adjusted to 4.5 and it was percolated through a column packed with a weak anion exchanger in the Cl^- form (Spheron-DEAE; Lachema). Hydrophilic acids (HyA-1) trapped on the column were eluted with a 10^{-1} mol/l aqueous solution of sodium hydroxide. The eluate was treated with Dowex 50W (H^+) cation exchanger and was finally lyophilized.

HA-2, FA-2 and HS-2. Nordic humic and fulvic acids, and lyophilized water from Hellerundmyra, a bog area near Oslo (Norway), were used [11]. HA-2 and FA-2 were isolated using the same method as for International Fulvic and Humic Acids [10]. HS-2 was prepared by 200-fold concentration of the filtered water (0.45 μm) by vacuum evaporation and lyophilization.

X1, I, II, IIIa and IIIb. Fractions of humic substances isolated from water from the Mirochovské blato peatbog, near Třeboň (South Bohemia) were used. The procedure of Mantoura and Riley [12] employing Amberlite XAD-2 resin was used to isolate the humic substances. They were neutralized with Dowex 50W (H^+) cation exchanger, freed from low-molecular-weight constituents by dialysis with a Spectra/Por 6 tube (see above) and lyophilized (sample X1). This sample was fractionated by gel chromatography on Sephadex using the procedures of Wershaw and Pinckney [13] and Hejzlar [14].

(a) A 1% solution of the sample X1 dissolved in distilled water at pH 12 (adjusted with sodium hydroxide) was applied on a Sephadex G-50 column. Water was used as the eluent (see Fig. 4a, separation 1). Three main fractions were collected (I, II and III).

(b) Fraction III was mixed with sodium chloride (15.5 g/l), its pH was adjusted to 7.0 and it was further separated on the same Sephadex G-50 column. On elution with water (Fig. 4a, separation 2) two fractions, IIIa and IIIb, were obtained.

The acids present in the fractions obtained from X1 were converted into the H^+ forms and lyophilized. These samples were reconstituted in water before the analysis (0.4 mg/ml). A detailed description of the isolation and characterization of X1 and related fractions can be found elsewhere [15].

1P, 2P, 3P and 4P. Fractions of HA-Fluka (see above) were obtained by hydrophobic chromatography on a Phenyl-Sepharose Cl-4B (Pharmacia, Uppsala, Sweden) column with a 4-ml bed volume.

A 1-ml sample volume (2 mg/ml) placed on the column was eluted with 3 ml of

distilled water and the eluate was trapped into three fractions (1P, 2P and 3P). Fraction 4P remained retained at the top of the sorbent bed (Fig. 5a). It was eluted with 8 ml of a 2% (w/v) solution of Triton X-100. No further preparation of the fractions was needed before their ITP analyses (differences in the concentrations of HS in the fractions were compensated for by sample injection volumes).

RESULTS AND DISCUSSION

ITP separation of humic substances

Humic substances migrate anionically and with high effective mobilities within the pH range currently employed in ITP. A large number of the constituents present in such samples are responsible for the appearance of the isotachopherograms (features typical of complex ionic mixtures). Their spectral properties [16] are favourable for achieving a high detection selectivity in ITP and, therefore, photometric detection at 405 nm was chosen. To improve the interpretability of the isotachopherograms obtained with the photometric detector, we preferred the work in the spike mode [17] with discrete spacing constituents added to the sample (Fig. 1b).

From the isotachopherogram in Fig. 1b it is apparent that also at a low pH of the leading electrolyte the main part of the acids migrated with effective mobilites close to that of the leading ion. Such a limited mobility span of HS indicates a poor capability of ITP from the point of view of differentiation of this group of constituents. A lower pH of the leading electrolyte (pH < 3.5) did not provide any improvement in this respect [18] and, in addition, it could be critical from the point of view of precipitation of some sample constituents [16]. A considerable improvement in the separation conditions was possible [18] when the counter-ionic constituent of an

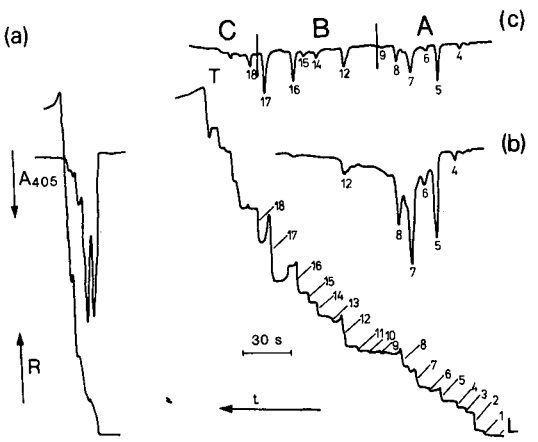

Fig. 1. Isotachopherogram from the separation of HA-Fluka. (a) Conductivity and photometric detector records as obtained for a 5-μl injection volume (for the sample description, see Experimental) in the electrolyte system (Table I) without PVP; (b) same as (a) except that a 30-μl volume of the spacers (each at a 0.05 m*M* concentration) was also injected; (c) same as (b) (the sample volume was 10 μl) except that the leading electrolyte contained 0.025% of PVP. The conductivity detector records were nearly identical for (b) and (c). A, B and C = symbols for the mobility regions in the span leading (L)–terminating (T) ions. 1–18 = Numbers of boundaries between discrete spacers [9].

appropriate charge number was present in the leading electrolyte [19]. However, this approach has the drawback that the effective mobilities of the spacing constituents are influenced to such an extent that a small difference in the concentration of the counter-ionic constituents may require a new search for suitable spacers. The use of β-cyclodextrin in the leading electrolyte to differentiate HS was also studied [18]. However, its influence on the effective mobilities of this group of separands was only marginal.

The best results were achieved on addition of PVP to the leading electrolyte. This polymer was used as it has already been shown [20] that it has a considerable influence on the effective mobilities of some acids representing monomeric units of HS. A detailed discussion of the interaction was given by Molyneux and Vekavakayanodha [21]. The influence of PVP on the effective mobilities of some of the HS was considerable also at a very low concentration of the polymer while the mobilities of the spacing constituents remained uninfluenced (see Fig. 1b and c).

A high run-to-run reproducibility of the profiles obtained from the photometric detector was achieved for given sample of HS. The record from the conductivity detector demonstrated a rapid loss of the detector performance owing to the adsorption of HS on its contacts. Hence, frequent electric cleaning of the conductivity detector was necessary.

From the many photometric detector profiles (see, *e.g.*, Fig. 3a or 4b), it is apparent that the humic substances did not migrate exclusively on the boundaries between the discrete spacers but mixed zones of HS and spacing constituents were also formed. This was also confirmed by the conductivity detector records, which differed from that shown in Fig. 1b for various HS samples tested. The principal of characterization of HS used in this work is based on a comparison of the distributions of various HS samples within the mobility span but not on the correct isotachophoretic separation of these complex mixtures. Therefore, the occurrence of mixed zone formation is not really a serious drawback in this respect.

The mobility span between the leading and terminating anions was divided into three regions (A, B and C as shown, *e.g.*, in Fig. 1c) for a more convenient visualization of the distribution of the HS along this span.

The influence of the concentration of PVP on the effective mobilites of HS is illustrated in Fig. 2. It can be seen that when its concentration in the leading electrolyte was higher than 0.1% (w/v) some of the analytes had effective mobilities lower than that of the terminating anion. At very high concentrations of the polymer (up to 2.5%), however, 15–30% of HS still migrated isotachophoretically. A 0.025% concentration of PVP in the leading electrolyte was the optimum as the desired distribution of the effective mobilites of the separands was achieved at the same time only a negligible part of the migrating constituents was lost (migration in the terminating electrolyte).

The compositions of the electrolyte systems used throughout are given in Table I.

Differentiation of humic and fulvic acids

On the basis of their solubilities, HS are traditionally classified into three groups, *viz.*, humic acids (HA), fulvic acids (FA) and humin (for details see, *e.g.* refs. 1 and 16).

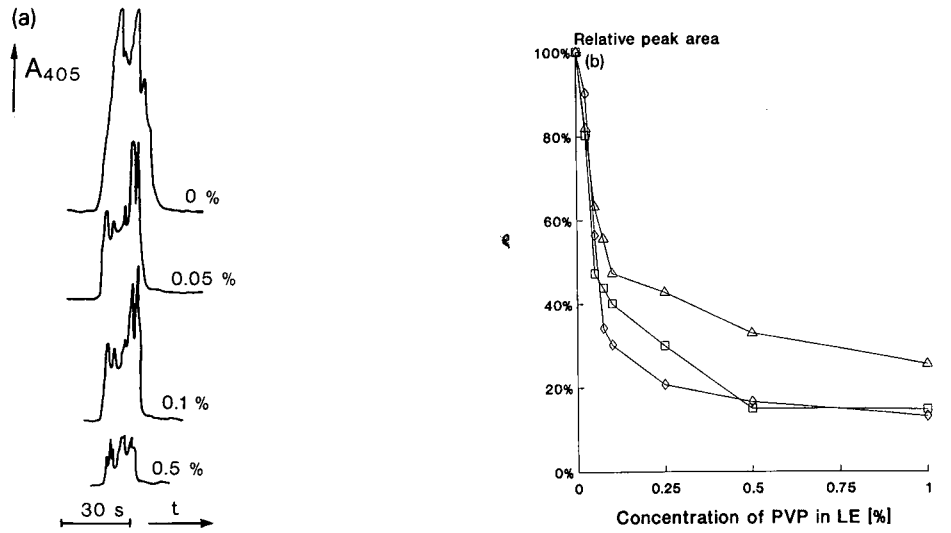

Fig. 2. Influence of PVP concentration on the migration of humic substances. (a) Profiles obtained from the photometric detector for various concentrations of PVP in the leading electrolyte (15-μl injection volumes); (b) graphical plots of dependence of the peak area on PVP concentration in the leading electrolyte. The peak areas are related to the area obtained in the run without PVP. Samples: □, HA-Fluka; ◇, HA-1; △, FA-1.

ITP profiles of some of the studied HA and FA (the acids were obtained as described under Experimental) are shown in Fig. 3a. The profiles, split into three regions (see above), show that the acids differ mainly in the occupancies of the C regions. Here, large parts of HS are present in HA samples whereas in FA this

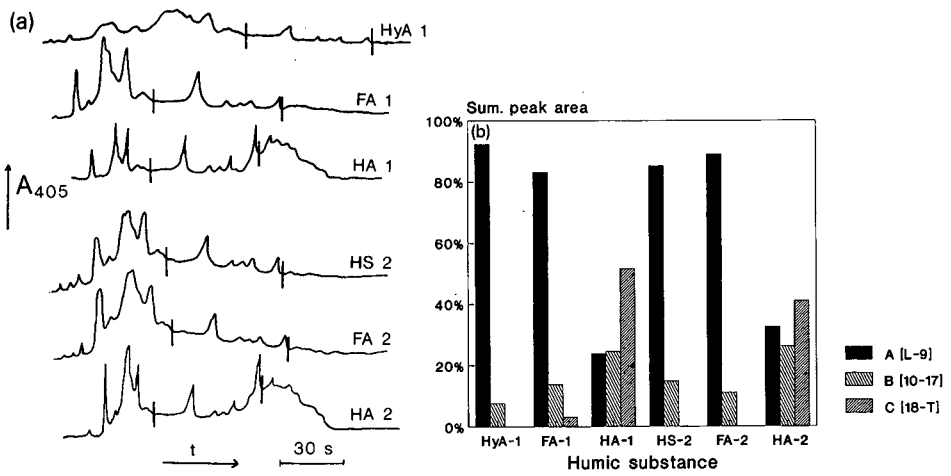

Fig. 3. Profiles of HS fractionated on an XAD resin. (a) Isotachopherograms obtained for 10-μl volumes of the XAD fractions of HS. The leading electrolyte contained 0.025% of PVP. The vertical bars divide the profiles into three mobility regions, A, B and C, from left to right. (b) Graphical representation of the profiles as evaluated on integration (sums of the relative peak areas within the mobility intervals, A, B and C are presented).

migration region is almost free of the analytes. It should be noted that without the use of PVP such a differentiation was impossible. This differentiation also did not exist when the concentration of the PVP in the leading electrolyte was higher than 0.1% (HS migrating in the C regions of the HA samples in Fig. 3 were retarded into the

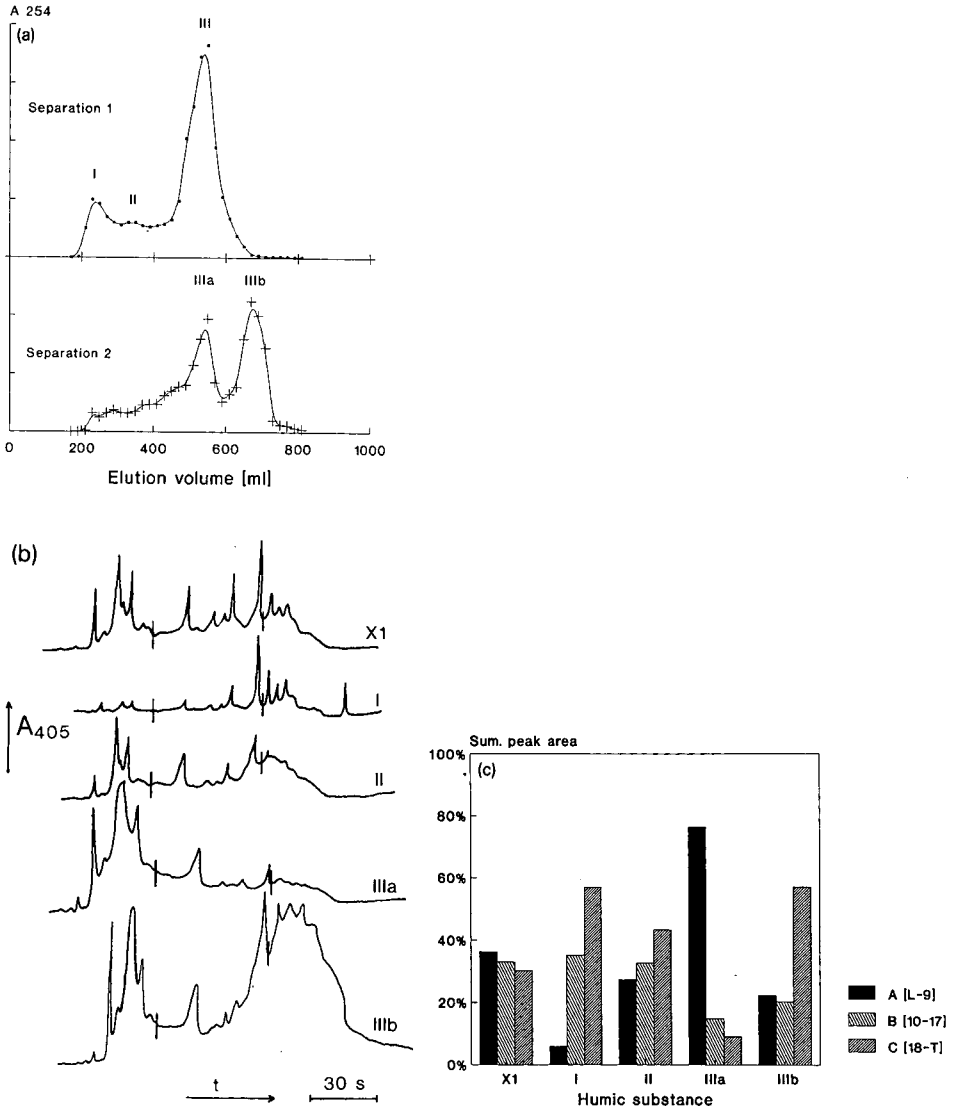

Fig. 4. Profiles of HS after fractionation on Sephadex G-50. (a) Chromatograms (254 nm) for gel chromatographic separation of X1 (separation 1) and for adsorption chromatography of fraction III (separation 2; see Experimental for details). (b) Isotachophoretic profiles of the original sample (X1) and the fractions. The leading electrolyte contained 0.025% PVP (10-μl injection volume). The vertical bars divide the profiles into three mobility regions, A, B and C, from left to right. (c) Graphical representation of the profiles of the sample and fractions (sums of the relative peak areas within the mobility intervals A, B and C are presented).

terminating zone). The effective mobilities of the constituents present in HyA-1 were influenced only negligibly by the use of PVP. It also apparent that the sample of water (HS-2) had a profile very similar to those of FA. This is in agreement with previous findings [22] that natural waters contain mainly FA.

It is known that HA have higher molecular weights and a higher content of aromatic structures than FA [1]. To decide which of these differences was responsible for the concentration of a large part of HA in the mobility region C, we carried out the experiments discussed below.

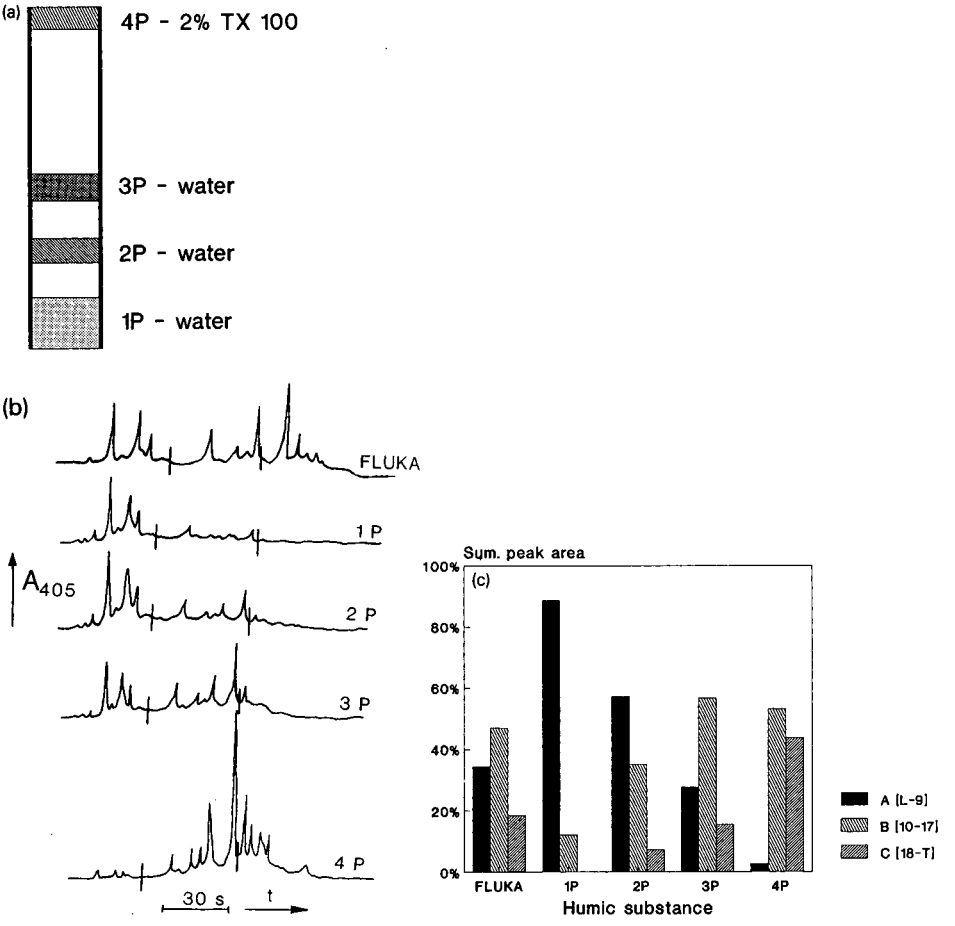

Fig. 5. Profiles of HS present in HA-Fluka after fractionation on Phenyl-Sepharose Cl-4B. (a) Schematic illustration of the fractionation of the sample on the column packed with Phenyl-Sepharose Cl-4B (for further details, see Experimental). (b) ITP profiles of the sample and fractions. The leading electrolyte contained 0.025% of PVP. Injection volumes were 5 μl for HA-Fluka, 1P, 2P and 3P and 50 μl for 4P. The vertical bars divide the profiles into three mobility regions A, B and C, from left to right. (c) Graphical representations of the profiles as in Figs. 3 and 4.

Separation on Sephadex G-50

The course of a two-step separation of X1 on a Sephadex G-50 column is shown in Fig. 4a. The first separation step was in fact gel chromatography, whereas during separation of fraction III (the second step) the experimental conditions (presence of sodium chloride) were such that adsorptive and hydrophobic effects also played a role [13]. Profiles of the original sample and fractions obtained by this two-step separation are shown in Fig. 4b. A graphical evaluation is shown in Fig. 4c. It is apparent that fraction I (containing the constituents with molecular weights > 50 000 dalton) hardly contains any of the most mobile constituents (poor A region in the profile). It is also clear that the presence of this group of constituents gradually increases in the fractions of lower molecular weight (Fig. 4c). The profile of fraction II is very close to that characteristic of the original sample (X1 in Fig. 4).

The elution volume of fraction IIIa coincided with the elution volume of fraction III (1000–5000 dalton). From its ITP profile (Fig. 4b), it can be seen that it consisted mainly of constituents with high effective mobilities. In contrast to other fractions these differences could be also detected in ITP experiments without PVP (not shown). The results suggest that HS fractions with higher molecular weights have lower effective mobilities than those with lower molecular weights. However, when PVP was present in the leading electrolyte, the behaviour of fraction IIIb (containing low-molecular-weight constituents when the elution data are considered) differed. It was found by ^{13}C NMR spectroscopy that this fraction contains a much higher ratio of aromatic structures [15], which are known to interact with PVP [20,21].

Separation on Phenyl-Sepharose Cl-4B

An HA-Fluka sample was fractionated on a Phenyl-Sepharose Cl-4B packed column (Fig. 5a). A comparison of the ITP profiles of the fractions and their graphical evaluations (Fig. 5b and c) with their elution orders (an increase with increasing hydrophobicity of the solute) shows that for the higher hydrophobicities of the fraction constituents a larger number of the constituents with low effective mobilities are present in it. However, in this instance low effective mobilities can be ascribed to the interaction of the separands with electroneutral PVP.

CONCLUSIONS

The results suggest that the presence of PVP in the leading electrolyte provides a means of determining the degree of hydrophobicity and thus the presence of aromatic structures of HA. In addition, the profiles also demonstrate differences in the molecular weights (or, better, molecular weight/charge number ratios).

Differences in hydrophobicities and molecular weights and associated solubilities of the constituents serve as a basis for classical differentiation schemes for HA and FA. The results indicate that the method employed here has potential to serve for this purpose with some obvious advantages (speed of analysis, less labour requirements, minimum sample preparation).

ACKNOWLEDGEMENTS

Dr.E. Gjessing is thanked for kindly providing samples of humic substances of Norwegian origin.

REFERENCES

1 E. M. Thurman and R. L. Malcolm, in R. F. Christman and E. T. Gjessing (Editors), *Aquatic and Terrestrial Humic Materials*, Ann Arbor Sci. Publ., Ann. Arbor, MI, 1983, p. 1.
2 V. V. Stepanov and A. N. Pakhomov, *Sov. Soil Sci.*, 6 (1969) 742.
3 R. Klocking, *J. Chromatogr.*, 78 (1973) 409.
4 E. T. Gjessing and T. Gjerdahl, in D. Povoledo and H. L. Golterman (Editors), *Humic Substances*, PUDOC, Wageningen, 1972, p. 43.
5 N. R. Curvetto, N. A. Balmaceda and G. A. Orioli, *J. Chromatogr.*, 93 (1974) 248.
6 N. R. Curvetto, N. A. Balmaceda and G. A. Orioli, *Turrialba*, 25 (1975) 365.
7 F. M. Everaerts, Th. P. E. M. Verheggen and F. E. P. Mikkers, *J. Chromatogr.*, 169 (1979) 21.
8 D. Kaniansky, *Thesis*, Komenský University, Bratislava, 1981.
9 V. Madajová, D. Kaniansky and J. Marák, *5th International Symposium on Isotachophoresis*, Maastricht, 3–5 September 1986, Symposium Abstracts, p. 58.
10 E. M. Thurman and R. L. Malcolm, *Environ. Sci. Technol.*, 15 (1981) 463.
11 J. Kukkonen, A. Oikari, S. Johnsen and E. Gjessing, *Sci. Total. Environ.*, 79 (1989) 197.
12 R. F. C. Mantoura and J. P. Riley, *Anal. Chim. Acta*, 76 (1975) 97.
13 R. L. Wershaw and D. J. Pinckney, *J. Res. U.S. Geol. Surv.*, 1 (1973) 361.
14 J. Hejzlar, *Water Res.*, 21 (1987) 1311.
15 J. Hejzlar, B. Spakowska and R. L. Wershaw, in preparation.
16 M. Schnitzer, in R. G. Burns, G. Dell'Agnola, S. Miele, S. Nardi, G. Savoini, M. Schnitzer, P. Segui, D. Vaughan and S. A. Visser (Editors), *Humic Substances: Effects on Soil and Plant*, Reda, Milan, 1986, p. 14.
17 L. Arlinger, *J. Chromatogr.*, 91 (1974) 785.
18 P. Kopáček, *Postgrad. Rep.*, Komenský University, Bratislava, 1988.
19 D. Kaniansky, V. Madajová, I. Zelenský and S. Stankoviansky, *J. Chromatogr.*, 194 (1980) 11.
20 M. Hutta, *Grad. Rep.*, Komenský University, Bratislava, 1978.
21 P. Molyneux and S. Vekavakayanodha, *J. Chem. Soc., Faraday Trans. 1*, 82 (1986) 291.
22 N. Plechanov, B. Josefsson, D. Dyrssen and K. Lundquist, in R. F. Christman and E. T. Gjessing (Editors), *Aquatic and Terrestrial Humic Materials*, Ann Arbor Sci. Publ., Ann Arbor, MI, 1983, p. 387.

Journal of Chromatography, 545 (1991) 471–474
Elsevier Science Publishers B.V., Amsterdam

CHROM. 23 152

Anomalous behaviour of sodium in isotachophoresis

J. C. REIJENGA* and Th. P. E. M. VERHEGGEN
Laboratory of Instrumental Analysis, Eindhoven University of Technology, P.O. Box 513, 5600 MB Eindhoven (The Netherlands)

ABSTRACT

Using a cationic operational system in capillary isotachophoresis, millimolar concentrations of sodium were determined in the absence and presence of serum proteins. With several internal standards, the reproducibility of the sodium determination was significantly poorer in the presence of proteins, even after partial thermal degradation. The results are explained by protein–sodium interaction in the injection port, where the electric field strength was sixteen times lower than in the separation capillary.

INTRODUCTION

The latest instrumental developments in capillary zone electrophoresis (CZE) prompted us to undertake a reassessment of the potential use of capillary isotachophoresis (ITP). In our view, future uses of ITP will mainly be focused on the following applications: (a) as a preparative, concentrating separation technique; (b) for the determination of non-UV-absorbing components at lower millimolar concentration levels as no sensitive universal detector is available for use in CZE; and (c) applications requiring high accuracy and precision, *e.g.*, as a reference method; this is not possible with any diluting separation technique, such as chromatography.

Our recent work has been focused on the third aspect. An example is the use of ITP as a reference method for the determination of barium and strontium in glass standards. In addition, the possibility of using ITP as a reference method for sodium in serum was the subject of an earlier publication [1]. Aqueous samples were analysed using different ITP equipment and a routine determination based on flame atomic emission spectrometry (FAES). The results were fairly promising. Determination in serum samples, however, showed a slight but significant intercept in favour of FAES [2]. Nevertheless, the calibration lines were still excellent with ITP.

It is well known that binding of many species to serum proteins does occur. Up to now, we have assumed that the electric field strength in the separation compartment was sufficiently high to free the bound components. In our example, irreversible binding of a tiny fraction of the sodium to serum proteins would explain the discrepancies found in the experiments mentioned. In this present work, experiments were designed to confirm this theory.

0021-9673/91/$03.50

EXPERIMENTAL

ITP equipment and system

Experiments were performed using laboratory-made ITP equipment described previously [3]. The separation compartment was a PTFE capillary with a length of 200 mm and 0.2 mm I.D. The detector was an a.c. conductivity detector. Chemicals used were all of analytical-reagent grade and were obtained from Merck (Darmstadt, Germany) unless stated otherwise. The operational system consisted of a solution of 0.01 mol/l $KHCO_3$ adjusted to pH 5.0 with citric acid as a leading electrolyte. The reason for not using KOH (Titrisol quality) was that the latter was difficult to keep sodium-free in a stock solution, essential in this experiment. In this system, calcium did not interfere in the separation, owing to complexation with the citric acid. The terminator was a solution of 0.005 mol/l creatinine, adjusted to pH 5 with citric acid.

The stabilized driving current of 30 μA was delivered by a modified Brandenburg (Thornton Health, U.K.) power supply. The conductivity detector signal and its differential were recorded with a Kipp (Delft, The Netherlands) Type BD41 flat-bed potentiometric recorder, with a paper speed of 5 mm/s.

The samples were injected with a 10-μl syringe (Hamilton, Bonaduz, Switzerland), equiped with a device to inject reproducibly at exactly the same location at the leading/terminator interface. The injection volume was 1 μl, which was adjusted and read under a microscope.

Samples and internal standards

Samples consisted of a healthy pooled serum and a solution of 40 g/l human serum albumin fraction V, HSA (Sigma, St. Louis, MO, U.S.A.). The effect of sodium binding to proteins was likely to be detected preferably at a low sodium content. Therefore, 1 ml of each of the samples was dialysed against 2 l of deionized water for 24 h to decrease the sodium content to *ca.* 1 mmol/l.

In addition, it was considered that if binding of sodium to serum proteins does occur, the effect will at least alter on degradation of the proteins. Therefore, half of each of the dialysed samples (after addition of the internal standard) was subjected to heat treatment for 30 min on a water-bath of 90°C. The protein-containing solutions turned opaque, indicating at least partial thermal degradation.

A blank sample, with respect to serum proteins, was prepared using a 2.50 mmol/l solution of sodium chloride. There were several reasons for using a mixture of three internal standards (I.S.). Solvent evaporation during thermal treatment can then be corrected for, using Na/I.S. zone-length ratios. Possible interactions between one of the internal standards and any of the other sample constituents can be verified by measuring the I.S./I.S. zone-length ratios. A solution of *ca.* 1 mmol/l of each of the following components was used as an internal standard: tetramethylammonium iodate (TMA), tetraethylammonium iodate (TEA) and histidine (HIS). Sample and internal standards were mixed in equal amounts of 1000 μl using a fixed-volume pipette with a disposable tip.

RESULTS AND DISCUSSION

A blank run indicated that the operational system was essentially sodium-free:

no additional zone transitions could be observed in the differential signal. In a typical isotachopherogram, only zones of sodium, TMA, TEA and HIS are visible (Fig. 1). Zone lengths were measured from the differential using a ruler. Zone-length ratios were calculated and are given in Table I.

The relative zone-length reproducibility of the internal standards was satisfactory, even for histidine, the mobility of which was close to that of the terminator. The I.S. reproducibility in the HSA solution was slightly lower less. It was concluded that all three internal standards performed satisfactorily.

Solvent evaporation during thermal treatment was *ca.* 3%, a seen from the average increase in absolute I.S. zone lengths. The determination of 2.50 mmol/l of sodium in the blank was found to be highly reproducible, with a 1% relative standard deviation. A small amount of sodium was found in both pooled serum and albumin solutions. The reproducibility of sodium determination in HSA-containing solutions was considered to be very poor.

Contrary to expectations the standard deviations for sodium determination in albumin-containing solutions did not allow conclusions regarding the effect of heat treatment. The interaction apparently is not manifested as an irreversible binding of a constant amount of sodium. In that event a significant increase on heat treatment would be expected.

The better reproducibility in the pooled serum than in the HSA solutions may be misinterpreted. It should be noted that with the pooled serum, a considerable dilution of the original protein content was the result of osmosis during dialysis, because of the high initial sodium content. It remains to be seen if further dilution of the sample, prior to injection, would decrease the effect to acceptable proportions.

In our view, the results indicate an irreproducible interaction between sodium

TABLE I

RELATIVE ZONE LENGTHS AND CORRESPONDING RELATIVE STANDARD DEVIATIONS (R.S.D.) OF SODIUM AND THE INTERNAL STANDARDS

Sample	Na/TMA	R.S.D. (%)	TMA/TEA	R.S.D. (%)	TEA/HIS	R.S.D. (%)
Pooled	0.81		0.84		0.81	
	0.76	9	0.85	1	0.80	1
	0.68		0.85		0.83	
Pooled, treated	0.67		0.85		0.81	
	0.67	5	0.84	1	0.84	1
	0.73		0.85		0.81	
HSA	0.73		0.85		0.83	
	0.67	11	0.85	1	0.83	1
	0.58		0.82		0.83	
HSA, treated	0.56		0.82		0.85	
	0.59	83	0.85	2	0.93	5
	1.47		0.83		0.81	
Blank	1.21		0.85		0.99	
	1.20	1	0.84	1	0.99	1
	1.21		0.84		0.97	
Blank, treated	1.23		0.86		0.98	

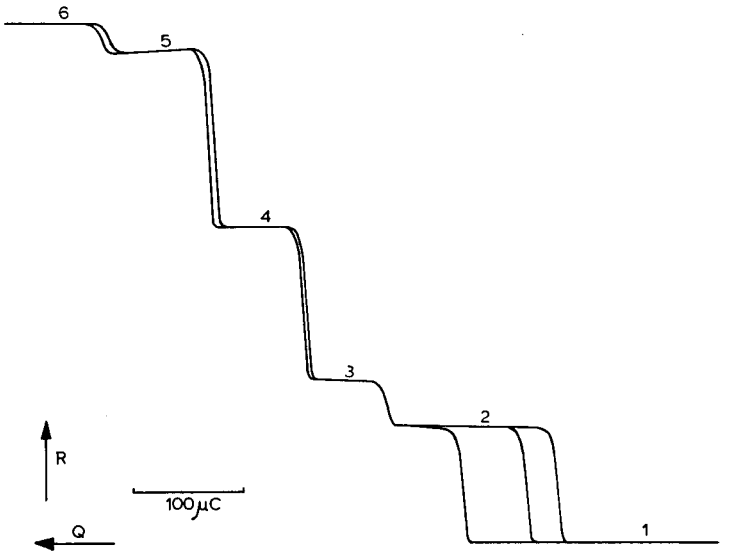

Fig. 1. Irreproducible results of the determination of millimolar concentrations of sodium in the presence of partially degradated pooled serum proteins. 1 = Potassium; 2 = sodium; 3 = trimethylammonium; 4 = triethylammonium; 5 = histidine; 6 = creatinine.

and albumin during ITP separation, inside the injection compartment. Here, the electric field strength is sixteen times lower than in the separation capillary. This sample matrix effect must be taken into account in the trace analysis of biological samples.

REFERENCES

1 A. A. G. Lemmens, J. C. Reijenga, F. M. Everaerts, R. T. P. Janssen, J. A. R. J. Hulsman and C. A. M. Meijer, *J. Chromatogr.*, 320 (1985) 193.
2 A. A. G. Lemmens, unpublished results.
3 F. M. Everaerts, Th. P. E. M. Verheggen and J. L. Beckers, *Isotachophoresis, Theory, Instrumentation and Applications*, (*Journal of Chromatography Libarary*, Vol. 5), Elsevier, Amsterdam, 1978.

Journal of Chromatography, 545 (1991) 475–479
Elsevier Science Publishers B.V., Amsterdam

CHROM. 23 150

Use of isotachophoresis as a reference method for the simultaneous determination of barium and strontium

R. G. TRIELING and J. C. REIJENGA*
Laboratory of Instrumental Analysis, University of Technology, P.O. Box 513, 5600 MB Eindhoven (The Netherlands)
and
H. D. JONKER
Nederlandse Philips Bedrijven, Technology Centre Glass, P.O. Box 218, 5600 MD Eindhoven (The Netherlands)

ABSTRACT

When using X-ray fluorescence spectrometry for the determination of alkali and alkaline earth metals in a silica matrix, frequent recalibration with reference samples is necessary. Determination of metals in these reference samples is carried out using classical analysis. The latter was not possible with barium and strontium in the presence of each other owing to mutual interference. Isotachophoresis, using a 0.02 mol/l potassium–citrate leading electrolyte of pH 5.0 and magnesium chloride as a terminator proved suitable. At concentration ratios in the range 1:10 to 10:1 the accuracy and precision were well within the 1% requirement.

INTRODUCTION

Routine methods require reference samples as analytical standards, the purpose being calibration, taking into account possible sample matrix effects. The average composition of glass consists of, in addition to SiO_2, oxides K_2O, MgO, CaO, TiO_2, Fe_2O_3, Sb_2O_3, CeO_2, ZrO_2, Al_2O_3, Na_2O, SrO, BaO. For X-ray fluorescence spectrometry which is a rapid routine method for the simultaneous determination of glass components, the silica matrix requires recalibration with reference samples including this matrix. The composition of the reference sample should be known with an accuracy and precision exceeding that obtained by the routine method.

Classical analysis, *e.g.*, titration, is often used. However, barium and strontium have almost identical physical and chemical properties and hence mutual interference occurs in most commonly used determinations. The use of a separation technique prior to determination is therefore essential.

With capillary isotachophoresis, separation and determination can be combined. Isotachophoresis has been used previously for the determination of cations in glass-related samples [1]. Complex-forming agents such as crown ethers, hydroxyiso-

0021-9673/91/$03.50

butyric acid (HIBA) and polyethylene glycol (PEG) are necessary to improve the separation of alkali and alkaline earth metals when analysed in one run [2–7]. HIBA is a mild complexing agent, also used for the separation of lanthanides [8]. In the system mentioned [1], separation is not optimized for alkaline earth metals and strontium will still interfere in the determination of calcium, magnesium and barium. In this study, attention was focused on the separation of barium and strontium, a highly selective operational system being sought for these two species.

EXPERIMENTAL

Equipment

Analyses were performed with laboratory-made equipment described previously [9]. The separation compartment was a PTFE capillary (200 mm × 0.2 mm I.D.). An a.c. conductivity detector was used. The constant driving current was ca. 50 μA during separation and 25.0 μA during detection. The conductivity signal and its differential were recorded on a potentiometric flat-bed recorder with a paper speed of 2 mm/s. The time of analysis was up to 20 min. The samples were injected with a Type 701 10-μl syringe (Hamilton, Bonaduz, Switzerland), equipped with a Chaney fixed-volume adaptor, adjusted to 1 μl. The sample was introduced 2 mm below the leading/terminating electrolyte boundary to ensure complete recovery of strontium.

Operational system

In earlier work [10] we investigated the decrease in the effective mobility of alkaline earth metals by citric acid as a co-counter ion at pH 5.0. The results showed that eventually the alkaline earth metal ions have a mobility lower than that of sodium. This is necessary for a good separation, because the mobility interval between sodium and potassium is not sufficient. A citrate concentration exceeding 0.001 mol/l is necessary. A leading electrolyte concentration of 0.02 mol/l potassium was chosen for two reasons: at increasing ionic strength the absolute mobilities of bivalent ions decrease more than those of monovalent ions, and a higher citrate concentrations at pH 5.0 is possible.

The leading electrolyte was prepared by dissolving analytical-reagent grade potassium hydrogencarbonate in water. This was preferred to potassium hydroxide because of the lower sodium content. Citric acid addition was calculated by weight. It should be noted that the order of mobility of the alkaline earth metal ions was reversed with respect to that with HIBA complexation [1]. This follows directly form the corresponding complex stability constants, found in the literature [11]. Therefore, magnesium could be used as a terminator, using 0.01 mol/l magnesium chloride solution. The effective mobilities of barium, strontium and magnesium were $30 \cdot 10^{-9}$, $27 \cdot 10^{-9}$ and $23 \cdot 10^{-9}$ $m^2/V \cdot s$, respectively. These 10% differences ensure adequate separation capability. Of the ions present in solution after pretreatment of the glass samples, only sodium, barium and strontium migrate within the leading–terminator mobility interval (Fig. 1).

Sample pretreatment

Approximately 1 g of solid glass sample was dissolved in 25 ml concentrated hydrofluoric acid–perchloric acid (1:1), the solution was evaporated to dryness, the

residue was dissolved in 40 ml of 6 mol/l hydrochloric acid and the mixture was evaporated to dryness. The latter procedure was repeated twice with 10 ml of 99% acetic acid instead of 40 ml 6 *M* hydrochloric acid. The residue was dissolved in deionized water with heating. After cooling to room temperature, the solution was filtered and transferred into a 200-ml volumetric flask, diluted to volume with deionized water and transferred into a polyethene container. The pH was measured. The filter-paper with the solid residue was ashed in a platinum crucible and checked for the absence of barium and strontium by energy-dispersive X-ray analysis.

Internal standard

A solution of 200 μl of triethylamine (Fluka) in 500 ml of deionized water (*ca.* 2.8 mmol/l) was used as an internal standard (I.S.). The pH of this solution was 8–9, resulting in partial neutralization of the acidic samples. The sample and I.S. were mixed in equal volumes, using a 1000-μl pipette with disposable tips. An analytical balance with a resolution of 0.1 mg was used to check the I.S. to sample ratio on a mass basis. The zone-length ratio measured on the isotachopherogram was multiplied by this mass ratio to correct for minor fluctuations in the use of the pipette. Owing to the extensive sample pretreatment, fluctuations in sample density were sufficiently small to allow this procedure.

Syringe-rinsing procedure

A syringe-rinsing procedure was developed to eliminate cross-contamination from subsequent injections. After sample injection, the syringe was rinsed successively in water, a tracer solution, water and the next sample solution. Each rinsing consisted of a fixed number of plunger displacements in the corresponding solution. The tracer solution consisted of 30 μl of *n*-butylamine in 50 ml of deionized water (*ca.* 6 mmol/l). The idea was that if no zone occurs at the *n*-butylamine step height (between sodium and I.S.), cross-contamination with the previously injected sample can be excluded. If an additional zone is present, the results of the analysis are not valid.

Calibration

Barium and strontium standards were prepared from standard solutions of 1000 ppm (Baker) and were used for calibration. Using calibrated precision glassware, a number of standard solutions were made containing both elements at concentrations of *ca.* 0, 1, 2, 3 and 5 mg/ml. These standards were subsequently kept in plastic containers.

RESULTS AND DISCUSSION

Calibration graphs were constructed by analysing each of the standards twice. A difference of 1% between the duplicate results was considered acceptable, otherwise the analysis was repeated until good duplicate results were obtained. The Ba/I.S. and Sr/I.S. zone length ratios were multiplied by the I.S./samples volume ratio and plotted against the concentration of the corresponding element. The resulting calibration graphs (see Fig. 2) have been a correlation coeffficient of 0.9998 or better. Duplicate analyses of samples were also within 1%.

Over a 1-month period, a number of calibration graphs were constructed. The

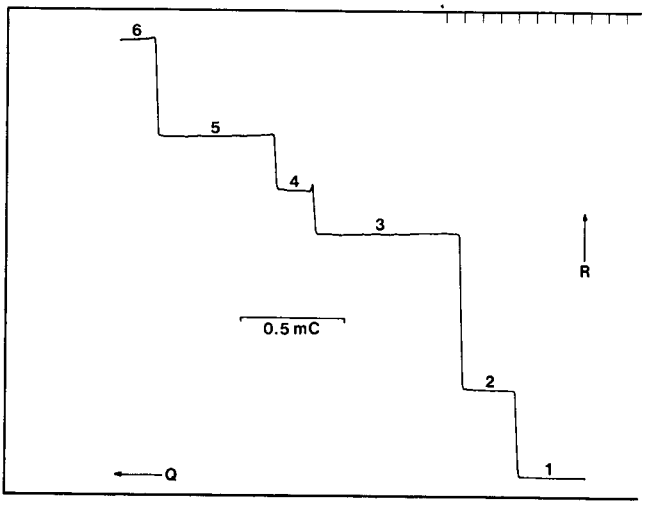

Fig. 1. Isotachopherogram of a typical glass sample. Resistance R is plotted against charge Q, the product of current and time. 1 = Potassium; 2 = sodium; 3 = triethylamine as I.S.; 4 = barium; 5 = strontium; 6 = magnesium. See text for operational conditions.

intercept of the calibration graphs was sufficiently small not to introduce an additional systematic error. The front of the barium zone shows a distinct detector overshoot, possibly owing to electrode reactions with the counter ion. This overshoot should be included in the zone length of barium because it does not orginate from an additional component. The slopes of the calibration graphs show a day-to-day variation of 3 and 2% for barium and strontium, respectively, which means that daily recalibration is necessary.

Precision was determined by analysing a sample fourteen times. This included dilution with the internal standard, injection, analysis and zone length measurement. The relative standard deviations of the calculated concentration were 0.8 and 0.7% for barium and strontium, respectively. Accuracy was determined by analysing dried

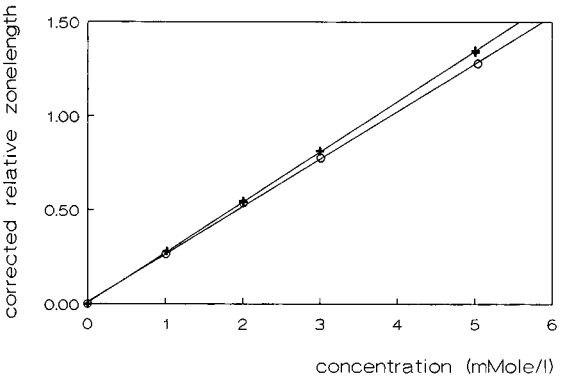

Fig. 2. Calibration graphs for (○) barium and (+) strontium. Correlation = 0.9998 and 0.9999, respectively (n = 10).

barium and strontium carbonates of super-pure quality. The result was 99.9% with a standard deviation of 0.2%.

The syringe-rinsing method was found useful and is recommended for precision analysis with any separation technique using syringe injection. An obvious requirement is that the tracer is not present in any of the samples. The sensitivity of the method can be changed by means of the tracer concentration.

It is concluded that isotachophoresis can be used as a reference method for glass standards containing both barium and strontium in the usual silica matrix. Provided that barium and strontium are not lost through precipitation in the sample pretreatment (this has been verified), it can be used to label reference samples for X-ray fluorescence spectrometry.

REFERENCES

1 A. A. G. Lemmens, F. M. Everaerts, J. W. Venema and H. D. Jonker, *J. Chromatogr.*, 439 (1988) 423.
2 A. A. G. Lemmens, *Thesis*, University of Technology, Eindhoven, 1989.
3 S. Fanali, F. Foret and P. Bocek, *Pharmazie*, 40 (1985) 653.
4 I. Nukatsuka, M. Taga and H. Yoshida, *Bull Chem. Soc. Jpn.*, 54 (1981) 2629.
5 D. Kaniansky, I. Zelenský, I. Valašková, J. Marak, V. Zelenská, *J. Chromatogr.*, 502 (1990) 143.
6 F. S. Stover, *J. Chromatogr.*, 298 (1984) 203.
7 F. S. Stover, *J. Chromatogr.*, 368 (1986) 476.
8 M. Tazaki, M. Tkagi and K. Ueno, *Chem. Lett.*, 5 (1982) 639.
9 F. M. Everaerts, J. L. Beckers and Th. P. E. M. Verheggen, *Isotachophoresis, Theory, Instrumentation and Applications*, Journal of chromatography Library, Vol. 6, Elsevier, Amsterdam, 1976.
10 J. C. Reijenga, *Graduation Report*, University of Technology, Eindhoven, 1978.
11 A. E. Martell and R. M. Smith, *Critical Stability Constants*, Plenum Press, New York, 1974.

Author Index Vol. 545

PUBLICATION SCHEDULE FOR 1991

Journal of Chromatography and Journal of Chromatography, Biomedical Applications

MONTH	D 1990–F 1991	M	A	M	J	J	
Journal of Chromatography	Vols. 535–539	540/1 + 2 541/1 + 2 542/1	542/2 543/1	543/2 544/1 + 2 545/1	545/2 546/1 + 2 547/1 + 2	548/1 + 2	The publication schedule for further issues will be published later
Cumulative Indexes, Vols. 501–550							
Bibliography Section		560/1			560/2		
Biomedical Applications	Vols. 562, 563	564/1	564/2 565/1 + 2	566/1 566/2	567/1	567/2	

INFORMATION FOR AUTHORS

(Detailed *Instructions to Authors* were published in Vol. 522, pp. 351–354. A free reprint can be obtained by application to the publisher, Elsevier Science Publishers B.V., P.O. Box 330, 1000 AH Amsterdam, The Netherlands.)

Types of Contributions. The following types of papers are published in the *Journal of Chromatography* and the section on *Biomedical Applications*: Regular research papers (Full-length papers), Review articles and Short Communications. Short Communmications are usually descriptions of short investigations, or they can report minor technical improvements of previously published procedures; they reflect the same quality of research as Full-length papers, but should preferably not exceed six printed pages. For Review articles, see inside front cover under Submission of Papers.

Submission. Every paper must be accompanied by a letter from the senior author, stating that he/she is submitting the paper for publication in the *Journal of Chromatography*.

Manuscripts. Manuscripts should be typed in double spacing on consecutively numbered pages of uniform size. The manuscript should be preceded by a sheet of manuscript paper carrying the title of the paper and the name and full postal address of the person to whom the proofs are to be sent. As a rule, papers should be divided into sections, headed by a caption (*e.g.*, Abstract, Introduction, Experimental, Results, Discussion, etc.). All illustrations, photographs, tables, etc., should be on separate sheets.

Introduction. Every paper must have a concise introduction mentioning what has been done before on the topic described, and stating clearly what is new in the paper now submitted.

Abstract. All articles should have an abstract of 50–100 words which clearly and briefly indicates what is new, different and significant.

Illustrations. The figures should be submitted in a form suitable for reproduction, drawn in Indian ink on drawing or tracing paper. Each illustration should have a legend, all the *legends* being typed (with double spacing) together on a *separate sheet*. If structures are given in the text, the original drawings should be supplied. Coloured illustrations are reproduced at the author's expense, the cost being determined by the number of pages and by the number of colours needed. The written permission of the author and publisher must be obtained for the use of any figure already published. Its source must be indicated in the legend.

References. References should be numbered in the order in which they are cited in the text, and listed in numerical sequence on a separate sheet at the end of the article. Please check a recent issue for the layout of the reference list. Abbreviations for the titles of journals should follow the system used by *Chemical Abstracts*. Articles not yet published should be given as "in press" (journal should be specified), "submitted for publication" (journal should be specified), "in preparation" or "personal communication".

Dispatch. Before sending the manuscript to the Editor please check that the envelope contains four copies of the paper complete with references, legends and figures. One of the sets of figures must be the originals suitable for direct reproduction. Please also ensure that permission to publish has been obtained from your institute.

Proofs. One set of proofs will be sent to the author to be carefully checked for printer's errors. Corrections must be restricted to instances in which the proof is at variance with the manuscript. "Extra corrections" will be inserted at the author's expense.

Reprints. Fifty reprints of Full-length papers and Short Communications will be supplied free of charge. Additional reprints can be ordered by the authors. An order form containing price quotations will be sent to the authors together with the proofs of their article.

Advertisements. Advertisement rates are available from the publisher on request. The Editors of the journal accept no responsibility for the contents of the advertisements.

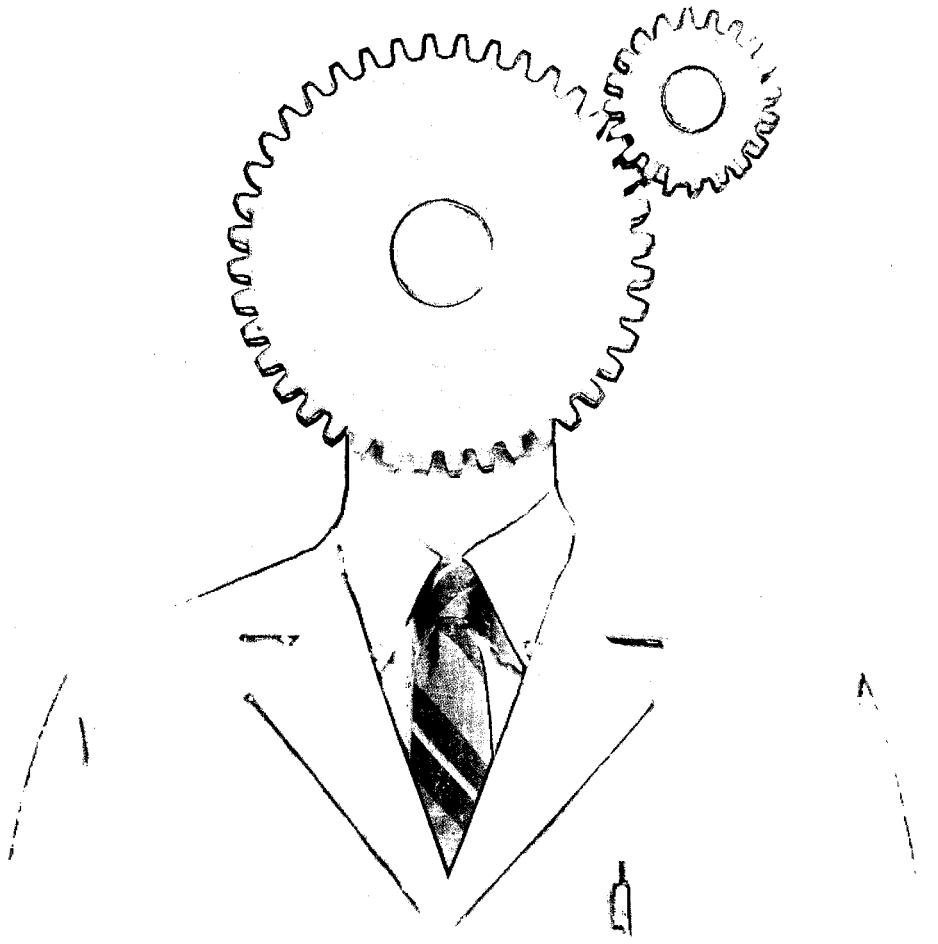

There's more to our CE autosampler than automation.

On the new Model 270A-HT High Throughput Capillary Electrophoresis System, a unique sample cooling system minimizes sample degradation. Our special design eliminates evaporation. Ion replenishment can be fully automated with the multiple buffer system. The software makes it easy to custom-tailor analysis parameters to each sample...Whether you need unattended overnight operation on 50 samples or just a few, optimal performance is ensured. The Model 270A-HT High Throughput Capillary Electrophoresis System. Higher sensitivity, greater reliability and more performance than ever. Contact Applied Biosystems today.

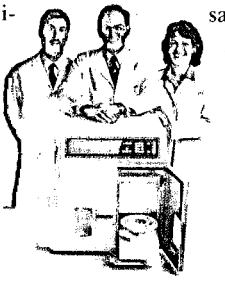

Applied Biosystems

oster City, U.S.A. Tel: (415) 570-6667. Telex: 470052 APBIO UI. Fax: (415) 572-2743.
Iissisauga, Canada. Tel: (416) 821-8183. Fax: (416) 821-8246.
Varrington, U.K. Tel: 0925-825650. Telex: 629611 APBIO G. Fax: 0925-828196.
Veiterstadt, Germany. Tel: 06151-87940. Telex: 4197318 Z ABI D. Fax: 06151-84899.
aris, France. Tel: (1) 48 63 24 44. Telex: 230458 ABIF. Fax: (1) 48 63 22 82.
Ilan, Italy. Tel: (0)2 89404561. Fax: (0)2 8321655.
Iaarssen, The Netherlands. Tel: (0) 3465-74868. Telex: 70896. Fax: (0) 3465-74904.
urwood, Australia. Tel: (03) 808-7777. Fax: (03) 887-1469.
okyo, Japan. Tel: (03) 699-0700. Fax: (03) 699-0733.